UMCEE 03-08 May 2003

VERIFICATION OF GIRDER DISTRIBUTION FACTORS FOR CONTINUOUS STEEL GIRDER BRIDGES

IDS CONTRACT NO. 95-0242

Report submitted to
the Michigan Department
of Transportation

Andrzej S. Nowak, Junsik Eom, and David Ferrand

Department of Civil and Environmental Engineering
University of Michigan
Ann Arbor, Michigan 48109-2125

DISCLAIMER

Technical Report Documentation Page

1. Report No. Research Report RC-1429	2. Government Accession No.	3. MDOT Project Manager	
4. Title and Subtitle Verification of Girder Distribution Factors for Continuous Steel Girder Bridges		5. Report Date May 2003	
7. Author(s) Andrzej S. Nowak, Junsik Eom, and David Ferrand		6. Performing Organization Code	
9. Performing Organization Name and Address University of Michigan 2340 G.G. Brown Bldg. Ann Arbor, MI 48109-2125		8. Performing Org Report No. UMCEE 03-08	
12. Sponsoring Agency Name and Address Michigan Department of Transportation Construction and Technology Division P.O. Box 30049 Lansing, MI 48909		10. Work Unit No. (TRAIS)	
		11. Contract Number: IDS Contract No. 95-0242	
		11(a). Authorization Number: 15	
15. Supplementary Notes		13. Type of Report & Period Covered Final Report	
		14. Sponsoring Agency Code	

16. Abstract

The Report documents the field testing and analysis of continuous steel girder bridges. The objective of the tests was to provide a basis for recommended girder distribution factors (GDF) for interior girders and dynamic load factors (DLF), suitable for evaluation of existing continuous steel girder bridges. A total of six bridges were instrumented and loaded with heavy 11-axle trucks. The maximum measured strain was about 240 με for positive moment at midspan, and 150 με for negative moment over support locations. Lower than expected strain values were due to partial fixity of supports, and flexural stiffness of the deck slab, sidewalks, parapets and curbs. An advanced finite element (FEM) analysis was performed using ABAQUS. The FEM results are compared with the test results. The field study confirmed some of the previous findings related to the dynamic load factors (DLF). In general, DLF's for continuous spans are lower than DLF's for simple spans. DLF's are lower for a negative moment (over the support) than for a positive moment (mid-span). The test results showed that DLF for a single heavy truck is less than 0.15. For two trucks side-by-side, DLF is 0.05-0.07 for the tested bridges. The field tests showed that the live load moment distribution is different for continuous spans compared with simple spans (tested in previous years). In general, the distribution is more uniform for continuous spans, and this applies mostly to the negative moment. The superposition of truck loads in one lane and two adjacent spans produces a larger strain than measured during the field tests. The tests confirmed that the code specified GDF's, for a single lane and for multi-lane traffic, are adequate or conservative, for both AASHTO LRFD (1998) and AASHTO Standard (2002). AASHTO Standard (2002) provides more conservative GDF's.

17. Key Words	18. Distribution Statement No restrictions. This document is available to the public through the Michigan Department of Transportation.		
19. Security Classification (report) Unclassified	20. Security Classification (Page) Unclassified	21. No of Pages 235	22. Price

Note:

Intentionally left blank

Executive Summary

The Report documents the field testing and analysis of continuous steel girder bridges. The objective of the tests was to provide a basis for recommended girder distribution factors (GDF) for interior girders and dynamic load factors (DLF), suitable for evaluation of existing continuous steel girder bridges.

A total of six bridges were instrumented and loaded with heavy 11-axle trucks. The results were obtained for one truck and two trucks side-by-side. The vehicles were moving at crawling speed for the static load measurement and at a regular speed for the dynamic load measurement. Two truck positions were considered for each case, close to the curb and center of the traffic lane. The strains for both trucks are practically the same, which confirms the repeatability of the results. The measured maximum strains were also the same for crawling speed and a regular speed. The maximum measured strain was about 240 με for positive moment at midspan, and 150 με for negative moment over support locations. Lower than expected strain values were due to partial fixity of supports, and flexural stiffness of the deck slab, sidewalks, parapets and curbs. An advanced finite element (FEM) analysis was performed using ABAQUS. The FEM results are compared with the test results.

The field study confirmed some of the previous findings related to the dynamic load factors (DLF). In general, DLF's for continuous spans are lower than DLF's for simple spans. DLF's are lower for a negative moment (over the support) than for a positive moment (mid-span). The test results showed that DLF for a single heavy truck is less than 0.15. For two trucks side-by-side, DLF is 0.05-0.07 for the tested bridges. Therefore, for evaluation of existing steel girder bridges it is recommended, conservatively, to use DLF = 0.10 for two lane loading, and DLF = 0.20 for a single truck load case.

The field tests showed that the live load moment distribution is different for continuous spans compared with simple spans (tested in previous years). In general, the distribution is more uniform for continuous spans, and this applies mostly to the negative moment. The superposition of truck loads in one lane and two adjacent spans produces a larger strain than measured during the field tests.

The tests confirmed that the code specified GDF's, for a single lane and for multi-lane traffic, are adequate or conservative, for both AASHTO LRFD (1998) and AASHTO Standard (2002). AASHTO Standard (2002) provides more conservative GDF's. Therefore, for the design of new bridges and evaluation of existing structures, it is recommended to use AASHTO LRFD (1998) GDF's.

The analysis and truck survey presented in the previous report (Nowak 2001) showed that the probability of a simultaneous occurrence of two fully loaded truck side-by-side is negligible. Therefore, for evaluation of existing continuous steel girder bridges, it is possible to use the GDF's specified in the AASHTO Standard (2002) for a single lane even for two lane structures.

TABLE OF CONTENTS

Acknowledgments

The presented research has been sponsored by the Michigan Department of Transportation which is gratefully acknowledged. The authors thank the technical staff of the Michigan DOT, Roger Till, Sudhakar Kulkarni, Steven Beck and other members of TAG for their useful comments, discussions and support.

The project team received help from other researchers, current and former students and staff of the University of Michigan. In particular, thanks are due to Dr. Aleksander Szwed, Dr. Maria Szerszen, and Taejun Cho. They were involved in field instrumentation, measurements, and processing of the results.

Thanks are due to the Michigan State Police for their cooperation.

The realization of the research program would not be possible without in kind support of the Michigan DOT and the University of Michigan. Measurements were taken using equipment purchased by the University of Michigan.

1. INTRODUCTION

1.1 Introduction

The objective of this study is validation of the code–specified girder distribution factors (GDF) and dynamic load factors (DLF) for continuous steel girder bridges by field tests and finite element analysis. Field testing is an increasingly important topic in the effort to deal with the deteriorating infrastructure, in particular this applies to bridges and pavements. There is a need for accurate and inexpensive methods for diagnostics, verification of load distribution, and determination of the actual load carrying capacity. A considerable number of Michigan bridges show signs of deterioration. In particular, there is a severe corrosion on many steel structures. By analytical methods, some of these bridges are not adequate to carry the normal highway traffic. However, the actual load carrying capacity is often much higher than what can be determined by analysis, due to more favorable load sharing, effect of non-structural components (parapets, railing, sidewalks), and other difficult to quantify factors. Field testing can reveal the hidden strength reserve and thus verify the adequacy of the bridge. One of the most important objectives of this study is to develop a field testing techniques to measure the actual GDF's and DLF's in continuous span bridges, with minimum traffic interruptions.

There is a growing need for developing efficient procedures for evaluation of the actual load spectra, load distribution, actual strength and predict the remaining life of the structure. There is a need to verify if the currently used girder distribution factors (GDF) are too conservative. Girder distribution factors (GDF) are very important in evaluation of existing bridges. Extensive analytical studies performed in conjunction with the development of AASHTO LRFD Code indicated that GDF's specified by the AASHTO Standard Specifications (1996) are often inaccurate, in some cases the specified values are overly conservative, and in other cases they are too permissive. Knowledge of the accurate GDF's is needed to determine the actual value of live load (truck load) for bridge girders. Overestimation of GDF's can have serious economic consequences, as deficient bridges must be repaired or rehabilitated.

Furthermore, the GDF's specified in AASHTO were derived for HS-20 trucks. On the other hand, the live load in Michigan is often governed by 11 axle trucks. Therefore, there is a need to determine the GDF's for 11 axle vehicles loaded to the legal limit.

It was observed in previous field tests performed on simple-span steel girder bridges that GDF can be considerably different than what is specified in the design code (AASHTO Standard or AASHTO LRFD). For bridges that have a marginal rating factor, a conservative GDF can have serious economic consequences (posting, repair, rehabilitation or replacement). Previous tests by the University of Michigan team were carried out to determine the GDF for simply supported steel girder bridges, representing about 65% of all bridges in Michigan. Continuous bridges require a different arrangement of instrumentation, as the strain transducers are placed not only at mid-span but also at the supports.

MDOT is anticipating a change in the method of load rating bridges from using a one lane girder distribution factor (GDF) [S/14] to using a two lane GDF [S/11] in certain instances. As a result, some bridges with a current operating rating of 98 tons (controlled by the 2-unit, 77 ton truck) may need posting when analyzed using a two lane GDF (77 X 14/11 = 98). The purpose of the project is to focus on GDF's for continuous steel beam bridges, and to check if the use of a one lane GDF can be applied. MDOT provided a listing of continuous steel beam bridges with an operating rating of 100 tons or less that include possible bridges for testing. The study is based on the experience of previous research carried out by the University of Michigan.

Dynamic load factors (DLF) calculated using AASHTO Standard Specifications and AASHTO LRFD can be very conservative compared to the actual values. In most cases the specified DLF is about 0.3. Previous field tests performed for simple span bridges using heavy trucks indicate that the actual DLF is less than about 0.15 for a single truck, and less than 0.1 for two trucks side-by-side. This study intends to verify the actual DLF's for continuous steel girder bridges by field testing.

2. SELECTED BRIDGES

This study is focused on steel continuous girder bridges. These structures constitute about 11% of all steel girder bridges in Michigan. A more accurate value of GDF is needed for evaluation of existing structures. Analytical studies also point to a reduced conservatism in code-specified GDF's for shorter spans. In this study, the selection of bridges was based of the following criteria:

- Structural type and material; steel continuous girder bridges.
- Skewness; Bridges with skew angle of more than 30 degrees were excluded.
- Accessibility; some structures could not be considered because of difficult access for testing equipment, in particular heavy traffic under the considered span.
- Traffic volume; very busy bridges were not considered because of the expected difficulties with traffic control. Therefore, only bridges with an average daily traffic of 7,000 were selected.

More than a thirty bridges were inspected to verify their feasibility for load test. Finally, six bridges were selected for this study as listed in Table 2.1. All bridges carry two lanes, except S12-82293 which carries 5 lanes. The detailed descriptions of each bridge are shown in the following chapters.

Table 2.1 Selected Bridges.

MDOT ID Number	Location (County)	No. of Span	No. of Lanes	Total Bridge Length (ft)	No. of Girders	Girder Spacing	Year Constructed	Skew Angle	Operating Rating (kips)	ADT
S08-77024	St. Clair	3	2	342	7	7’2’’	1982	1	264	164
S05-44044	Lapeer	3	2	388	7	6’11”	1983	17	212	315
S01-12034	Coldwater	2	2	216	4	8’6”	1967	0	176	900
S09-77023	St.Clair	3	2	370	6	8’4”	1980	19	246	1460
S13-59012	Montcalm	4	2	459	5	8’10”	1979	7	264	550
S12-82293	Wayne	2	5*	594	9	8’8”	1971	25	280	6840

* 4 traffic lanes plus a left turn lane

Note:

Intentionally left blank

3. LOAD TESTING PROCEDURE

3.1 Instrumentation and data acquisition

The strain transducers were attached to the lower and/or upper surface of the bottom flange of steel girders at midspan (Figure 3.1), depending on the accessibility. In addition, they were installed on girders at the support to measure the negative moment The deflection of the most loaded girder was measured at the midspan using the optical device (PSM-R) manufactured by Noptel, Co. in Finland. This device is suitable for long distance remote displacement measurements. It is based on a combined LED transmitter and opto-electronic receiver that measures the position of the reflector or prism attached to the target. Figures 3.2 and 3.3 illustrate the actual setup of the PSM-R deflection measurement system.

Strain transducers were connected to the SCXI data acquisition system from the National Instruments. The data acquisition mode is controlled from the external PC notebook computer, and acquired data are processed and directly saved in PC's hard drive (Figure 3.4).

The data acquisition system consists of a four slot SCXI-1000 chassis, one SCXI-1200 data acquisition module and two SCXI-1100 multiplexers. Each multiplexer can handle up to 32 channels of input data. The current system is capable of handling 64 channels of strain or deflection inputs. Up to 32 additional channels can be added if required. A portable field computer is used to store, process and display the data on site. A typical data acquisition setup is shown in Figure 3.4. The data from all instruments is collected after placing the trucks in desired positions or while trucks are passing on the bridge. For the normal speed tests, a sampling rate of 300 per second was used for calculation of dynamic effects. This is equivalent to 11.4 samples per meter at a truck speed of 95 km/h. The real time responses of all transducers are displayed on the monitor during all stages of testing, assuring the safety of the bridge load test.

Figure 3.1 Removable Strain Transducer Mounted to the Lower Flange.

Figure 3.2 Infrared Beam Projector Manufactured by Noptel Inc.
for Deflection Measurement

Figure 3.3 Prism Attached under Girder for Deflection Measurement

A new strain measurement system was purchased from Bridge Diagnostics, Inc. in Boulder, Colorado. This system can simultaneously handle 16 channels of strain measurements. It has been designed expressly for performing live-load tests on highway bridges. One of the main advantages of using this system is that the strain transducers are automatically recognized by the main data logger, thereby eliminating the need for tracking channel numbers or calibration factors. Also, the main cable used in the system can accommodate multiple numbers of input signals. Therefore, it eliminates a complicated cable management on the bridge test site. The system was installed together with previous strain measurement system during the actual bridge tests to ensure the accuracy of the readings. Figure 3.5 shows the actual installation of the strain transducers used for the system from Bridge Diagnostics, Inc.

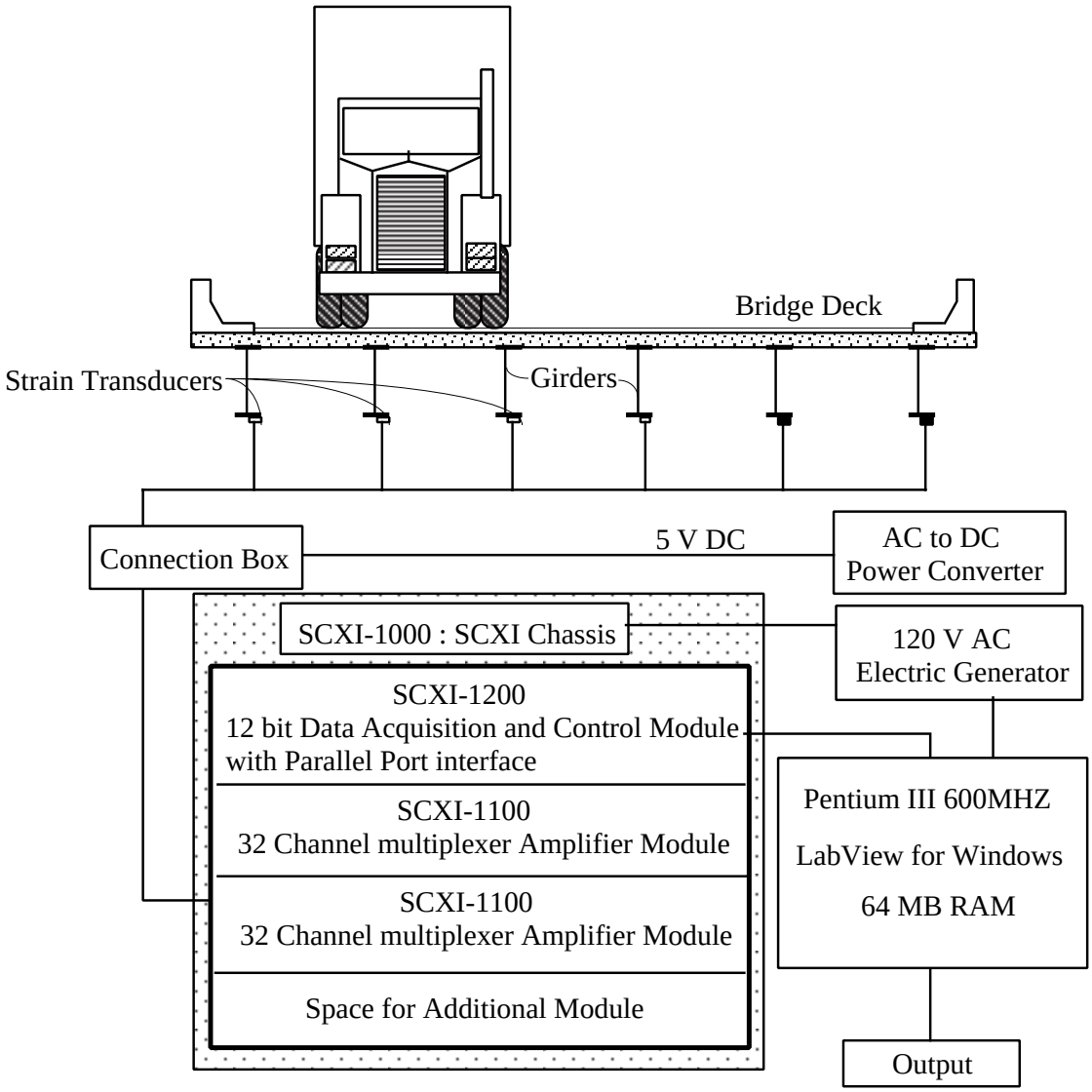

Figure 3.4. SCXI Data Acquisition System Setup.

3.2 Test loads for load distribution tests

Strain data for calculation of the girder distribution factors and dynamic load factors were taken on bottom-flanges of girders in the middle of a span, and near supports over pier and/or abutment. The measurements were taken under passages of one and two vehicles, each being a three-unit 11-axle truck with known weight and axle configuration. The actual axle weights of the test trucks were measured at the weigh stations prior to the test for all bridges.

Figure 3.5 Installation of New Strain Transducer Purchased from Bridge Diagnostics, Inc.

Strain data was used to calculate load distribution and dynamic load factors. Superposition of strain data for single trucks was compared to the results obtained for two trucks side-by-side, as the verification of the linear-elastic behavior of the bridge.

Trucks were driven over the bridge at crawling speed as static load and at normal speed to obtain dynamic effect on the bridge, except Bridge S12-82293. For bridge S12-82293, only static test was performed due to the difficulty in controlling heavy traffic. For each location, normal speed was the maximum possible speed for the test truck. Table 3.1 shows typical sequence of test runs. Lane 1 indicates north or west lane, and lane 2 indicates south or east lane, depending on the orientation of the tested bridge. In addition to crawling speed tests, the trucks were stopped at the predetermined position to confirm the pre-test analysis.

Table 3.1 Sequence of Typical Test Runs for Tested Bridges

Run#	Truck	Lane Side	Position	Truck Speed
1	Truck A	Lane 1	Center	Crawling
2	Truck B	Lane 1	Center	Crawling
3	Truck A	Lane 2	Center	Crawling
4	Truck B	Lane 2	Center	Crawling
5	Truck A	Lane 1	Curb	Crawling
6	Truck B	Lane 1	Curb	Crawling
7	Truck A	Lane 2	Curb	Crawling
8	Truck B	Lane 2	Curb	Crawling
9	Truck A	Lane 1	Center	Normal
10	Truck B	Lane 1	Center	Normal
11	Truck A	Lane 2	Center	Normal
12	Truck B	Lane 2	Center	Normal
13	Truck A and Bboth	side-by-side	Center	Crawling
14	Truck B and Aboth	side-by-side	Center	Crawling
15	Truck A and Bboth	side-by-side	Center	Normal
16	Truck B and Aboth	side-by-side	Center	Normal
17	Truck A followed by B	Lane 1	Center	Crawling
18	Truck A followed by B	Lane 2	Center	Crawling
19	Truck B followed by A	Lane 1	Center	Crawling
20	Truck B followed by A	Lane 2	Center	Crawling
21	Truck A followed by B	Lane 1	Center	Stop at fixed position
22	Truck A followed by B	Lane 2	Center	Stop at fixed position
23	Truck B followed by A	Lane 1	Center	Stop at fixed position
24	Truck B followed by A	Lane 2	Center	Stop at fixed position

3.3 Load distribution factor and dynamic load factor calculation from test results

Collected strain data from the tests were processed to identify dynamic load and girder distribution factors. Girder Distribution Factors (GDF) are calculated from the maximum static strain obtained from the static loading at each girder at the same section along the length of the bridge. Ghosn *et al*. (1986) assumed that GDF was equal to the ratio of the static strain at the girder to the sum of all the static strains. Stallings and Yoo (1993) used the weighted strains to account for different section moduli of the girders. Accordingly, GDF for the *i*-th girder, GDF_i, can be derived as follows:

$$GDF_i = \frac{M_i}{\sum_{j=1}^{k} M_j} = \frac{ES_i\varepsilon_i}{\sum_{j=1}^{k} ES_j\varepsilon_j} = \frac{\frac{S_i}{S_\ell}\varepsilon_i}{\sum_{j=1}^{k} \frac{S_j}{S_\ell}\varepsilon_j} = \frac{\varepsilon_i w_i}{\sum_{j=1}^{k} \varepsilon_j w_j} \qquad (3\text{-}1)$$

where M_i = bending moment at the *i*-th girder; E = modulus of elasticity; S_i = section modulus of the *i*-th girder; S_ℓ = typical interior section modulus; ε_i = maximum bottom-flange static strain at the *I*-th girder; w_i = ratio of the section modulus of the *i*th girder to that of a typical interior girder; and k = number of girders. When all girders have the same section modulus (that is, when weigh factors, w_i, are equal to one for all girders), Eq. (3-1) is equivalent to that of Ghosn *et al*. (1986). Because of edge stiffening effect due to curbs and barrier walls, the section modulus in exterior girders is slightly greater than in interior girders. In other words, the weigh factors, w_i, for exterior girders are greater than one. Therefore, from Eq. (3-1), the assumption of the weigh factors, w_i, equal to one will cause slightly overestimated girder distribution factors in interior girders and underestimated girder distribution factors in exterior girders. In this study, the weigh factors, w_i, are assumed to be one.

For multi-lane loading, the girder distribution factors calculated from Eq. (3-1) must be multiplied by the numbers of loaded lanes to be comparable with the bridge code because the AASHTO code specified girder distribution factors are based on the effect of one truck load.

Dynamic load factors (DLF's) are defined in several ways, as discussed in previous studies (Paultre *et al*. 1992; Bakht and Pinjarkar 1989). In this study, the dynamic load factor was taken as the ratio of the maximum dynamic strain and the maximum static strain (Figure 3.6):

$$DLF = \frac{\varepsilon_{dyn}}{\varepsilon_{stat}} \qquad (3\text{-}2)$$

where ε_{dyn} = absolute maximum dynamic strain under the vehicle traveling at normal speed; and ε_{stat} = maximum equivalent static strain from normal speed test, obtained by filtering out the dynamic portion. Collected data are filtered by applying some numerical procedures, such as averaging filtering technique, to increase the signal-to-noise ratio, and to reduce the effect of random, and non-periodic noise.

Dynamic load factor is calculated for all instrumented girders. However, for comparison with the code specified DLF, it is necessary to consider DLF corresponding to the largest static strains, because this is the governing case.

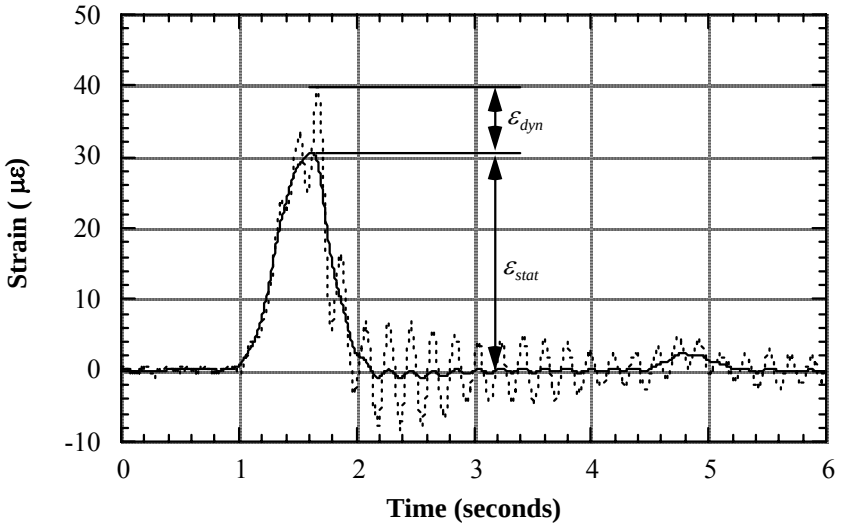

Figure 3.6. Dynamic and Static Strain under a Truck at Highway Speed.

4. SPECIFIED LOAD DISTRIBUTION FACTORS AND DYNAMIC LOAD FACTORS

Measured girder distribution factors (GDF) and dynamic load factors (DLF) are compared in tables and figures with the values calculated according to the current design codes. Throughout the report, distribution factors are expressed in terms of axle load for the full truck rather than a line of wheel loads for the half truck. For the bending moment in interior girders, the AASHTO Standard (1996) specifies GDF's as follows. For steel girder and prestressed concrete girder bridges, with one lane, GDF is:

$$GDF = \frac{S}{14} \tag{4-1}$$

and for steel and prestressed concrete girder bridges, with multi lanes,

$$GDF = \frac{S}{11} \tag{4-2}$$

where S = girder spacing (ft).

The AASHTO LRFD Code (1998) specifies GDF as a function of girder spacing, span length, stiffness parameters, and bridge skew. For the bending moment in interior girders with one lane loading, GDF is:

$$GDF = \left\{0.06 + \left(\frac{S}{14}\right)^{0.4}\left(\frac{S}{L}\right)^{0.3}\left(\frac{K_g}{12.0Lt_s^3}\right)^{0.1}\right\}\left\{1 - c_1(\tan\theta)^{1.5}\right\} \tag{4-3}$$

and for multi lane loading:

$$GDF = \left\{0.075 + \left(\frac{S}{9.5}\right)^{0.6}\left(\frac{S}{L}\right)^{0.2}\left(\frac{K_g}{12.0Lt_s^3}\right)^{0.1}\right\}\left\{1 - c_1(\tan\theta)^{1.5}\right\} \tag{4-4}$$

$$c_1 = 0.25\left(\frac{K_g}{12.0Lt_s^3}\right)^{0.25}\left(\frac{S}{L}\right)^{0.5} \qquad \text{for } 30° < \theta < 60° \tag{4-5}$$

$$c_1 = 0 \qquad \text{for } \theta < 30° \tag{4-6}$$

where S = girder spacing (ft); L = span length (ft); $K_g = n(I + Ae_g^2)$; t_s = thickness of concrete slab (in); n = modular ratio between girder and slab materials; I = moment of inertia of the girder (in^4); A = area of the girder (in^2); e_g = distance between the centers of gravity of the girder and the slab (in); and θ = skew angle in degrees. In practice, the term $K_g/(Lt_s^3)$ is within 0.9 and 1.1, but it may imply more accuracy than exists for bridge evaluation. Therefore, in this report the term $K_g/(Lt_s^3)$ is assumed equal to 1.0, for positive and negative moment analysis.

The AASHTO LRFD (1998) formulas were developed based on the NCHRP Project 12-26 (Zokaie *et al*. 1991). The method includes the longitudinal stiffness parameter, K_g, and the span length, L, in addition to the girder spacing, S. AASHTO Guide for Load Distribution (1994) specifies similar load factors to those of AASHTO LRFD (1998).

For GDF's specified in AASSHTO LRFD (1998), the span length, L, is the span length for the calculation of GDF at midspan, and the average span length of two adjacent spans for the calculation of GDF at the support. There is no difference between those GDF's specified for positive moment and negative moment in AASHTO Standard (2002)

Most bridge design codes specify the dynamic load as an additional static live load. In the AASHTO Standard (1996), dynamic load factors are specified as a function of span length only:

$$\text{DLF} = \frac{50}{3L + 125} \leq 0.30 \qquad (4\text{-}7)$$

where DLF = dynamic load factor (maximum 30 percent); and L= span length (ft). This empirical equation has been used since 1944. In the AASHTO LRFD (1998), live load is specified as a combination of HS20 truck (AASHTO 1996) and a uniformly distributed load of 0.64 kip/ft. The dynamic load factor is equal to 0.33 of the truck effect, with no dynamic load applied to the uniform loading.

5. FINITE ELEMENT ANALYSIS

The field test results were compared with analytical computations. The analysis was performed using ABAQUS finite element program available at the University of Michigan. Material and other structural parameters are based on the collected information about the bridge supplemented with engineering judgement.

5.1. Types of finite element models for bridges

In the finite element analysis, the geometry of a bridge superstructure can be idealized in many different ways. The following types of models are used:

- Plane grillage model,
- 3-dimensional grillage model,
- 2-dimensional model with shell elements for slab and beam elements for girders,
- 3-dimensional model with shell elements for slab and beam elements for girders,
- 3-dimensional model with shell elements for slab and girders,
- 3-dimensional model with solid elements for slab and shell elements for girders.

For this study, a three-dimensional finite element method (FEM) was applied to investigate the structural behavior of the considered bridges. The concrete slab is modeled using isotropic, eight node solid elements, with three degrees of freedom at each node. The girder flanges and web are modeled using three-dimensional, quadrilateral, four node shell elements with six degrees of freedom at each node (Tarhini and Frederic 1992). The structural effects of the secondary members, such as sidewalk and parapet, are also taken into account in the finite element analysis models.

5.2 Applied Loads

The load was applied in form of two 11-axle, three unit trucks, the same as those used in field tests. The input data included axle loads and axle spacings.

The trucks were positioned as in the field test. The transverse position of the trucks was as measured during the actual test. The longitudinal position of trucks was calculated as the position producing the maximum positive bending moment at midspan, and near supports for the maximum negative bending moment, where the strain transducers were located. Theoretically, the maximum bending moment for simple span bridges does not occur at midspan. However, the difference is very small, usually less than 2 percent. Therefore, the strain transducers were attached at midspan for all tested bridges. Bending moment at the midspan is calculated using influence curves for the bridge span treated as a simply supported beam. The maximum negative bending moment occurs right over the piers. However, the strain concentration right over the supports prevents from accurate strain measurements. Therefore, for the field tests, strain gages were installed on the girder about one and half foot apart from the center of the supports. To compare the test results with FEM analysis, the values from FEM are taken at the same location as the strain gages installed. The strain values obtained from FEM analysis show that the differences between the strains at the girders right over the support and the strain values taken at the girders one and half foot apart from the center of support are usually less than 5 percent.

After determining the truck position on the bridge, concentrated loads are linearly distributed to adjacent nodes based on the location of the load, as shown in Figure 5.1. The detailed descriptions of the bridge models are explained in later chapters.

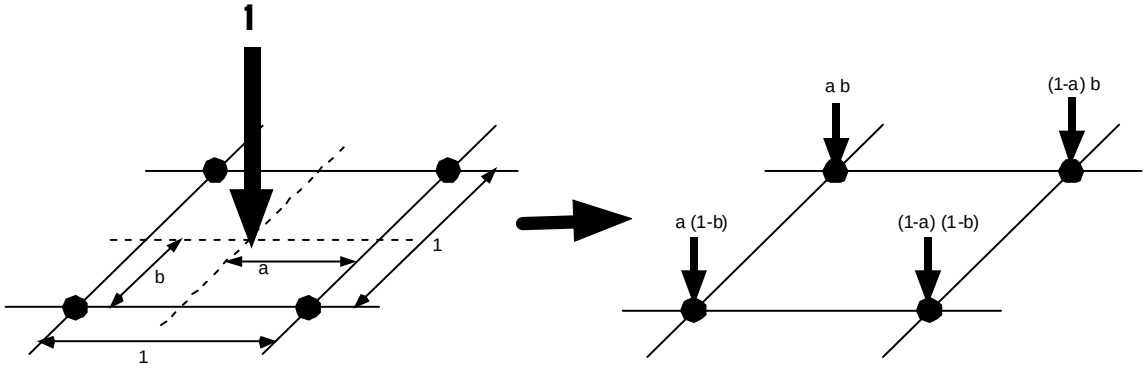

Figure 5.1 Distribution of a concentrated load to adjacent nodes

6. BRIDGE ON BRAIDWOOD ROAD OVER I-69, IN ST.CLAIR COUNTY (S08-77024)

6.1 Bridge Description

This bridge was built in 1982 and it is located on Braidwood Road over I-69 near Emmet in St.Clair County, Michigan. It is a three span, continuous steel girder bridge, designed as a composite section. It has six steel girders spaced at 7 ft 2 in, as shown in Figure 6.1, with 1 degree skew. The total bridge length is 342 ft. The side elevation is shown in Figure 6.2. The bridge has one lane in each direction and it carries an average daily traffic (ADT) of 164. The operating load rating is 264 kips, according to the Michigan Structure Inventory.

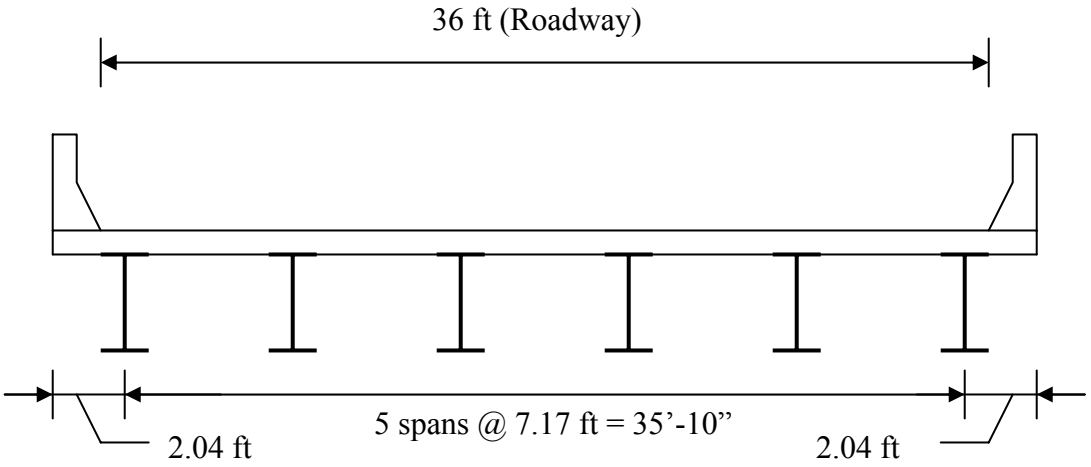

Figure 6.1 Cross Section of the bridge (S08-77024)

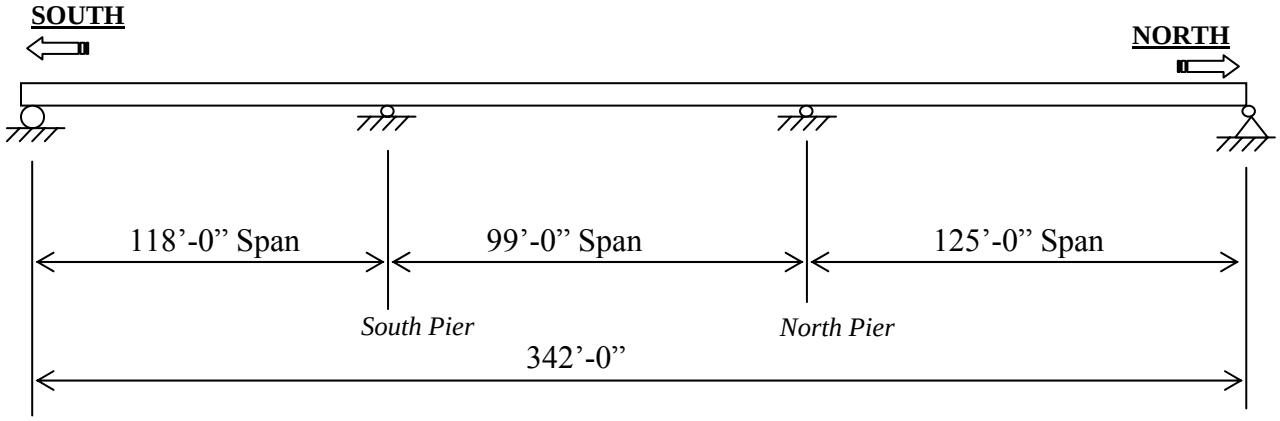

Figure 6.2 Side Elevation of Bridge (S08-77024)

6.2 Instrumentation

Strain transducers were installed on the bottom flanges of girders at midspan and at support locations, as shown in Figure 6.3. The reflector for the PSM-R device from Noptel was installed at the girder No. 3 to measure deflection. The bridge was instrumented on May 14, 2002, and bridge test were performed on May 15, 2002.

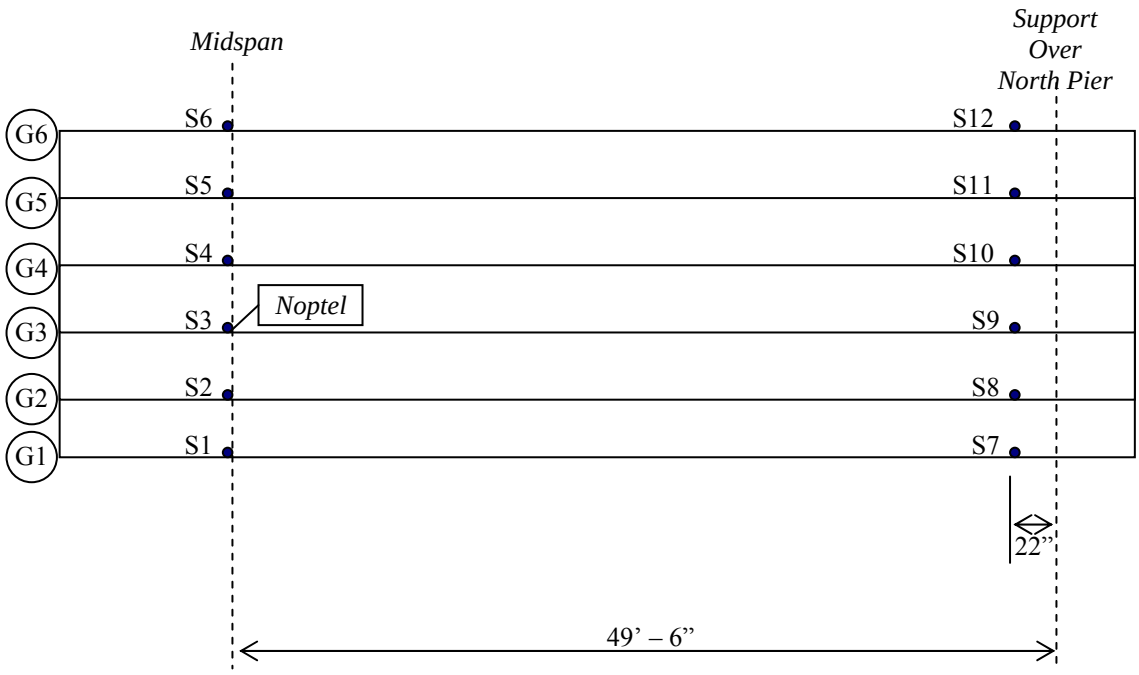

Figure 6.3 Strain Gage Location in Center Span of Bridge (S08-77024)

6.3 Load cases

The girder distribution factors (GDF) and dynamic load factors (DLF) were calculated using the strains measured at midspan and near support. The bridge was loaded with two 11-axle trucks (three-unit vehicles).

The truck A and truck B have gross weights of 146 kips and 145 kips, with wheelbases of 57 ft and 58 ft, respectively. Truck configurations are shown in Figures 6.4 and 6.5.

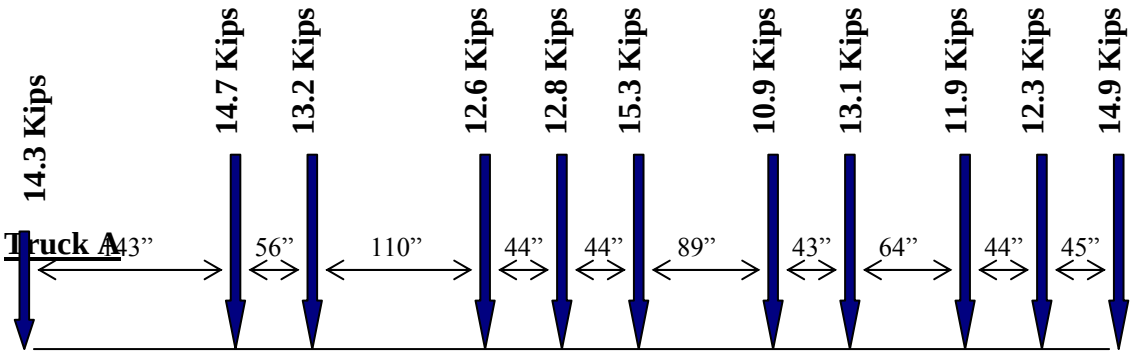

Figure 6.4 Truck A configuration, Bridge (S08-77024)

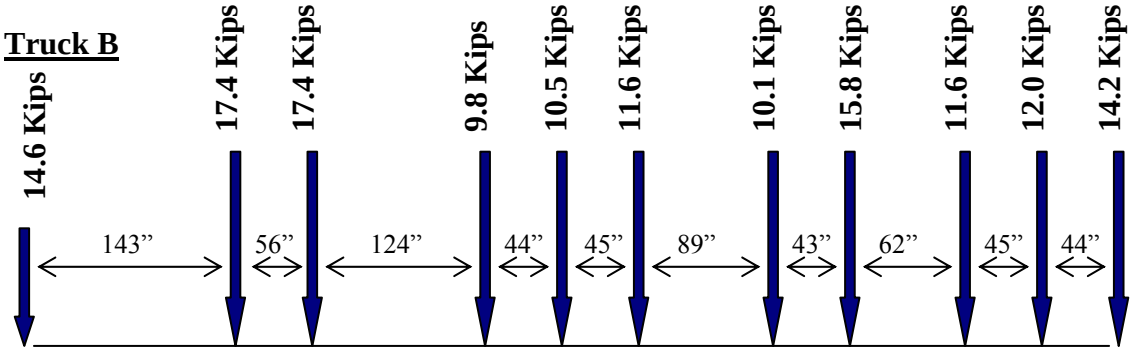

Figure 6.5 Truck B configuration, Bridge (S08-77024)

A total of 24 load cases were considered, as shown in Table 6.1. First each truck was driven by itself at the center of each lane, at crawling speed. Then, the same truck was driven close to the curb. The runs in the center of the lane were repeated at a normal highway speed. In addition, two trucks were driven simultaneously, side-by-side, at crawling speed and normal highway speed. For side-by-side cases, the runs were repeated after the trucks switched lanes, i.e. first truck A was in east lane, and B in west lane, then truck A was in west lane, and B in east lane. Then one truck was driven, followed by the other truck for each lane. In addition, trucks were stopped at predetermined position to verify pre-test calculation.

Table 6.1. Sequence of Test Runs, Bridge (S08-77024)

Run#	Truck	Lane Side	Position	Truck Speed
1	Truck A	East	Center	Crawling
2	Truck B	East	Center	Crawling
3	Truck A	West	Center	Crawling
4	Truck B	West	Center	Crawling
5	Truck A	East	Curb	Crawling
6	Truck B	East	Curb	Crawling
7	Truck A	West	Curb	Crawling
8	Truck B	West	Curb	Crawling
9	Truck A	East	Center	25 MPH
10	Truck B	East	Center	30 MPH
11	Truck A	West	Center	27 MPH
12	Truck B	West	Center	37 MPH
13	Truck A and Bboth	side-by-side	Center	Crawling
14	Truck B and Aboth	side-by-side	Center	Crawling
15	Truck A and Bboth	side-by-side	Center	27 MPH
16	Truck B and Aboth	side-by-side	Center	26 MPH
17	Truck A followed by B	East	Center	Crawling
18	Truck A followed by B	West	Center	Crawling
19	Truck B followed by A	East	Center	Crawling
20	Truck B followed by A	West	Center	Crawling
21	Truck A followed by B	East	Center	Stop at fixed position
22	Truck A followed by B	West	Center	Stop at fixed position
23	Truck B followed by A	East	Center	Stop at fixed position
24	Truck B followed by A	West	Center	Stop at fixed position

6.4 Test results

The resulting strains and GDF's are shown in Figures 6.6 through 6.17. Figures 6.6 to 6.13 present the results for one truck on the bridge under crawling-speed (static) tests. For each loading condition, strains are measured and the corresponding GDF's are calculated from the strain measurement. For comparison, GDF are also calculated according to AASHTO Standard (2002) and AASHTO LRFD Code (1998). The resulting GDF's are shown in Figures 6.6 through 6.13. Figures 6.6 to 6.9 show positive strain values recorded at the midspan of centerspan, and also resulting GDF's. Figures 6.10 to 6.13 present the negative strain values and corresponding GDF's near supports over north pier. For single lane loading, the maximum positive strain is about 120 με. This strain value corresponds about 3.5 ksi. The maximum negative strain near support is less than 100 με. This corresponds about 2.9 ksi. Strain values tend to be higher when the truck is positioned close to curb. In all considered single lane loadings, the measured GDF's do not exceed code specified values.

Figures 6.14 to 6.17 present the results for side-by-side static loading on the bridge under crawling-speed (static) tests. For two trucks side-by-side, strains are measured and the corresponding GDF's are calculated from the strain measurement. For comparison, GDF are also calculated according to code specified values. Figure 6.14 presents the measured positive strains under two trucks side by side, and Figure 6.15 show corresponding GDF's compared with code specified values. For two trucks side by side, the maximum recorded positive strain at the midspan is about 200 με, which corresponds about 5.8 ksi. Figure 6.15 shows that code specified GDF's are conservative. Even the single lane GDF's specifed in AASHTO Standard (2002) is sufficient for two trucks side by side. However, single lane GDF's specified in AASHTO LRFD (1998) is not sufficient for two lane load case in this bridge.

Figures 6.16 and 6.17 present the negative strains under two truck side by side loading measured near support over north pier. Figure 6.16 presents the measured negative strains, and Figure 6.17 shows corresponding GDF's compared with code specified

values. The maximum recorded negative strain near support at the midspan is about 140 με, which corresponds about 4 ksi. Figure 6.17 shows that code specified GDF's are conservative. As in GDF's for positive moments, even the single lane GDF's specifed in AASHTO Standard (2002) is sufficient for two trucks side by side. However, single lane GDF's specified in AASHTO LRFD (1998) is not sufficient for two lane load case in this bridge.

In all cases, the superposition of strains due to a single truck in West and East lanes produces almost the same results as strain due to two trucks side-by-side, as shown in Figures 6.14 and 6.16.

Figures 6.18 and 6.19 present the comparison of GDF's for positive and negative moment obtained from single lane loadings. In all cases, the code specified values are conservative. Particularly, GDF's specified in AASHTO Standard (2002) is very conservative.

Figure 6.20 compares the GDF's for positive and negative moment obtained from side-by-side loading. The figure indicates that code-specified GDF's are conservative for two truck side-by-side loading. For all considered two truck load cases, a single lane GDF specified in AASHTO Standard (2002) is also sufficient for two lane load cases for this bridge. However, a single lane GDF specified in AASHTO LRFD (1998) is not enough for two lane load cases for this bridge.

In Figures 6.21 and 6.22, DLF's are plotted for all load cases involving normal speed (no dynamic load was measured for crawling speed runs). Figure 6.21 shows DLF's measured at the midspan (positive moment), and Figure 6.22 for negative moment (near support). As shown in the figures, dynamic load factors for exterior girders are high because the static strains in these girders are very low. In other words, large values of DLF in exterior girders correspond to load cases with a single truck in the opposite lane (resulting in very low static strain).

The relationship between DLF and static and dynamic strains is shown in Figures 6.23 and 6.24, for positive moment and negative moment, respectively. The open circles correspond to static strain, ε_{stat}, and black solid squares correspond to dynamic strain, ε_{dyn}. For each static strain value (open circle), the corresponding dynamic strain is denoted by solid square (the numbers of circles and squares are same). Dynamic strains remain nearly constant, while static strains increase as truck loading increases. This results in large dynamic load factors for low static strains. DLF corresponding to the maximum strain caused by two trucks side-by-side, is less than 0.05 for the most heavily loaded girder.

Girder No. 4 was instrumented with a remote deflection measurement device manufactured by Noptel. The reflector was installed at midspan. The result is shown in Table 6.2. The maximum deflection recorded during the test is 13.9 mm for girder No. 3 for two side-by-side trucks.

Table 6.2. Maximum deflections measured at the center of Girder No.3, Bridge (S08-77024)

Run #	Vertical Deflection (mm)
1	7.6
2	7.8
3	5.8
4	5.8
5	6
6	6.1
7	3.5
8	3.6
13	13.8
14	13.9

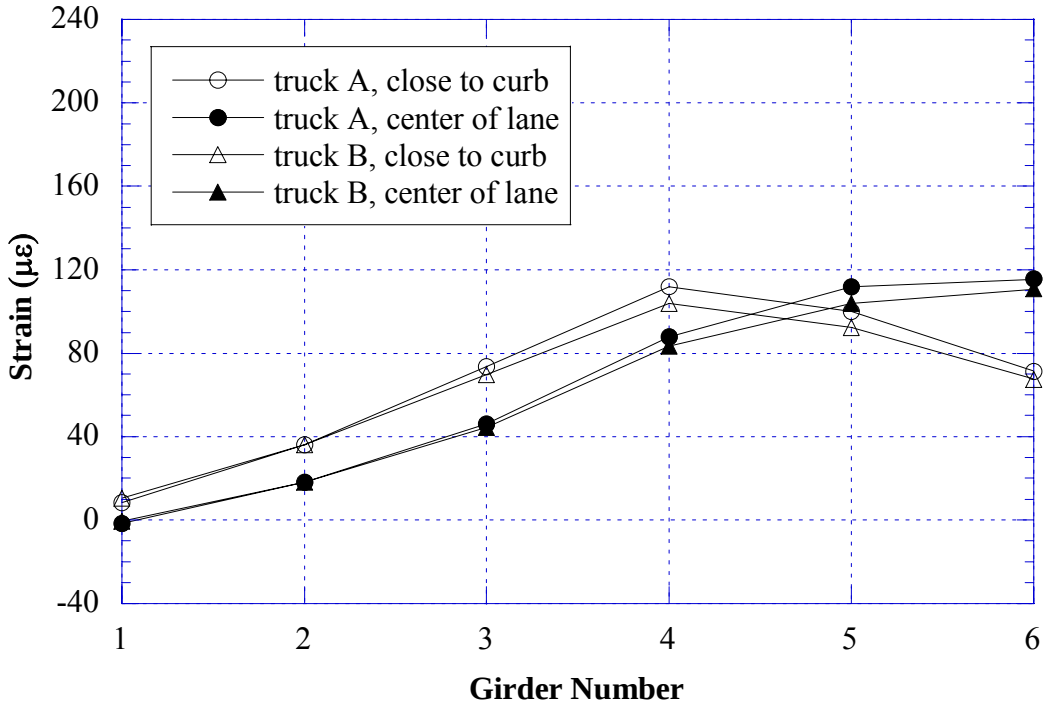

Figure 6.6 Positive Strain at Midspan of Centerspan, West Lane Loading (S08-77024)

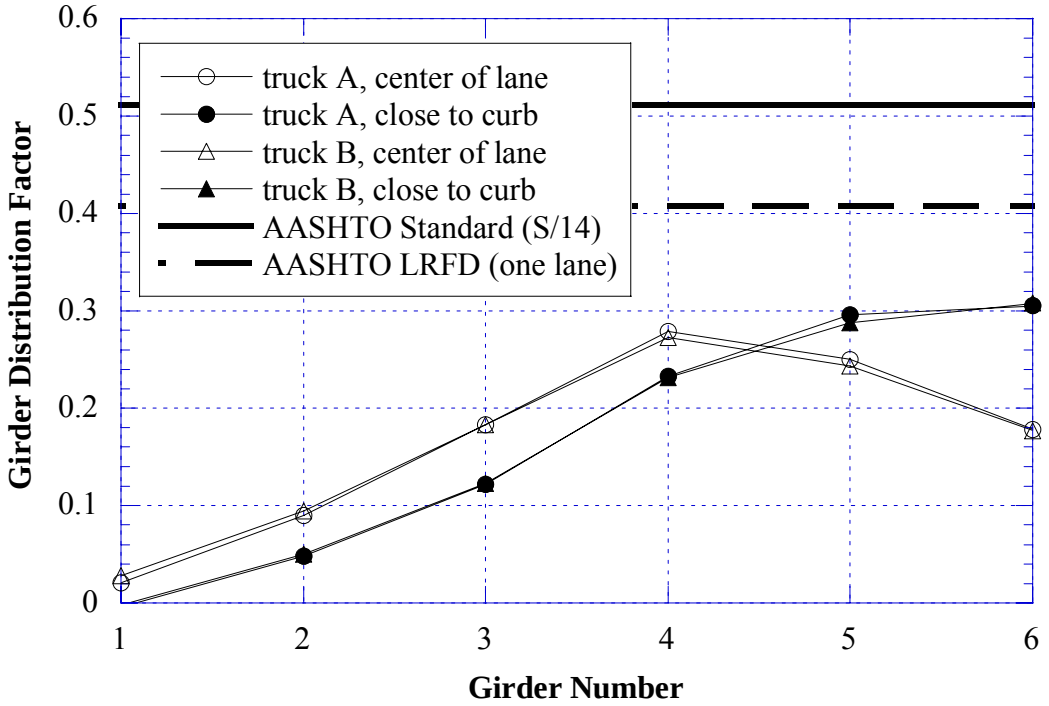

Figure 6.7 GDF from Positive Strain at Midspan of Centerspan, West Lane Loading (S08-77024)

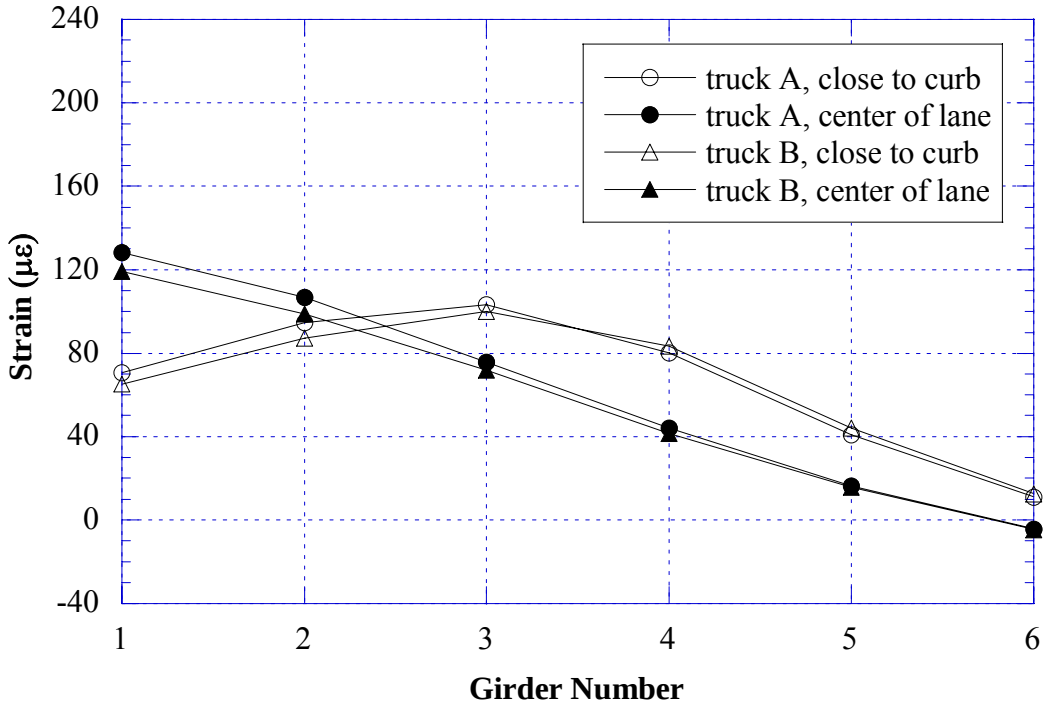

Figure 6.8 Positive Strain at Midspan of Centerspan, East Lane Loading (S08-77024)

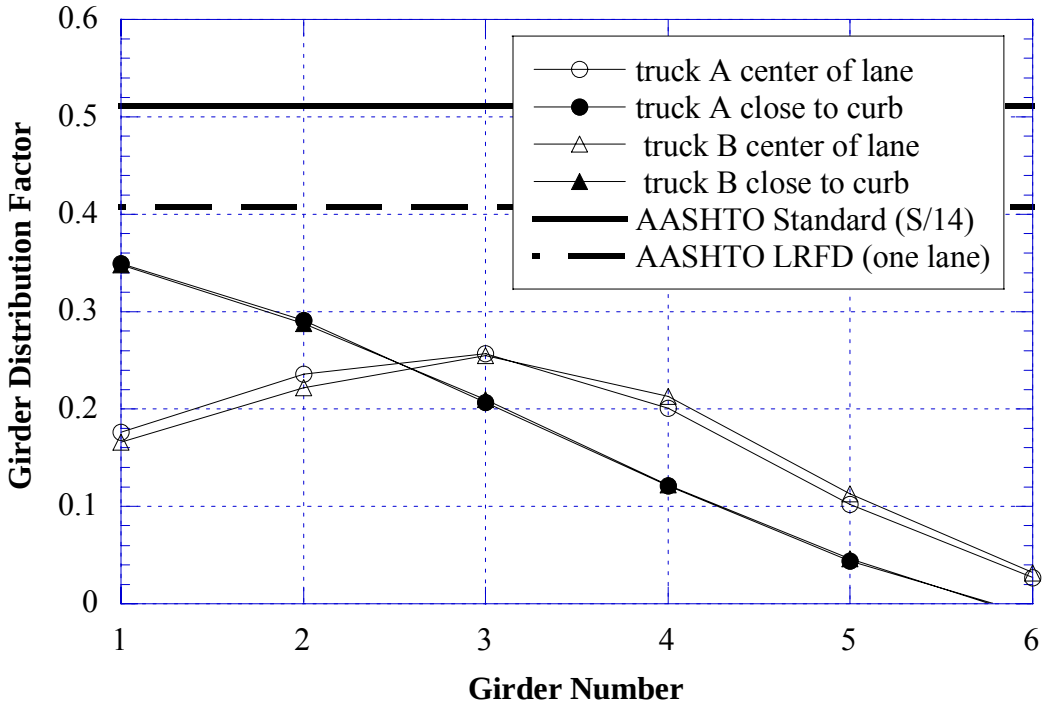

Figure 6.9 GDF from Positive Strain at Midspan of Centerspan, West Lane Loading (S08-77024)

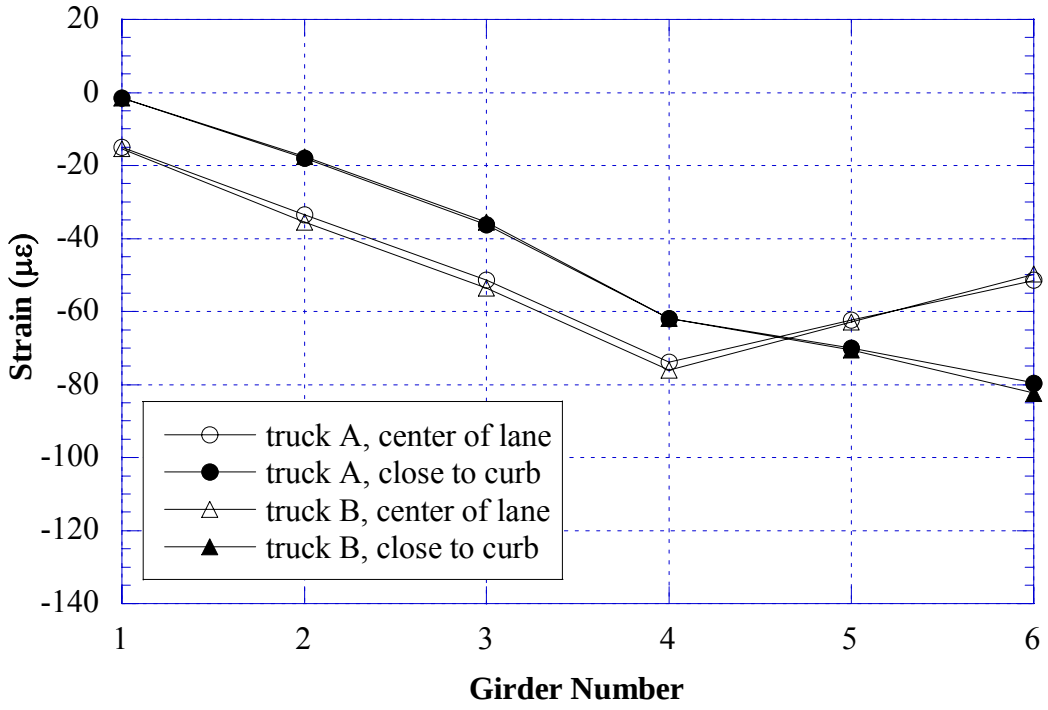

Figure 6.10 Negative Strain near Support over North Pier,
West Lane Loading (S08-77024)

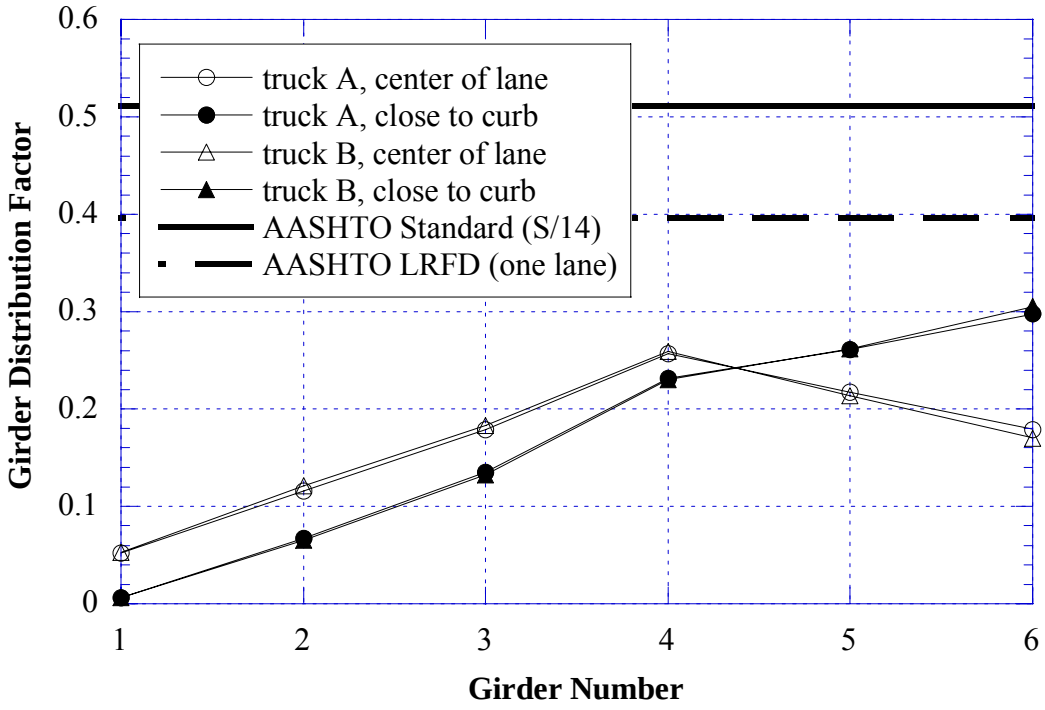

Figure 6.11 GDF from Negative Strain near Support over North Pier,
West Lane Loading (S08-77024)

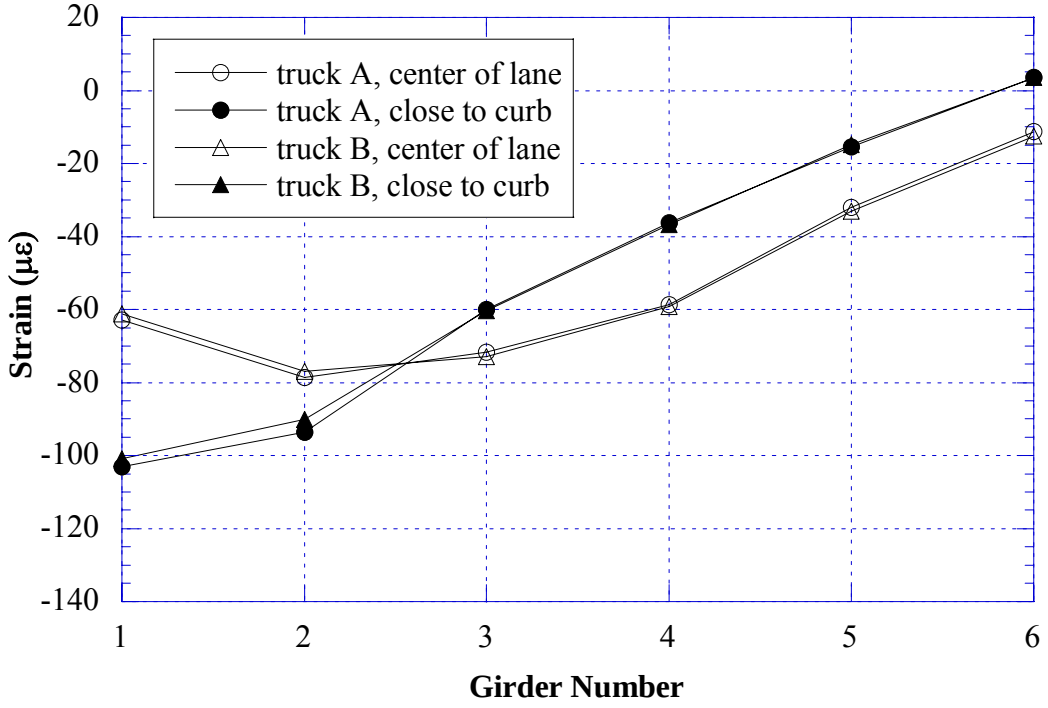

Figure 6.12 Negative Strain near Support over North Pier,
East Lane Loading (S08-77024)

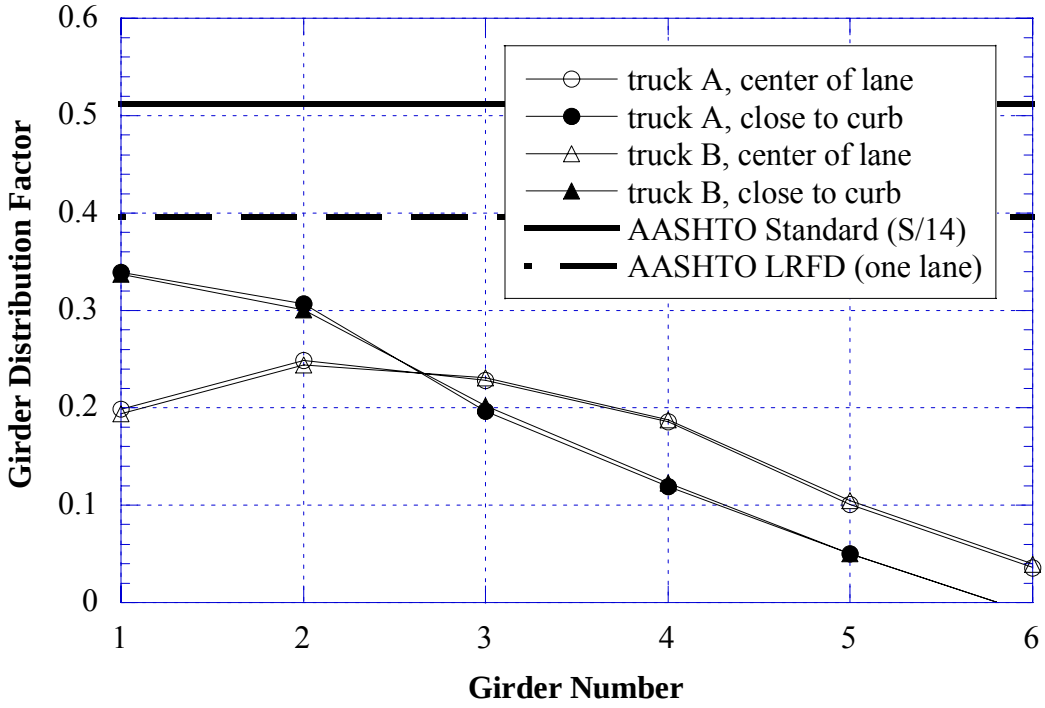

Figure 6.13 GDF from Negative Strain near Support over North Pier,
East Lane Loading (S08-77024)

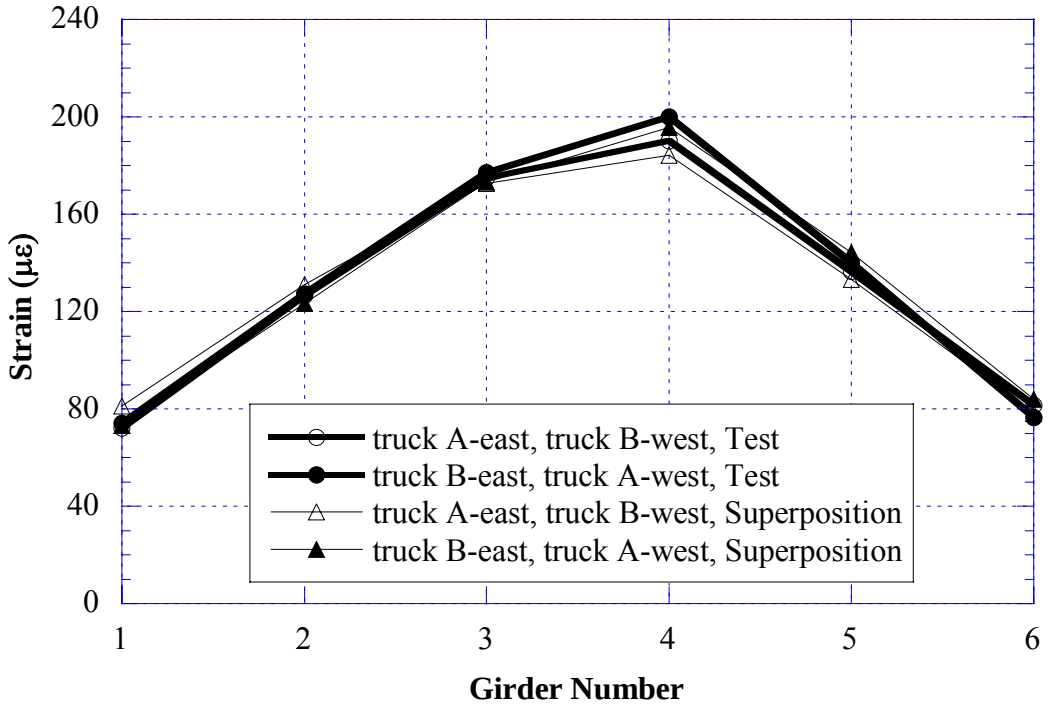

Figure 6.14 Positive Strain at Midspan of Centerspan, Side-by-Side Loading (S08-77024)

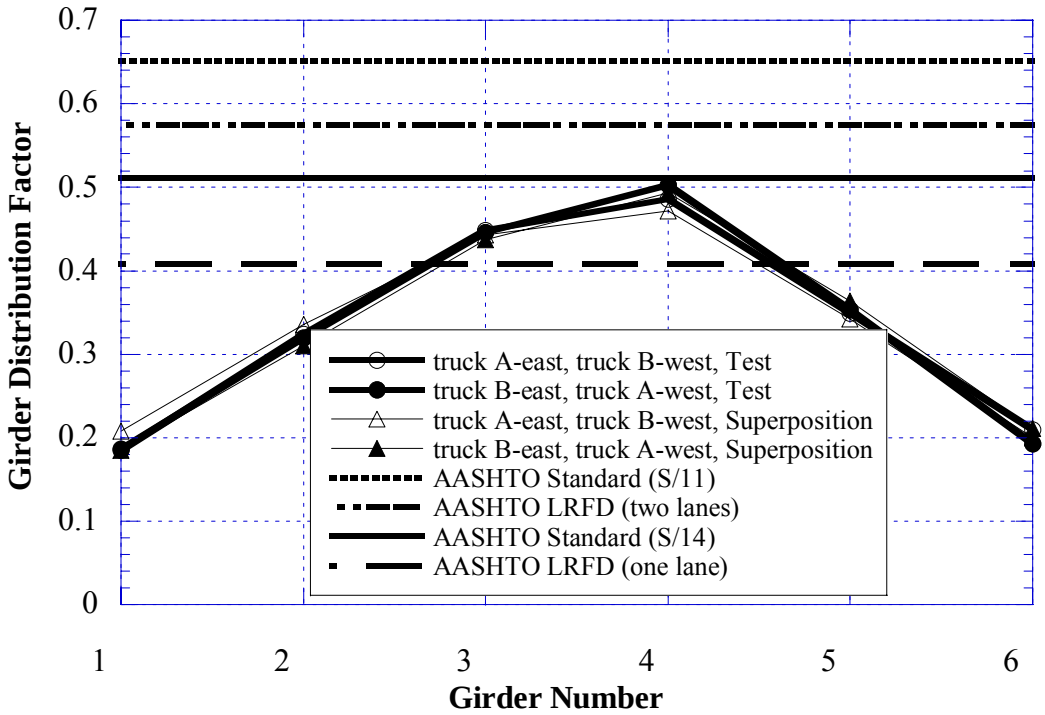

Figure 6.15 GDF from Positive Strain at Midspan of Centerspan, Side-by-Side Loading (S08-77024)

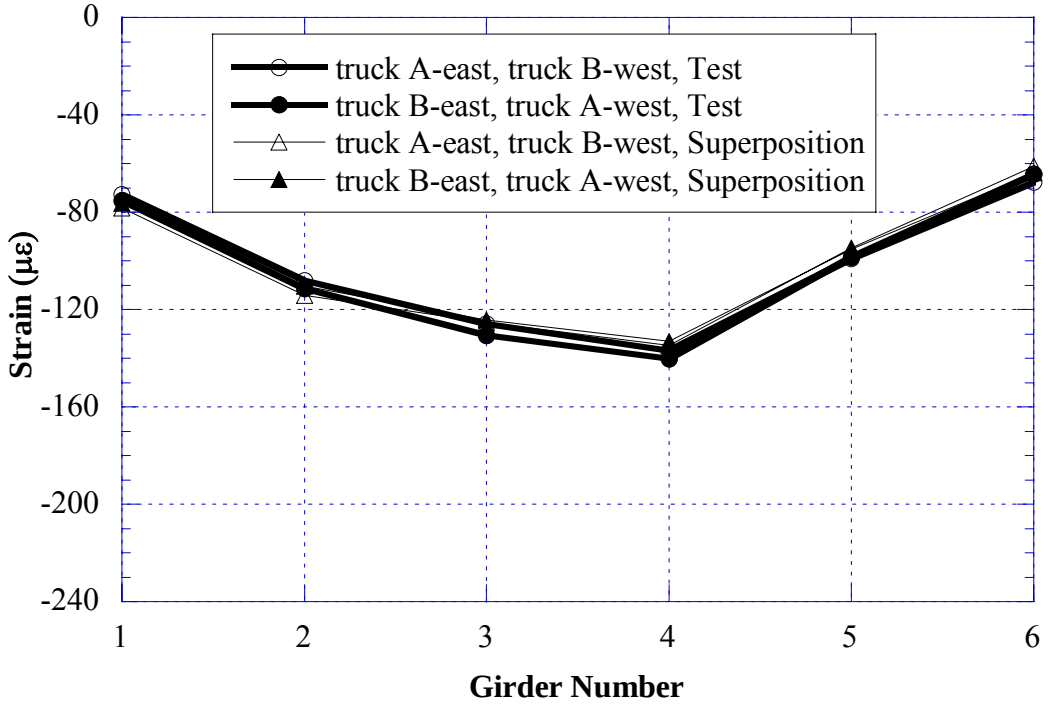

Figure 6.16 Negative Strain near Support over North Pier,
Side-by-Side Loading (S08-77024)

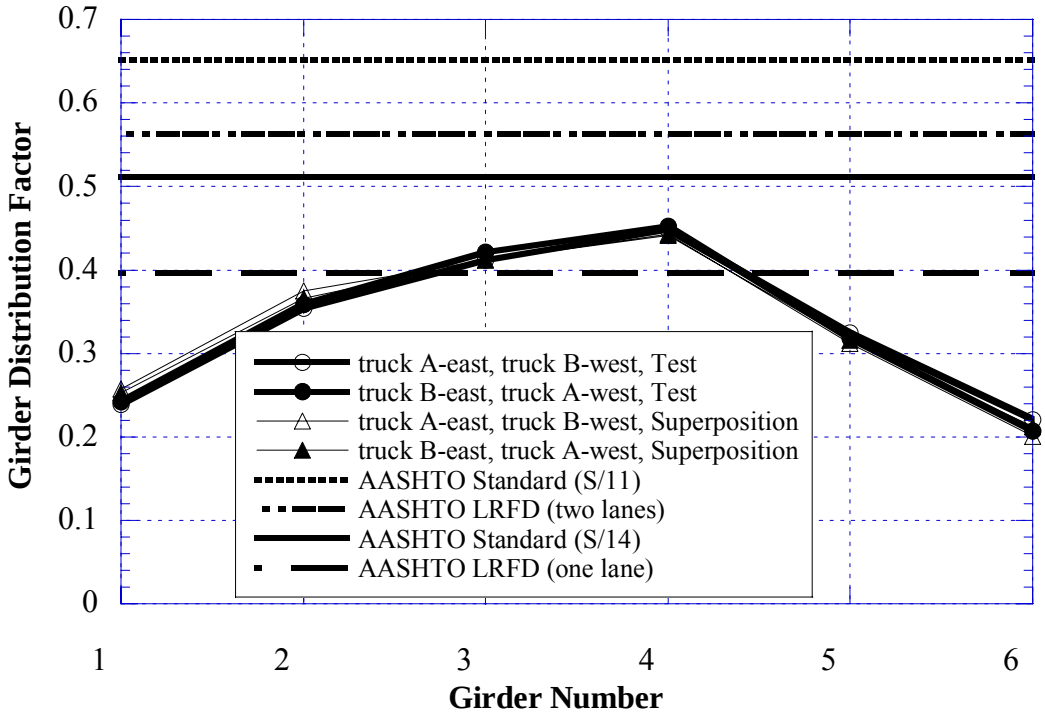

Figure 6.17 GDF from Negative Strain near Support over North Pier,
Side-by-Side Loading (S08-77024)

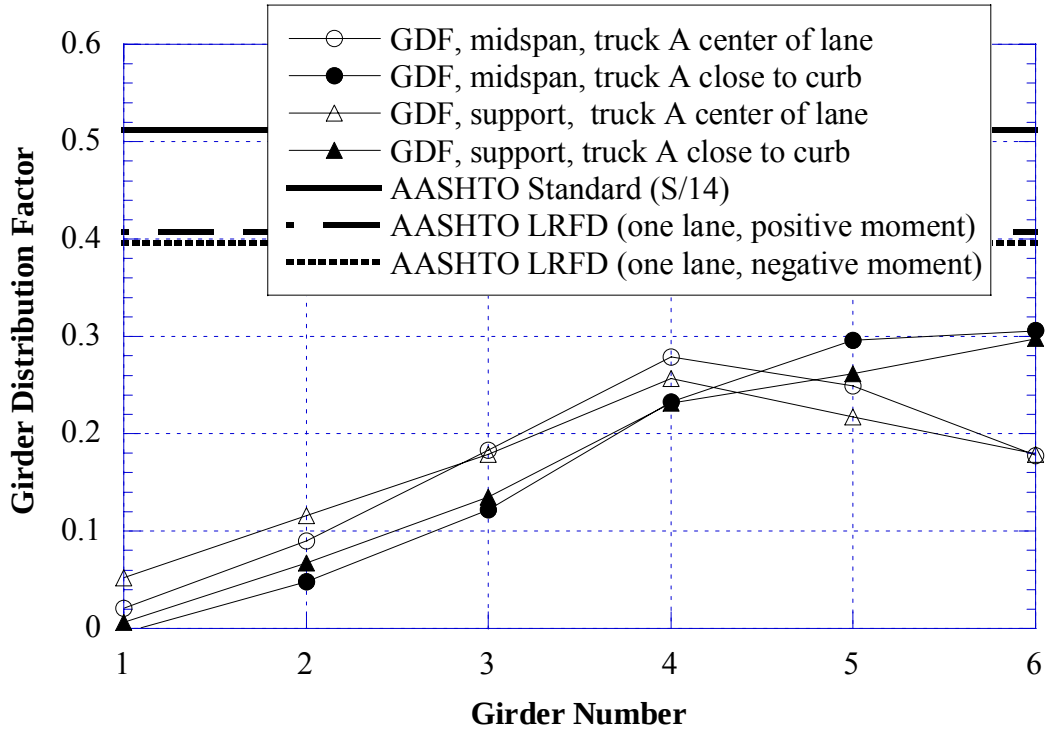

Figure 6.18 Comparison, GDF obtained from Positive Strain vs. GDF from Negative Strain, East Lane Loading, Bridge (S08-77024)

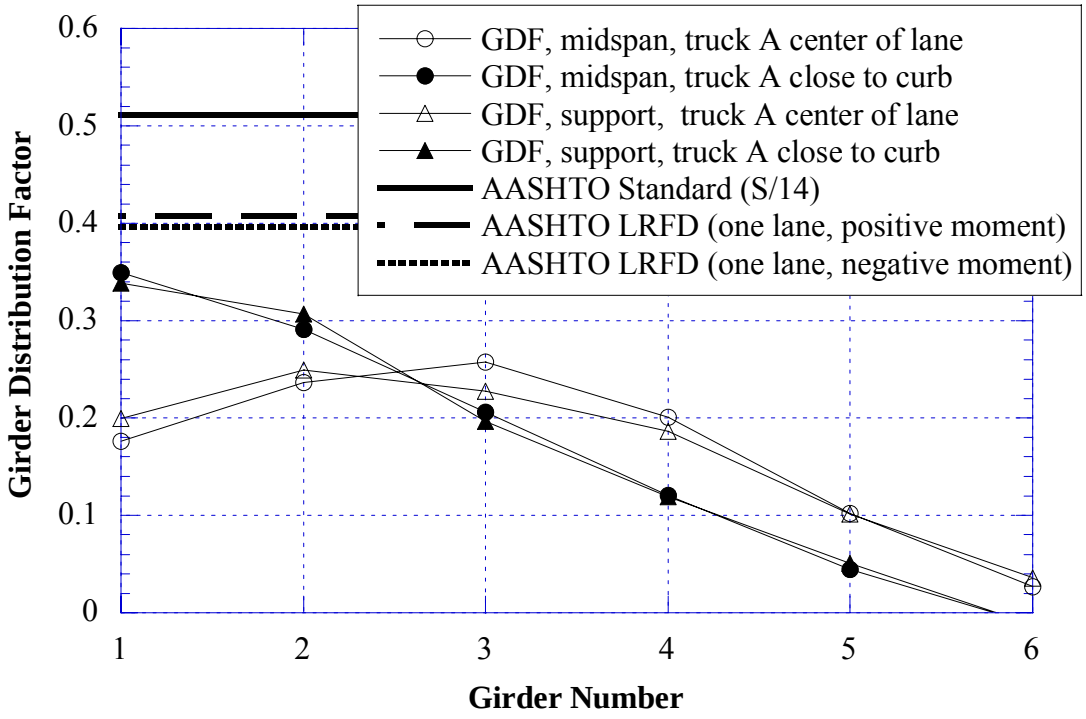

Figure 6.19 Comparison, GDF obtained from Positive Strain vs. GDF from Negative Strain, West Lane Loading, Bridge (S08-77024)

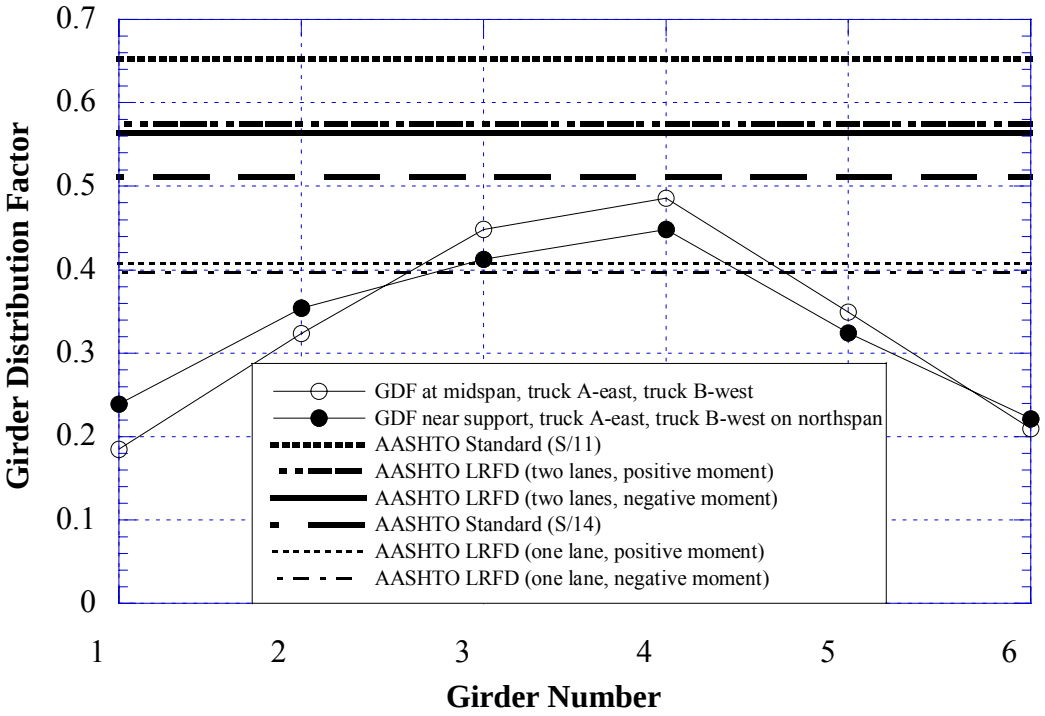

Figure 6.20 Comparison, GDF obtained from Positive Strain vs. GDF from Negative Strain, side-by-side loading, Bridge (S08-77024)

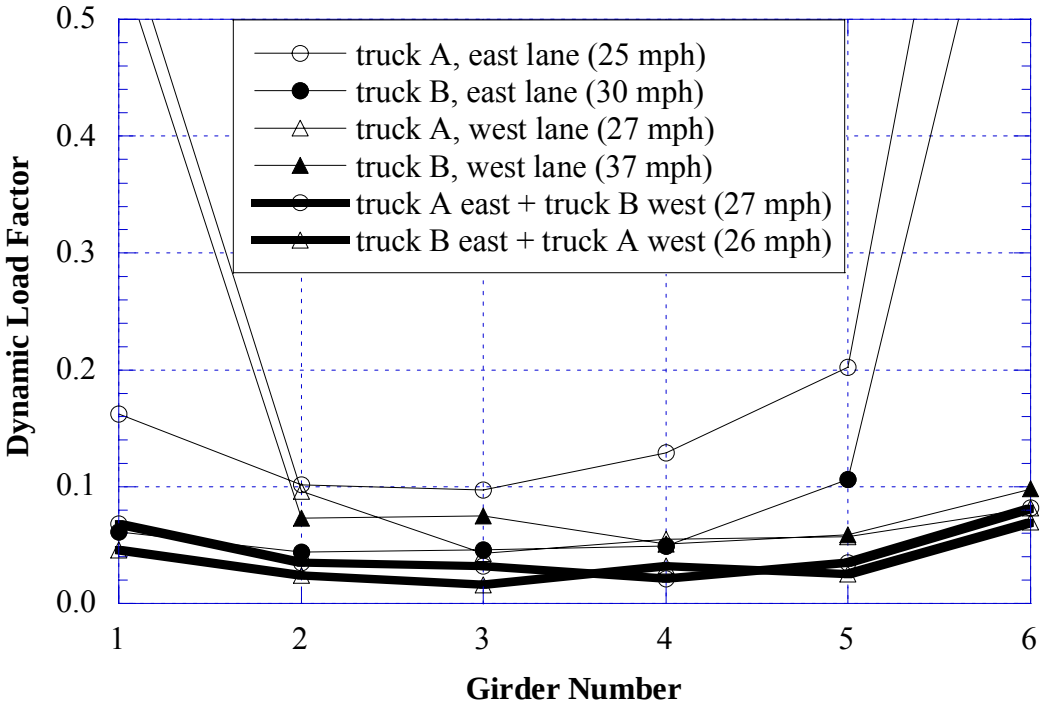

Figure 6.21 Dynamic Load Factors obtained from Positive Strain at Midspan of Centerspan, Bridge (S08-77024)

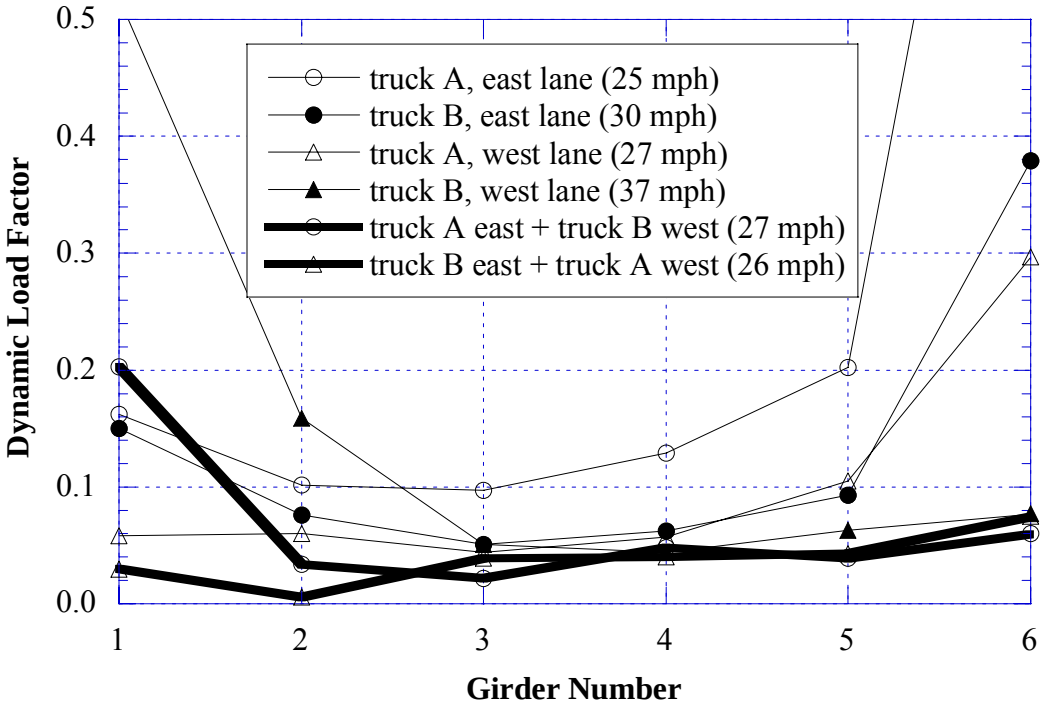

Figure 6.22 Dynamic Load Factors obtained from Negative Strain near Support over North Pier, Bridge (S08-77024)

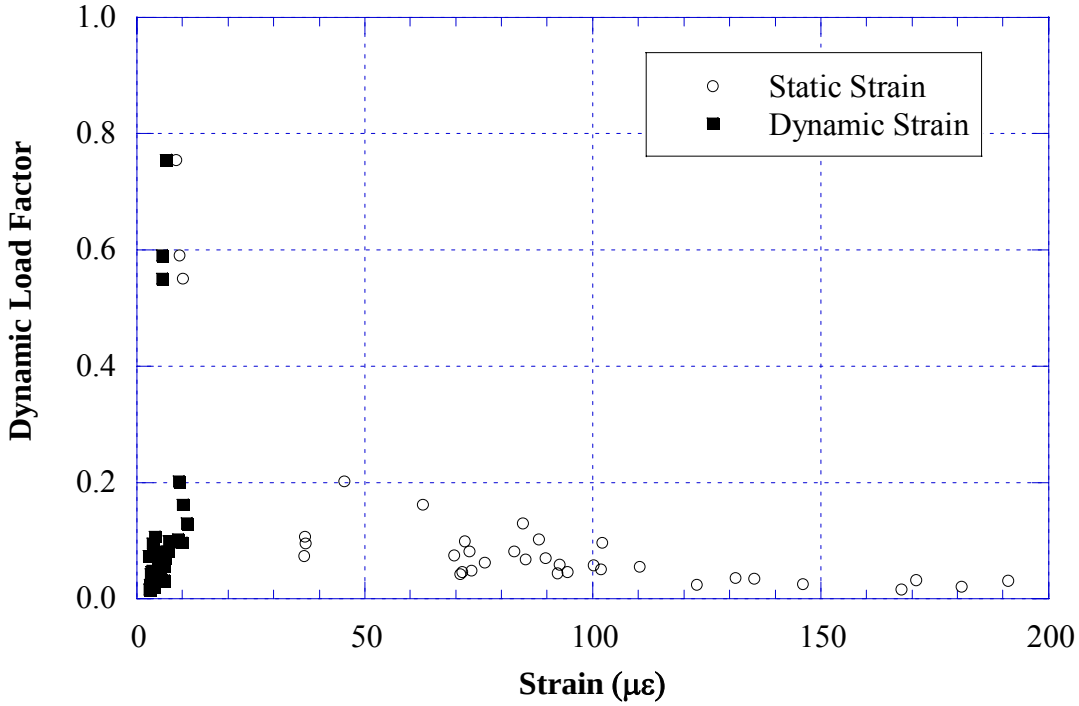

Figure 6.23 Strain vs. Dynamic Load Factors,
Based on Positive Strain at Midspan of Centerspan, Bridge (S08-77024)

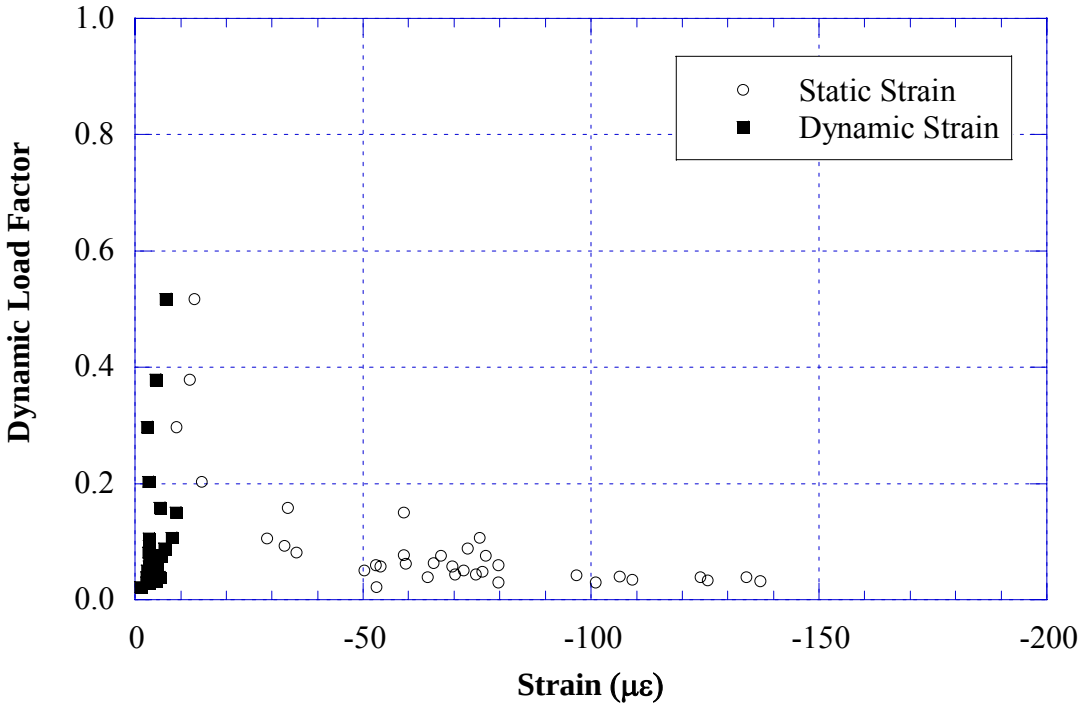

Figure 6.24 Strain vs. Dynamic Load Factors,
Based on Negative Strain near Support over North pier, Bridge (S08-77024)

6.5 Results of Finite Element Analysis

A three-dimensional finite element method (FEM) was applied to investigate the structural behavior of the bridge S08-77024. The concrete slab was modeled with isotropic, eight node solid elements, with three degrees of freedoms at each node. The girder flanges and web were modeled using three-dimensional, quadrilateral, four node shell elements with six degrees of freedom at each node. The structural effects of the secondary members, such as the sidewalk and parapet, were also taken into account in the finite element analysis models.

The mesh of the FEM model is shown in Figure 6.25. Total number of elements is 18,641, and total number of nodes is 24,629 for this model.

Strains and GDF's calculated for the considered model is shown in Figures 6.26 to 6.30. Figures 6.26 and 6.27 present strains and GDF's from FEM model for positive moment at the midspan under two trucks side-by-side loading. Figure 6.28 and 6.29 shows the strains and GDF's from FEM model for negative moment near support over north pier under two trucks side-by-side loading. In the figures, the values obtained from FEM analysis are compared with the corresponding measured values.

The resulting strain values obtained from field tests are lower than those from the finite element analysis for considered bridges. The main reason for low strains is due to the partial fixity of supports. In the previous study for simply supported bridges by University of Michigan (Nowak 2001 and 2002), the boundary conditions are simulated using the elastic spring elements in FEM models. However, for continuous bridges, it is almost impossible to obtain accurate spring coefficients satisfying multiple locations of supports with varied partial fixity condition. Therefore, in the study, the supports are assumed to behave as designed in the FEM models.

Figure 6.30 compares the GDF values for both positive moment and negative moment obtained from FEM analysis. The difference between GDF's for positive moment and negative moments is less than 10 percent.

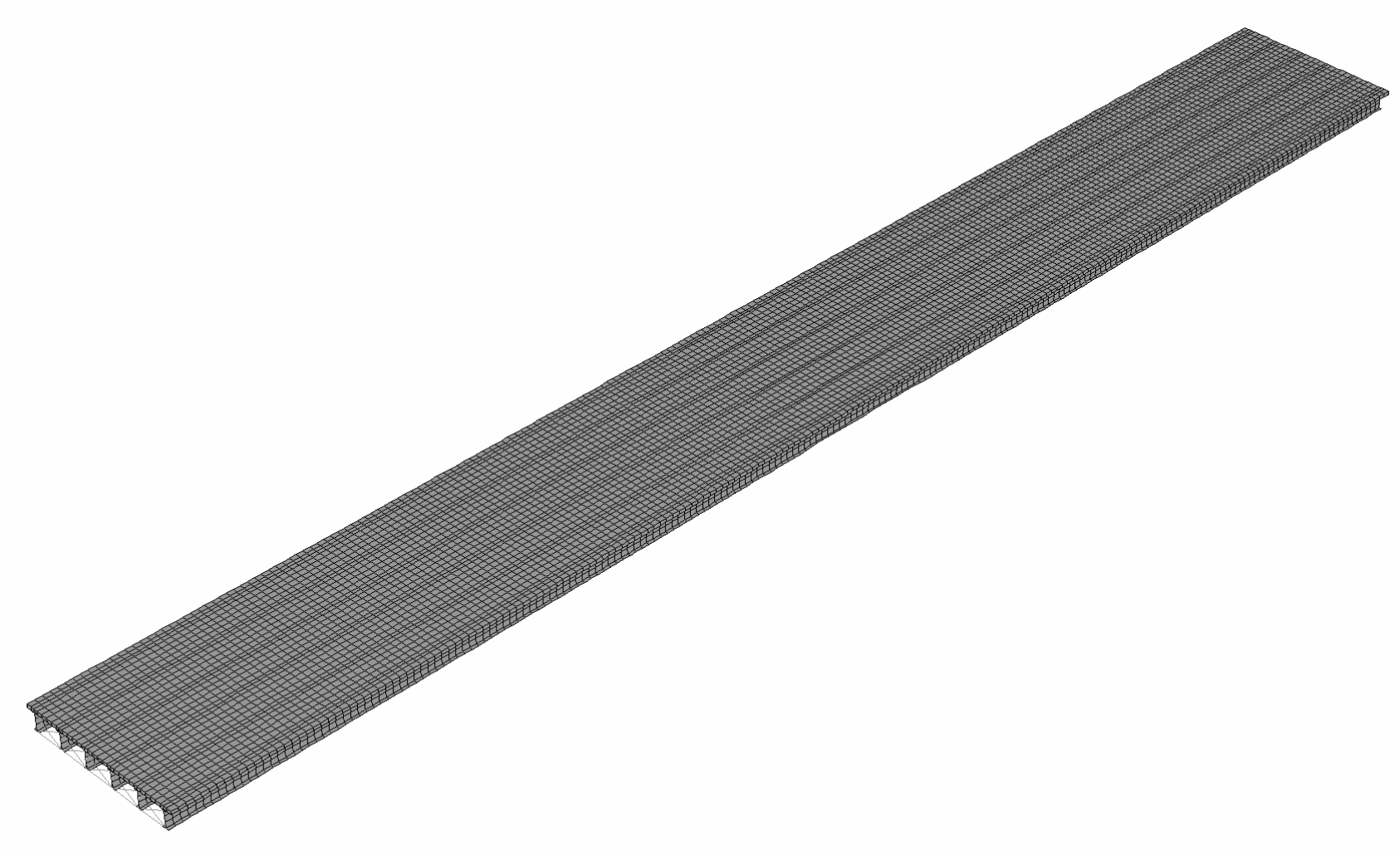

Figure 6.25 The Mesh of Finite Element Model, Bridge (S08-77024)

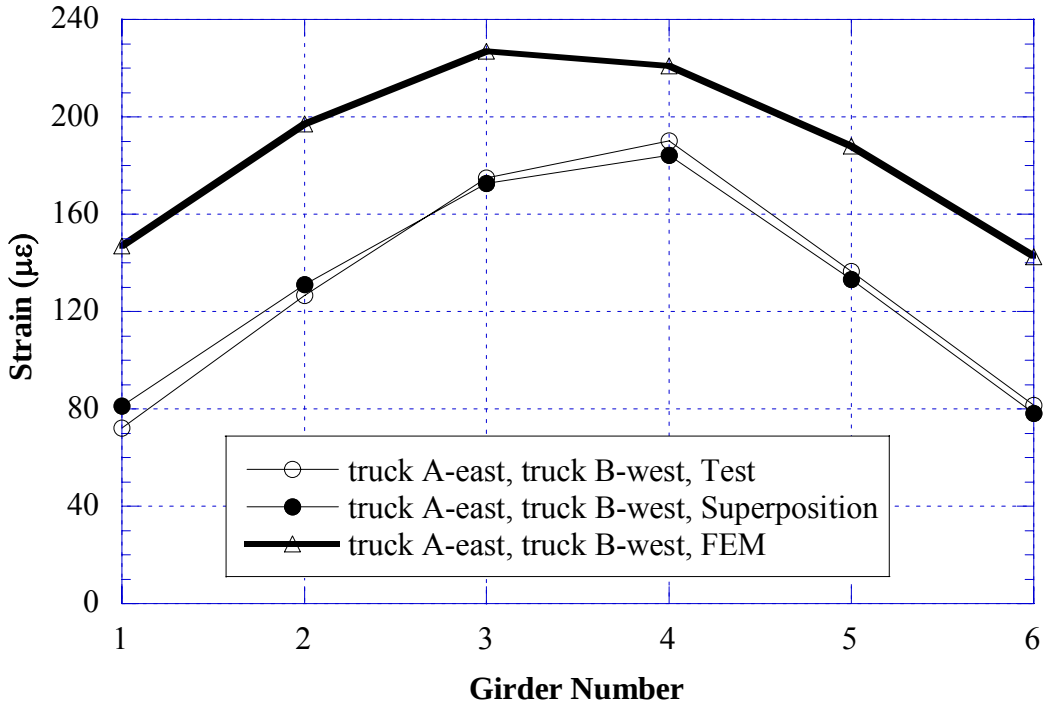

Figure 6.26 Comparison of FEM vs. Test, Positive Strain at Midspan of Centerspan, Side-by-Side Loading, Bridge (S08-77024)

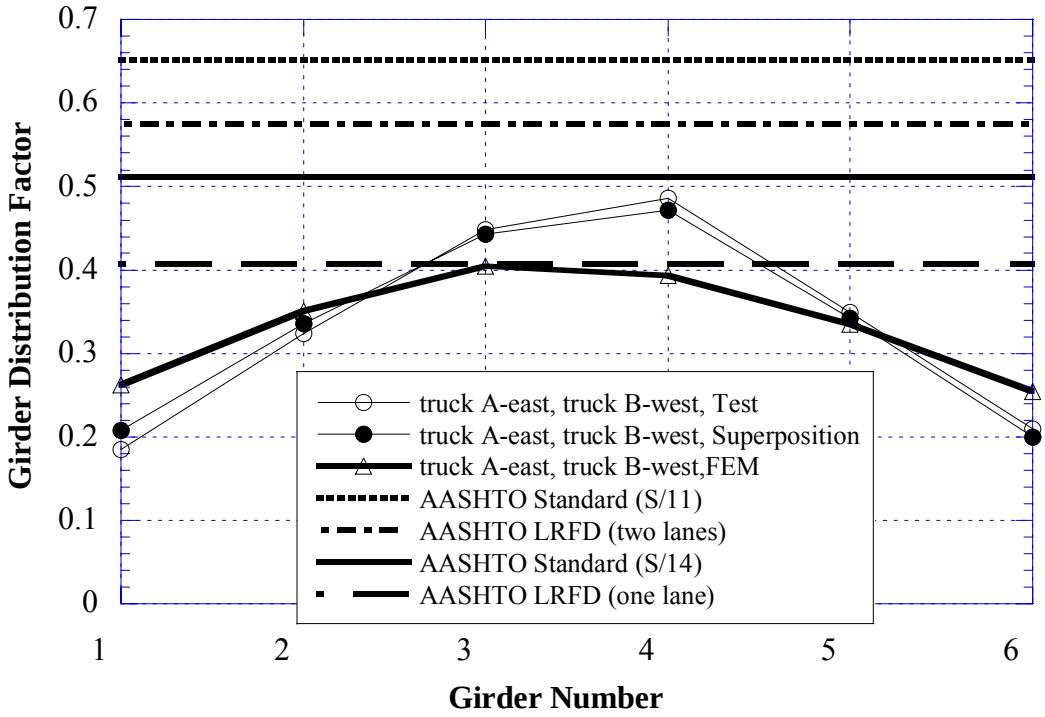

Figure 6.27 Comparison of FEM vs. Test, GDF Obtained from Positive Strain at Midspan of Centerspan, Side-by-Side Loading, Bridge (S08-77024)

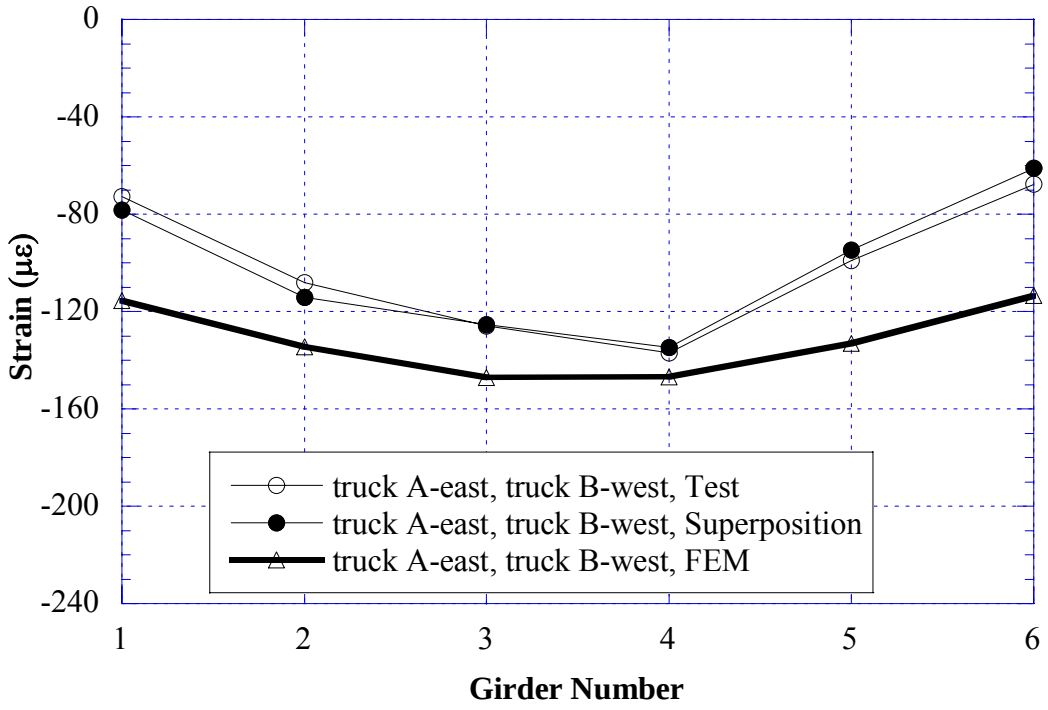

Figure 6.28 Comparison of FEM vs. Test, Negative Strain near Support over North Pier, Side-by-Side Loading, Bridge (S08-77024)

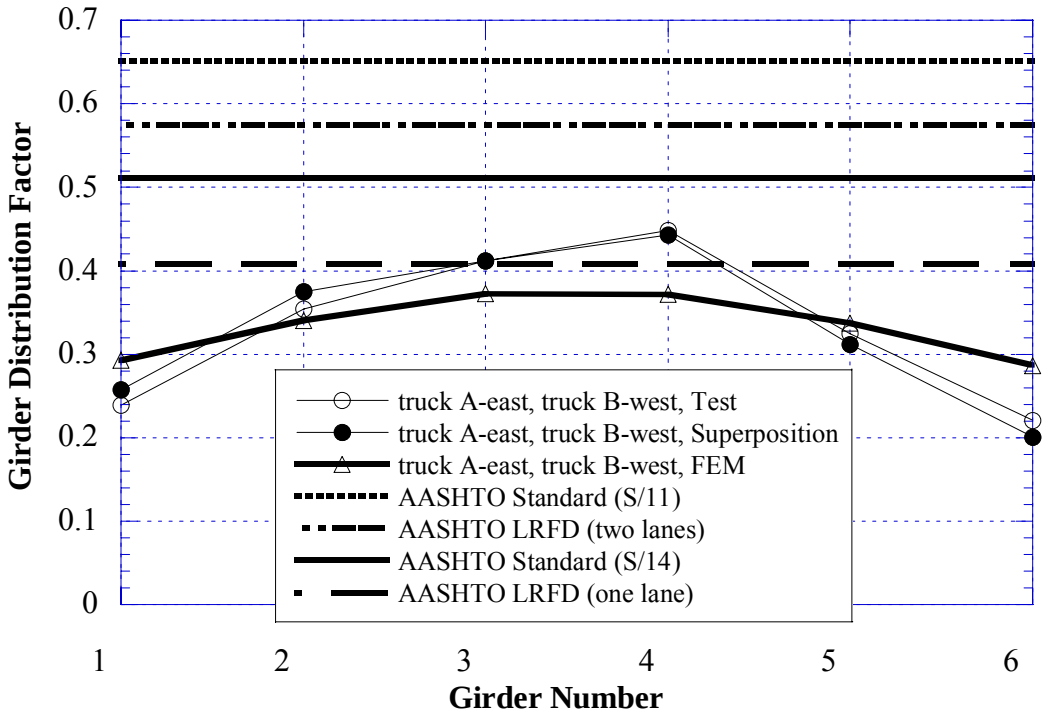

Figure 6.29 Comparison of FEM vs. Test, GDF Obtained From Negative Strain near Support over North Pier, Side-by-Side Loading, Bridge (S08-77024)

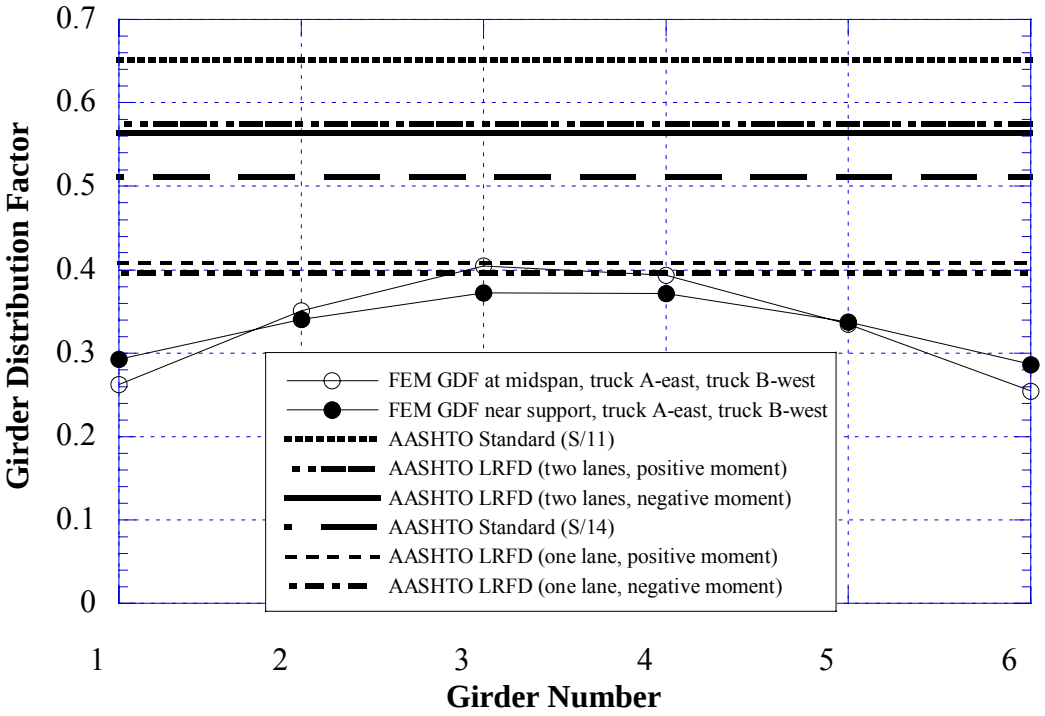

Figure 6.30 Comparison, GDF obtained from positive strain vs. GDF from Negative Strain, Based on Finite Element Analysis, Side-by-Side Loading, Bridge (S08-77024)

Note:

Intentionally left blank

7. BRIDGE ON FIVE LAKES ROAD OVER I-69, IN LAPEER COUNTY (S05-44044)

7.1 Bridge Description

This bridge was built in 1983 and it is located on Five Lakes Road over I-69, 4 miles east of Lapeer in Lapeer County, Michigan. It is a three span, continuous steel girder bridge, designed as a composite section. It has seven steel girders spaced at 6 ft 11 in, as shown in Figure 7.1, with 17 degree skew. The total bridge length is 387 ft. The side elevation is shown in Figure 7.2. The bridge has one lane in each direction and it carries an average daily traffic (ADT) of 315. The operating load rating is 212 kips, according to the Michigan Structure Inventory.

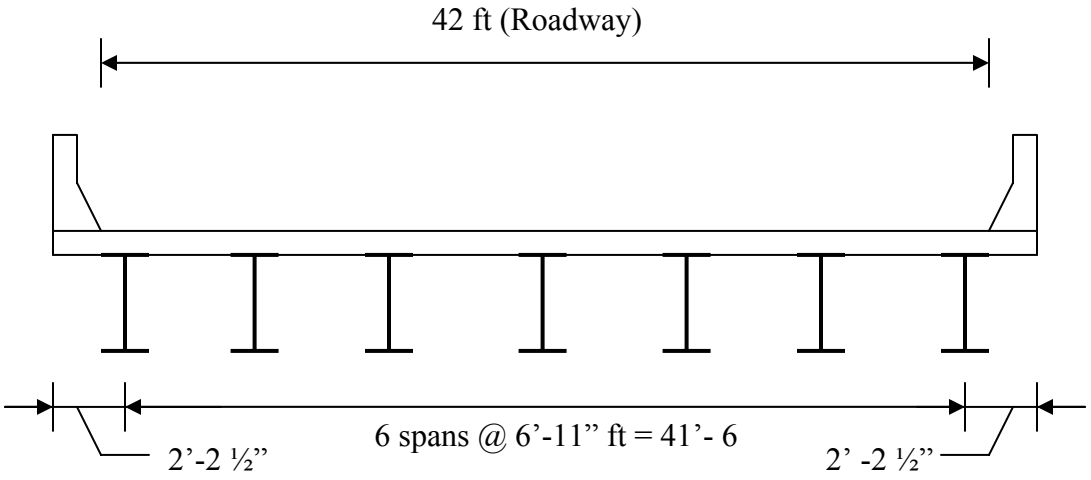

Figure 7.1 Cross Section of the bridge (S05-44044)

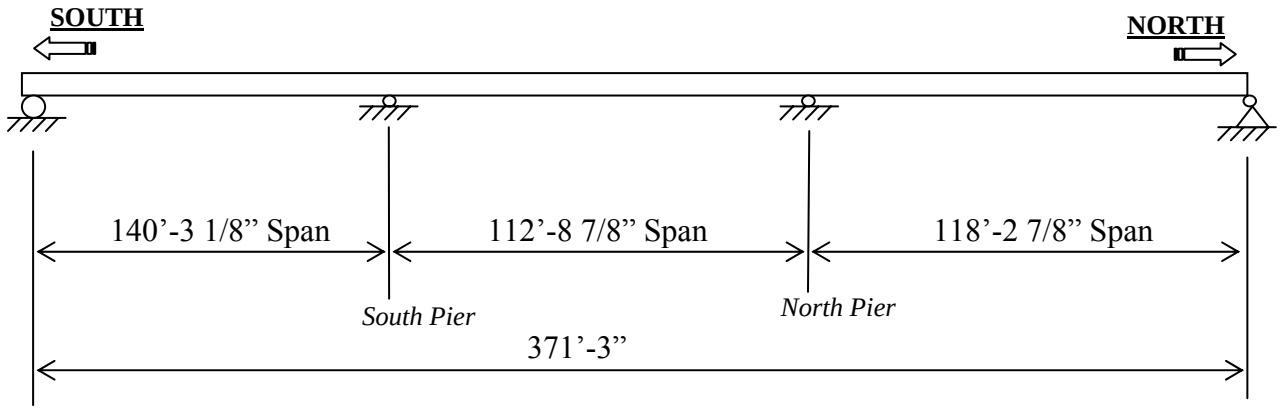

Figure 7.2 Side Elevation of Bridge (S05-44044)

7.2 Instrumentation

Strain transducers were installed on the bottom flanges of girders at midspan and at support locations, as shown in Figure 7.3. The reflector for the PSM-R device from Noptel was installed at the girder No. 4 to measure deflection. The bridge was instrumented on May 28, 2002, and bridge test were performed on May 29, 2002.

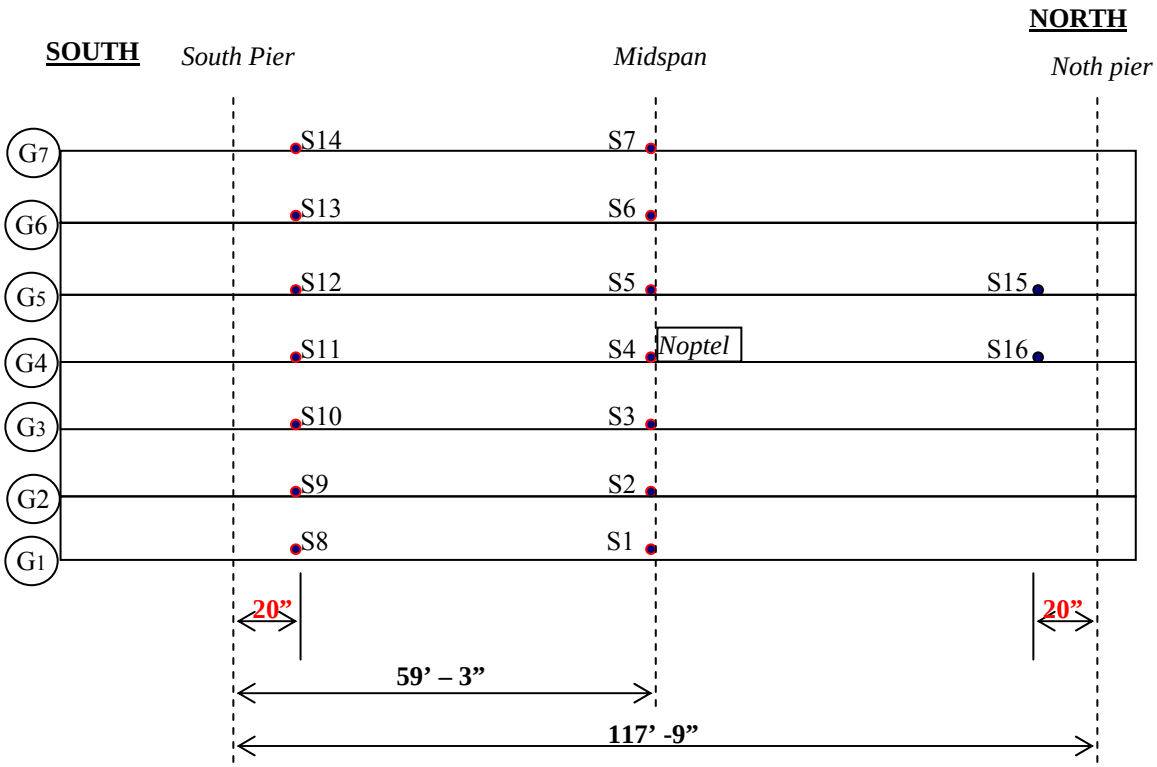

Figure 7.3 Strain Gage Location in Center Span of Bridge (S05-44044)

7.3 Load cases

The girder distribution factors (GDF) and dynamic load factors (DLF) were calculated using the strains measured at midspan. The bridge was loaded with two 11-axle trucks (three-unit vehicles).

The truck A and truck B have gross weights of 144 kips and 141 kips, with wheelbases of 59 ft and 52 ft, respectively. Truck configurations are shown in Figures 7.4 and 7.5.

Truck A

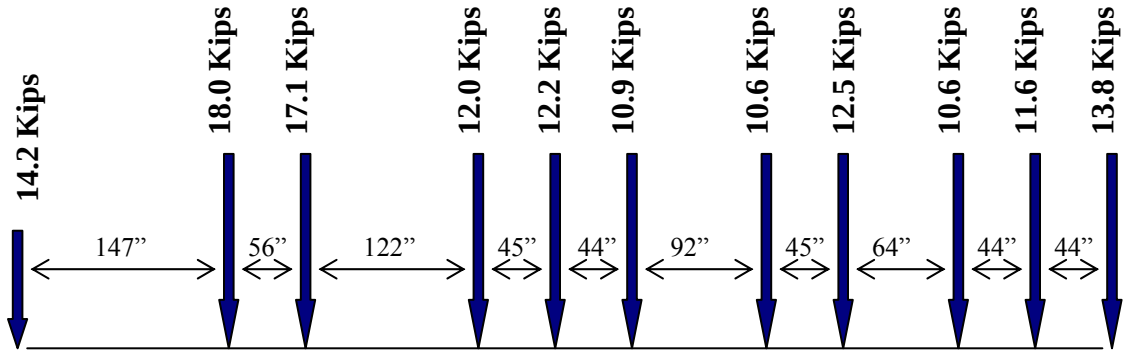

Figure 7.4 Truck A configuration, Bridge (S05-44044)

Truck B

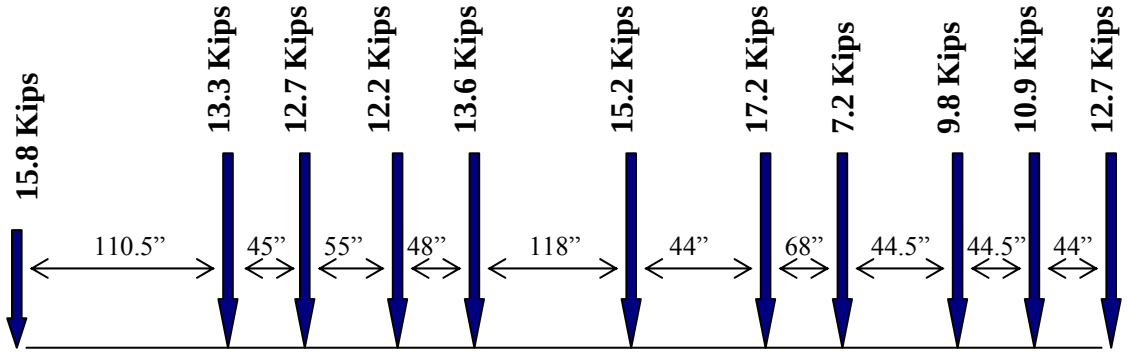

Figure 7.5 Truck B configuration, Bridge (S05-44044)

A total of 24 load cases were considered, as shown in Table 7.1. First each truck was driven by itself at the center of each lane, at crawling speed. Then, the same truck was driven close to the curb. The runs in the center of the lane were repeated at a normal highway speed. In addition, two trucks were driven simultaneously, side-by-side, at crawling speed and normal highway speed. For side-by-side cases, the runs were repeated after the trucks switched lanes, i.e. first truck A was in east lane, and B in west lane, then truck A was in west lane, and B in east lane. Then one truck was driven, followed by the other truck for each lane. In addition, trucks were stopped at predetermined position to verify the pre-test calculation.

Table 7.1. Sequence of Test Runs, Bridge (S05-44044)

Run#	Truck	Lane Side	Position	Truck Speed
1	Truck A	East	Center	Crawling
2	Truck B	East	Center	Crawling
3	Truck A	West	Center	Crawling
4	Truck B	West	Center	Crawling
5	Truck A	East	Curb	Crawling
6	Truck B	East	Curb	Crawling
7	Truck A	West	Curb	Crawling
8	Truck B	West	Curb	Crawling
9	Truck A	East	Center	25 MPH
10	Truck B	East	Center	27 MPH
11	Truck A	West	Center	32 MPH
12	Truck B	West	Center	30 MPH
13	Truck A and Bboth	side-by-side	Center	Crawling
14	Truck B and Aboth	side-by-side	Center	Crawling
15	Truck A and Bboth	side-by-side	Center	28 MPH
16	Truck B and Aboth	side-by-side	Center	30 MPH
17	Truck A followed by B	East	Center	Crawling
18	Truck A followed by B	West	Center	Crawling
19	Truck B followed by A	East	Center	Crawling
20	Truck B followed by A	West	Center	Crawling
21	Truck A followed by B	East	Center	Stop at fixed position
22	Truck A followed by B	West	Center	Stop at fixed position
23	Truck B followed by A	East	Center	Stop at fixed position
24	Truck B followed by A	West	Center	Stop at fixed position

7.4 Test results

The resulting strains and GDF's are shown in Figures 7.6 through 7.17. Figures 7.6 to 7.13 present the results for one truck on the bridge under crawling-speed (static) tests. For each loading condition, strains are measured and the corresponding GDF's are calculated from the strain measurement. For comparison, GDF are also calculated according to AASHTO Standard (2002) and AASHTO LRFD Code (1998). The resulting GDF's are shown in Figures 7.6 through 7.13. Figures 7.6 to 7.9 show positive strain values recorded at the midspan of centerspan, and also resulting GDF's. Figures 7.10 to 7.13 present the negative strain values and corresponding GDF's near supports over south pier. For single lane loading, the maximum positive strain is about 160 με. This strain value corresponds about 4.6 ksi. The maximum negative strain near support is less than 120 με. This corresponds about 3.5 ksi. Strain values tend to be higher when the truck is positioned close to curb. For single lane loadings on the center of lanes, the measured GDF's do not exceed code specified values. However, when the truck is very close to curb, GDF's can exceed the specified values in AASHTO LRFD (1998) for single lane loading. Still, GDF specified in AASHTO Standard (2002) is conservative in all considered cases.

Figures 7.14 to 7.17 present the results for side-by-side static loading on the bridge under crawling-speed (static) tests. For two trucks side-by-side, strains are measured and the corresponding GDF's are calculated from the strain measurement. For comparison, GDF are also calculated according to code specified values. Figure 7.14 presents the measured positive strains under two trucks side by side, and Figure 7.15 shows corresponding GDF's compared with code specified values. For two trucks side by side, the maximum recorded positive strain at the midspan is about 110 με, which corresponds about 3.2 ksi. Figure 7.15 shows that code specified GDF's are conservative. Even the single lane GDF's specifed in AASHTO Standard (2002) and AASHTO LRFD (1998) is sufficient for two trucks side-by-side.

Figures 7.16 and 7.17 present the negative strains under two truck side by side loading measured near support over south pier. Figure 7.16 presents the measured negative strains, and Figure 7.17 shows corresponding GDF's compared with code specified values. The maximum recorded negative strain near supportat the midspan is about 120 με, which corresponds about 3.5 ksi. Figure 7.17 shows that code specified GDF's are conservative. As in GDF's for positive moments, even the single lane GDF's specifed in AASHTO Standard (2002) is sufficient for two trucks side by side. However, single lane GDF's specified in AASHTO LRFD (1998) is not sufficient for two lane load case in this bridge.

In all cases, the superposition of strains due to a single truck in West and East lanes produces almost the same results as strain due to two trucks side-by-side, as shown in Figures 7.14 and 7.16.

Figures 7.18 and 7.19 present the comparison of GDF's for positive and negative moment obtained from single lane loadings. The code specified values are conservative. However, if the truck is very close to curb, the measured GDF's can exceed the GDF's specified in AASHTO LRFD (1998).

Figure 7.20 compares the GDF's for positive and negative moment obtained from side-by-side loading. The figure indicates that code-specified GDF's are conservative for two truck side-by-side loading. For all considered two truck load cases, a single lane GDF specified in AASHTO Standard (2002) is also sufficient for two lane load cases for this bridge. However, a single lane GDF specified in AASHTO LRFD (1998) is not enough for two lane load cases for this bridge.

In Figures 7.21 and 7.22, DLF's are plotted for all load cases involving normal speed (no dynamic load was measured for crawling speed runs). Figure 7.21 shows DLF's measured at the midspan (positive moment), and Figure 7.22 for negative moment (near support). As shown in the figures, dynamic load factors for exterior girders are high because the static strains in these girders are very low. In other words, large values of

DLF in exterior girders correspond to load cases with a single truck in the opposite lane (resulting in very low static strain).

The relationship between DLF and static and dynamic strains is shown in Figures 7.22 and 7.23, for positive moment and negative moment, respectively. The open circles correspond to static strain, ε_{stat}, and black solid squares correspond to dynamic strain, ε_{dyn}. For each static strain value (open circle), the corresponding dynamic strain is denoted by solid square (the numbers of circles and squares are same). Dynamic strains remain nearly constant, while static strains increase as truck loading increases. This results in large dynamic load factors for low static strains. DLF corresponding to the maximum strain caused by two trucks side-by-side, is less than 0.10 for the most heavily loaded girder.

Girder No. 4 was instrumented with a remote deflection measurement device manufactured by Noptel. The reflector was installed at midspan. The result is shown in Table 7.2. The maximum deflection recorded during the test is 19.9 mm for girder No. 4 for two side-by-side trucks.

Table 7.2. Maximum deflections measured at the center of Girder No.4, Bridge (S05-44044)

Run #	Vertical Deflection (mm)
1	9.7
2	9.6
3	8.9
4	8.8
5	5.4
6	5.9
7	4.1
8	4.2
13	19.7
14	19.9

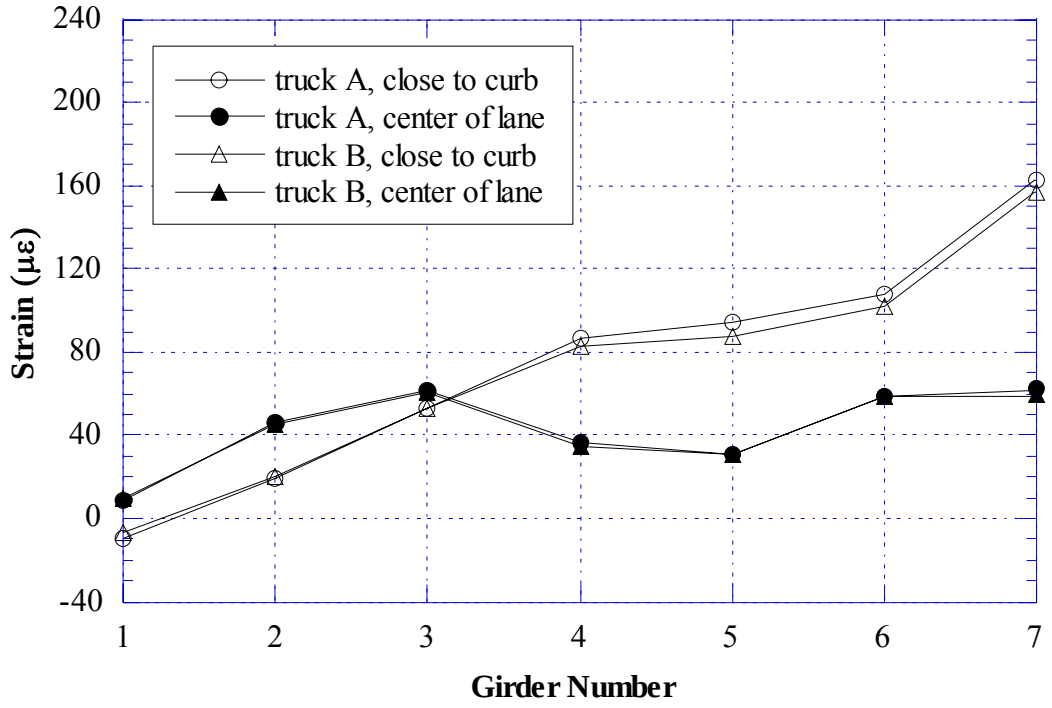

Figure 7.6 Positive Strain at Midspan of Centerspan, West Lane Loading (S05-44044)

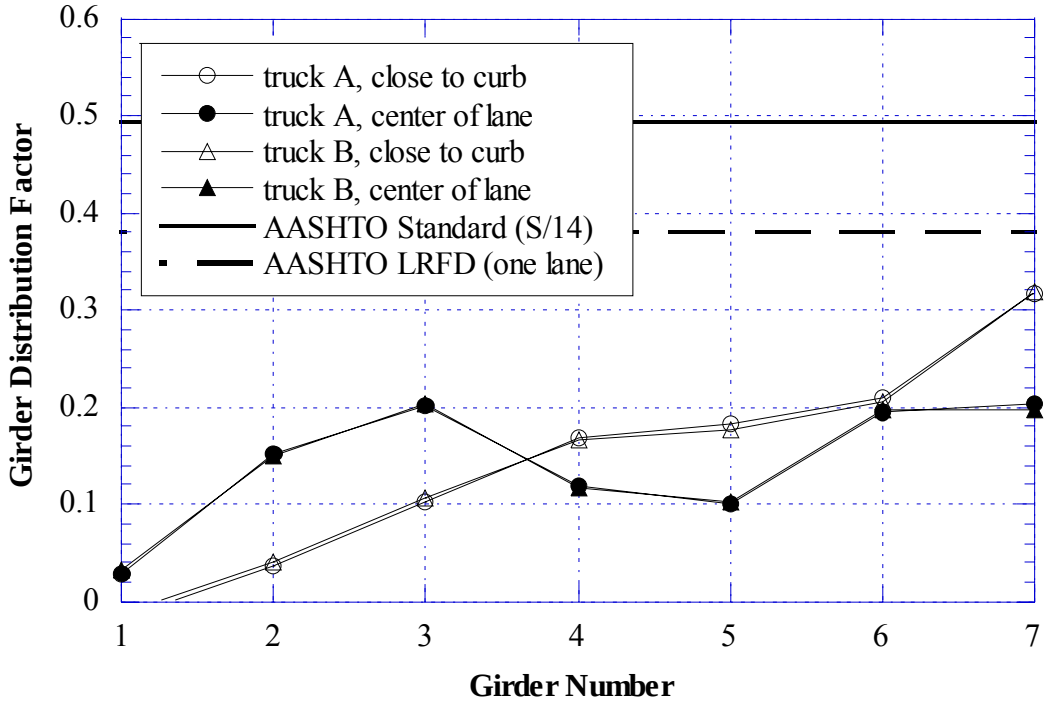

Figure 7.7 GDF from Positive Strain at Midspan of Centerspan, West Lane Loading (S05-44044)

Figure 7.8 Positive Strain at Midspan of Centerspan, East Lane Loading (S05-44044)

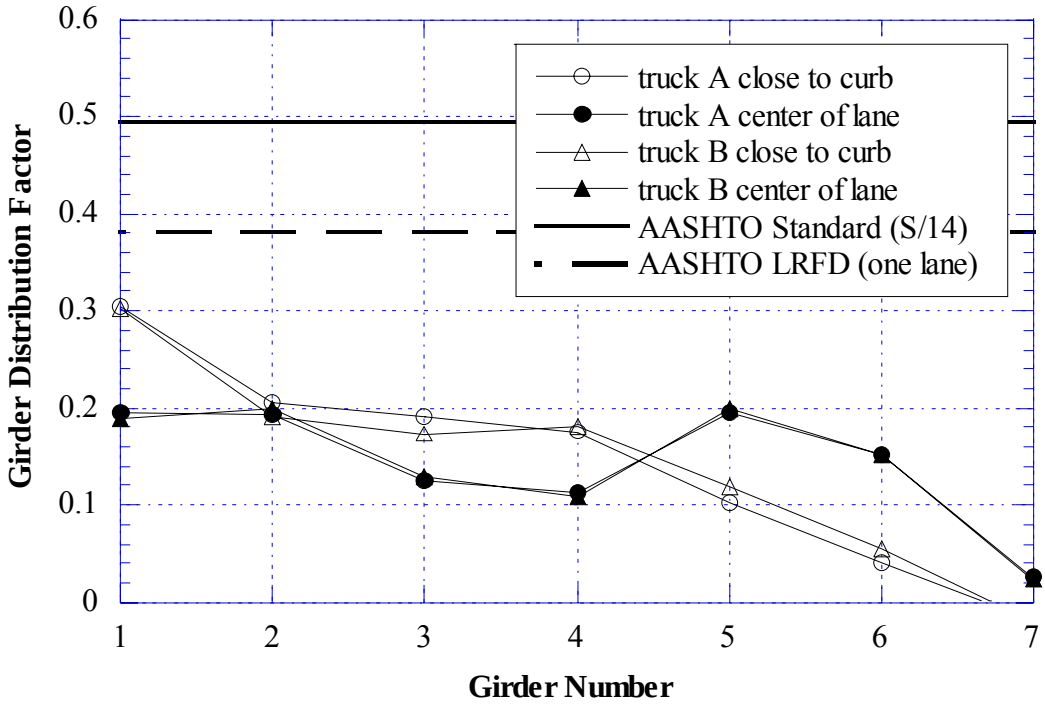

Figure 7.9 GDF from Positive Strain at Midspan of Centerspan, East Lane Loading (S05-44044)

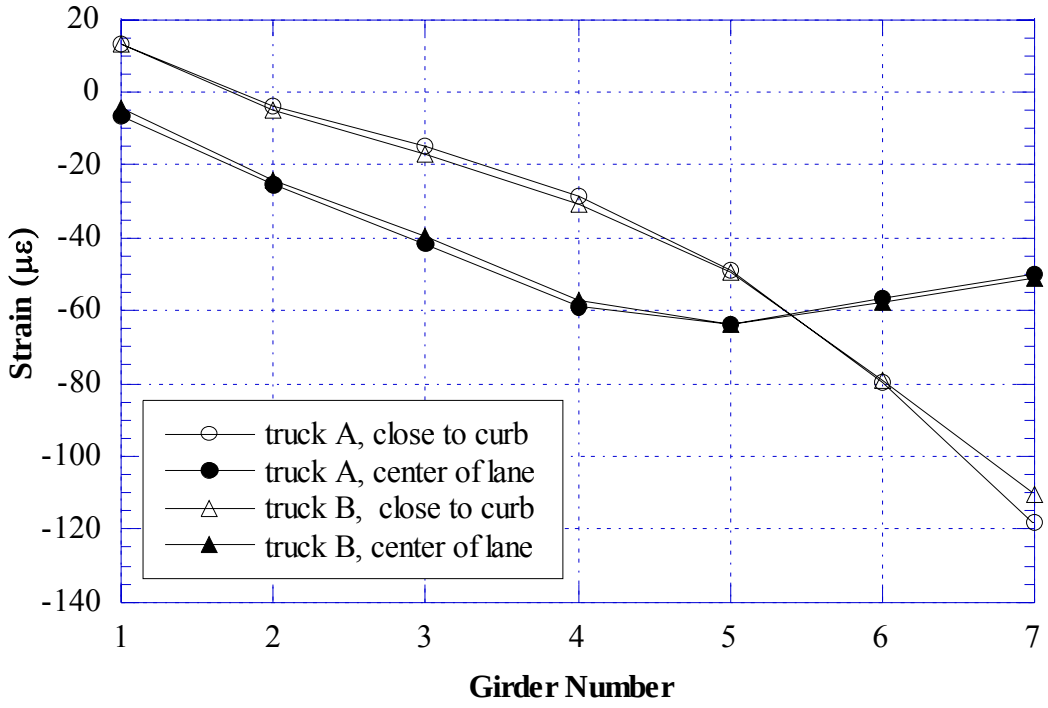

Figure 7.10 Negative Strain near Support over South Pier,
West Lane Loading (S05-44044)

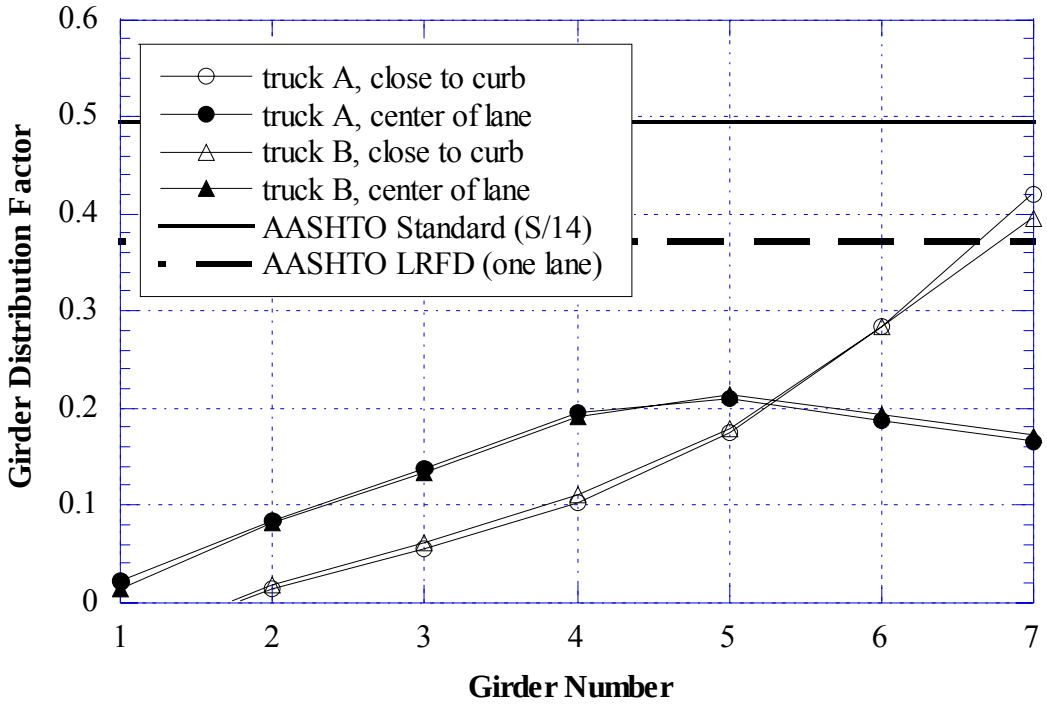

Figure 7.11 GDF from Negative Strain near Support over South Pier,
West Lane Loading (S05-44044)

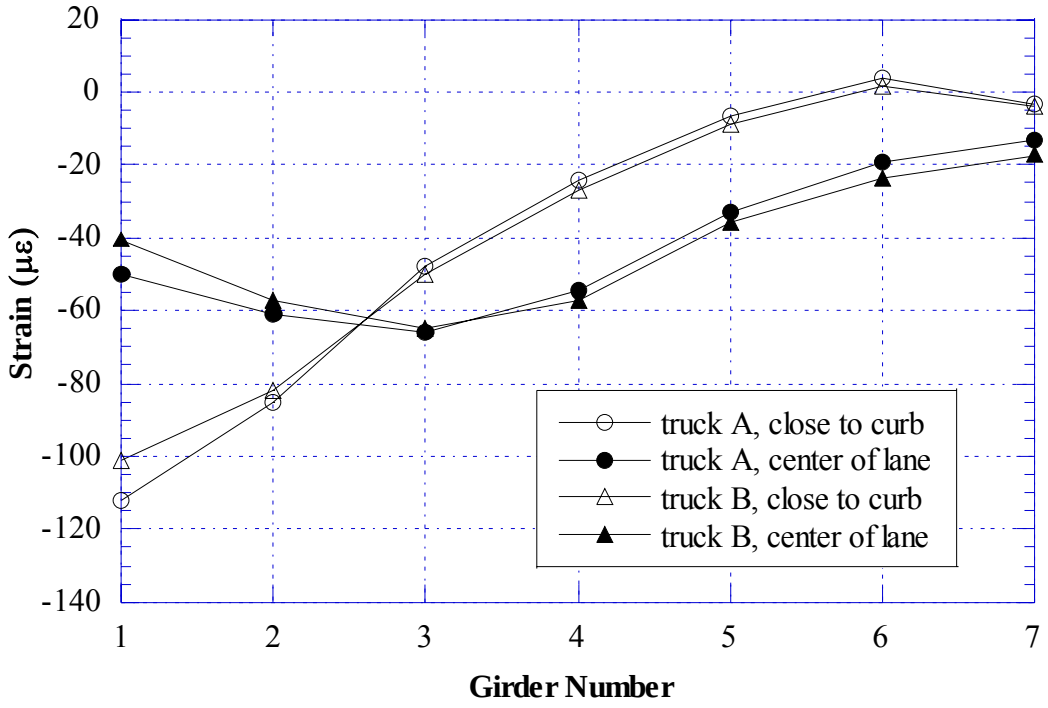

Figure 7.12 Negative Strain near Support over South Pier,
East Lane Loading (S05-44044)

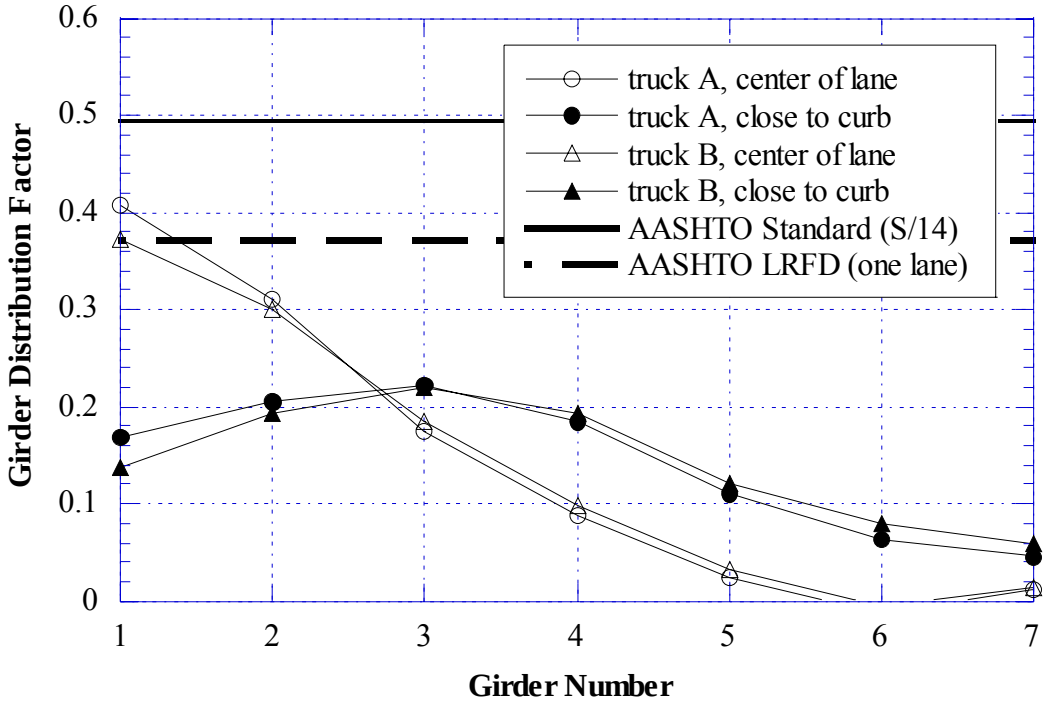

Figure 7.13 GDF from Negative Strain near Support over South Pier,
East Lane Loading (S05-44044)

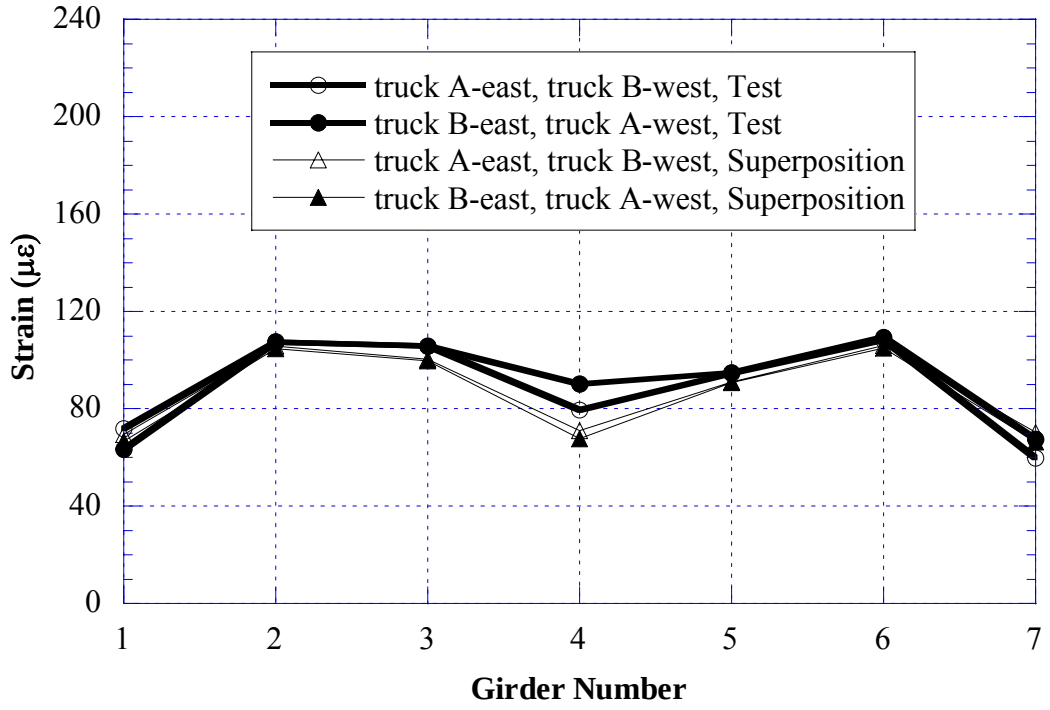

Figure 7.14 Positive Strain at Midspan of Centerspan, Side-by-Side Loading (S05-44044)

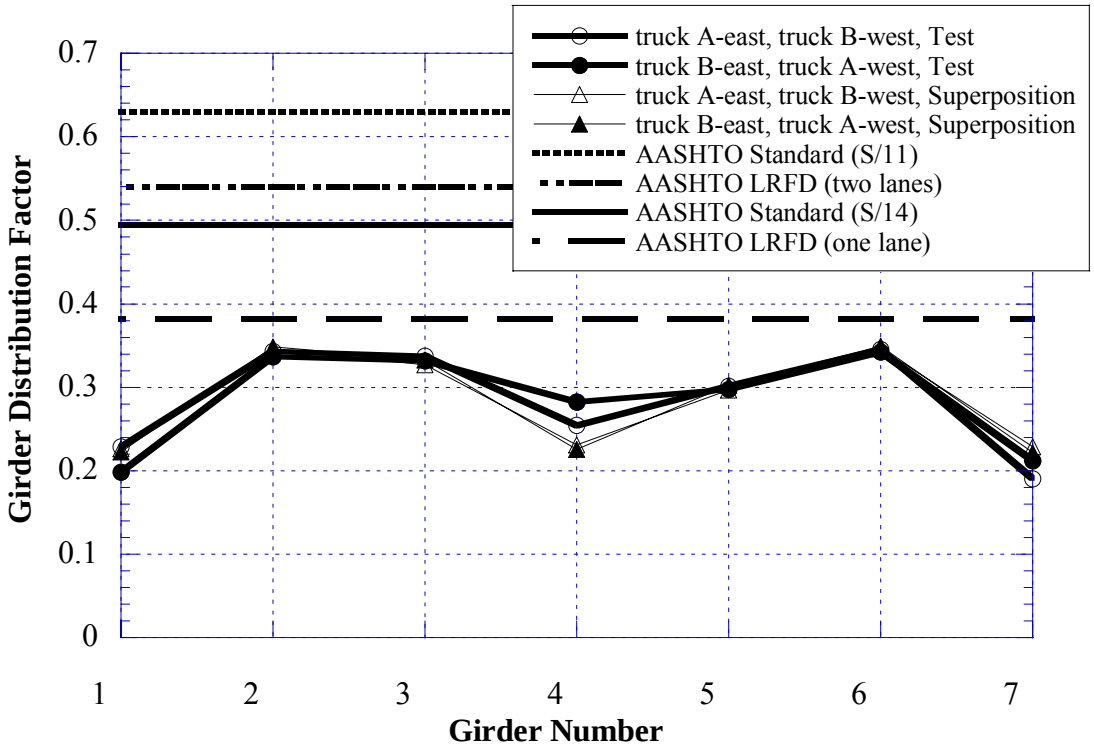

Figure 7.15 GDF from Positive Strain at Midspan of Centerspan, Side-by-Side Loading (S05-44044)

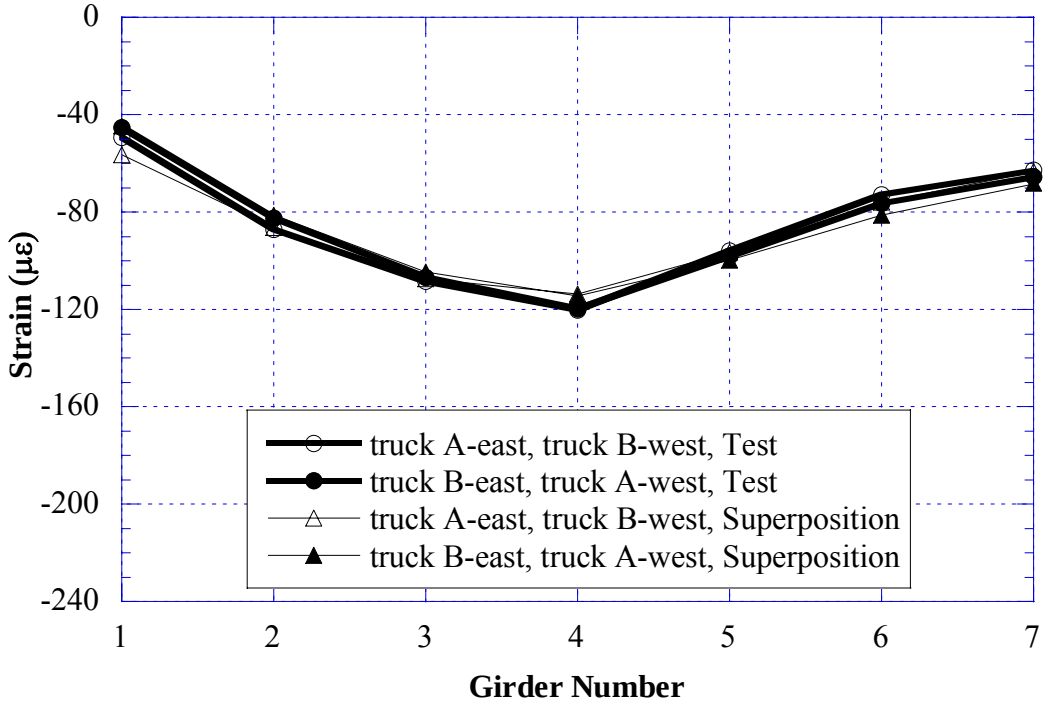

Figure 7.16 Negative Strain near Support over South Pier,
Side-by-Side Loading (S05-44044)

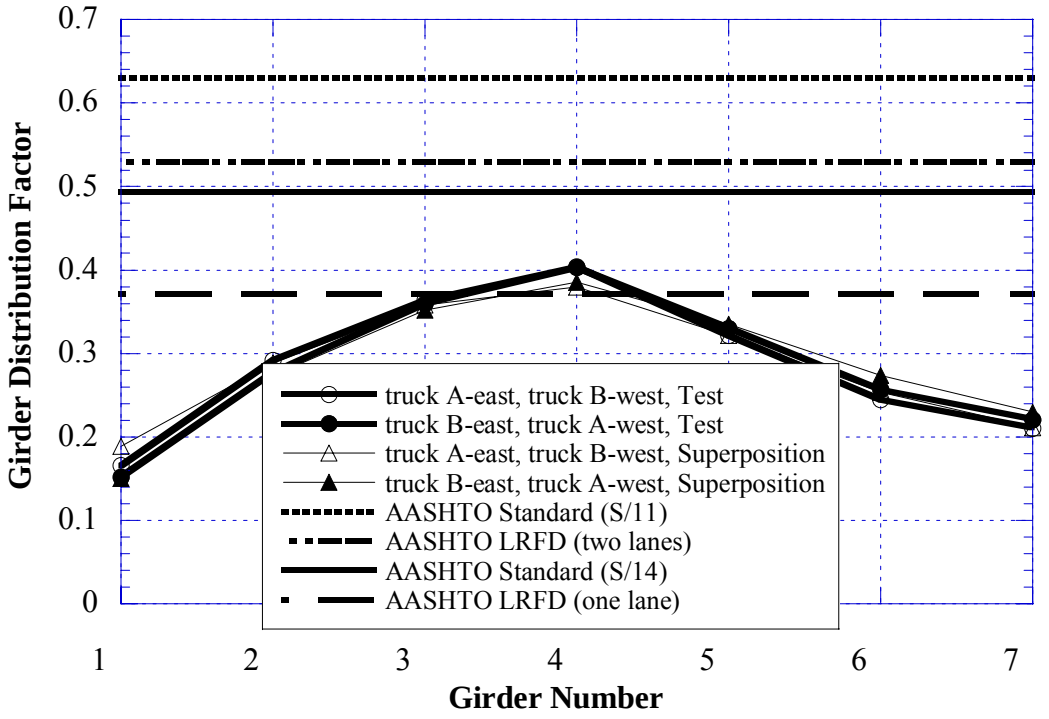

Figure 7.17 GDF from Negative Strain near Support over South Pier,
Side-by-Side Loading (S05-44044)

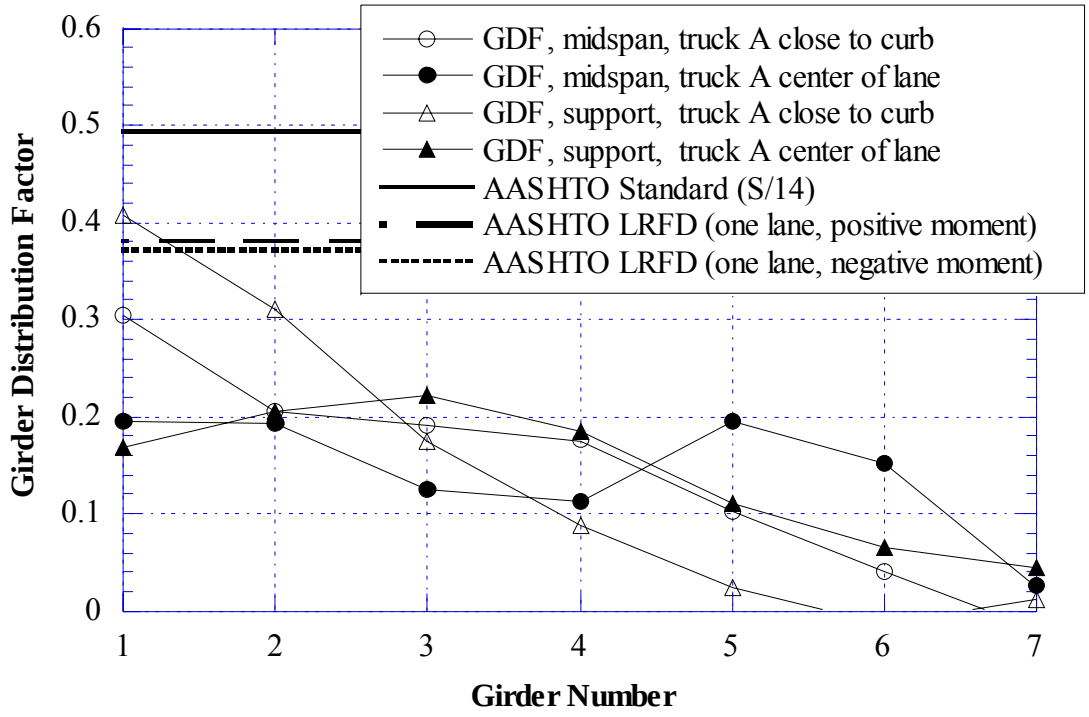

Figure 7.18 Comparison, GDF obtained from Positive Strain vs. GDF from Negative Strain, East Lane Loading (S05-44044)

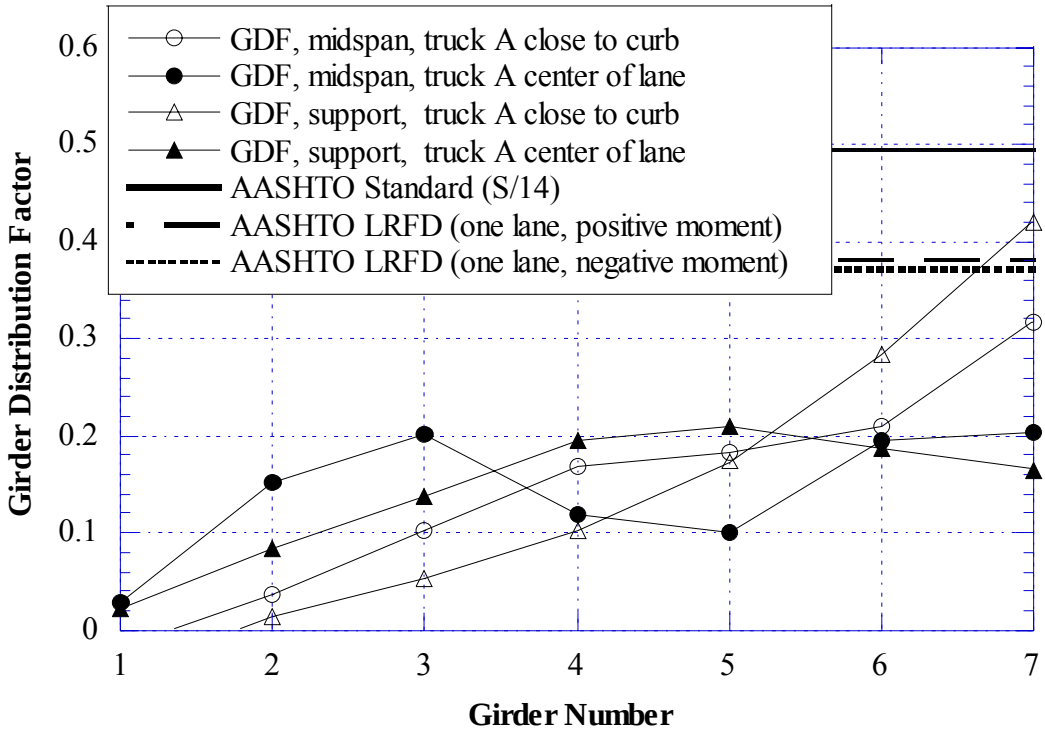

Figure 7.19 Comparison, GDF obtained from Positive Strain vs. GDF from Negative Strain, West Lane Loading (S05-44044)

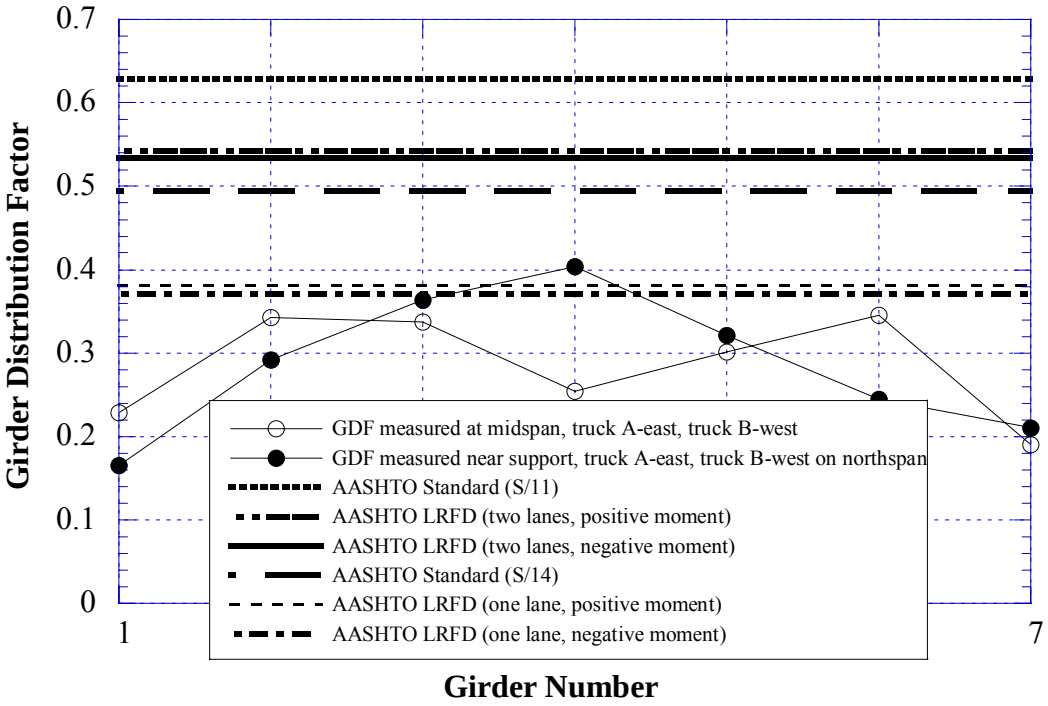

Figure 7.20 Comparison, GDF obtained from Midspan vs. GDF from Support, side-by-side loading (S05-44044)

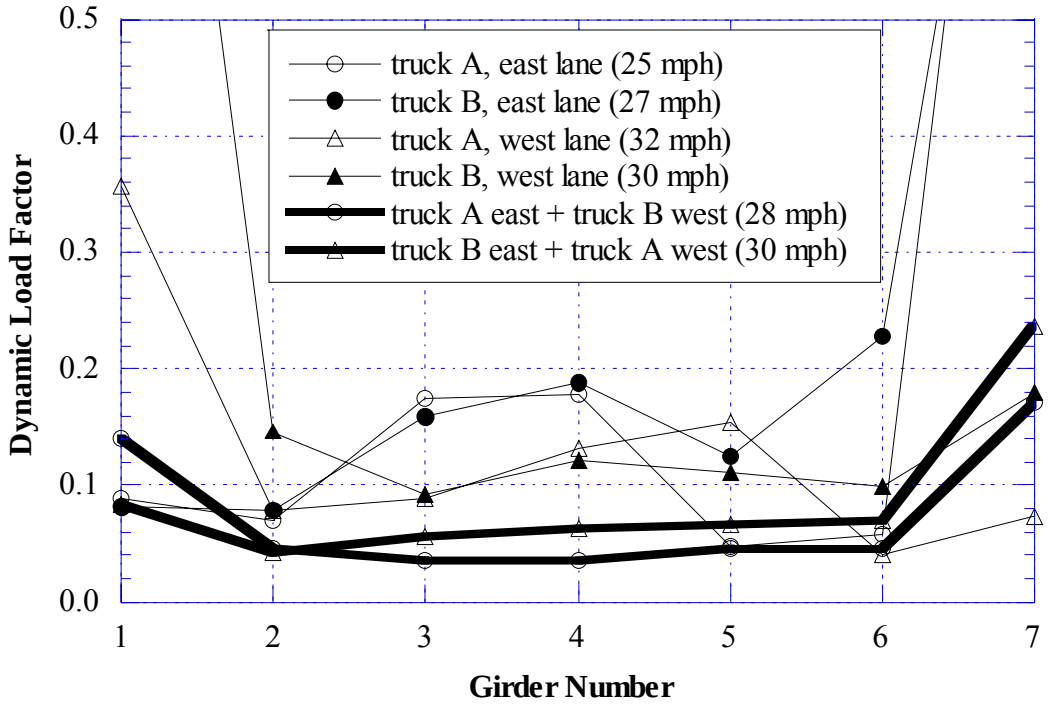

Figure 7.21 Dynamic Load Factors obtained from Positive Strain at Midspan of Centerspan (S05-44044)

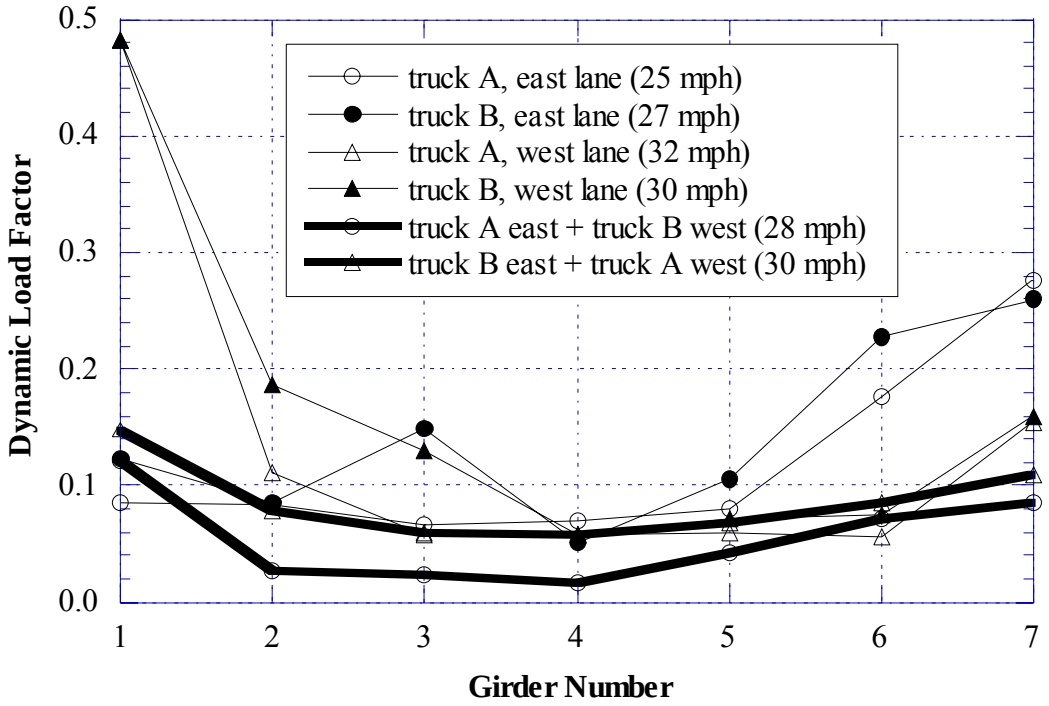

Figure 7.22 Dynamic Load Factors obtained from Negative Strain near Support over South Pier (S05-44044)

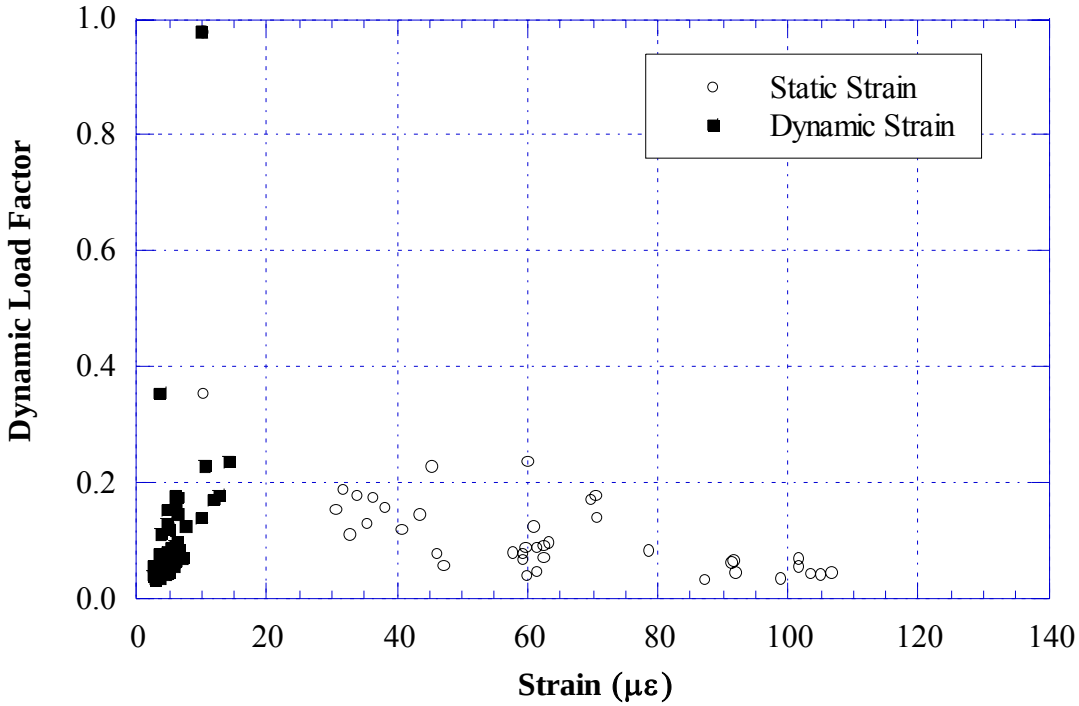

Figure 7.23 Strain vs. Dynamic Load Factors,
Based on Positive Strain at Midspan of Centerspan (S05-44044)

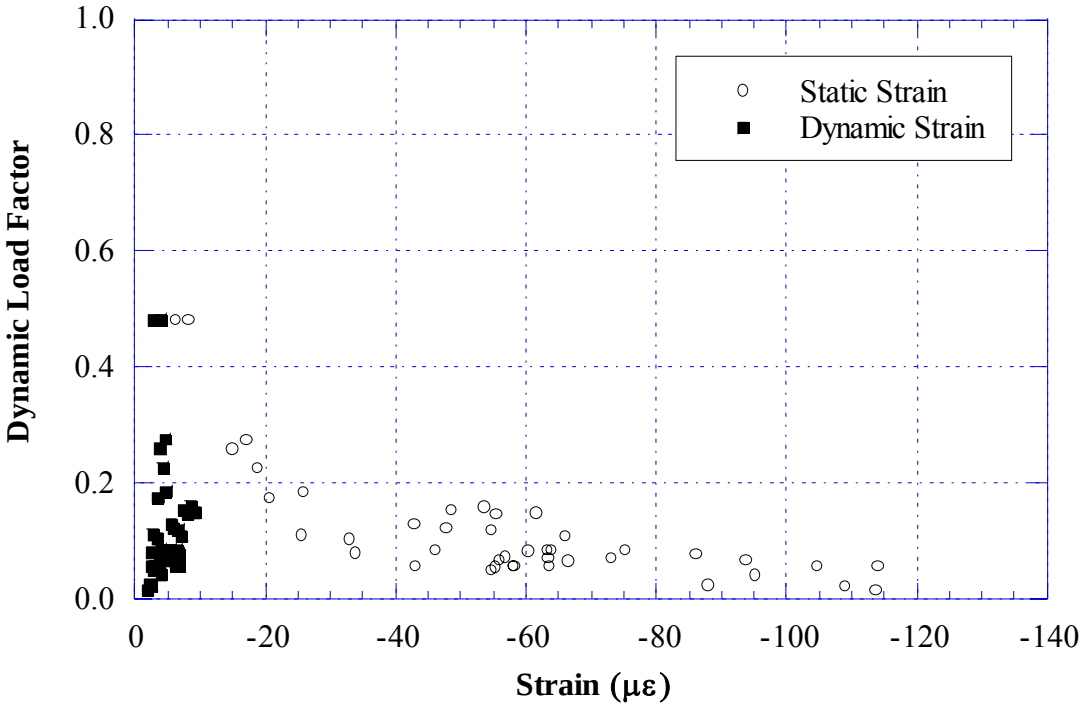

Figure 7.24 Strain vs. Dynamic Load Factors,
Based on Negative Strain near Support over South Pier (S05-44044)

7.5 Results of Finite Element Analysis

A three-dimensional finite element method (FEM) was applied to investigate the structural behavior of the bridge S05-44044. The concrete slab was modeled with isotropic, eight node solid elements, with three degrees of freedoms at each node. The girder flanges and web were modeled using three-dimensional, quadrilateral, four node shell elements with six degrees of freedom at each node. The structural effects of the secondary members, such as the sidewalk and parapet, were also taken into account in the finite element analysis models.

The mesh of the FEM model is shown in Figure 7.25. Total number of elements is 24,462, and total number of nodes is 32,430 for this model.

Strains and GDF's calculated for the considered model is shown in Figures 7.26 to 7.31. Figures 7.26 and 7.27 present strains and GDF's from FEM model for positive moment at the midspan under two trucks side-by-side loading. Figure 7.28 and 7.29 shows the strains and GDF's from FEM model for negative moment near support over north pier under two trucks side-by-side loading. In the figures, the values obtained from FEM analysis are compared with the corresponding measured values.

The resulting strain values obtained from field tests are close to or lower than those from the finite element analysis for considered bridges. For positive strain, there is a large difference in strain values from test and FEM analysis. It indicates that the FEM model did not accurately predicted the actual bridge behavior, due to various structural parameters not included in the FEM model. However, for negative strain, the values are very close. The main reason for this difference between the measured values and FEM results may be due to the partial fixity of supports. In the previous study for simply supported bridges by University of Michigan (Nowak 2001 and 2002), the boundary conditions are simulated using the elastic spring elements in FEM models. However, for continuous bridges, it is almost impossible to obtain accurate spring coefficients

satisfying multiple locations of supports with varied partial fixity condition. Therefore, in the study, the supports are assumed to behave as designed in the FEM models.

Figure 7.30 compares the GDF values for both positive moment and negative moment obtained from FEM analysis. The difference between GDF's from FEM analysis for positive moment and negative moments is less than 10 percent.

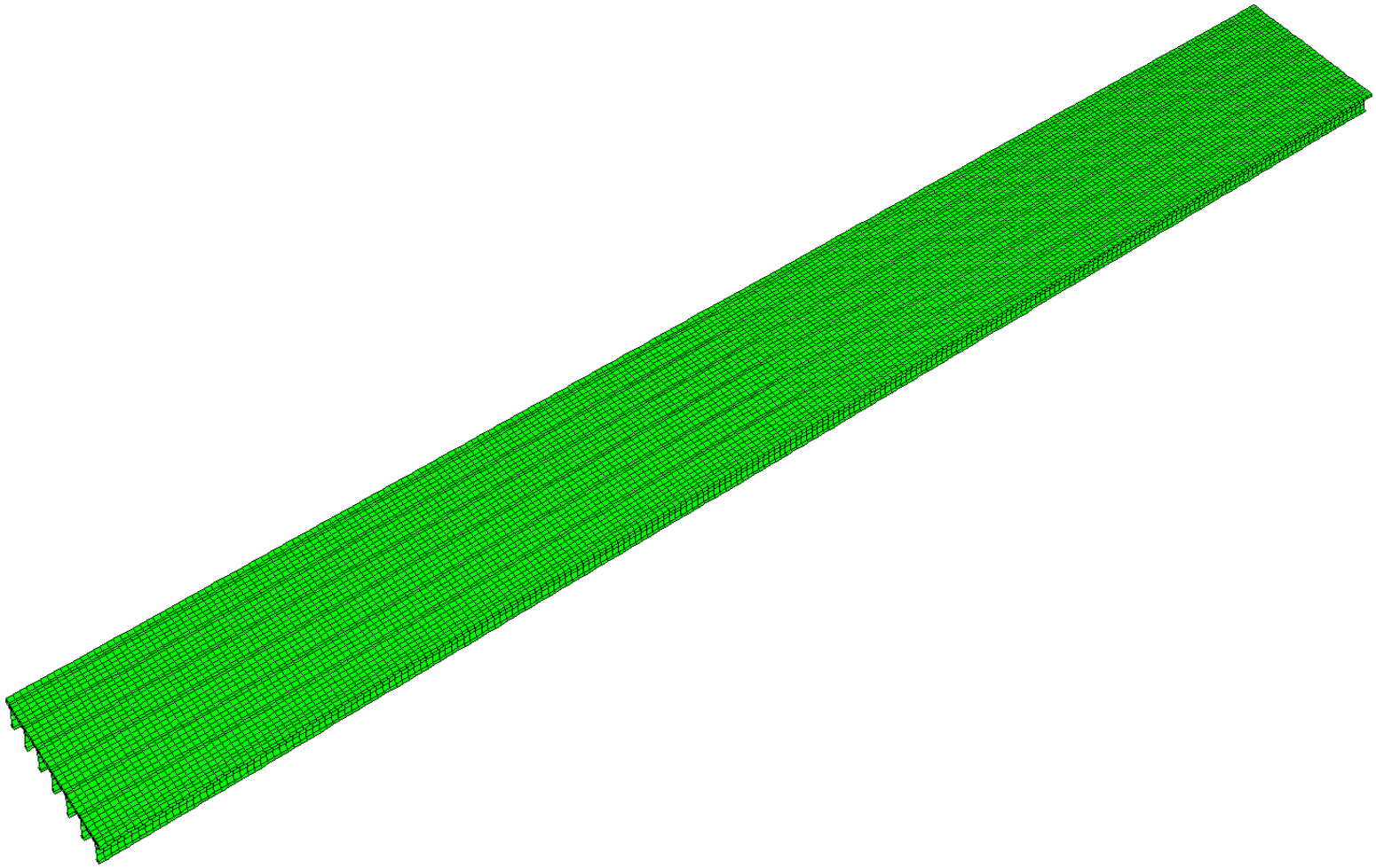

Figure 7.25 The Mesh of Finite Element Model (S05-44044)

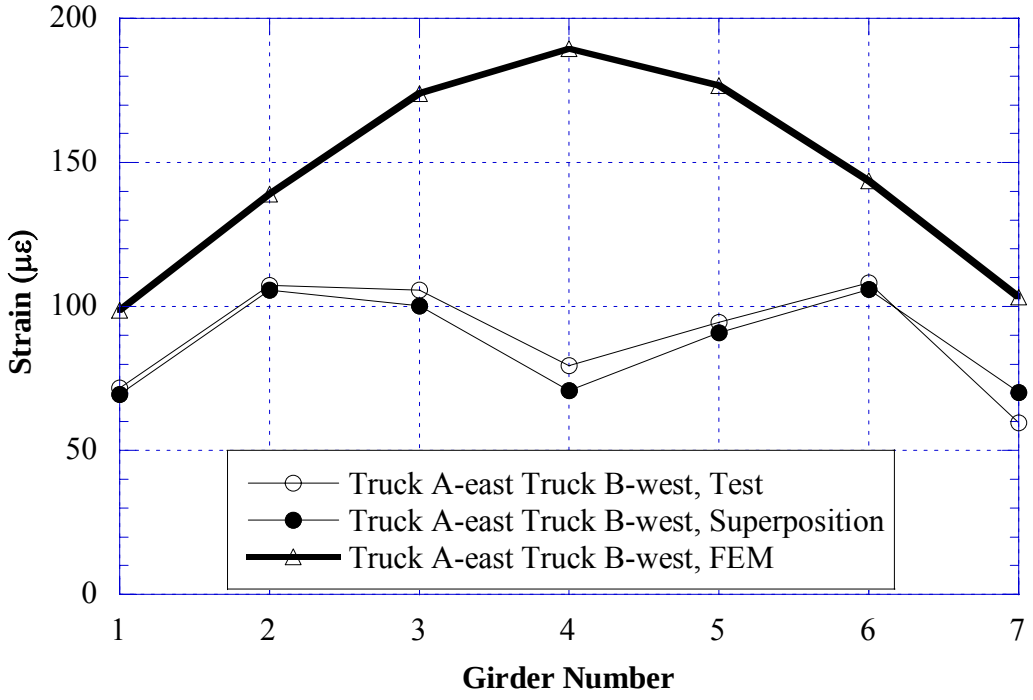

Figure 7.26 Comparison of FEM vs. Test, Positive Strain at Midspan of Centerspan, Side-by-Side Loading (S05-44044)

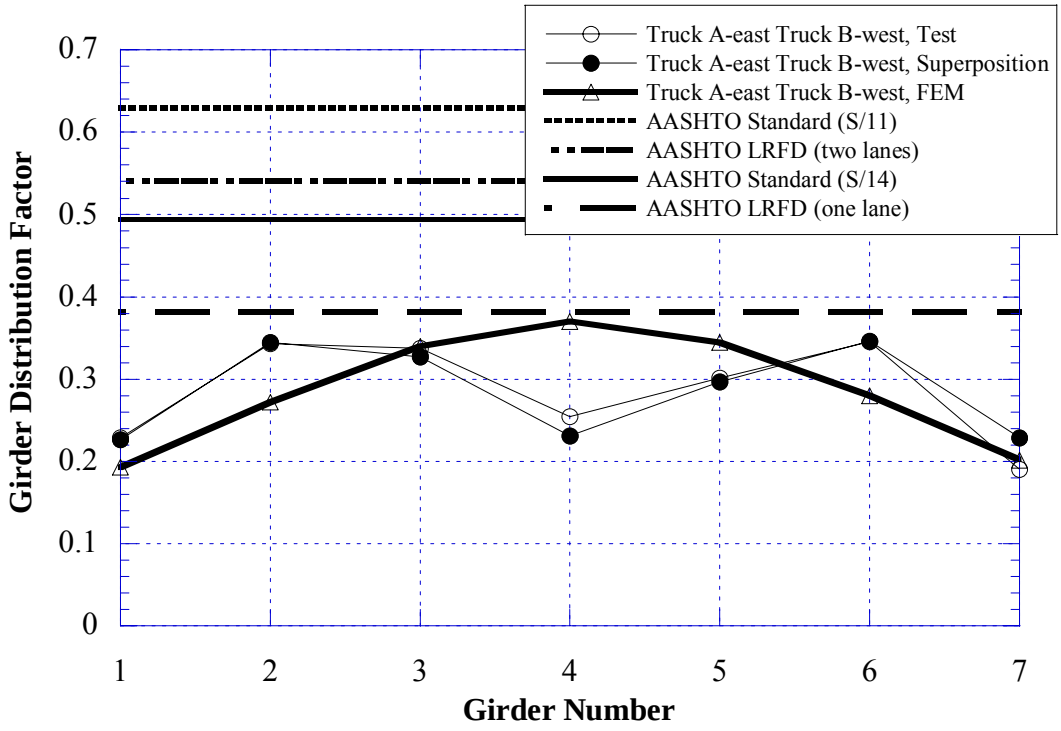

Figure 7.27 Comparison of FEM vs. Test, GDF Obtained from Positive Strain at Midspan of Centerspan, Side-by-Side Loading (S05-44044)

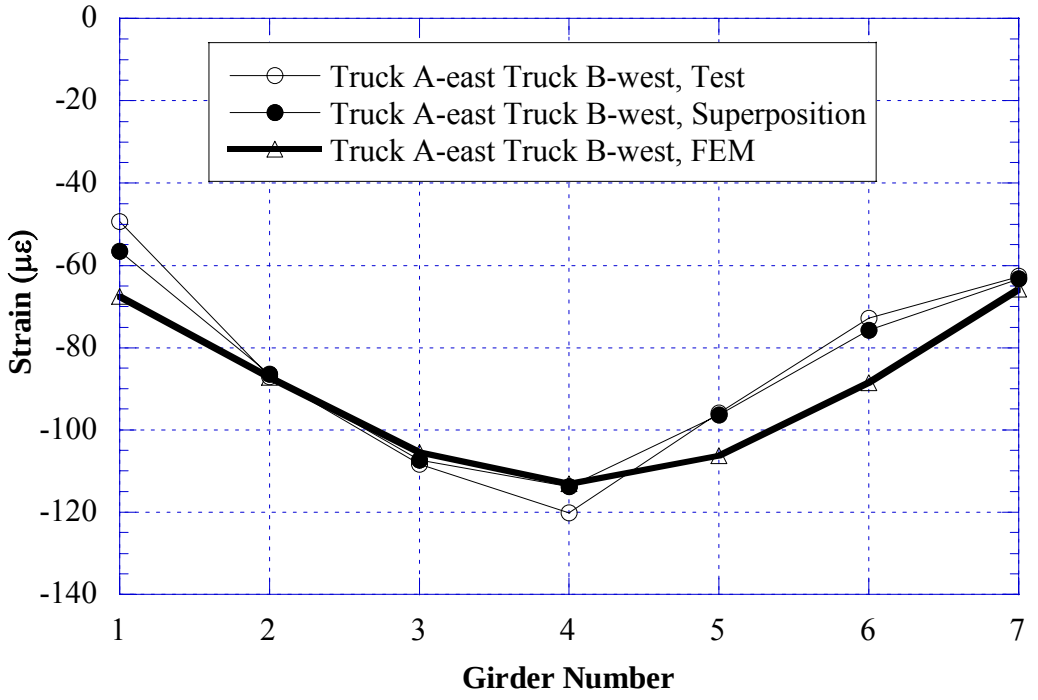

Figure 7.28 Comparison of FEM vs. Test, Negative Strain near Support over South Pier, Side-by-Side Loading (S05-44044)

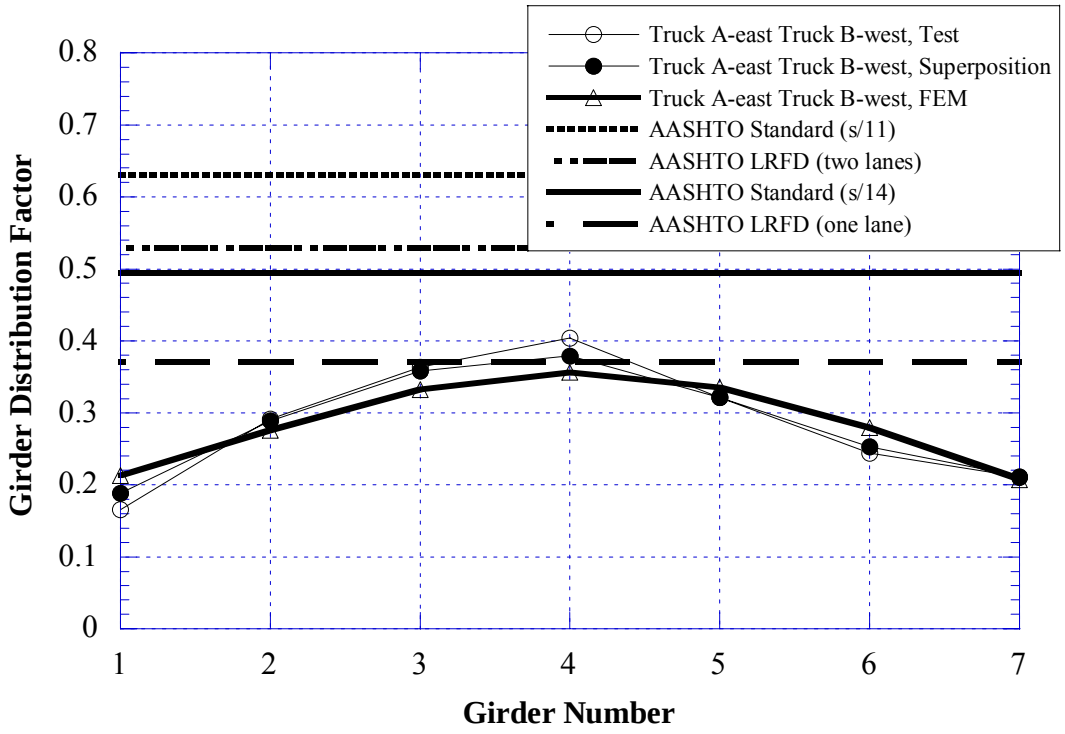

Figure 7.29 Comparison of FEM vs. Test, GDF Obtained From Negative Strain near Support over South Pier, Side-by-Side Loading (S05-44044)

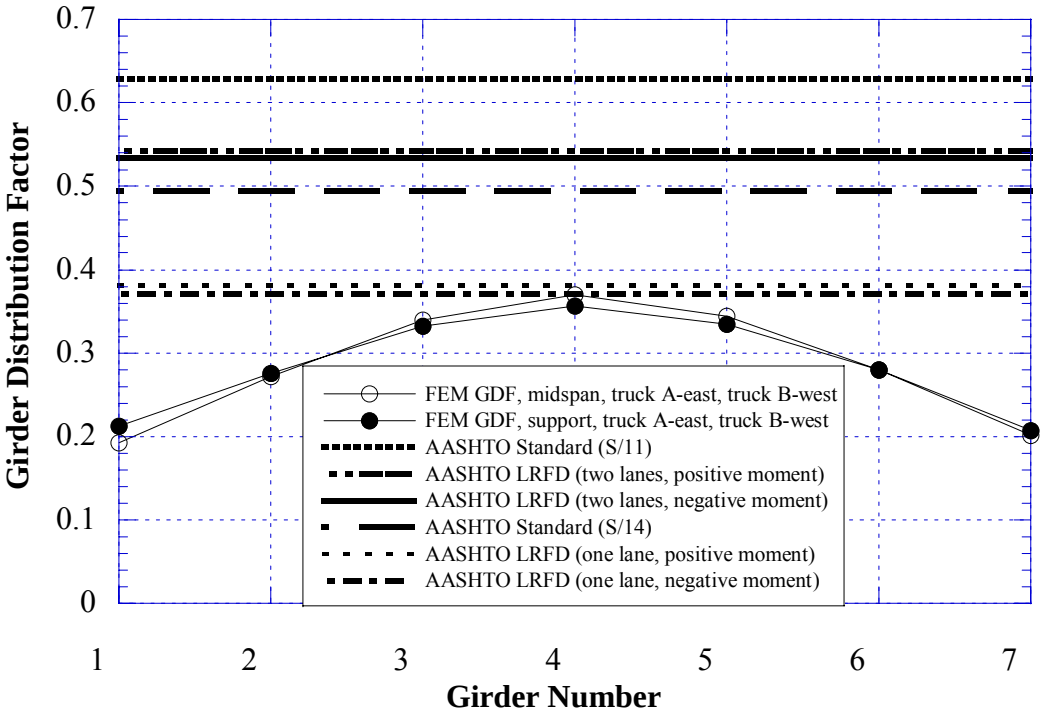

Figure 7.30 Comparison, GDF obtained from positive strain vs. GDF from Negative Strain, Based on Finite Element Analysis, Side-by-Side Loading (S05-44044)

Note:

Intentionally left blank

8.BRIDGE ON STATE ROAD OVER I-69, NEAR COLDWATER, BRANCH COUNTY (S01-12034)

8.1 Bridge Description

This bridge was built in 1967 and it is located on State Road over I-69 near Coldwater in Branch County, Michigan. It is a two span, continuous steel girder bridge with varying web height over pier, designed as a composite section. It has four steel girders spaced at 8 ft 6 in, as shown in Figure 8.1, with no skew. The total bridge length is 216 ft. The side elevation is shown in Figure 8.2. The bridge has one lane in each direction and it carries an average daily traffic (ADT) of 900. The operating load rating is 176 kips, according to the Michigan Structure Inventory.

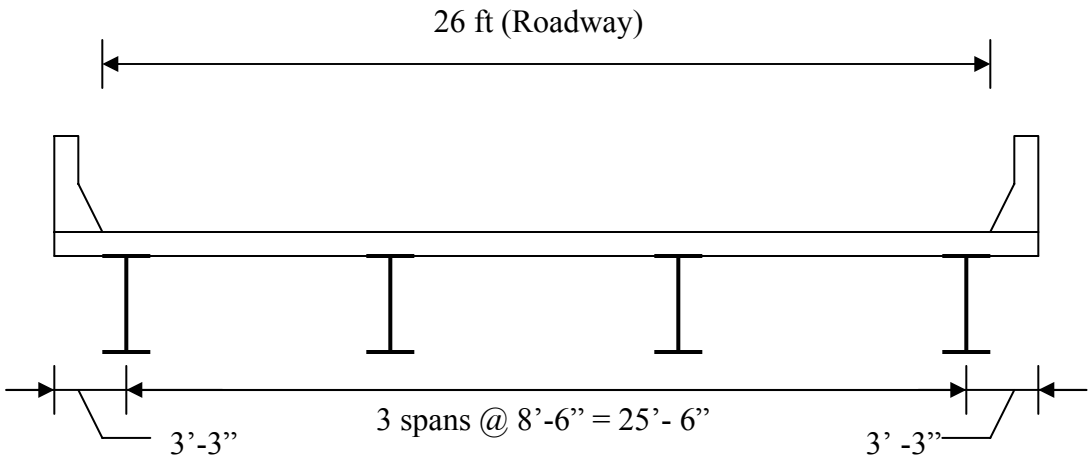

Figure 8.1 Cross Section of the bridge (S01-12034)

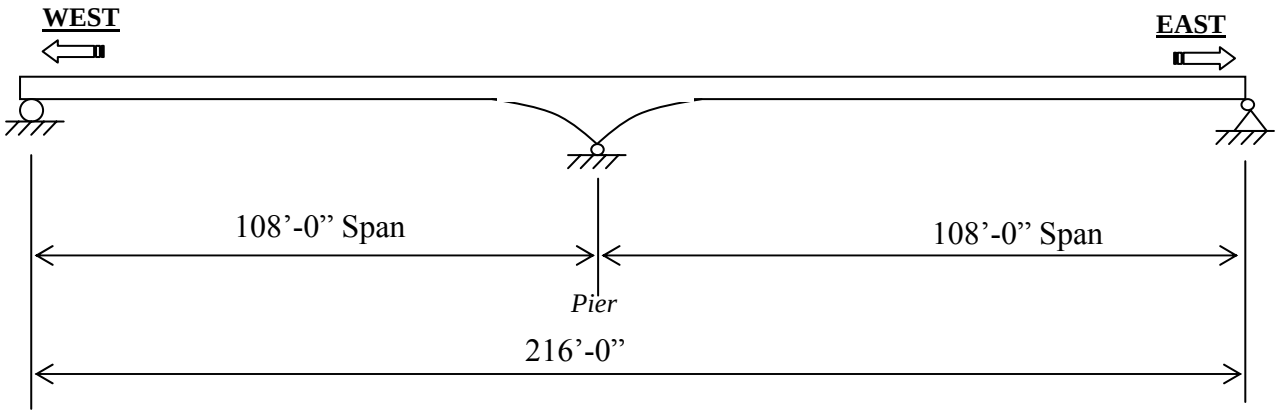

Figure 8.2 Side Elevation of Bridge (S01-12034)

8.2 Instrumentation

Strain transducers were installed on the bottom flanges of girders at midspan and at support locations, as shown in Figure 8.3. The reflector for the PSM-R device from Noptel was installed at the girder No. 2 to measure deflection. The bridge was instrumented on June 11, 2002, and bridge test were performed on June 12, 2002.

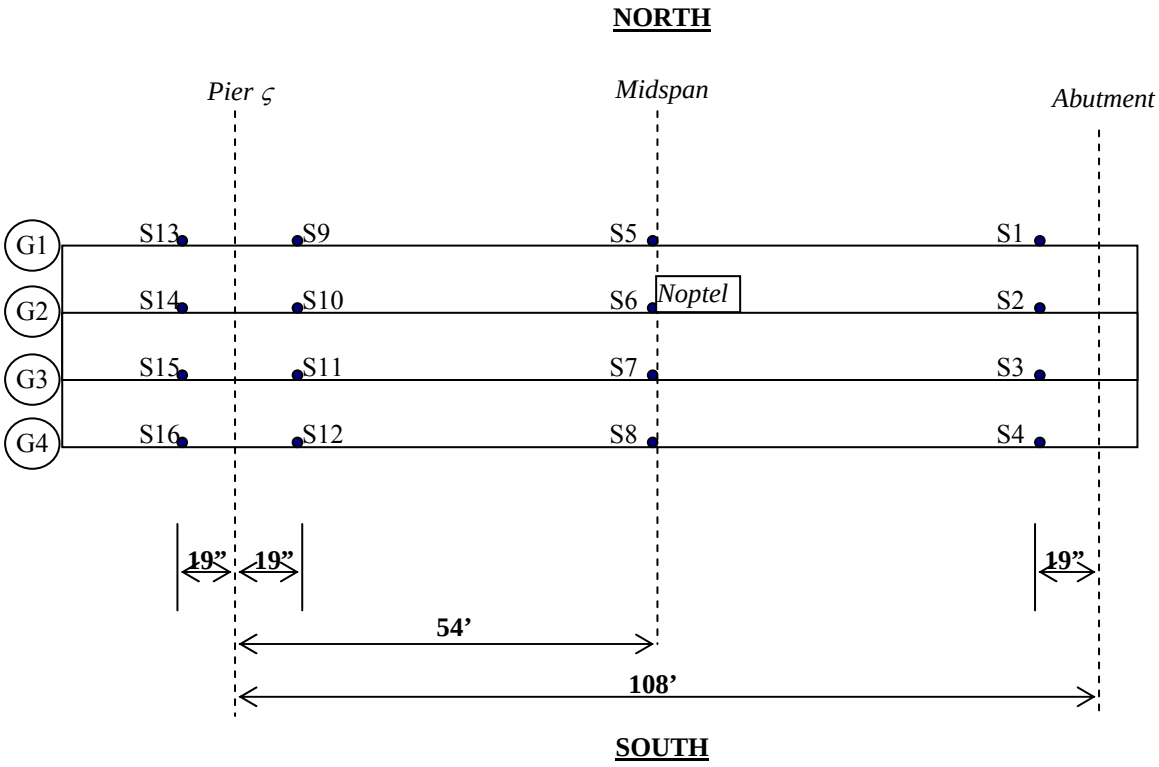

Figure 8.3 Strain Gage Location in East Span of Bridge (S01-12034)

8.3 Load cases

The girder distribution factors (GDF) and dynamic load factors (DLF) were calculated using the strains measured at midspan and near support. The bridge was loaded with one 11-axle truck (three-unit vehicle). Before the test, two trucks were arranged for the test, and weighed at the weigh station. However, one truck was broken down on the way to the bridge test site. Therefore, only one truck was used for the test.

The truck used has a gross weight of 145 kips, with a wheelbase of 57 ft. Truck configuration is shown in Figure 8.4.

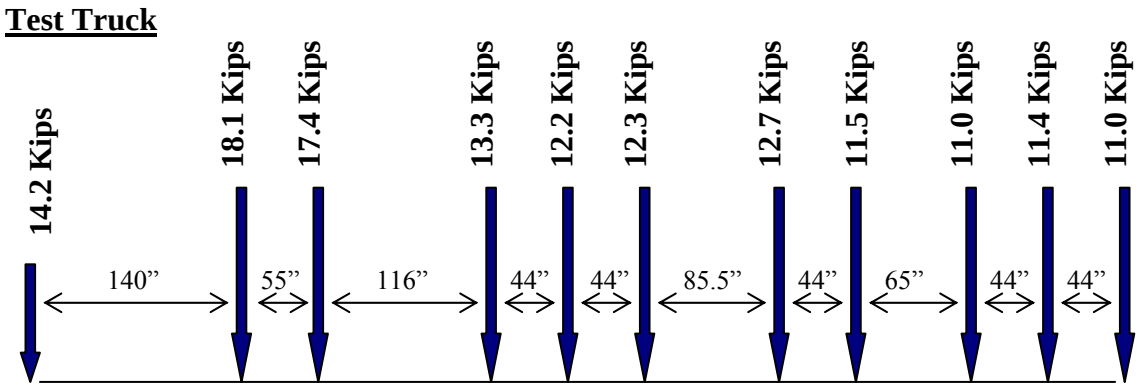

Figure 8.4 Truck configuration, Bridge (S01-12034)

Initially, a total of 18 load cases were considered, assuming two trucks would be available. However, due to the unexpected situation that one truck had mechanical problem on the way to the bridge, only 8 runs were performed, as shown in Table 8.1. The truck was driven at the center of each lane, at crawling speed. The runs in the center of the lane were repeated at a normal highway speed. The test truck was also stopped at the predetermined position to confirm pre-test calculation.

Table 8.1. Sequence of Test Runs, Bridge (S01-12034)

Run#	Lane Side	Position	Truck Speed
1	South	Center	Crawling
2	South	Center	Crawling
3	North	Center	Crawling
4	North	Center	Crawling
5	South	Center	25 MPH
6	North	Center	28 MPH
7	South	Center	Fixed Position
8	North	Center	Fixed Position

8.4 Test results

The resulting strains and GDF's are shown in Figures 8.5 through 8.16. Figures 8.5 to 8.12 present the results for one truck on the bridge under crawling-speed (static) tests. For each loading condition, strains are measured and the corresponding GDF's are calculated from the strain measurement. For comparison, GDF are also calculated according to AASHTO Standard (2002) and AASHTO LRFD Code (1998). The resulting GDF's are shown in Figures 8.6 through 8.12. Figures 8.5 to 8.8 show positive strain values recorded at the midspan of eastspan, and also resulting GDF's. Figures 8.9 to 8.12 present the negative strain values and corresponding GDF's near supports over center pier. For single lane loading, the maximum positive strain is about 140 με. This strain value corresponds about 4.1 ksi. The maximum negative strain near support is about 75 με. This corresponds about 2.2 ksi. In all considered single lane loadings, the measured GDF's do not exceed code specified values.

Figures 8.13 to 8.16 present the results for superposition of single lane loading on the bridge under crawling-speed (static) tests to simulate the two trucks side-by-side. For comparison, GDF are also calculated according to code specified values. Figure 8.13 presents the measured positive strains based on superposition, and Figure 8.14 show corresponding GDF's compared with code specified values. For superposition, the maximum positive strain at the midspan is about 220 με, which corresponds about 6.4 ksi. Figure 8.14 shows that code specified GDF's are conservative. Even the single lane GDF's specifed in AASHTO Standard (2002) is very close to the value from superposition. However, single lane GDF's specified in AASHTO LRFD (1998) is not sufficient for two lane load case in this bridge.

Figures 8.15 and 8.16 present the negative strains under two truck side by side loading measured near support over pier. Figure 8.15 presents the measured negative strains, and Figure 8.16 show corresponding GDF's compared with code specified values. The maximum recorded negative strain near support at the midspan is about 110 με, which corresponds about 3.2 ksi. Figure 8.16 shows that code specified GDF's are conservative.

As in GDF's for positive moments, even the single lane GDF's specifed in AASHTO Standard (2002) is sufficient for two trucks side by side. However, single lane GDF's specified in AASHTO LRFD (1998) is not sufficient for two lane load case in this bridge.

Figures 8.17 and 8.18 present the comparison of GDF's for positive and negative moment obtained from single lane loadings. In all cases, the code specified values are conservative. Particularly, GDF specified in AASHTO Standard (2002) is very conservative.

Figure 8.19 compares the GDF's for positive and negative moment obtained from side-by-side loading. The figure indicates that code-specified GDF's are conservative for two truck side-by-side loading (superposition). For two truck load cases, a single lane GDF specified in AASHTO Standard (2002) is also sufficient for two lane load cases for this bridge. However, a single lane GDF specified in AASHTO LRFD (1998) is not enough for two lane load cases for this bridge.

Strains were also measured near east abutment. The results are shown in Figures 8.20 to 8.22. Theoretically, there should be no strain recorded at this location. However, it was observed that the strain values can be up to 100 □□ under single lane loading. This indicates that the supports over east abutment are partially fixed , and do not behave as designed. This likely reduces the overall moment taken by the bridge girders.

In Figures 8.23 and 8.24, DLF's are plotted for load cases involving normal speed (no dynamic load was measured for crawling speed runs). Figure 8.23 shows DLF's measured at the midspan (positive moment), and Figure 8.24 for negative moment (near support). As shown in the figures, dynamic load factors for exterior girders are high because the static strains in these girders are very low. In other words, large values of DLF in exterior girders correspond to load cases with a single truck in the opposite lane (resulting in very low static strain).

The relationship between DLF and static and dynamic strains is shown in Figures 8.25 and 8.26, for positive moment and negative moment, respectively. The open circles correspond to static strain, ε_{stat}, and black solid squares correspond to dynamic strain, ε_{dyn}. For each static strain value (open circle), the corresponding dynamic strain is denoted by solid square (the numbers of circles and squares are same). Dynamic strains remain nearly constant, while static strains increase as truck loading increases. This results in large dynamic load factors for low static strains. DLF corresponding to the maximum strain due to single lane loading is less than 0.10 for the most heavily loaded girder.

Girder No. 2 was instrumented with a remote deflection measurement device manufactured by Noptel. The reflector was installed at midspan. The result is shown in Table 8.2. The maximum deflection recorded during the test is 13.2 mm for girder No. 3 for single lane loading.

Table 8.2. Maximum deflections measured at the center of Girder No.2, Bridge (S01-12034)

Run #	**Vertical Deflection (mm)**
1	8.3
2	8.7
3	13.1
4	13.2

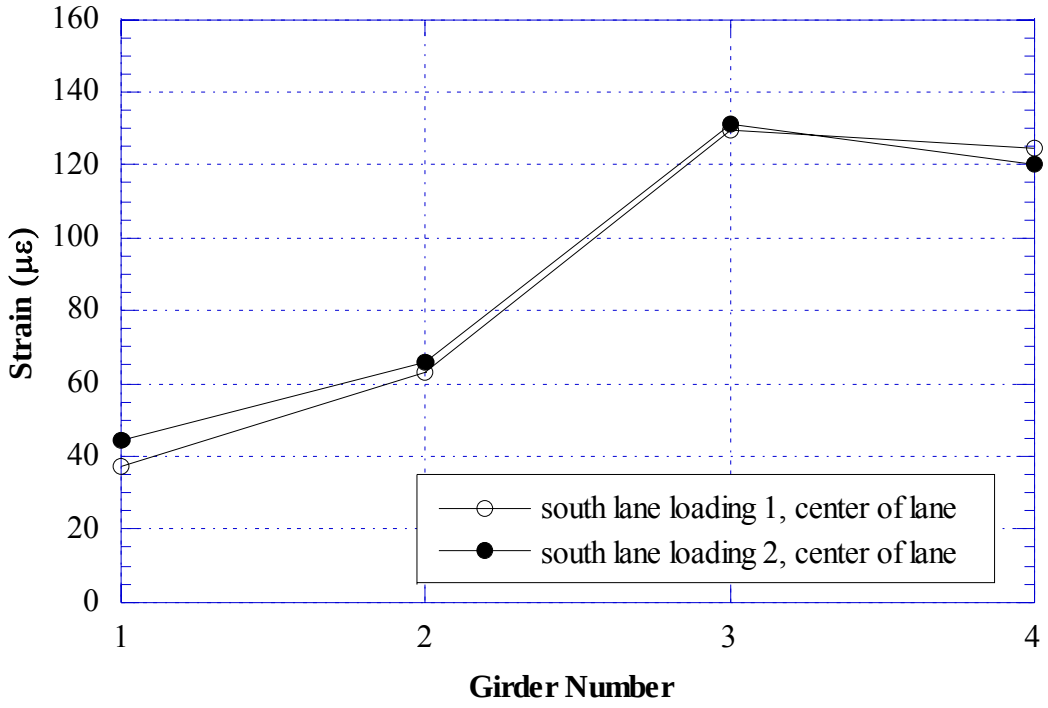

Figure 8.5 Positive Strain at Midspan of Eastspan, South Lane Loading (S01-12034)

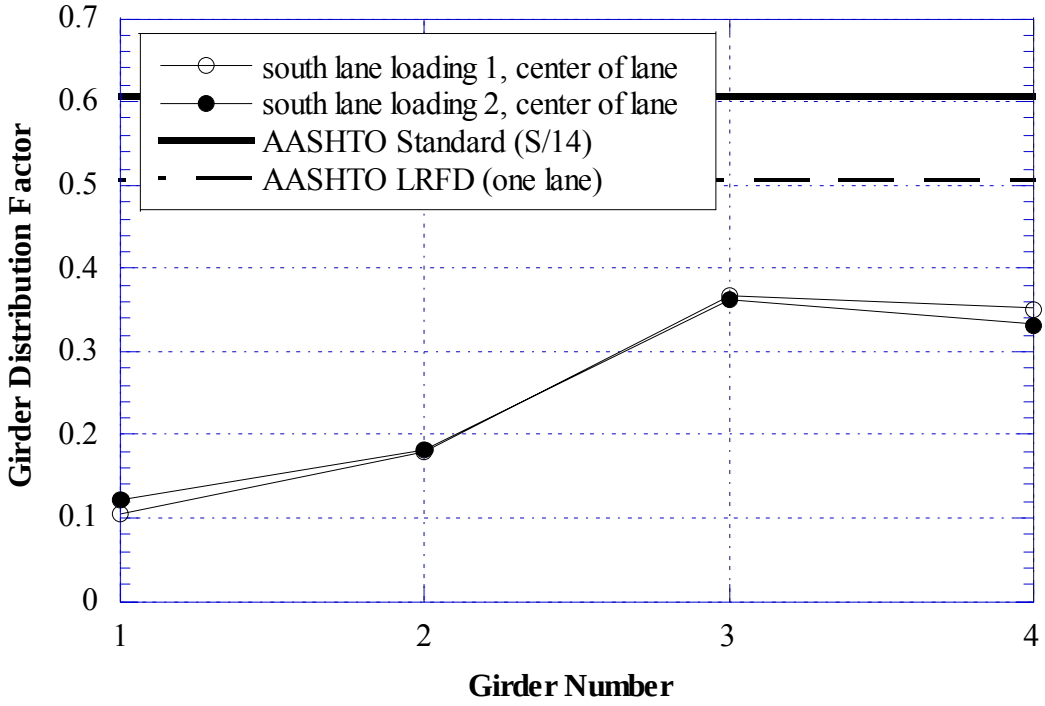

Figure 8.6 GDF from Positive Strain at Midspan of Eastspan, South Lane Loading (S01-12034)

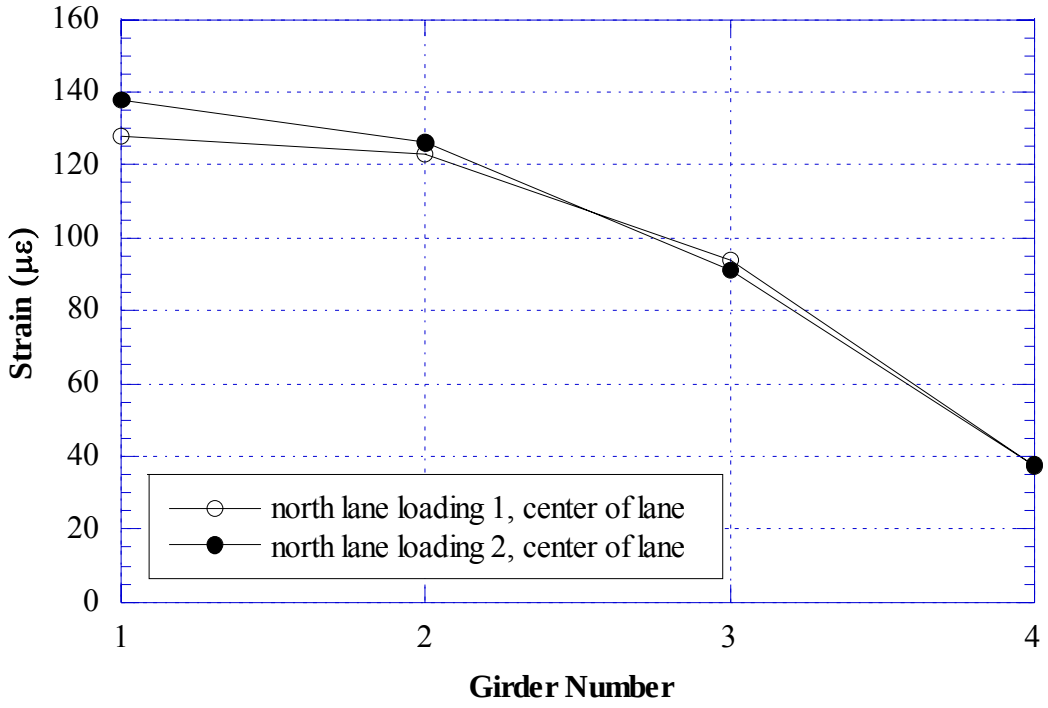

Figure 8.7 Positive Strain at Midspan of Eastspan, North Lane Loading (S01-12034)

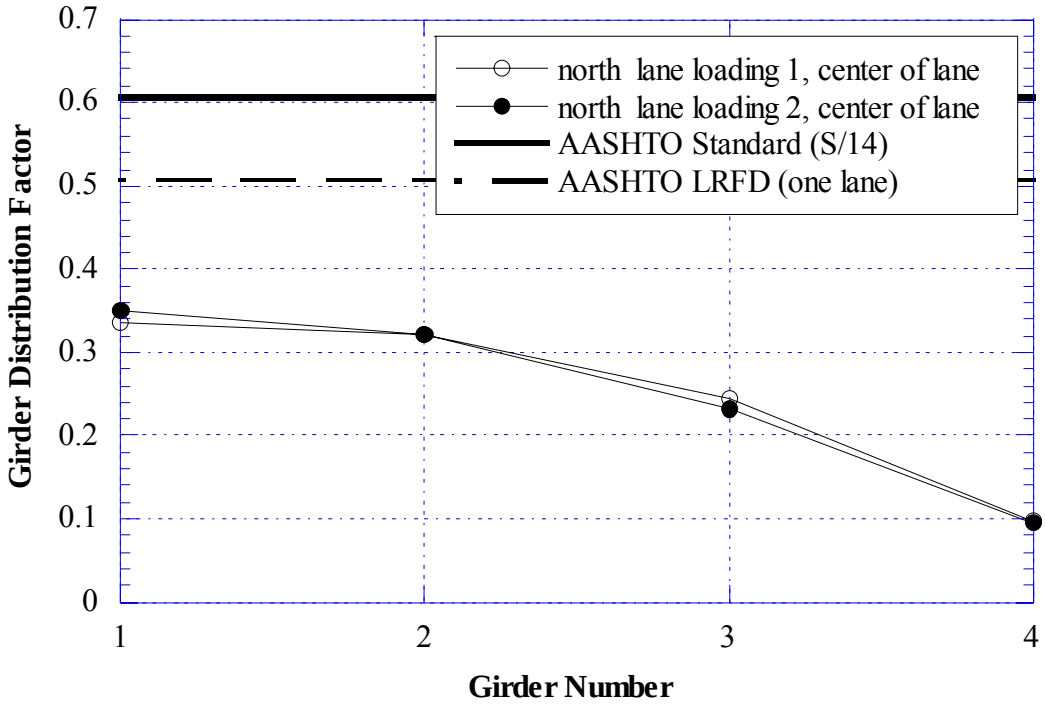

Figure 8.8 GDF from Positive Strain at Midspan of Eastspan, North Lane Loading ((S01-12034)

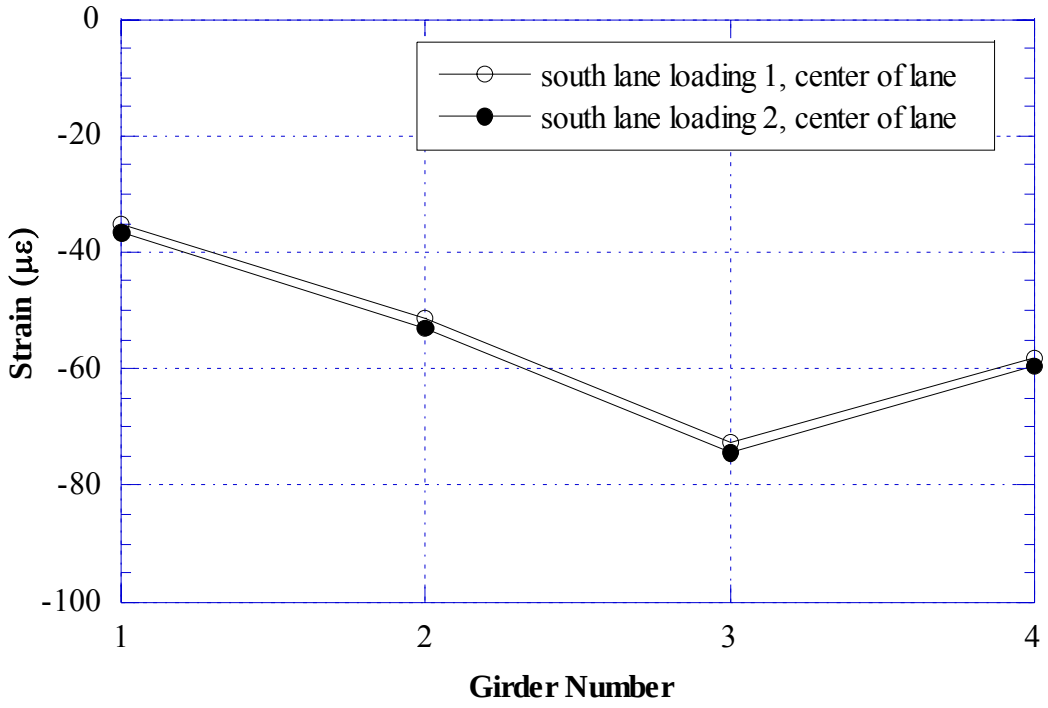

Figure 8.9 Negative Strain near Support over Pier, South Lane Loading (S01-12034)

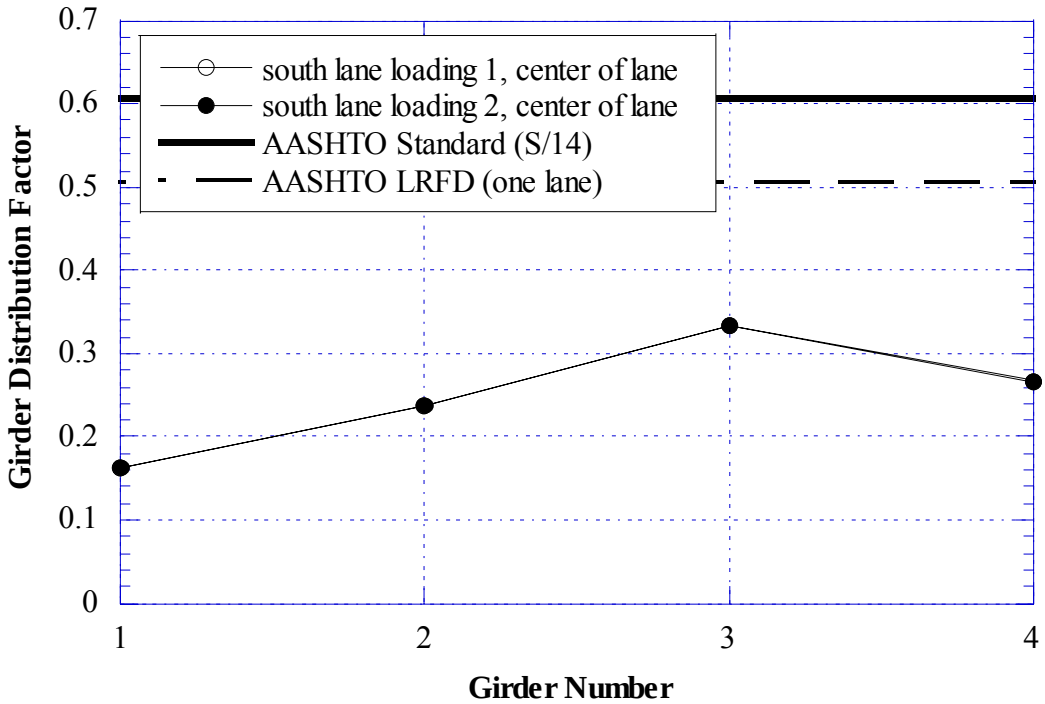

Figure 8.10 GDF from Negative Strain near Support over Pier, South Lane Loading (S01-12034)

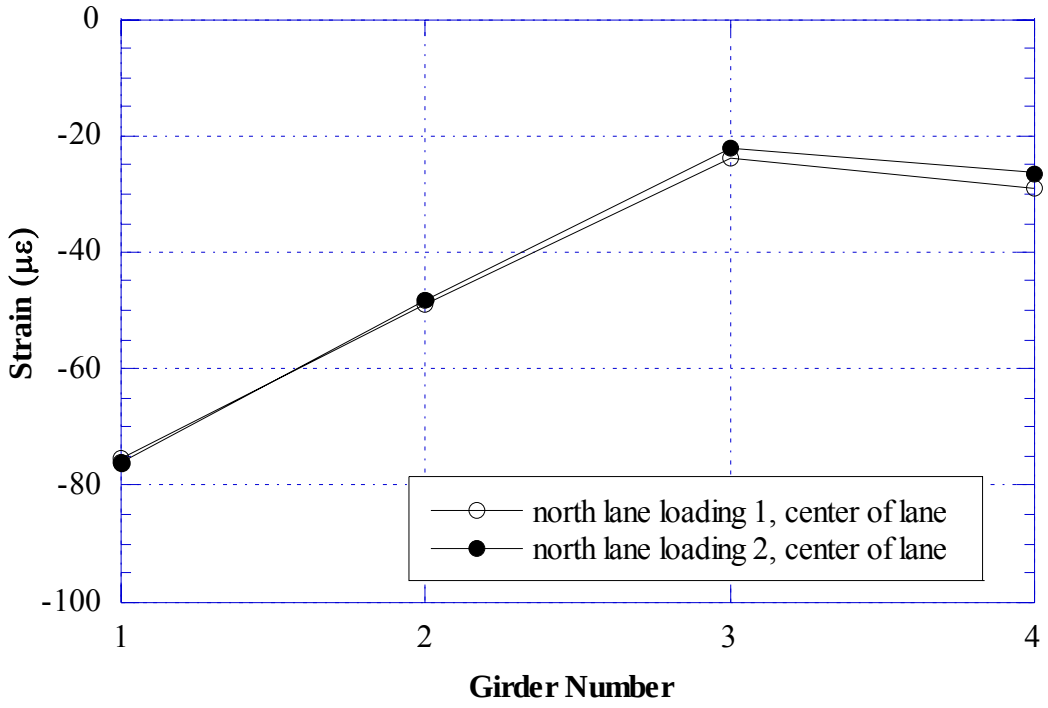

Figure 8.11 Negative Strain near Support over Pier, North Lane Loading (S01-12034)

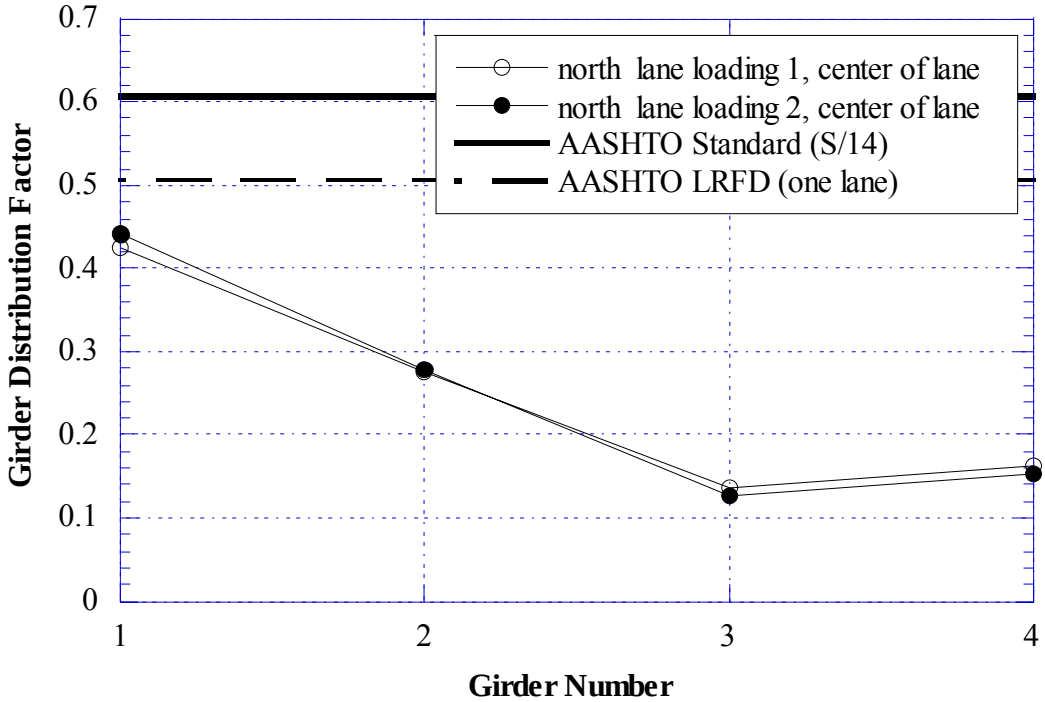

Figure 8.12 GDF from Negative Strain near Support over Pier, North Lane Loading (S01-12034)

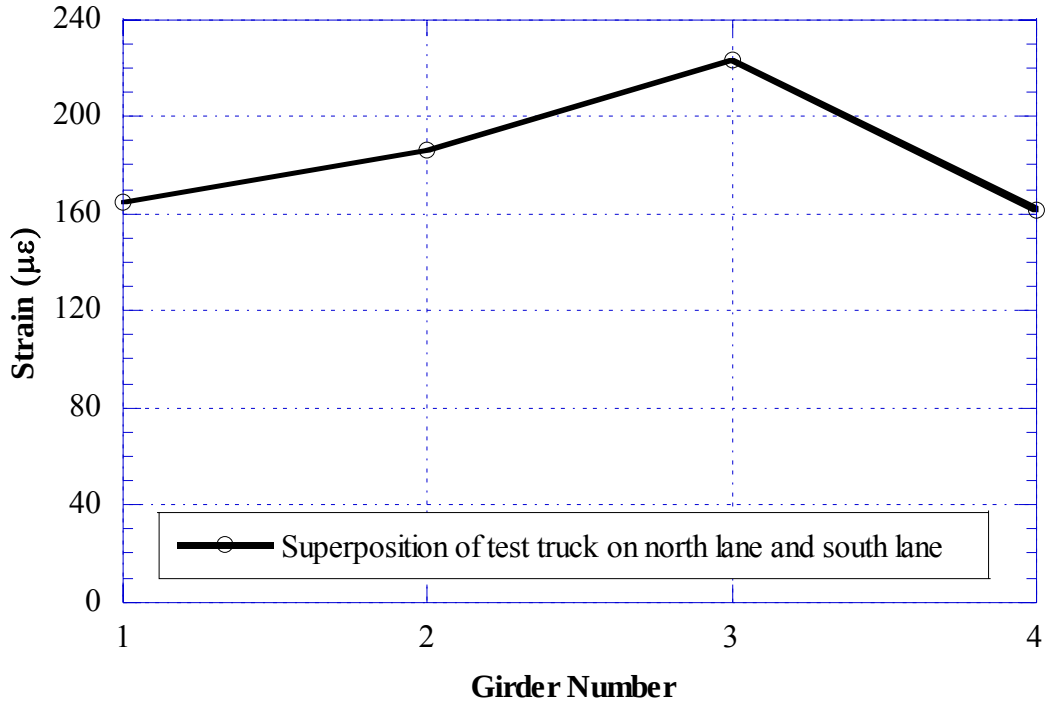

Figure 8.13 Positive Strain at Midspan of Eastspan, Side-by-Side Loading, Superposition (S01-12034)

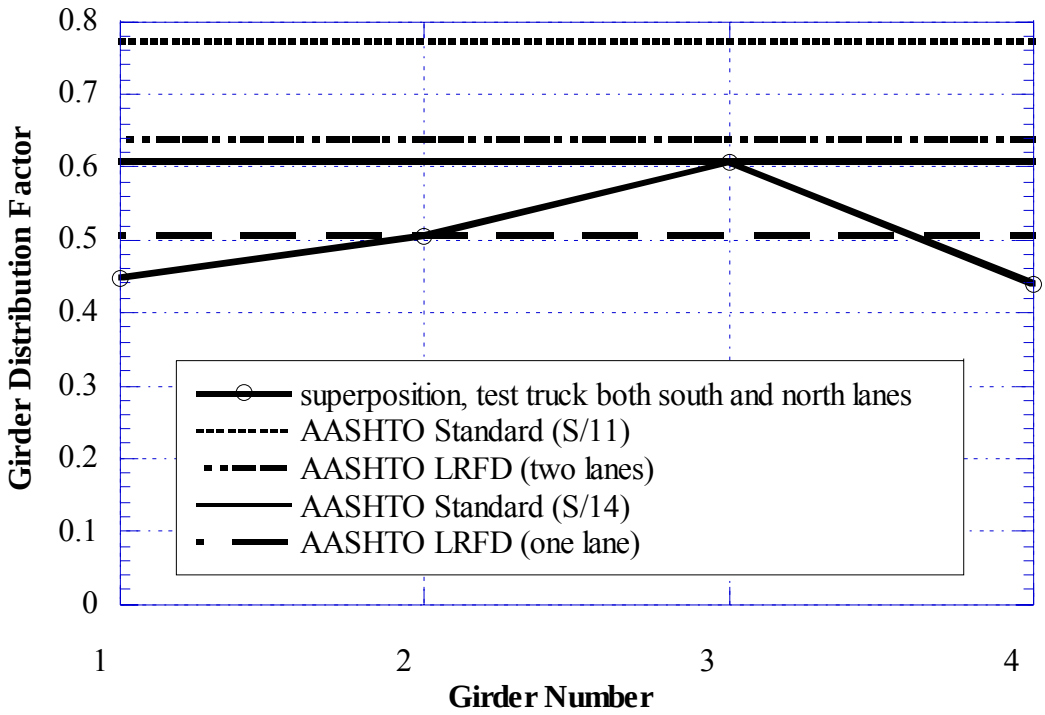

Figure 8.14 GDF from Positive Strain at Midspan of Eastspan, Side-by-Side Loading, Superposition (S01-12034)

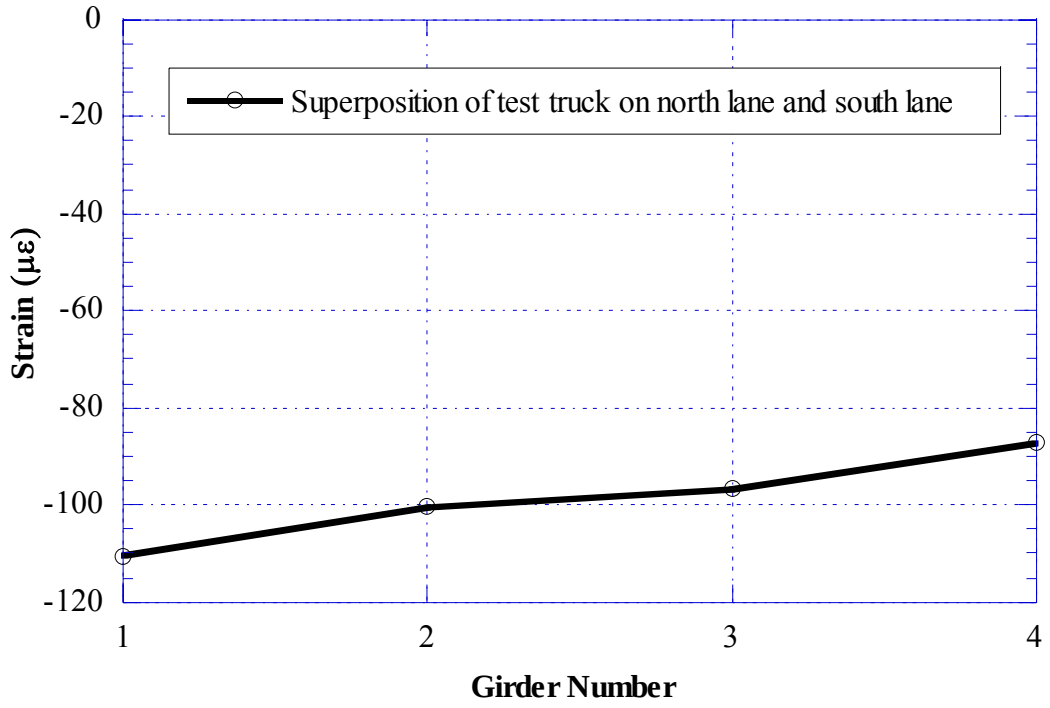

Figure 8.15 Negative Strain near Support over Pier, Side-by-Side Loading, Superposition (S01-12034)

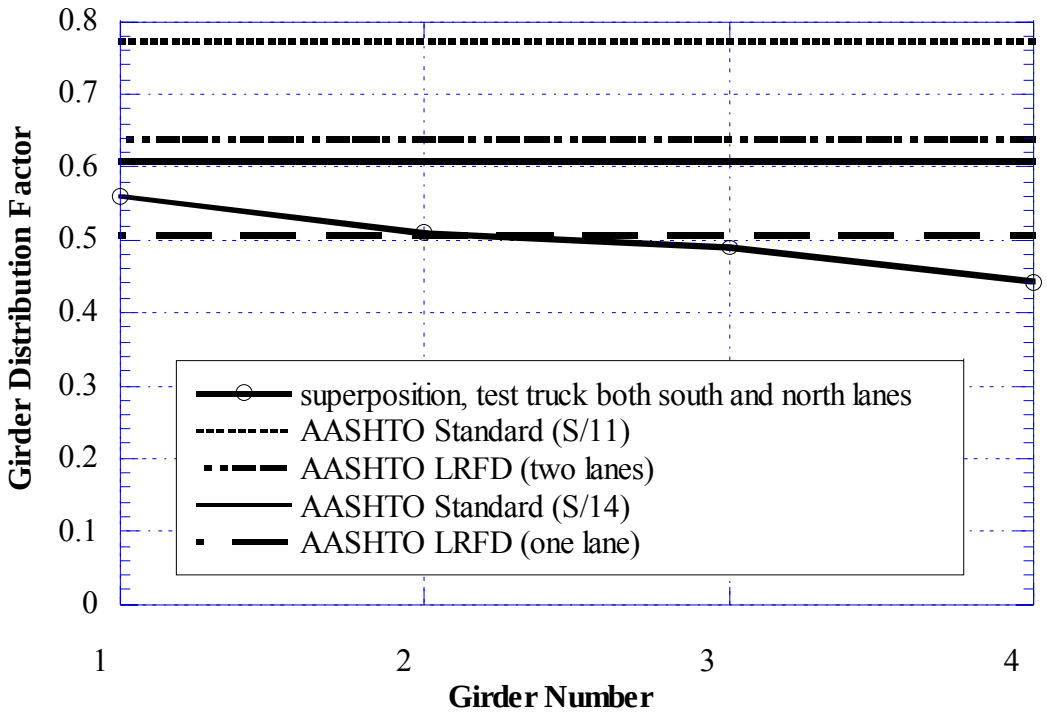

Figure 8.16 GDF from Negative Strain near Support over Pier, Side-by-Side Loading, Superposition (S01-12034)

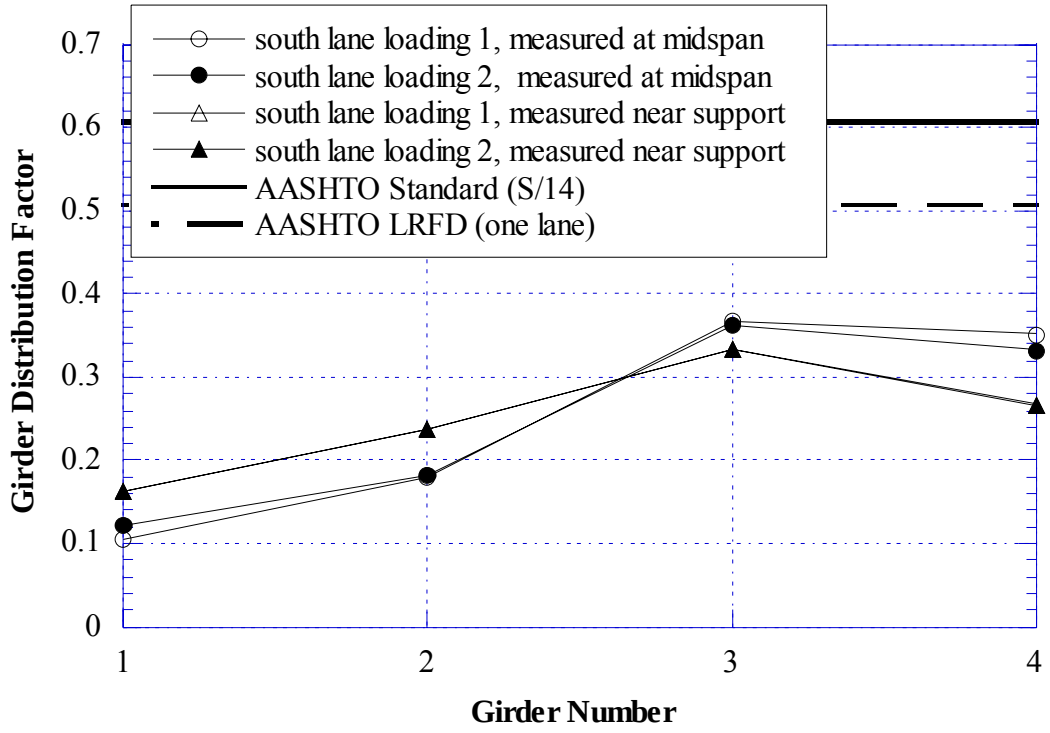

Figure 8.17 Comparison, GDF obtained from Positive Strain vs. GDF from Negative Strain, South Lane Loading (S01-12034)

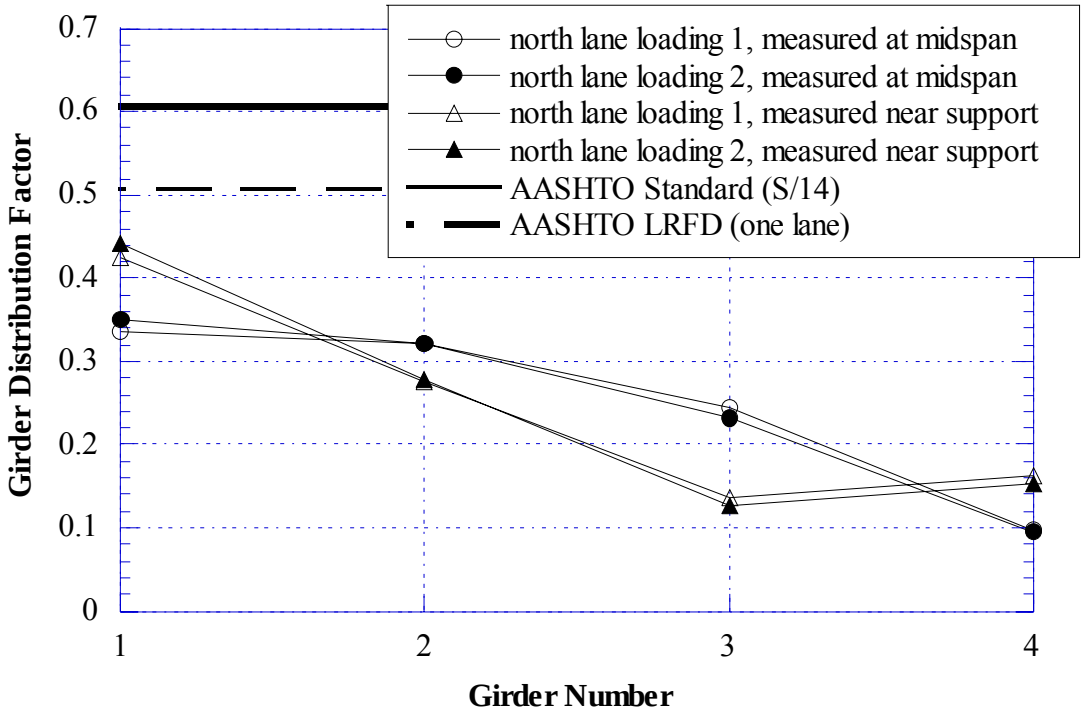

Figure 8.18 Comparison, GDF obtained from Positive Strain vs. GDF from Negative Strain, North Lane Loading (S01-12034)

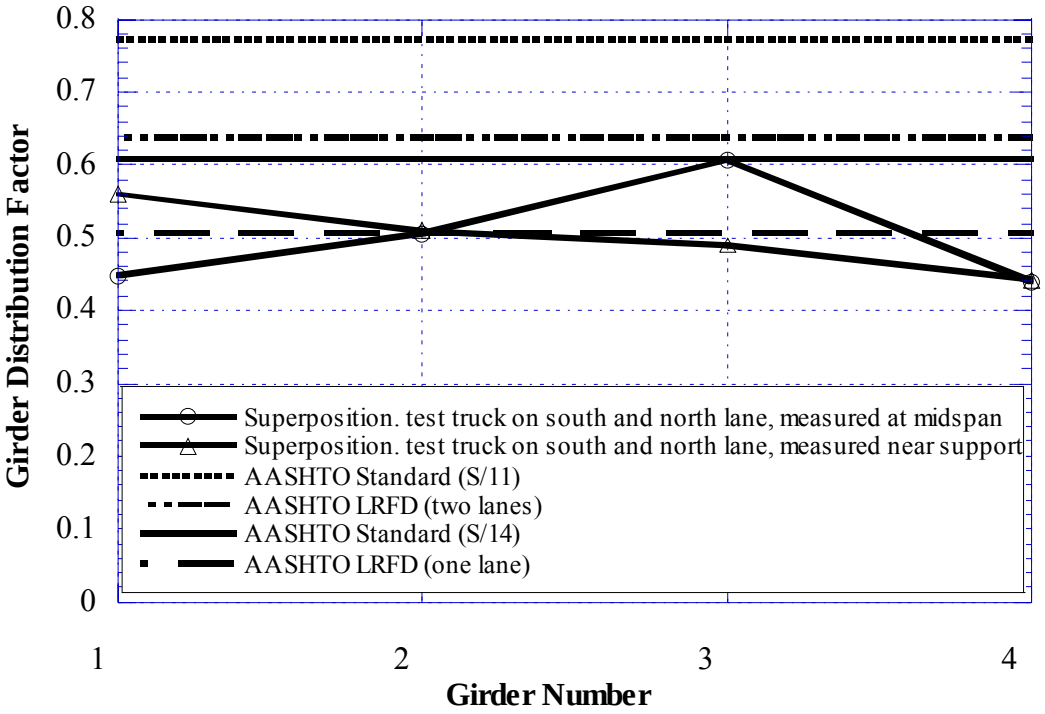

Figure 8.19 Comparison, GDF obtained from Positive Strain vs. GDF from Negative Strain, side-by-side loading (S01-12034)

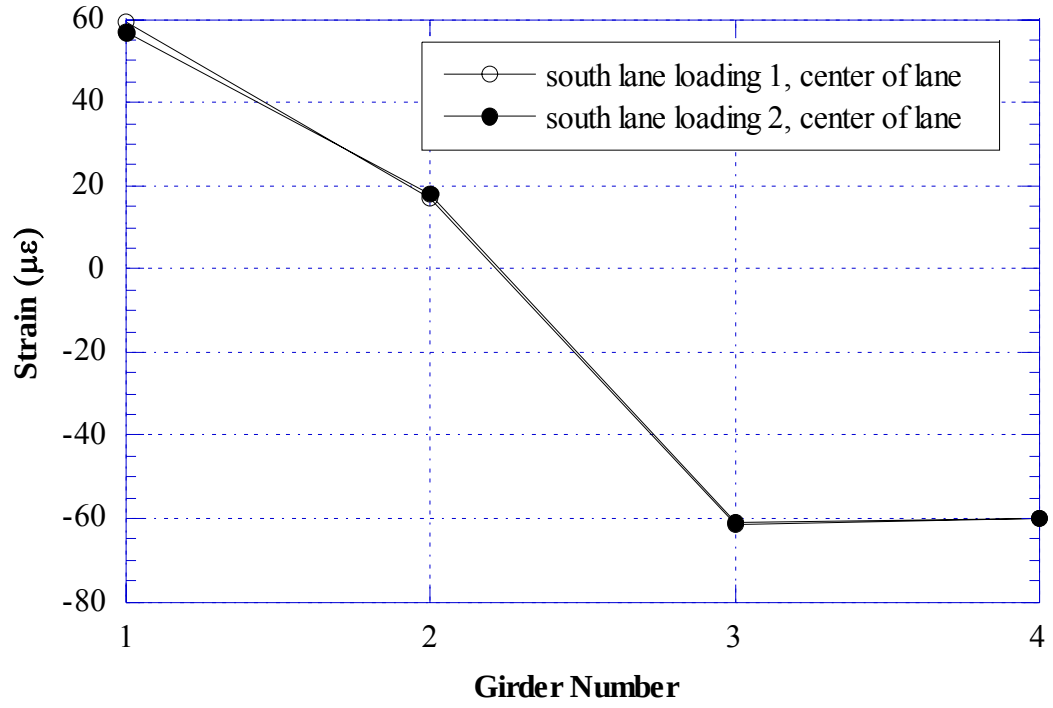

Figure 8.20 Strain near Support over East Abutment, South Lane Loading (S01-12034)

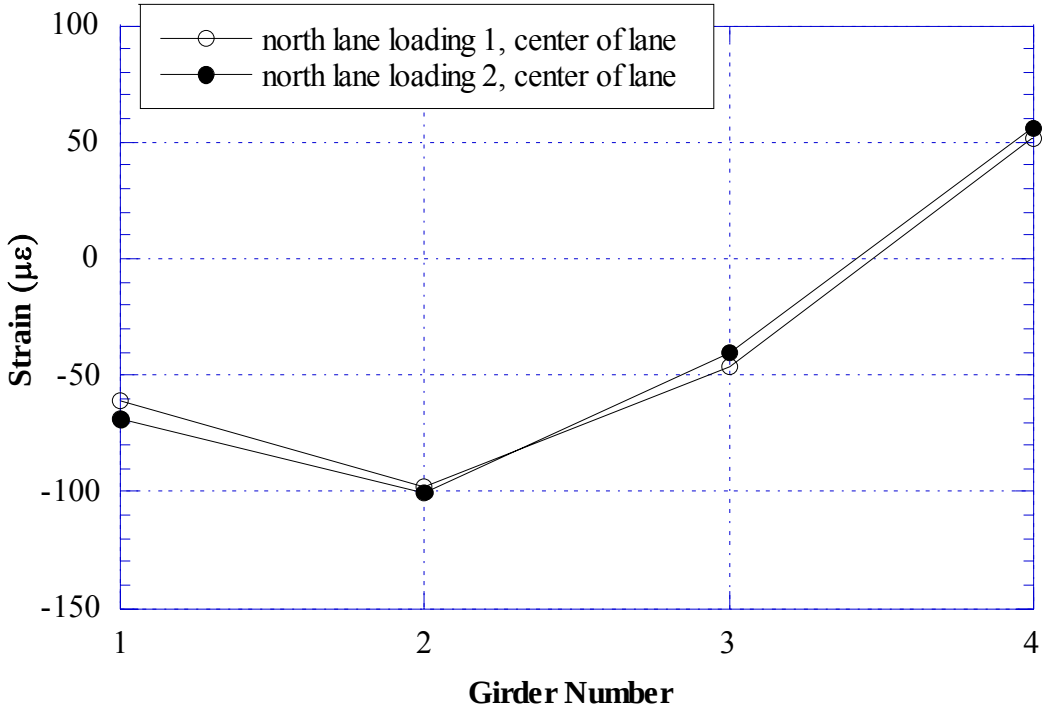

Figure 8.21 Strain near Support over East Abutment, North Lane Loading (S01-12034)

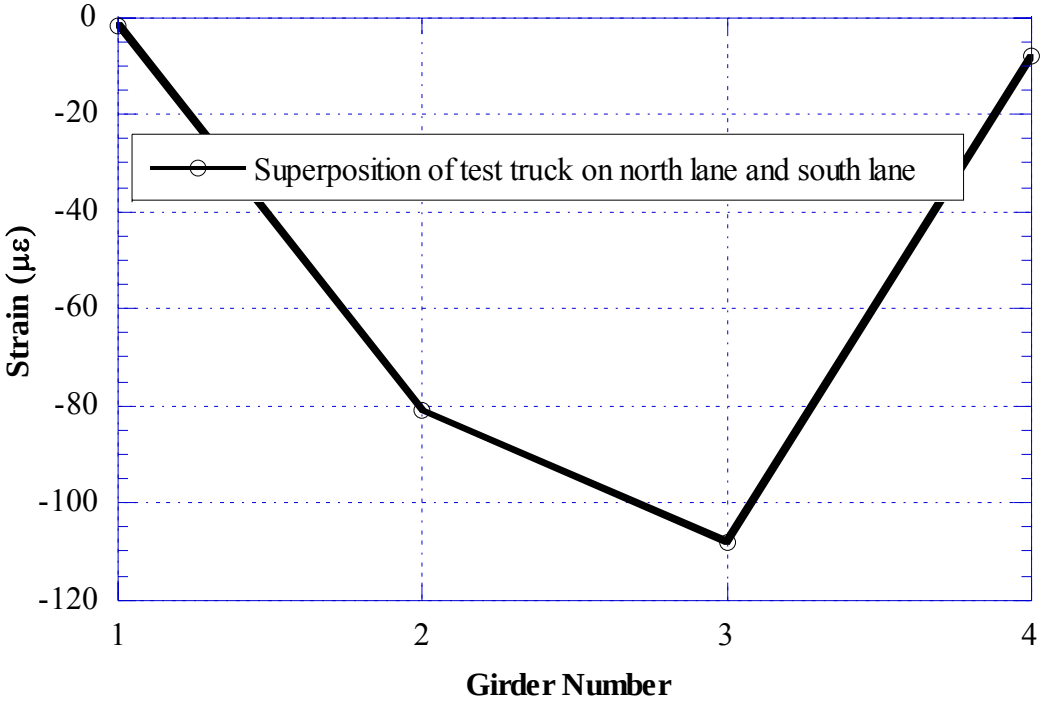

Figure 8.22 Strain near Support over East Abutment, Superposition of South and North Lane Loading (S01-12034)

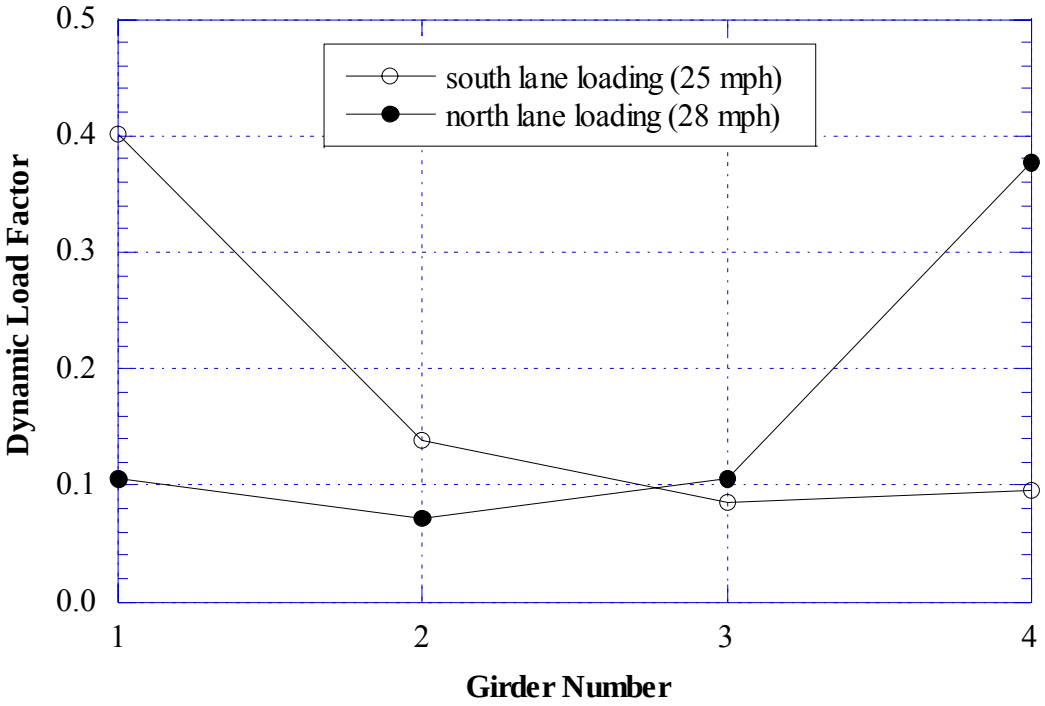

Figure 8.23 Dynamic Load Factors obtained from Positive Strain at Midspan of Southspan (S01-12034)

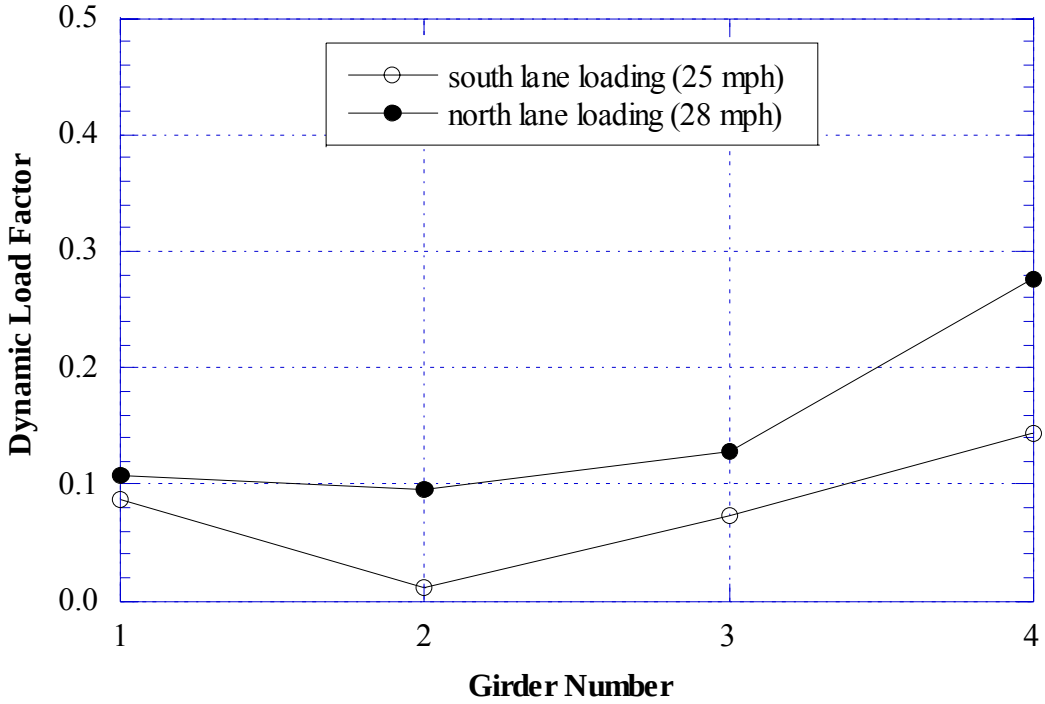

Figure 8.24 Dynamic Load Factors obtained from Negative Strain near Support over Pier (S01-12034)

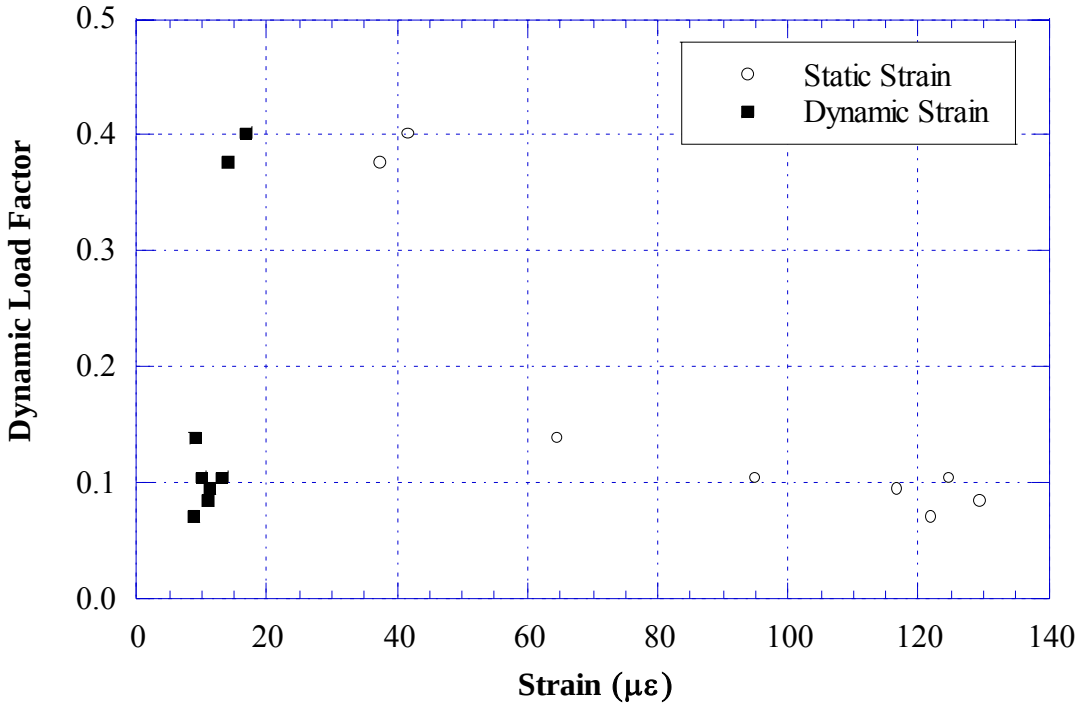

Figure 8.25 Strain vs. Dynamic Load Factors,
Based on Positive Strain at Midspan of Eastspan (S01-12034)

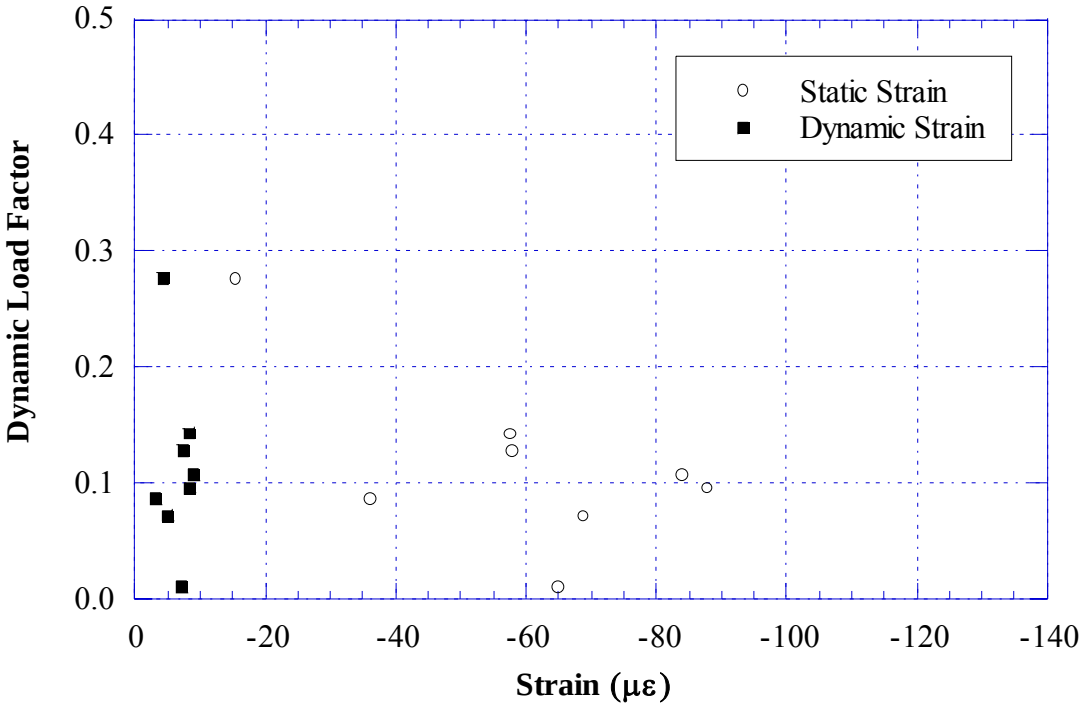

Figure 8.26 Strain vs. Dynamic Load Factors,
Based on Negative Strain near Support over pier (S01-12034)

8.5 Results of Finite Element Analysis

A three-dimensional finite element method (FEM) was applied to investigate the structural behavior of the bridge S01-12034. The concrete slab was modeled with isotropic, eight node solid elements, with three degrees of freedoms at each node. The girder flanges and web were modeled using three-dimensional, quadrilateral, four node shell elements with six degrees of freedom at each node. The structural effects of the secondary members, such as the sidewalk and parapet, were also taken into account in the finite element analysis models.

The mesh of the FEM model is shown in Figure 8.27. Total number of elements is 12,465, and total number of nodes is 17,193 for this model.

Strains and GDF's calculated for the considered model is shown in Figures 8.28 to 8.32. Figures 8.28 and 8.29 present strains and GDF's from FEM model for positive moment at the midspan under two trucks side-by-side loading. Figures 8.30 and 8.31 show the strains and GDF's from FEM model for negative moment near support over pier under two trucks side-by-side loading. In the figures, the values obtained from FEM analysis are compared with the superposition of corresponding measured values.

The resulting strain values obtained from field tests are lower than those from the finite element analysis for considered bridges. The main reason for low strains is due to the partial fixity of supports, as shown in Figures 8.20 to 8.22. In the previous study for simply supported bridges by University of Michigan (Nowak 2001 and 2002), the boundary conditions are simulated using the elastic spring elements in FEM models. However, for continuous bridges, it is almost impossible to obtain accurate spring coefficients satisfying multiple locations of supports with varied partial fixity condition. Therefore, in the study, the supports are assumed to behave as designed in the FEM models.

Figure 8.32 compares the GDF values for both positive moment and negative moment obtained from FEM analysis. The difference between GDF's for positive moment and negative moments is less than 10 percent.

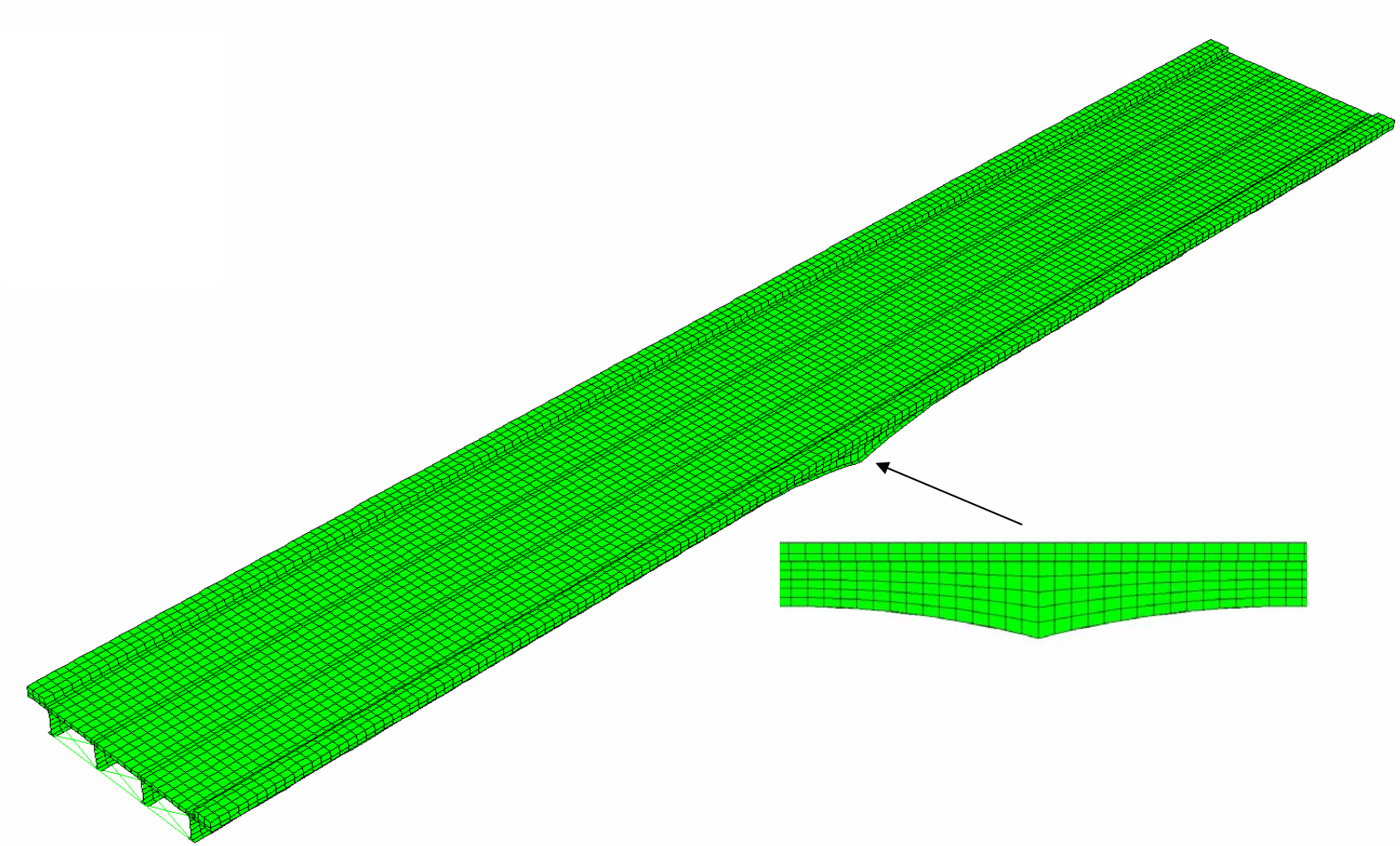

Figure 8.27 The Mesh of Finite Element Model, Bridge (S01-12034)

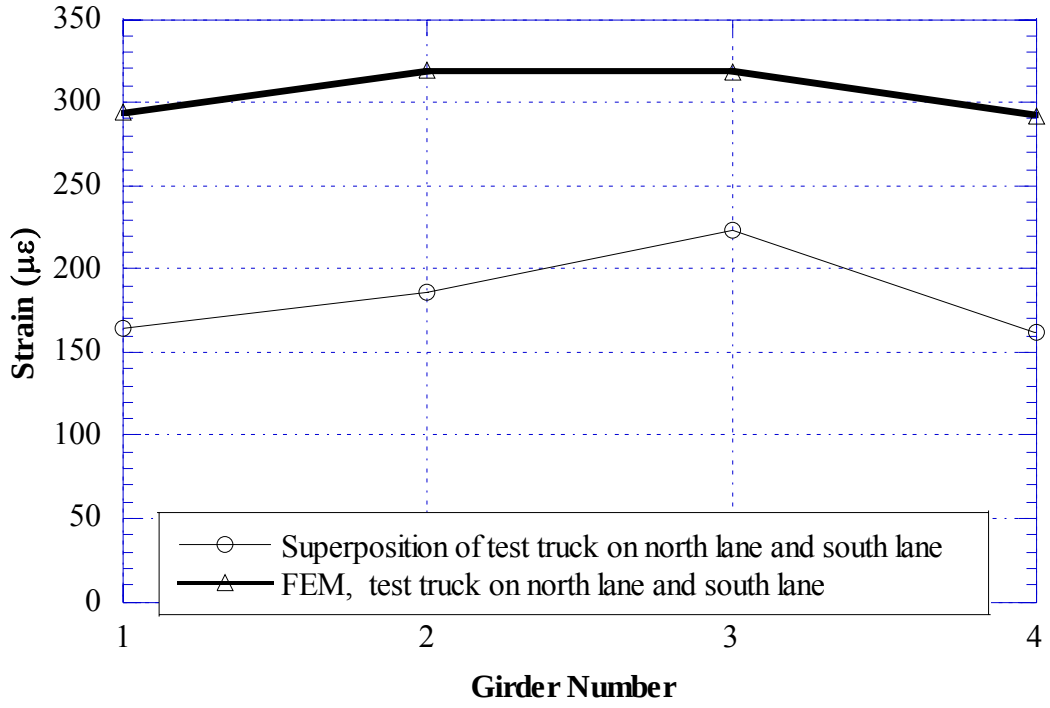

Figure 8.28 Comparison of FEM vs. Test, Positive Strain at Midspan of Eastspan, Side-by-Side Loading (S01-12034)

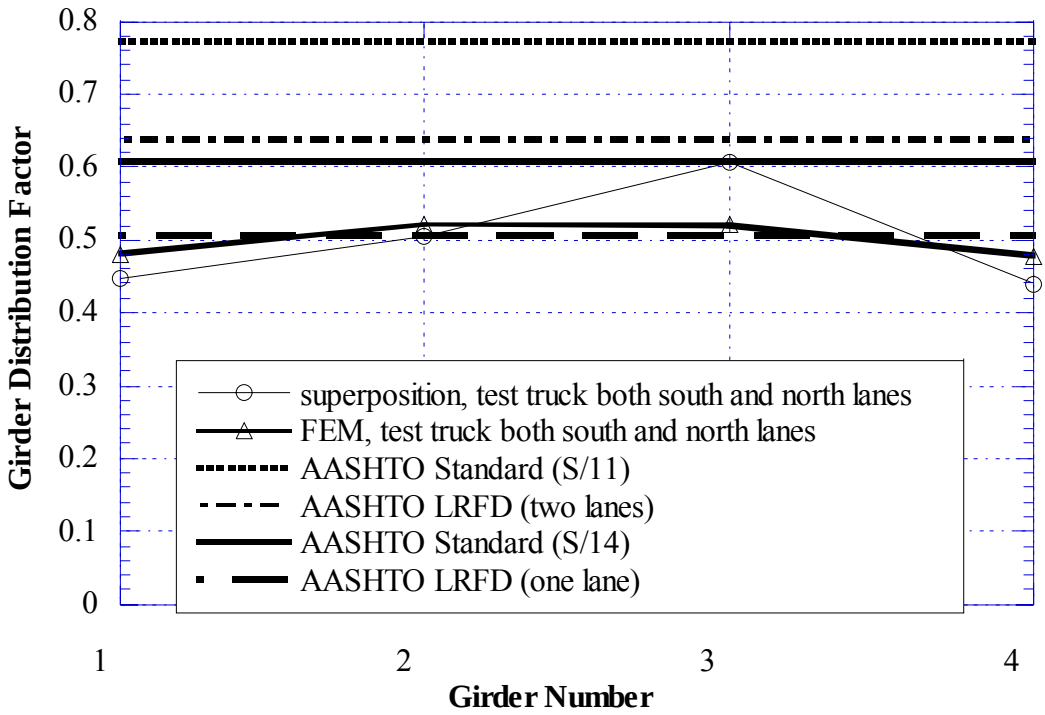

Figure 8.29 Comparison of FEM vs. Test, GDF Obtained from Positive Strain at Midspan of Eastspan, Side-by-Side Loading (S01-12034)

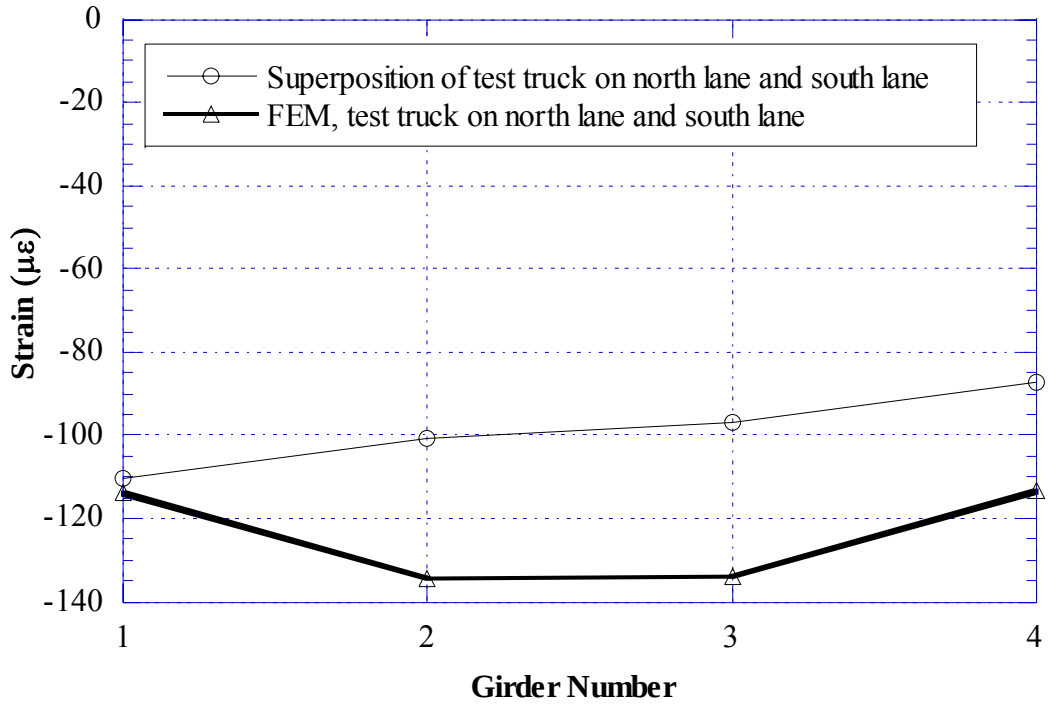

Figure 8.30 Comparison of FEM vs. Test, Negative Strain near Support over Pier, Side-by-Side Loading (S01-12034)

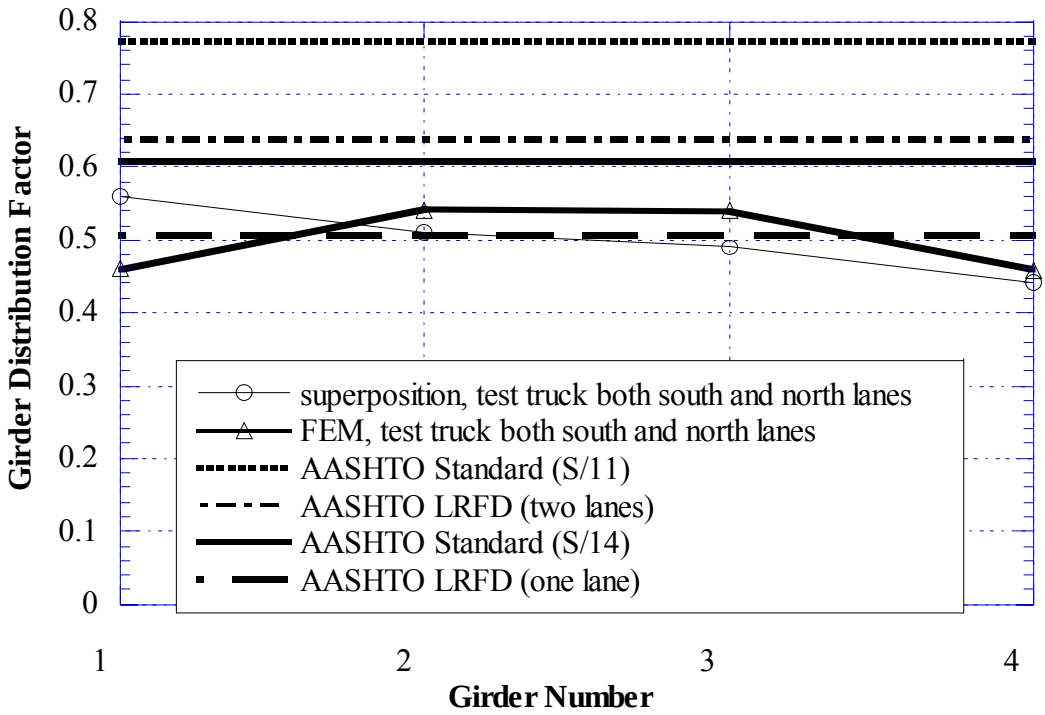

Figure 8.31 Comparison of FEM vs. Test, GDF Obtained from Negative Strain near Support over Pier, Side-by-Side Loading (S01-12034)

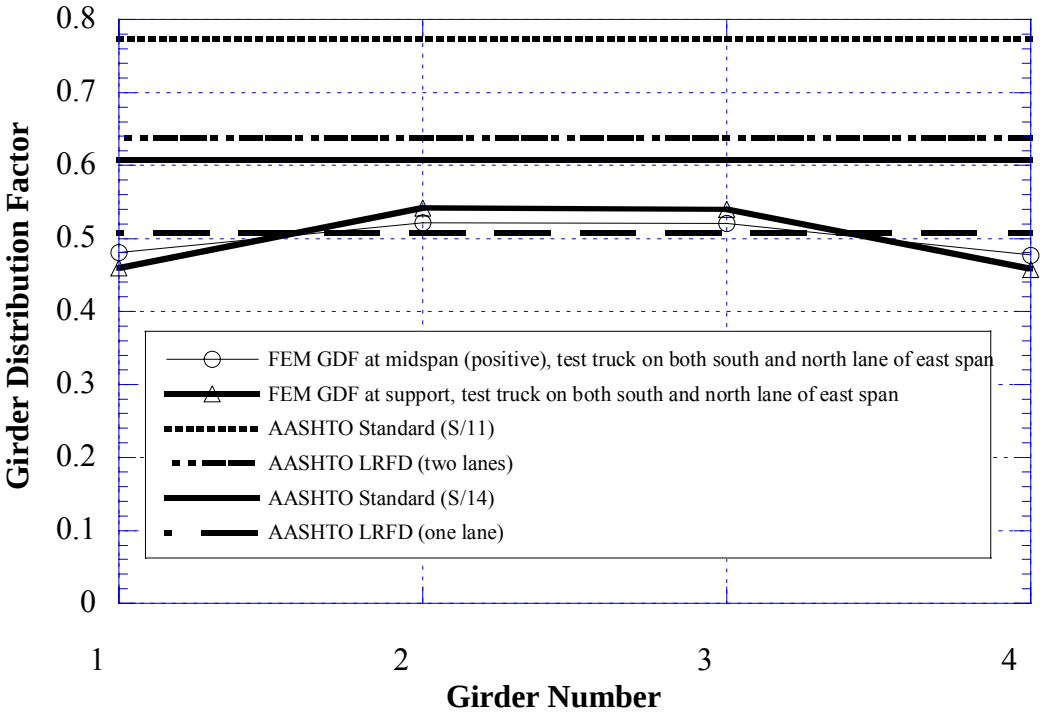

Figure 8.32 Comparison, GDF obtained from positive strain vs. GDF from Negative Strain, Based on Finite Element Analysis, Side-by-Side Loading (S01-12034)

Note:

Intentionally left blank

9. BRIDGE ON GOODELLS ROAD OVER I-69, ST.CLAIR COUNTY (S09-77023)

9.1 Bridge Description

This bridge was built in 1980 and it is located on Goodells Road over I-69, in St.Clair County, Michigan. It is a three span, continuous steel girder bridge, designed as a composite section. It has seven steel girders spaced at 8 ft 4 in, as shown in Figure 9.1, with 19 degree skew. The total bridge length is 370 ft. The side elevation is shown in Figure 9.2. The bridge has one lane in each direction and it carries an average daily traffic (ADT) of 1,460. The operating load rating is 246 kips, according to the Michigan Structure Inventory.

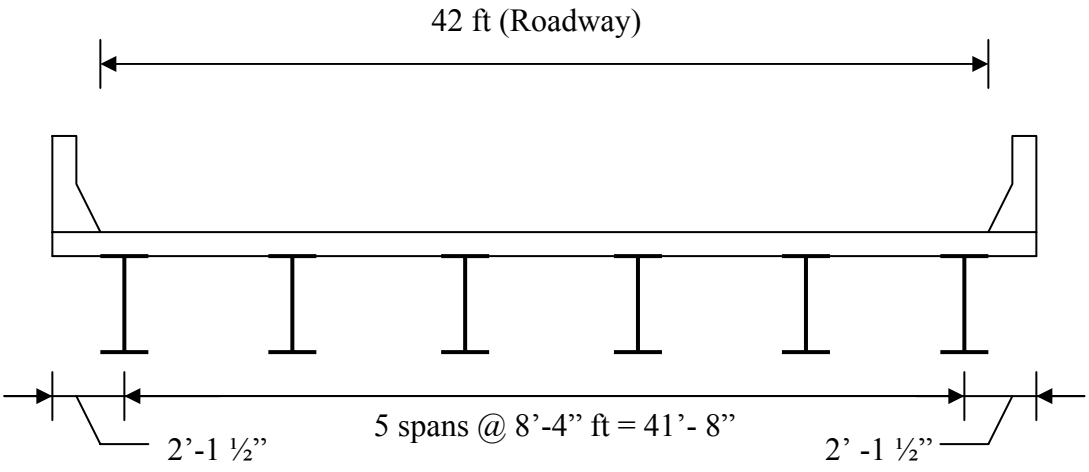

Figure 9.1 Cross Section of the bridge (S09-77023)

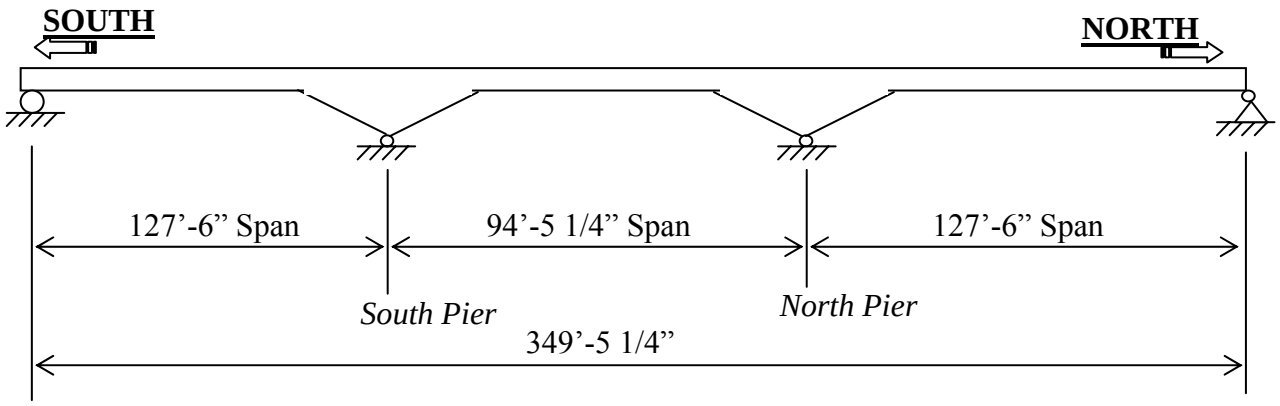

Figure 9.2 Side Elevation of Bridge (S09-77023)

9.2 Instrumentation

Strain transducers were installed on the bottom flanges of girders at midspan and at support locations, as shown in Figure 9.3. Strain gages were installed at all girders near support over south pier. However, over north pier only four interior girders were instrumented. The reflector for the PSM-R device from Noptel was installed at the girder No. 3 to measure deflection. The bridge was instrumented on July 9, 2002, and bridge test were performed on July 10, 2002.

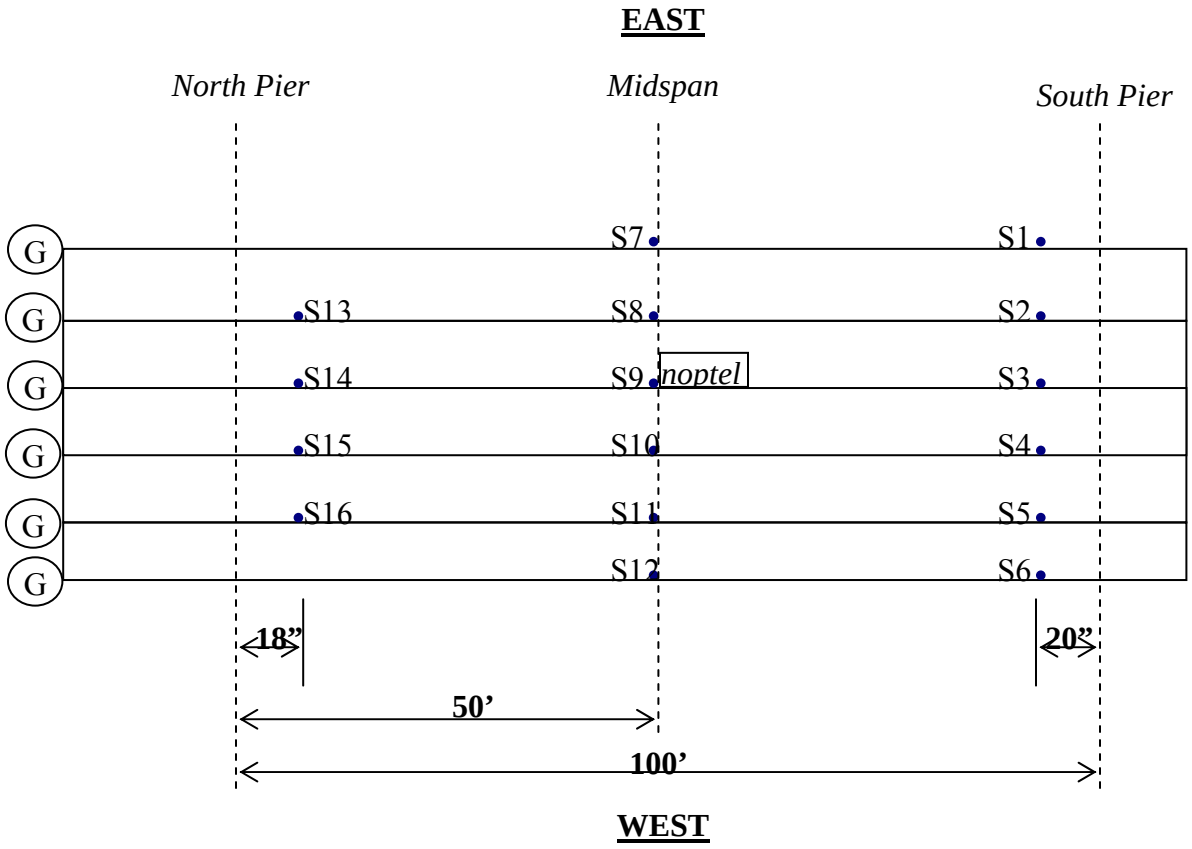

Figure 9.3 Strain Gage Location in Center Span of Bridge (S09-77023)

9.3 Load cases

The girder distribution factors (GDF) and dynamic load factors (DLF) were calculated using the strains measured at midspan. The bridge was loaded with two 11-axle trucks (three-unit vehicles).

The truck A and truck B have gross weights of 138 kips and 139 kips, with wheelbases of both 51 ft. Truck configurations are shown in Figures 9.4 and 9.5.

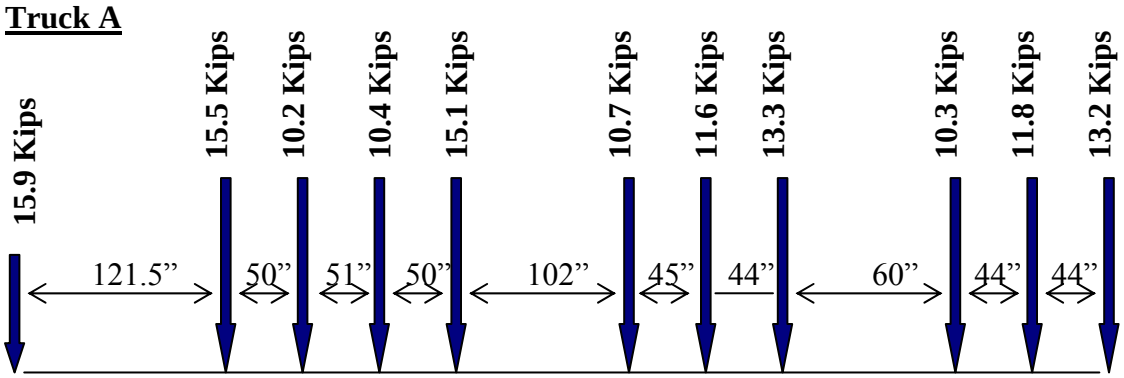

Figure 9.4 Truck A configuration, Bridge (S09-77023)

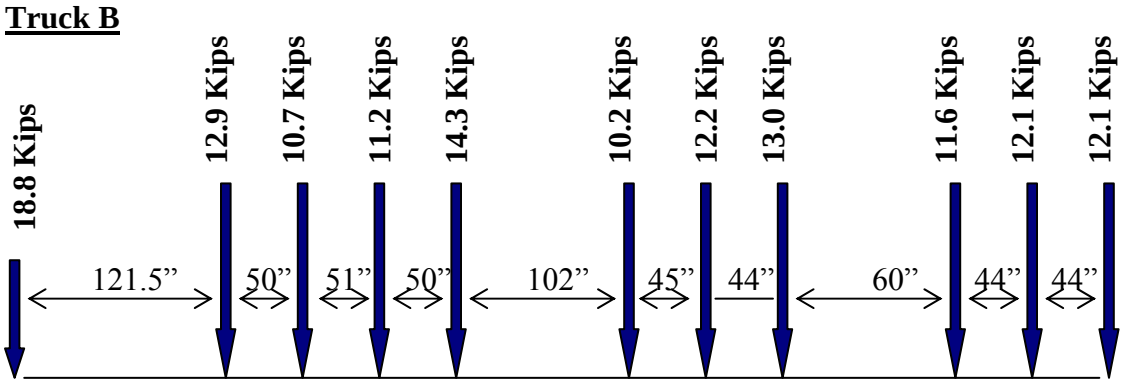

Figure 9.5 Truck B configuration, Bridge (S09-77023)

A total of 24 load cases were considered, as shown in Table 9.1. First each truck was driven by itself at the center of each lane, at crawling speed. Then, the same truck was driven close to the curb. The runs in the center of the lane were repeated at a normal highway speed. In addition, two trucks were driven simultaneously, side-by-side, at crawling speed and normal highway speed. For side-by-side cases, the runs were repeated after the trucks switched lanes, i.e. first truck A was in east lane, and B in west lane, then truck A was in west lane, and B in east lane. Then one truck was driven, followed by the other truck for each lane. In addition, trucks were stopped at predetermined position to verify pre-test calculation.

Table 9.1. Sequence of Test Runs, Bridge (S09-77023)

Run#	Truck	Lane Side	Position	Truck Speed
1	Truck A	East	Center	Crawling
2	Truck B	East	Center	Crawling
3	Truck A	West	Center	Crawling
4	Truck B	West	Center	Crawling
5	Truck A	East	Curb	Crawling
6	Truck B	East	Curb	Crawling
7	Truck A	West	Curb	Crawling
8	Truck B	West	Curb	Crawling
9	Truck A	East	Center	25 MPH
10	Truck B	East	Center	28 MPH
11	Truck A	West	Center	27 MPH
12	Truck B	West	Center	28 MPH
13	Truck A and Bboth	side-by-side	Center	Crawling
14	Truck B and Aboth	side-by-side	Center	Crawling
15	Truck A and Bboth	side-by-side	Center	17 MPH
16	Truck B and Aboth	side-by-side	Center	19 MPH
17	Truck A followed by B	East	Center	Crawling
18	Truck A followed by B	West	Center	Crawling
19	Truck B followed by A	East	Center	Crawling
20	Truck B followed by A	West	Center	Crawling
21	Truck A followed by B	East	Center	Stop at fixed position
22	Truck A followed by B	West	Center	Stop at fixed position
23	Truck B followed by A	East	Center	Stop at fixed position
24	Truck B followed by A	West	Center	Stop at fixed position

9.4 Test results

The resulting strains and GDF's are shown in Figures 9.6 through 9.17. Figures 9.6 to 9.13 present the results for one truck on the bridge under crawling-speed (static) tests. For each loading condition, strains are measured and the corresponding GDF's are calculated from the strain measurement. For comparison, GDF are also calculated according to AASHTO Standard (2002) and AASHTO LRFD Code (1998). The resulting GDF's are shown in Figures 9.6 through 9.13. Figures 9.6 to 9.9 show positive strain values recorded at the midspan of centerspan, and also resulting GDF's. Figures 9.10 to 9.13 present the negative strain values and corresponding GDF's near supports over south pier. For single lane loading, the maximum positive strain is about 160 με. This strain value corresponds about 4.6 ksi. The maximum negative strain near support is less than 125 με. This corresponds about 3.6 ksi. Strain values tend to be higher when the truck is positioned close to curb. For single lane loadings on the center of lanes, the measured GDF's do not exceed code specified values. However, when the truck is very close to curb, GDF's can exceed the specified values in AASHTO LRFD (1998) for single lane loading. Still, GDF specified in AASHTO Standard (2002) is conservative in all considered cases.

Figures 9.14 to 9.17 present the results for side-by-side static loading on the bridge under crawling-speed (static) tests. For two trucks side-by-side, strains are measured and the corresponding GDF's are calculated from the strain measurement. For comparison, GDF are also calculated according to code specified values. Figure 9.14 presents the measured positive strains under two trucks side by side, and Figure 9.15 show corresponding GDF's compared with code specified values. For two trucks side by side, the maximum recorded positive strain at the midspan is about 200 με, which corresponds about 5.8 ksi. Figure 9.15 shows that code specified GDF's are conservative. Even the single lane GDF specifed in AASHTO Standard (2002) is sufficient for two trucks side by side. However, single lane GDF specified in AASHTO LRFD (1998) is not sufficient for two lane load case in this bridge.

Figures 9.16 and 9.17 present the negative strains and GDF's under two truck side by side loading measured near support over north pier. Figure 9.16 presents the measured negative strains, and Figure 9.17 shows corresponding GDF's compared with code specified values. The maximum recorded negative strain near support at the midspan is about 130 με, which corresponds about 3.8 ksi. Figure 9.17 shows that code specified GDF's are conservative. As in GDF's for positive moments, even the single lane GDF specifed in AASHTO Standard (2002) is sufficient for two trucks side by side. However, single lane GDF specified in AASHTO LRFD (1998) is not sufficient for two lane load case in this bridge.

In all cases, the superposition of strains due to a single truck in West and East lanes produces almost the same results as strain due to two trucks side-by-side, as shown in Figures 9.14 and 9.16.

Figures 9.18 and 9.19 present the comparison of GDF's for positive and negative moment obtained from single lane loadings. GDF's specified in AASHTO Standard (2002) is very conservative in all cases. However, when the truck is very close to curb, the measured GDF can exceed the GDF's specified in AASHTO LRFD (1998).

Figure 9.20 compares the GDF's for positive and negative moment obtained from side-by-side loading. The figure indicates that code-specified GDF's are conservative for two truck side-by-side loading. For all considered two truck load cases, a single lane GDF specified in AASHTO Standard (2002) is also sufficient for two lane load cases for this bridge. However, a single lane GDF specified in AASHTO LRFD (1998) is not enough for two lane load cases for this bridge.

Figures 9.21 to 9.22 show the strain values measured near support over north pier. For the test, 16 strain gages were available. Therefore, It was decided during the instrumentation that at the midspan and south pier location, all girders should be instrumented, and only interior girders at north pier location. Therefore, GDF's were not calculated at north pier location. The maximum strain obtained at this location is about 130 με, which is very

close to the value from the south pier. Figure 9.23 compares the GDF's for positive and negative moment obtained from side-by-side loading.

In Figures 9.24 and 9.25, DLF's are plotted for all load cases involving normal speed (no dynamic load was measured for crawling speed runs). Figure 9.24 shows DLF's measured at the midspan (positive moment), and Figure 9.25 for negative moment (near support). As shown in the figures, dynamic load factors for exterior girders are high because the static strains in these girders are very low. In other words, large values of DLF in exterior girders correspond to load cases with a single truck in the opposite lane (resulting in very low static strain).

The relationship between DLF and static and dynamic strains is shown in Figures 9.26 and 9.27, for positive moment and negative moment, respectively. The open circles correspond to static strain, ε_{stat}, and black solid squares correspond to dynamic strain, ε_{dyn}. For each static strain value (open circle), the corresponding dynamic strain is denoted by solid square (the numbers of circles and squares are same). Dynamic strains remain nearly constant, while static strains increase as truck loading increases. This results in large dynamic load factors for low static strains. DLF corresponding to the maximum strain caused by two trucks side-by-side, is less than 0.05 for the most heavily loaded girder.

Girder No. 3 was instrumented with a remote deflection measurement device manufactured by Noptel. The reflector was installed at midspan. The result is shown in Table 9.2. The maximum deflection recorded during the test is 11.2 mm for girder No. 3 for two side-by-side trucks.

Table 9.2. Maximum deflections measured at the center of Girder No.3, Bridge (S09-77023)

Run #	Vertical Deflection (mm)
1	6.3
2	5.7
3	4.6
4	4.6
5	3.5
6	3.4
7	2.5
8	2.5
13	11.2
14	11.1

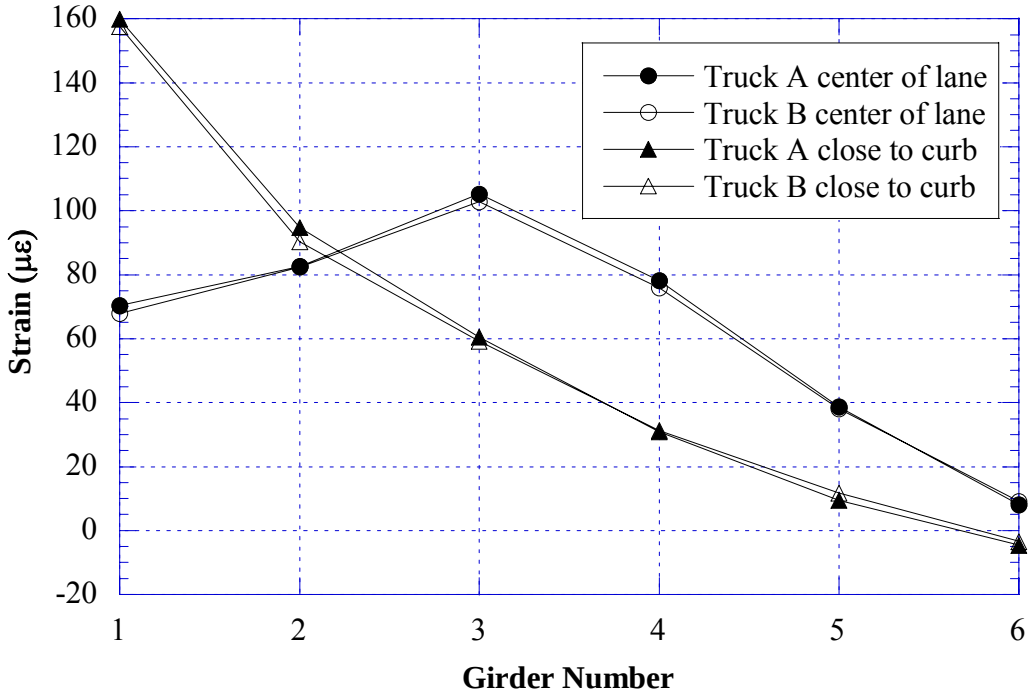

Figure 9.6 Positive Strain at Midspan of Centerspan, East Lane Loading (S09-77023)

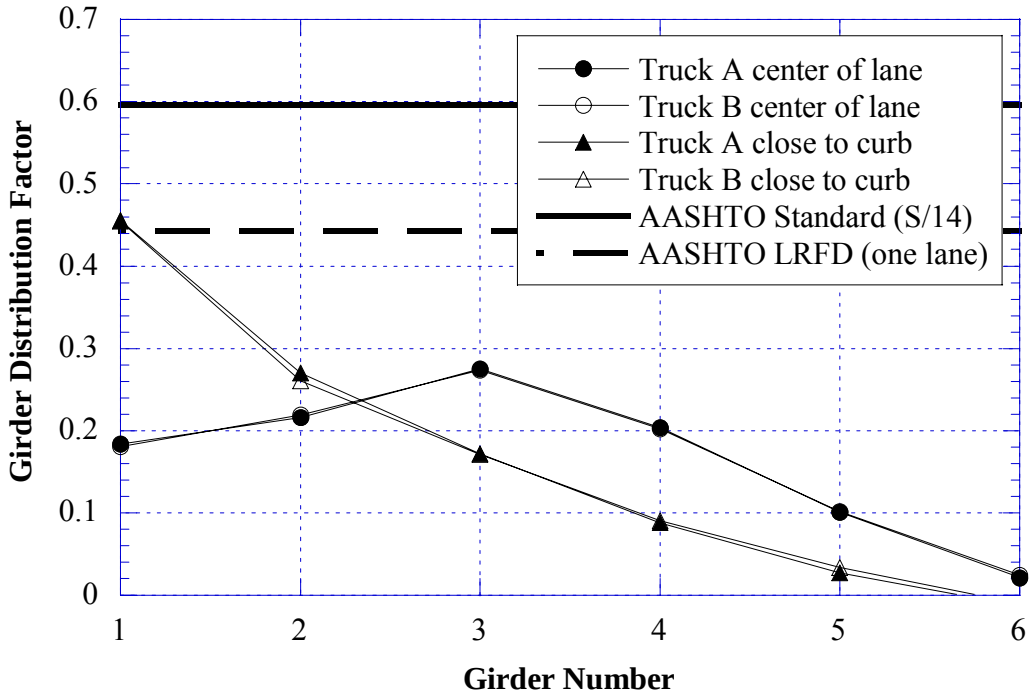

Figure 9.7 GDF from Positive Strain at Midspan of Centerspan, East Lane Loading (S09-77023)

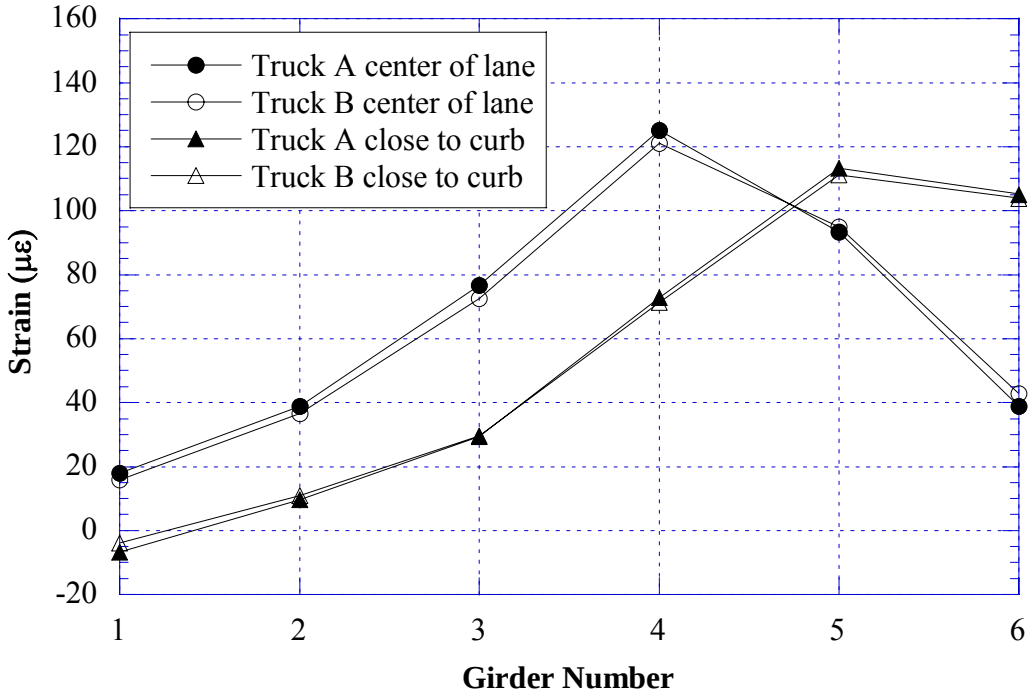

Figure 9.8 Positive Strain at Midspan of Centerspan, West Lane Loading (S09-77023)

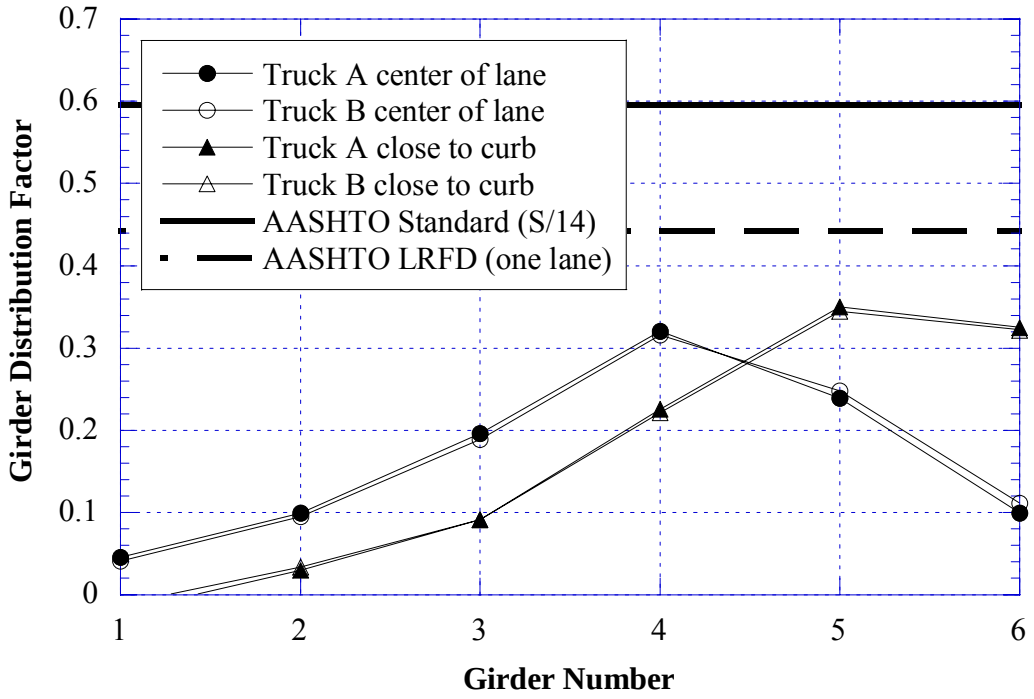

Figure 9.9 GDF from Positive Strain at Midspan of Centerspan, West Lane Loading (S09-77023)

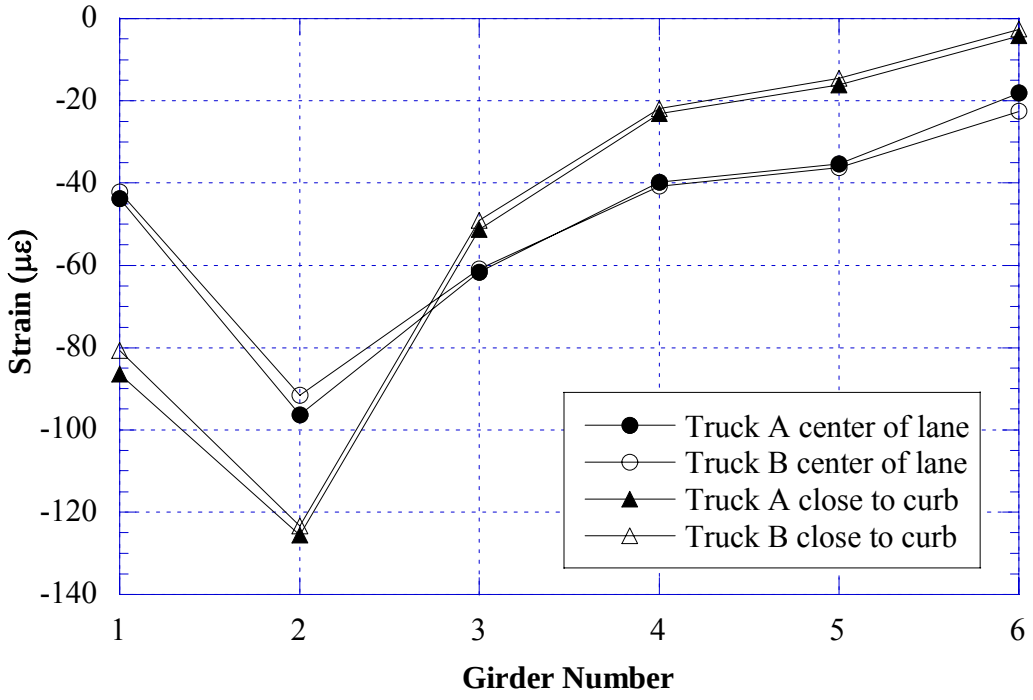

Figure 9.10 Negative Strain near Support over South Pier,
East Lane Loading (S09-77023)

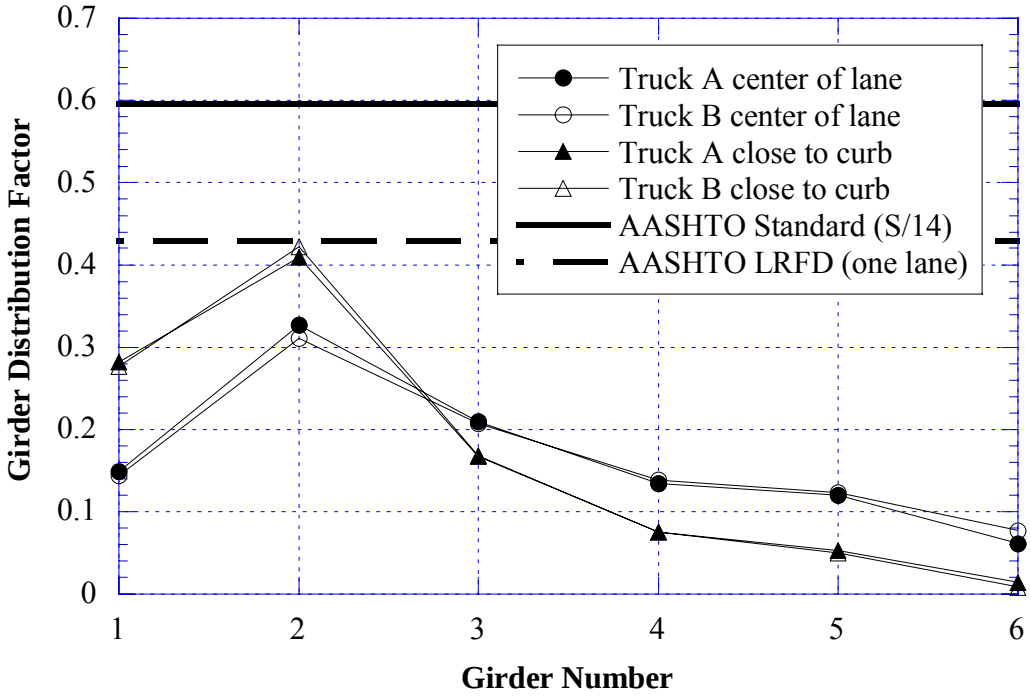

Figure 9.11 GDF from Negative Strain near Support over South Pier,
East Lane Loading (S09-77023)

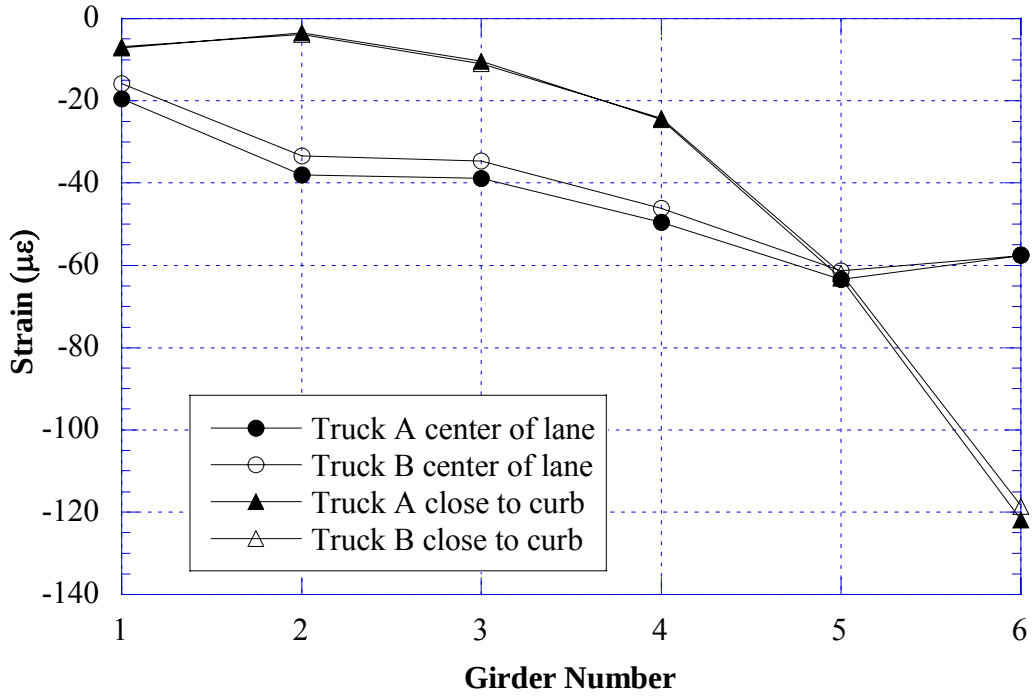

Figure 9.12 Negative Strain near Support over South Pier,
West Lane Loading (S09-77023)

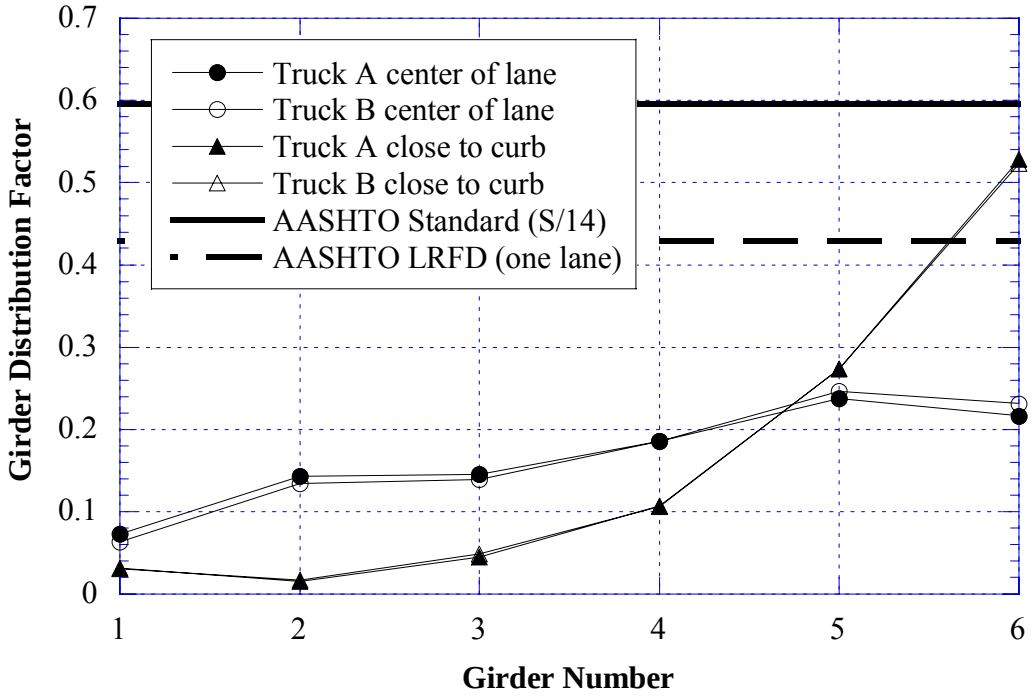

Figure 9.13 GDF from Negative Strain near Support over South Pier,
West Lane Loading (S09-77023)

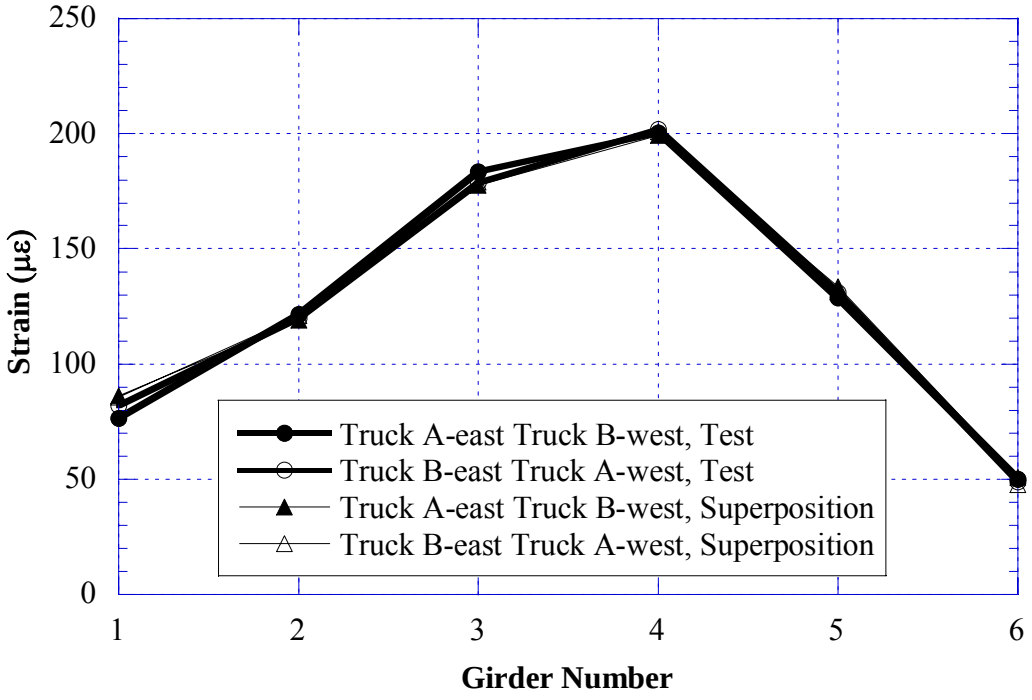

2Figure 9.14 Positive Strain at Midspan of Centerspan, Side-by-Side Loading (S09-77023)

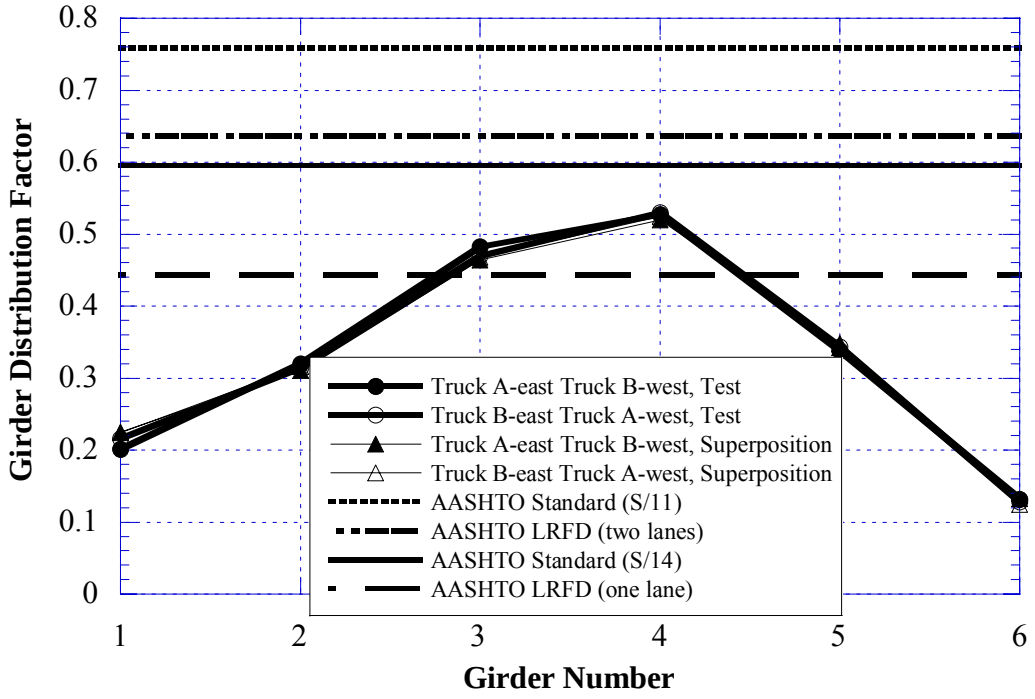

Figure 9.15 GDF from Positive Strain at Midspan of Centerspan, Side-by-Side Loading (S09-77023)

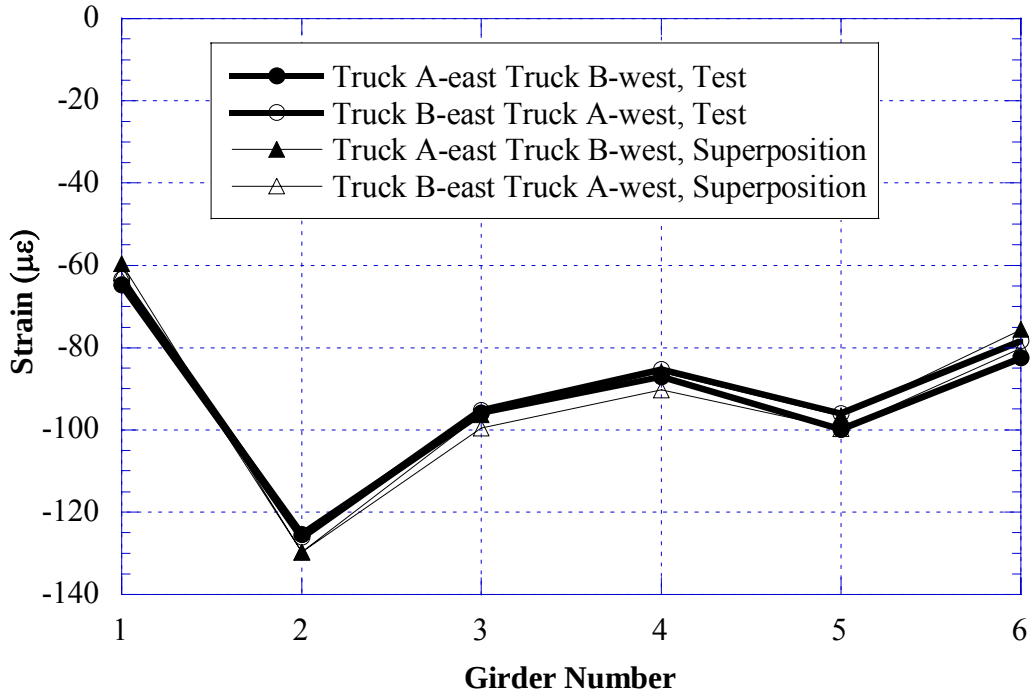

Figure 9.16 Negative Strain near Support over South Pier,
Side-by-Side Loading (S09-77023)

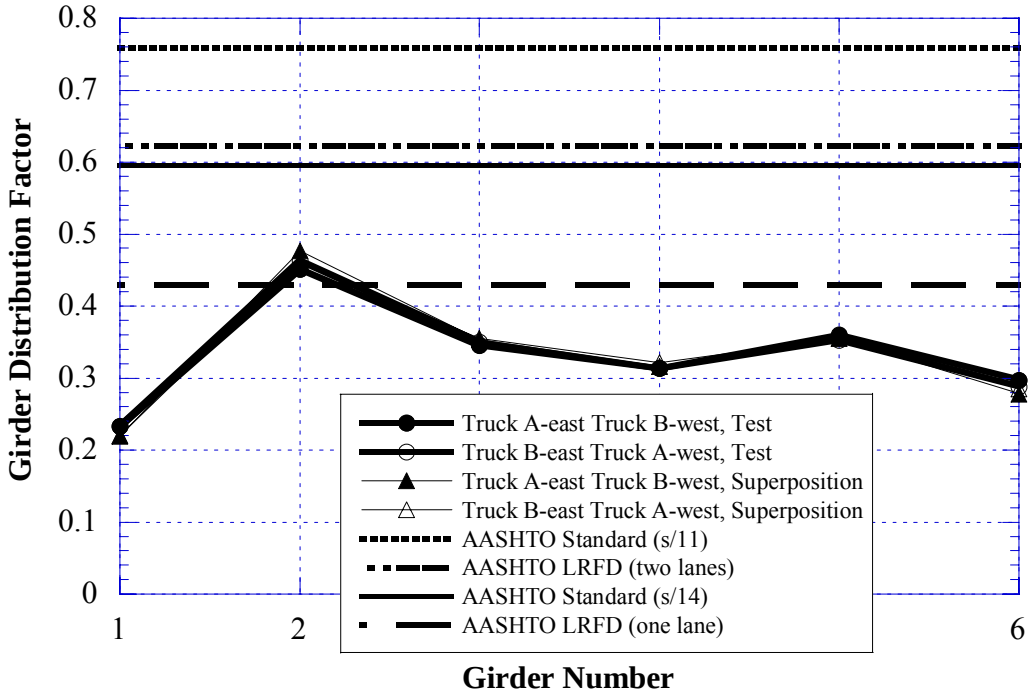

Figure 9.17 GDF from Negative Strain near Support over South Pier,
Side-by-Side Loading (S09-77023)

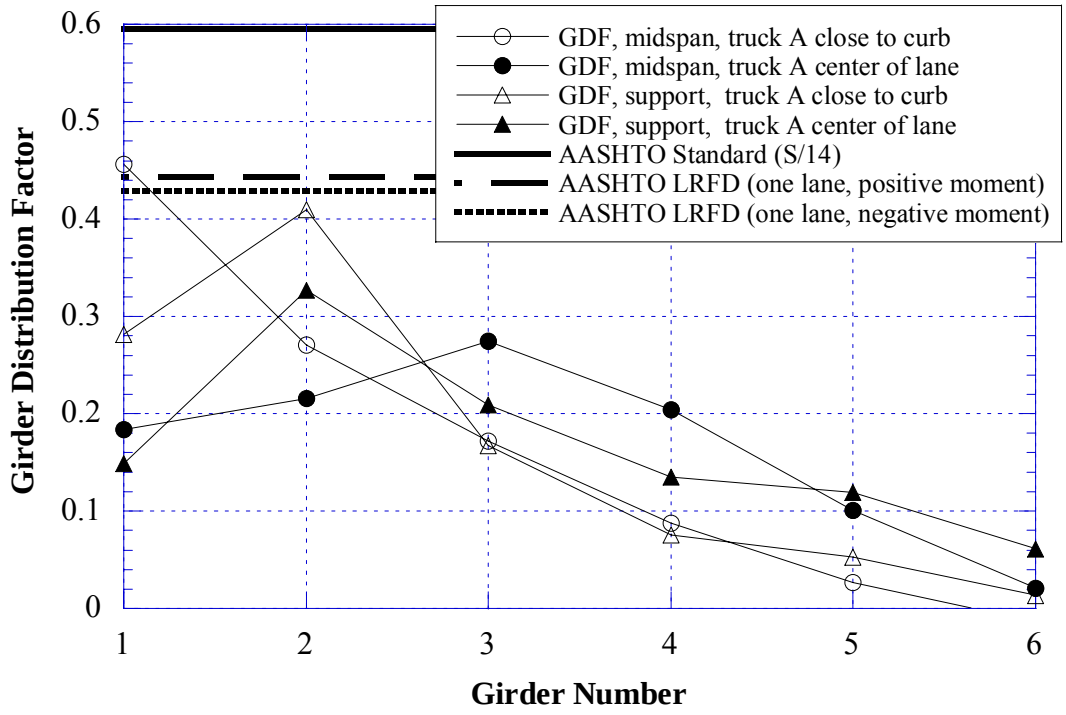

Figure 9.18 Comparison, GDF obtained from Positive Strain vs. GDF from Negative Strain, East Lane Loading (S09-77023)

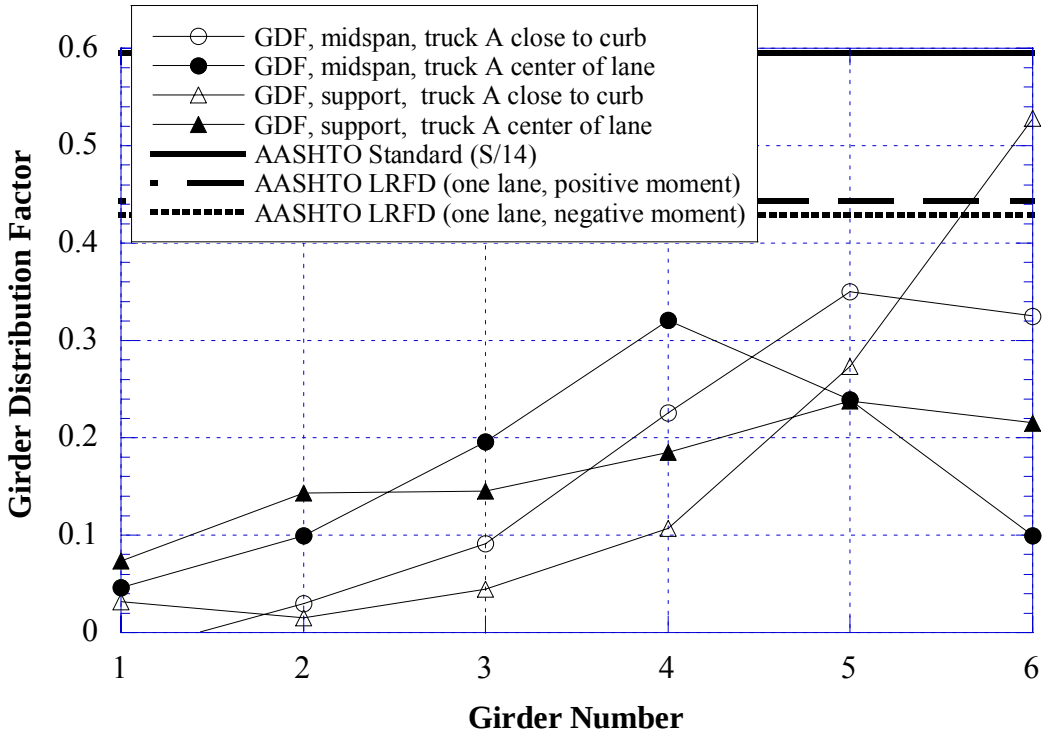

Figure 9.19 Comparison, GDF obtained from Positive Strain vs. GDF from Negative Strain, West Lane Loading (S09-77023)

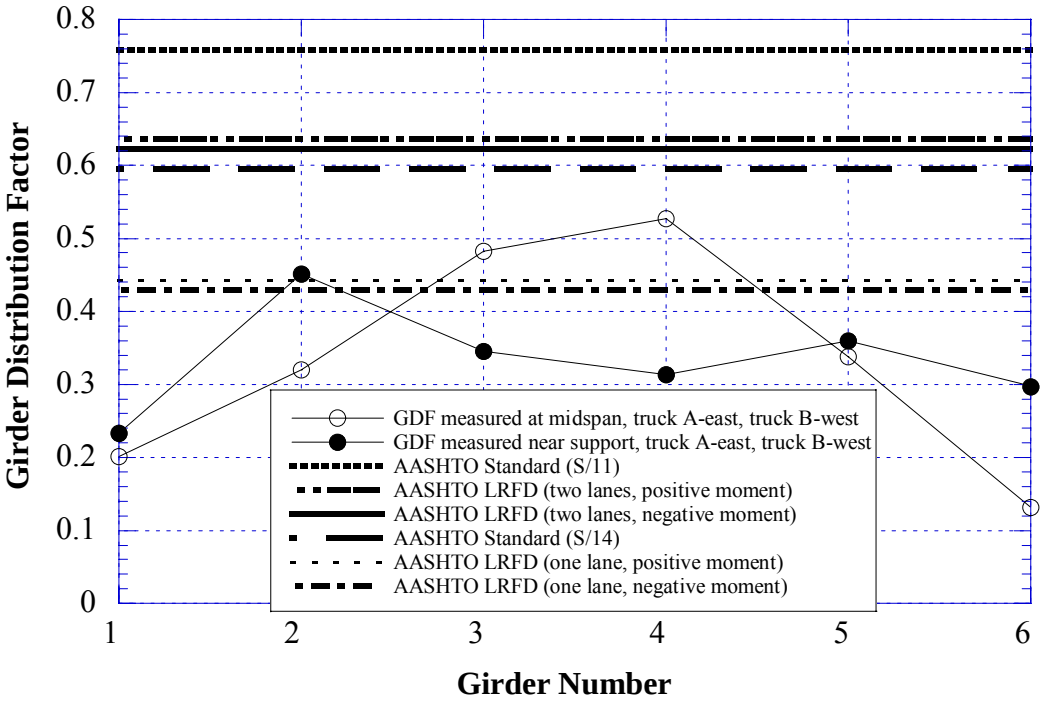

Figure 9.20 Comparison, GDF obtained from Midspan vs. GDF from Support, Side-by-Side Loading (S09-77023)

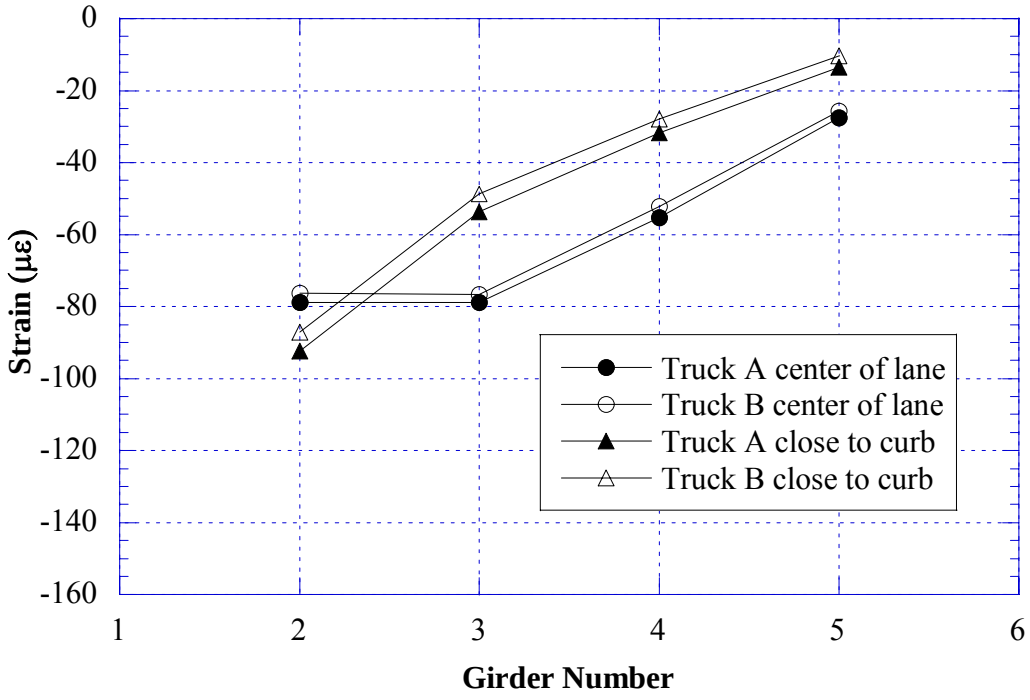

Figure 9.21 East Lane, Supports on North Pier, Crawling Speed (S09-77023)

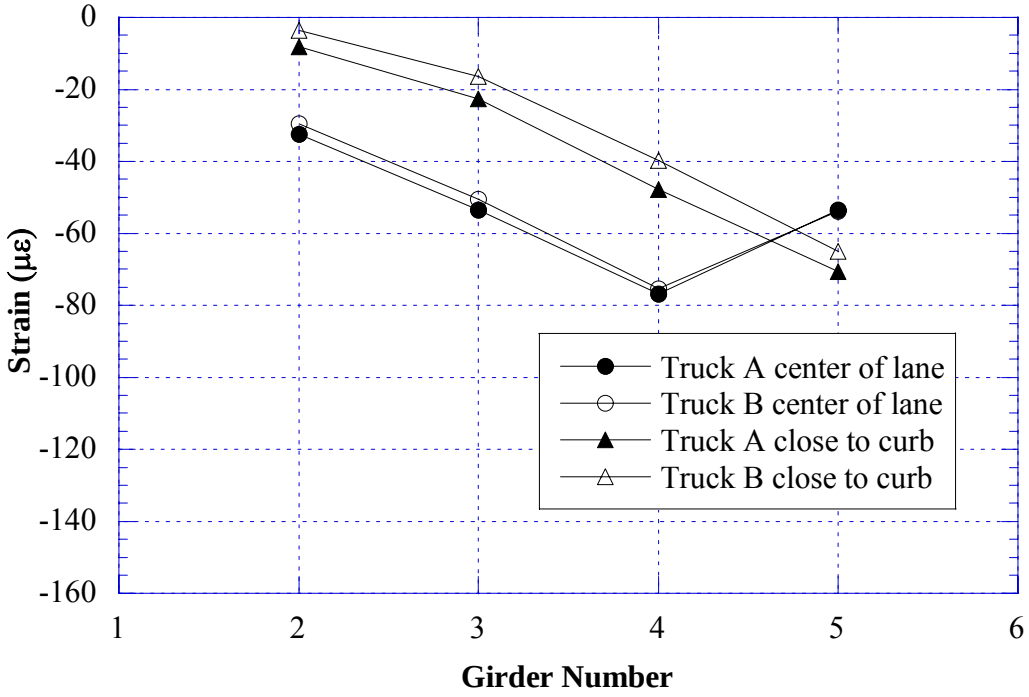

Figure 9.22 West Lane, Strain measured near Supports on North Pier, Crawling Speed (S09-77023)

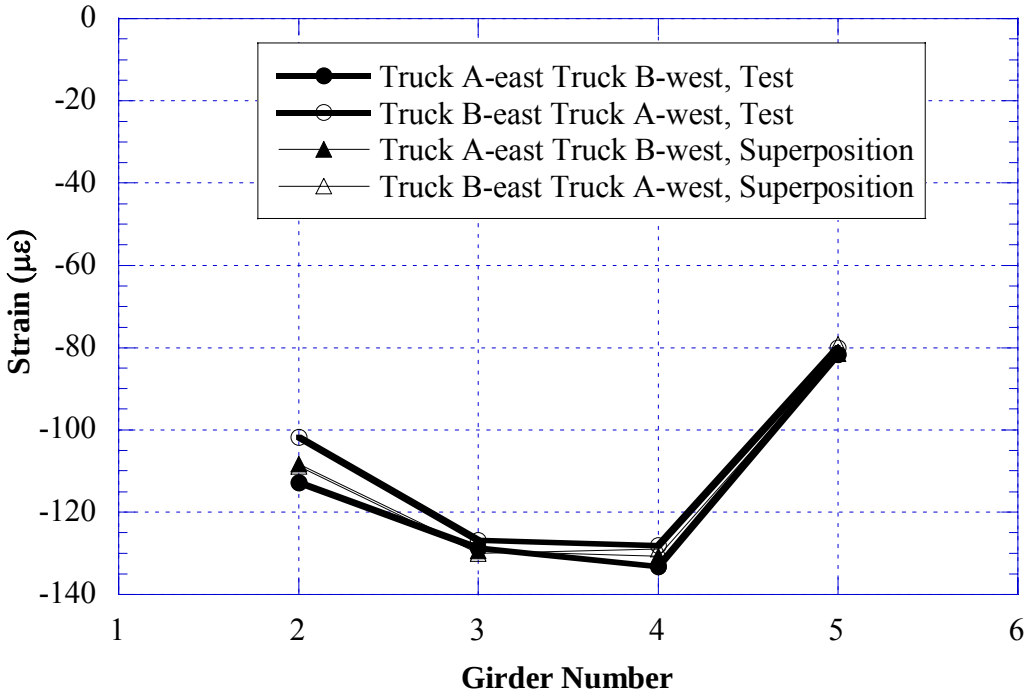

Figure 9.23 Side-by-Side Loading, Center of Lane, Strain measured near Supports on North Pier, Crawling Speed (S09-77023)

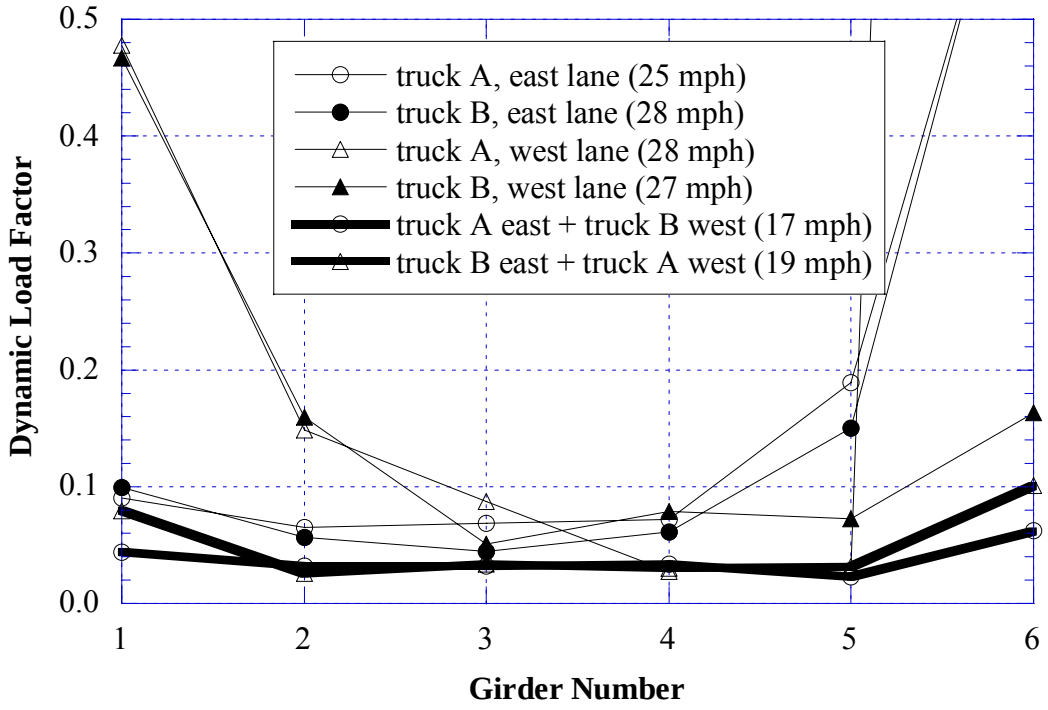

Figure 9.24 Dynamic Load Factors obtained from Positive Strain at Midspan of Centerspan (S09-77023)

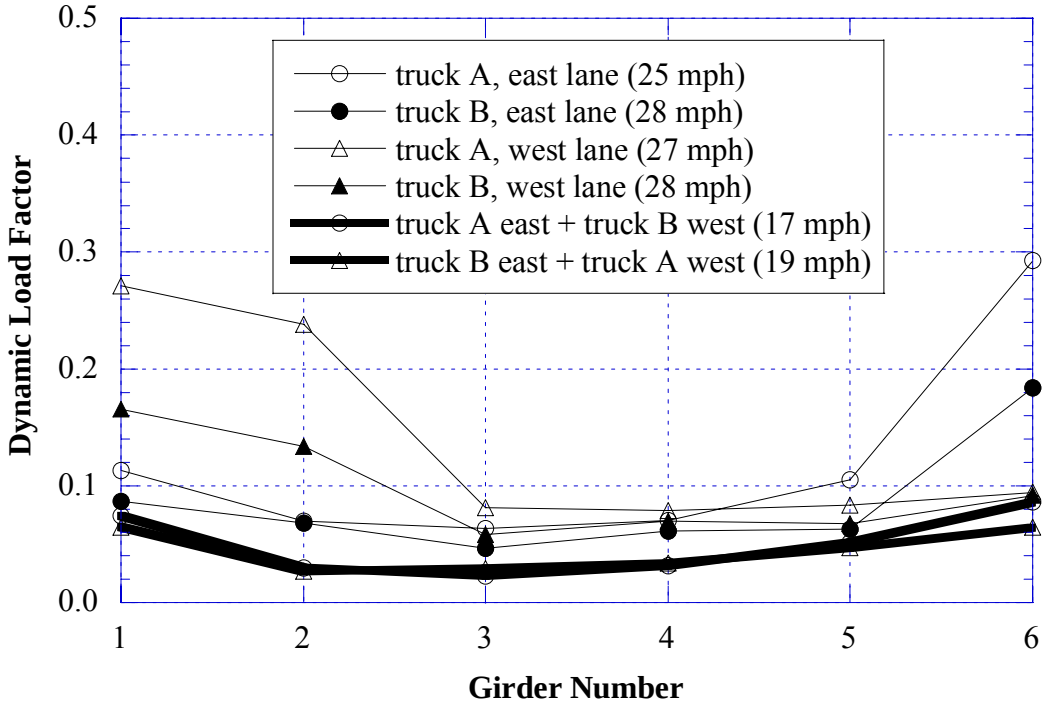

Figure 9.25 Dynamic Load Factors obtained from Negative Strain near Support over South Pier (S09-77023)

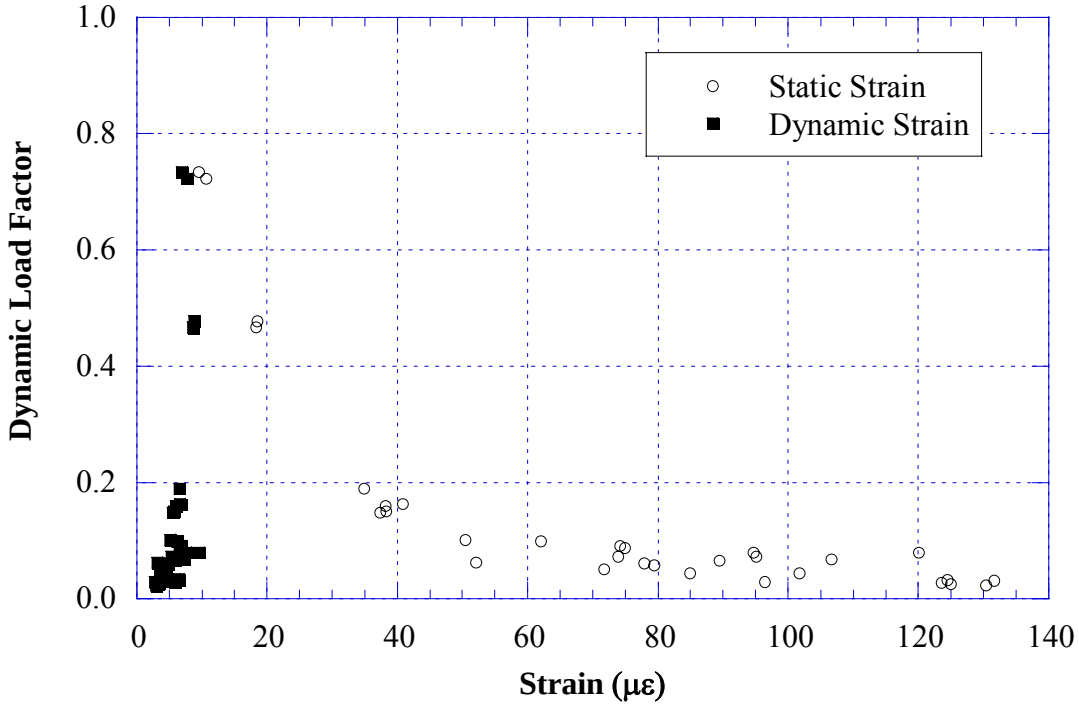

Figure 9.26 Strain vs. Dynamic Load Factors,
Based on Positive Strain at Midspan of Centerspan (S09-77023)

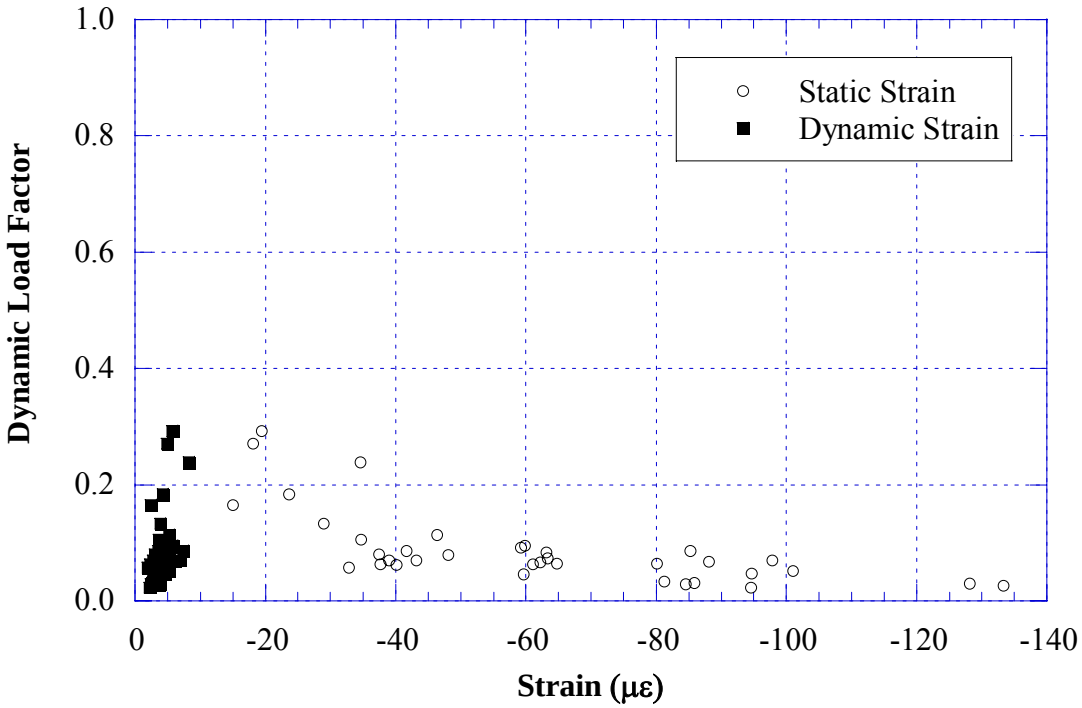

Figure 9.27 Strain vs. Dynamic Load Factors,
Based on Negative Strain near Support over South Pier (S09-77023)

9.5 Results of Finite Element Analysis

A three-dimensional finite element method (FEM) was applied to investigate the structural behavior of the bridge S09-77023. The concrete slab was modeled with isotropic, eight node solid elements, with three degrees of freedoms at each node. The girder flanges and web were modeled using three-dimensional, quadrilateral, four node shell elements with six degrees of freedom at each node. The structural effects of the secondary members, such as the sidewalk and parapet, were also taken into account in the finite element analysis models.

The mesh of the FEM model is shown in Figure 9.28. Total number of elements is 18,850, and total number of nodes is 24,510 for this model.

Strains and GDF's calculated for the considered model is shown in Figures 9.29 to 9.32. Figures 9.29 and 9.30 present strains and GDF's from FEM model for positive moment at the midspan under two trucks side-by-side loading. Figures 9.31 and 9.32 show the strains and GDF's from FEM model for negative moment near support over south pier under two trucks side-by-side loading. In the figures, the values obtained from FEM analysis are compared with the corresponding measured values.

The resulting strain values obtained from field tests are lower than those from the finite element analysis for considered bridges. The main reason for low strains is due to the partial fixity of supports. In the previous study for simply supported bridges by University of Michigan (Nowak 2001 and 2002), the boundary conditions are simulated using the elastic spring elements in FEM models. However, for continuous bridges, it is almost impossible to obtain accurate spring coefficients satisfying multiple locations of supports with varied partial fixity condition. Therefore, in the study, the supports are assumed to behave as designed in the FEM models.

Figure 9.33 compares the GDF values for both positive moment and negative moment obtained from FEM analysis. The difference between GDF's for positive moment and negative moments is less than 10 percent.

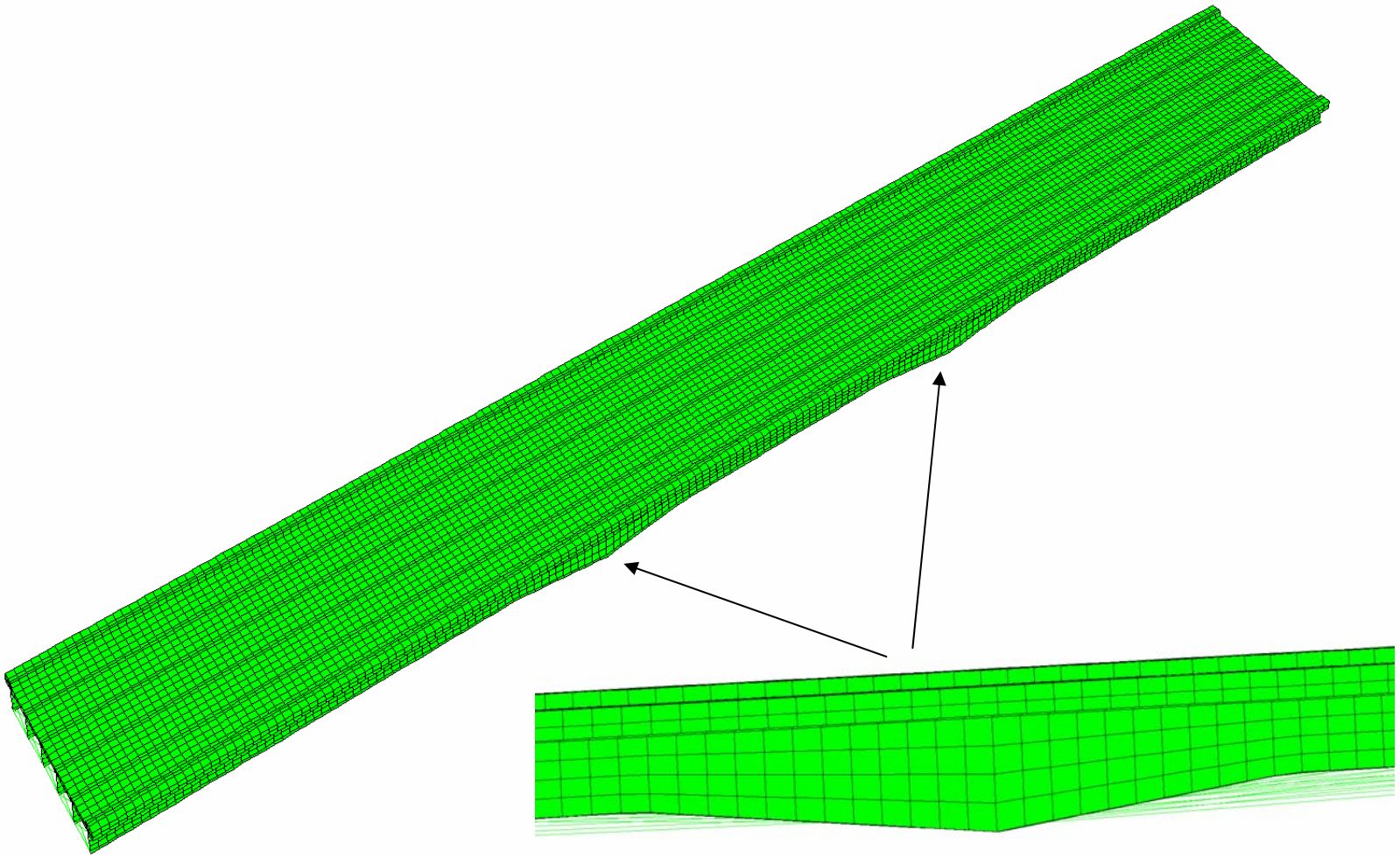

Figure 9.28 The Mesh of Finite Element Model (S09-77023)

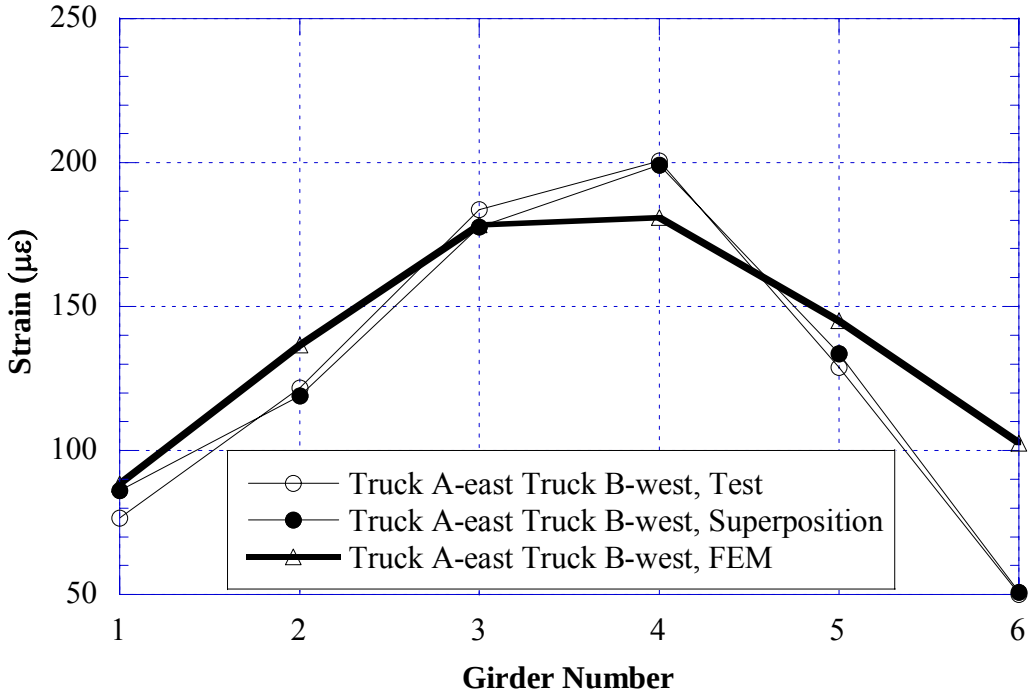

Figure 9.29 Comparison of FEM vs. Test, Positive Strain at Midspan of Centerspan, Side-by-Side Loading (S09-77023)

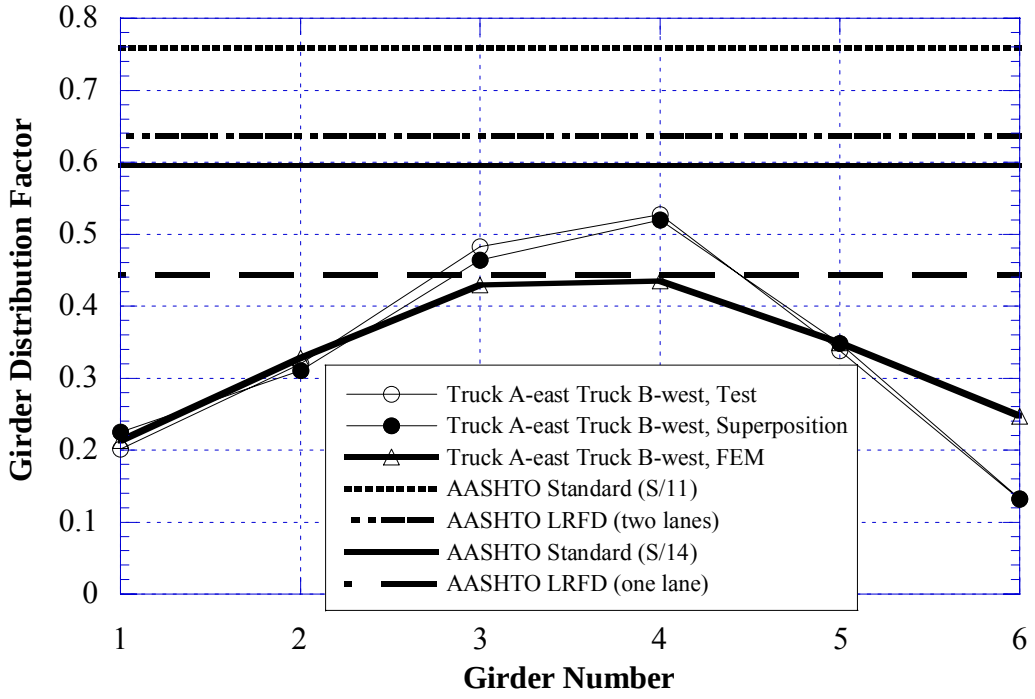

Figure 9.30 Comparison of FEM vs. Test, GDF Obtained from Positive Strain at Midspan of Centerspan, Side-by-Side Loading (S09-77023)

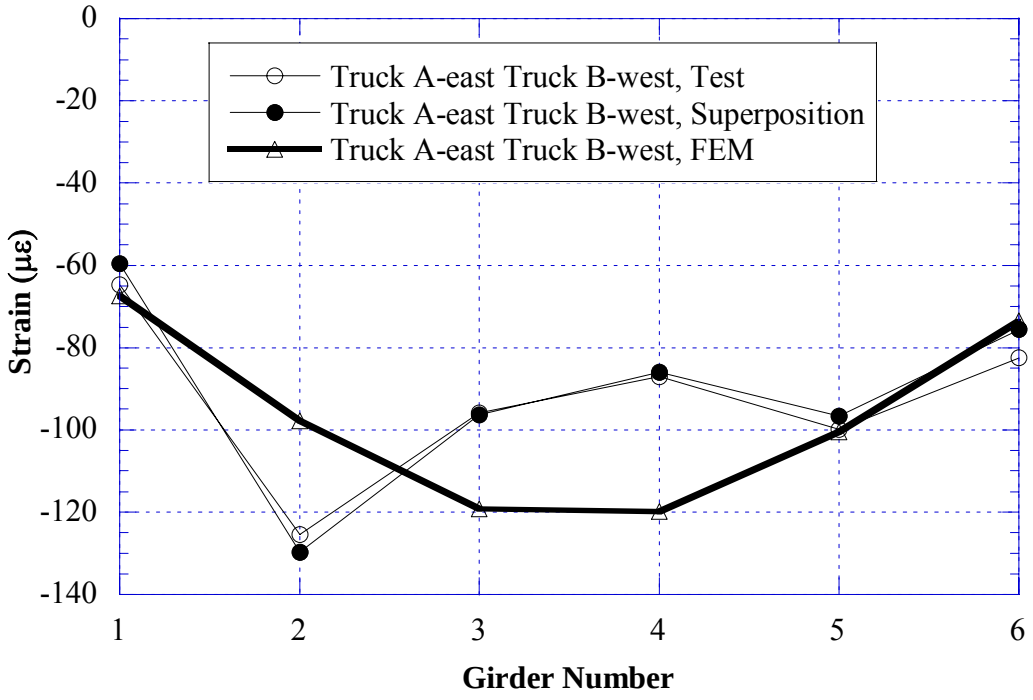

Figure 9.31 Comparison of FEM vs. Test, Negative Strain near Support over South Pier, Side-by-Side Loading (S09-77023)

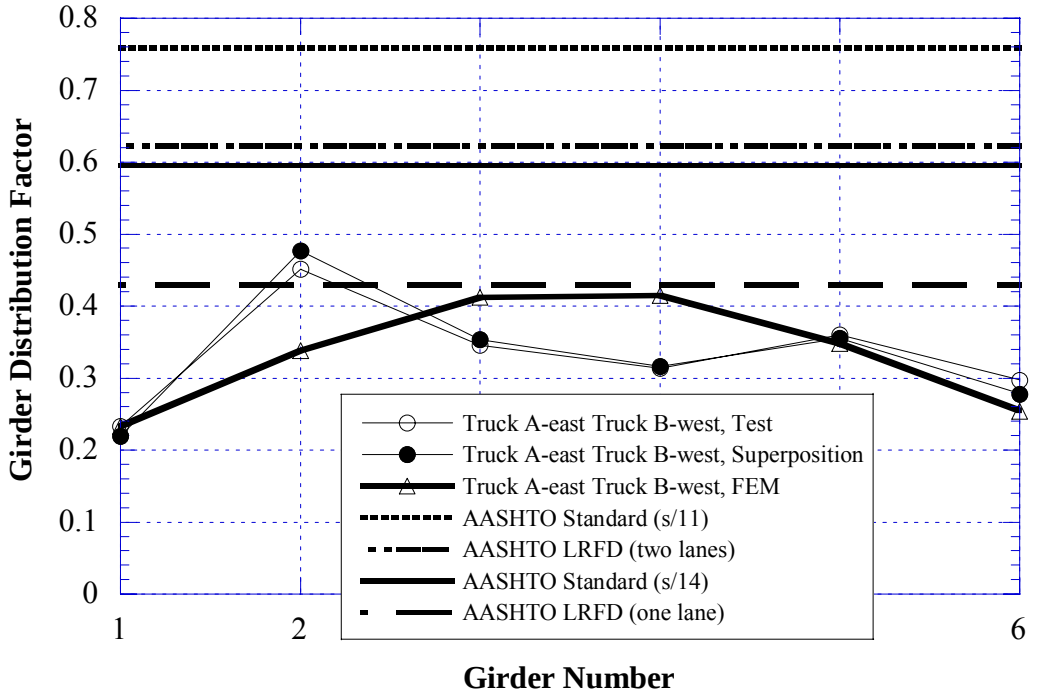

Figure 9.32 Comparison of FEM vs. Test, GDF Obtained From Negative Strain near Support over South Pier, Side-by-Side Loading (S09-77023)

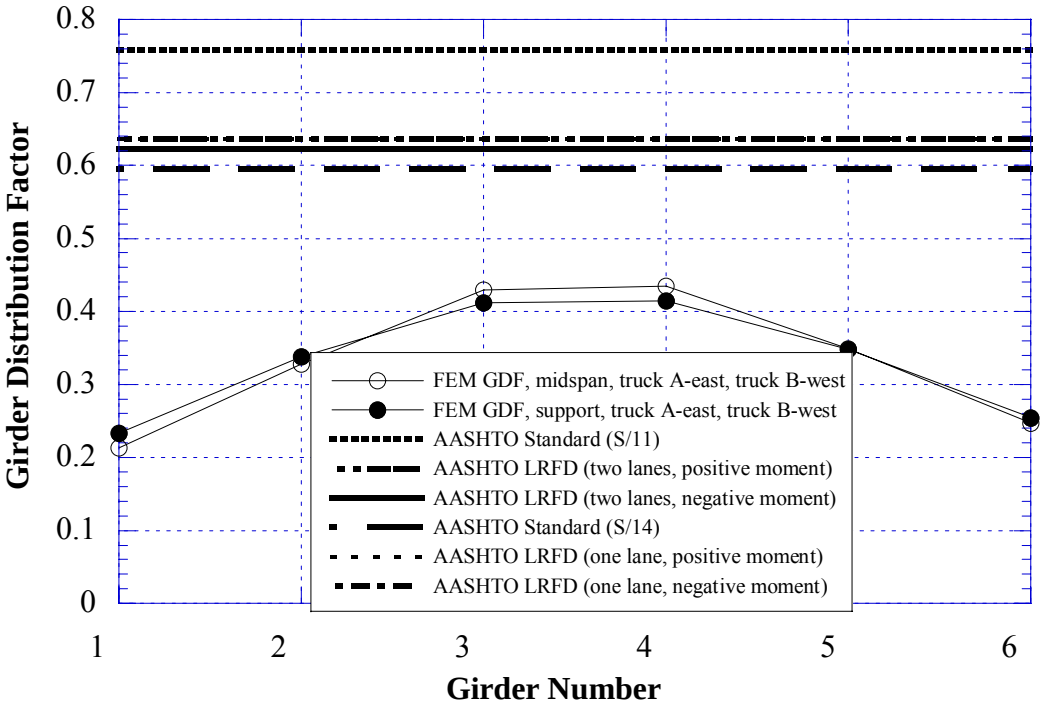

Figure 9.33 Comparison, GDF obtained from positive strain vs. GDF from Negative Strain, Based on Finite Element Analysis, Side-by-Side Loading (S09-77023)

Note:

Intentionally left blank

10. BRIDGE ON TAMARACK ROAD OVER US-131, MONTCALM COUNTY (S13-59012)

10.1 Bridge Description

This bridge was built in 1979 and it is located on Tamarack Road over US-131 in Montcalm County, Michigan. It is a four span, continuous steel girder bridge, designed as a composite section. It has five steel girders spaced at 8 ft 10 in, as shown in Figure 10.1, with 7 degree skew. The total bridge length is 459 ft. The side elevation is shown in Figure 10.2. The bridge has one lane in each direction and it carries an average daily traffic (ADT) of 550. The operating load rating is 264 kips, according to the Michigan Structure Inventory.

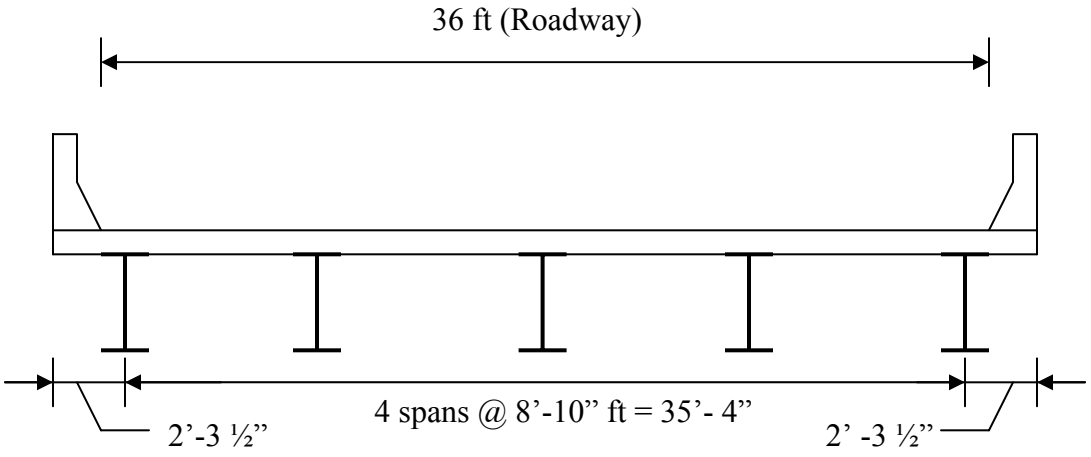

Figure 10.1 Cross Section of the bridge (S13-59012)

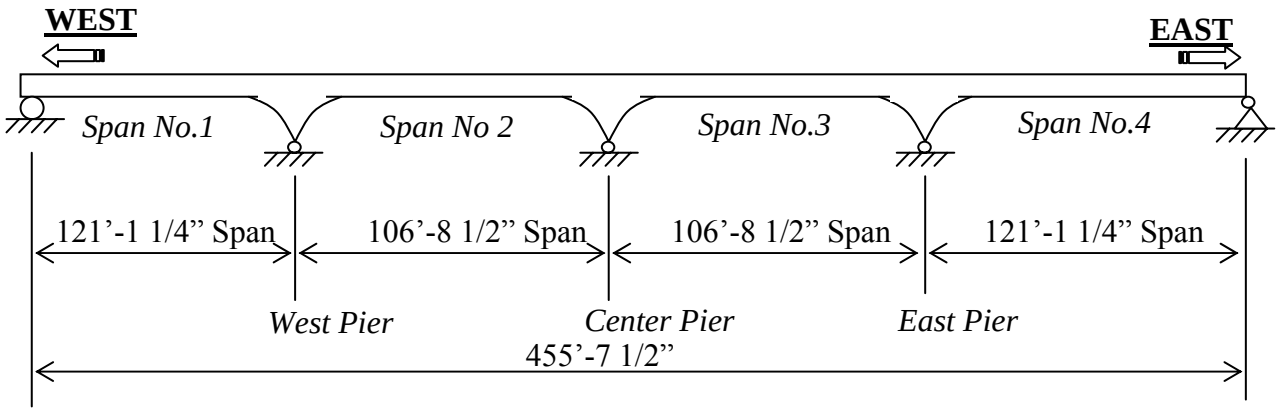

Figure 10.2 Side Elevation of Bridge (S13-59012)

10.2 Instrumentation

Strain transducers were installed on the bottom flanges of girders at midspan and at support locations, as shown in Figure 10.3. The reflector for the PSM-R device from Noptel was installed at the girder No. 3 to measure deflection. The bridge was instrumented on July 23, 2002, and bridge test were performed on July 24, 2002.

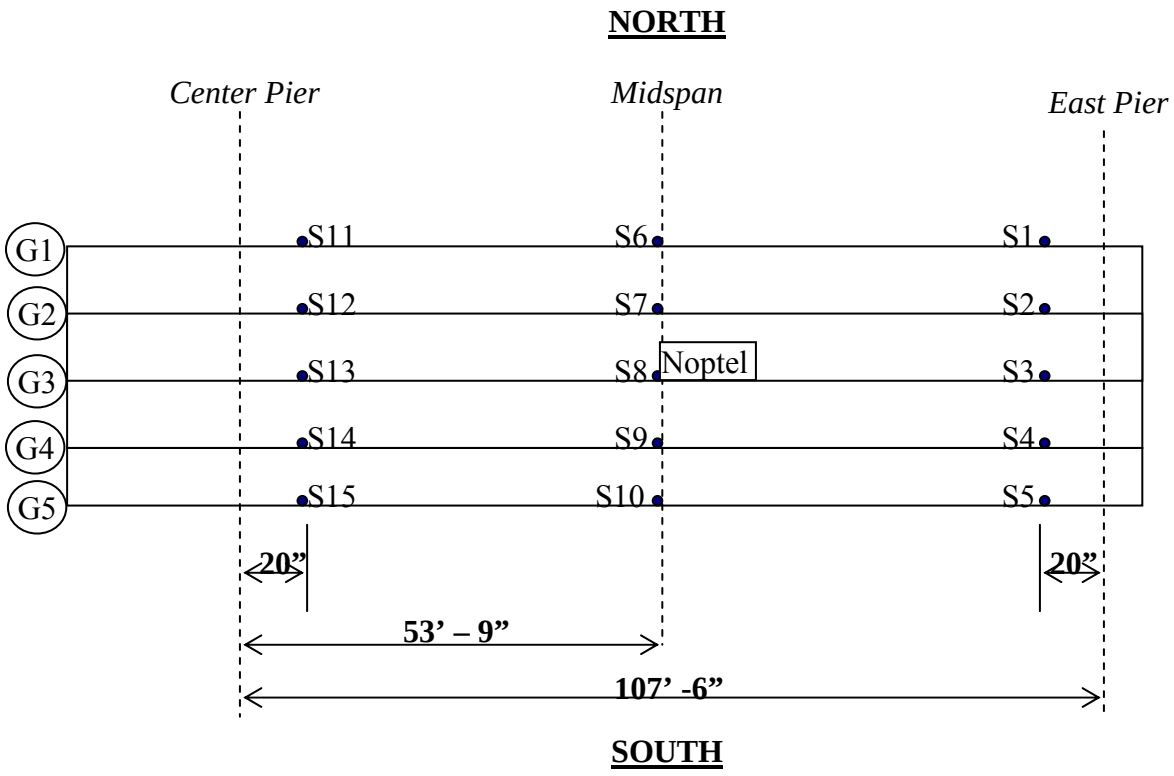

Figure 10.3 Strain Gage Location in overall view of the bridge (S13-59012)

10.3 Load cases

The girder distribution factors (GDF) and dynamic load factors (DLF) were calculated using the strains measured at midspan and near support. The bridge was loaded with two 11-axle trucks (three-unit vehicles).

The truck A and truck B have gross weights of 134 kips and 136 kips, with wheelbases of 59 ft and 58 ft, respectively. Truck configurations are shown in Figures 10.4 and 10.5.

Truck A

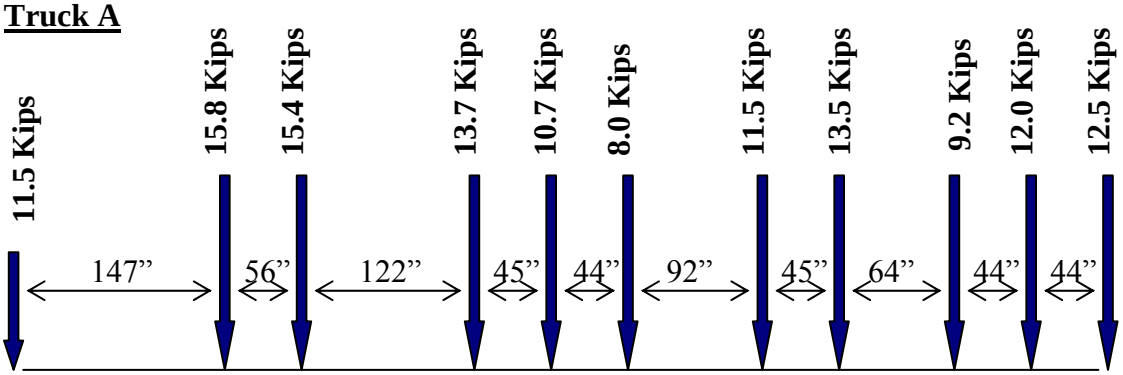

Figure 10.4 Truck A configuration, Bridge (S13-59012)

Truck B

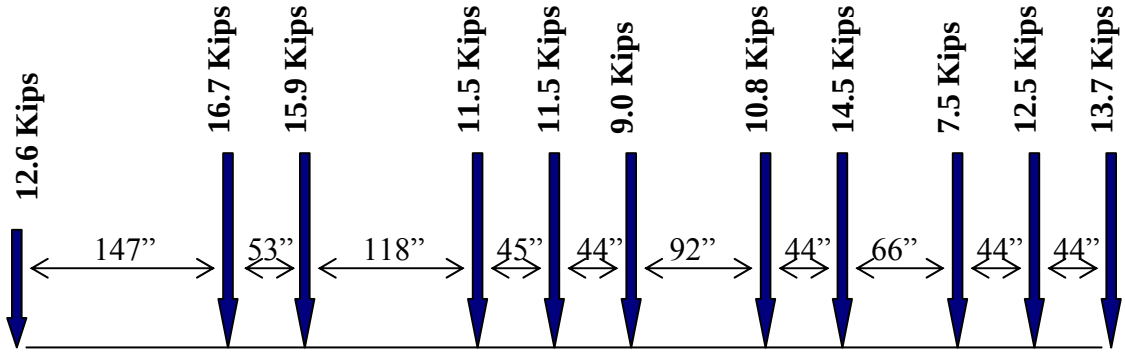

Figure 10.5 Truck B configuration, Bridge (S13-59012)

A total of 20 load cases were considered, as shown in Table 10.1. First each truck was driven by itself at the center of each lane, at crawling speed. Then, the same truck was driven close to the curb. The runs in the center of the lane were repeated at a normal highway speed. In addition, two trucks were driven simultaneously, side-by-side, at crawling speed and normal highway speed. For side-by-side cases, the runs were repeated after the trucks switched lanes, i.e. first truck A was in south lane, and B in north lane, then truck A was in north lane, and B in south lane. Then one truck was driven, followed by the other truck for each lane. In addition, trucks were stopped at predetermined position to verify pre-test calculation.

Table 10.1. Sequence of Test Runs, Bridge (S13-59012)

Run#	Truck	Lane Side	Position	Truck Speed
1	Truck A	South	Center	Crawling
2	Truck B	South	Center	Crawling
3	Truck A	North	Center	Crawling
4	Truck B	North	Center	Crawling
5	Truck A	South	Curb	Crawling
6	Truck B	South	Curb	Crawling
7	Truck A	North	Curb	Crawling
8	Truck B	North	Curb	Crawling
9	Truck A	South	Center	35 MPH
10	Truck B	South	Center	36 MPH
11	Truck A	North	Center	35 MPH
12	Truck B	North	Center	36 MPH
13	Truck A(South) and B(North)	side-by-side	Center	Crawling
14	Truck B(South) and A(North)	side-by-side	Center	Crawling
15	Truck B(South) and A(North)	side-by-side	Center	32 MPH
16	Truck A(South) and B(North)	side-by-side	Center	34 MPH
17	Truck A followed by B	South	Center	Crawling
18	Truck A followed by B	North	Center	Crawling
19	Truck A followed by B	South	Center	Stop at fixed position
20	Truck A followed by B	North	Center	Stop at fixed position

10.4 Test results

The resulting strains and GDF's are shown in Figures 10.6 through 10.23. Figures 10.6 to 10.17 present the results for one truck on the bridge under crawling-speed (static) tests. For each loading condition, strains are measured and the corresponding GDF's are calculated from the strain measurement. For comparison, GDF are also calculated according to AASHTO Standard (2002) and AASHTO LRFD Code (1998). The resulting GDF's are shown in Figures 10.6 through 10.17. Figures 10.6 to 10.9 show positive strain values recorded at the midspan of span 3, and also resulting GDF's. Figures 10.10 to 10.13 present the negative strain values and corresponding GDF's near supports over center pier. Figures 10.14 to 10.17 present the negative strain values and corresponding GDF's near supports over east pier. For single lane loading, the maximum positive strain is about 160 με. This strain value corresponds about 4.6 ksi. The maximum negative strain near support is less than 105 με. This corresponds about 3.0 ksi. Strain values tend to be higher when the truck is positioned close to curb. For single lane loadings on the center of lanes, the measured GDF's are below/very close to code specified values. However, when the truck is very close to curb, GDF's can exceed the specified values in AASHTO LRFD (1998) for single lane loading.

Figures 10.18 to 10.23 present the results for side-by-side static loading on the bridge under crawling-speed (static) tests. For two trucks side-by-side, strains are measured and the corresponding GDF's are calculated from the strain measurement. For comparison, GDF are also calculated according to code specified values. Figure 10.18 presents the measured positive strains under two trucks side by side, and Figure 10.19 shows corresponding GDF's compared with code specified values. For two trucks side by side, the maximum recorded positive strain at the midspan is about 240 με, which corresponds about 7.0 ksi. Figure 10.19 shows that code specified GDF's are conservative. Even the single lane GDF specifed in AASHTO Standard (2002) is sufficient for two trucks side by side. However, single lane GDF specified in AASHTO LRFD (1998) is not sufficient for two lane load case in this bridge.

Figures 10.20 and 10.21 present the negative strains and corresponding GDF's, respectively, under two truck side by side loading measured near support over center pier. Figures 10.22 and 10.23 show the negative strains and corresponding GDF's, respectively, under two truck side by side loading measured near support over east pier. The maximum recorded negative strain near support is about 140 με, which corresponds about 4 ksi. Figures 10.21 and 10.23 show that code specified GDF's are conservative.

The GDF's specifed in AASHTO Standard (2002) is conservative for two trucks side by side. However, The measured value exceeds GDF's specified in AASHTO LRFD (1998) for two lane load case near support over center pier.

In all cases, the superposition of strains due to a single truck in north and south lanes produces almost the same results as strain due to two trucks side-by-side.

Figures 10.24 and 10.25 present the comparison of GDF's for positive and negative moment obtained from single lane loadings. For single lane loadings on the center of lanes, the measured GDF's are below/very close to code specified values. However, when the truck is very close to curb, GDF's can exceed the specified values in AASHTO LRFD (1998) for single lane loading.

Figure 10.26 compares the GDF's for positive and negative moment obtained from side-by-side loading. The figure indicates that the test values are below or very close to the code specified GDF's for two truck side-by-side loading.

In Figures 10.27 to 10.29, DLF's are plotted for all load cases involving normal speed (no dynamic load was measured for crawling speed runs). Figure 10.27 shows DLF's measured at the midspan (positive moment), and Figure 10.28 and 10.29 for negative moment (near support) over center pier and east pier, respectivly. As shown in the figures, dynamic load factors for exterior girders are high because the static strains in these girders are very low. In other words, large values of DLF in exterior girders

correspond to load cases with a single truck in the opposite lane (resulting in very low static strain).

The relationship between DLF and static and dynamic strains is shown in Figures 10.30 for positive moment, and Figures 10.31 and 10.32, for negative moment. The open circles correspond to static strain, ε_{stat}, and black solid squares correspond to dynamic strain, ε_{dyn}. For each static strain value (open circle), the corresponding dynamic strain is denoted by solid square (the numbers of circles and squares are same). Dynamic strains remain nearly constant, while static strains increase as truck loading increases. This results in large dynamic load factors for low static strains. DLF corresponding to the maximum strain caused by two trucks side-by-side, is less than 0.10 for the most heavily loaded girder.

Girder No. 3 was instrumented with a remote deflection measurement device manufactured by Noptel. The reflector was installed at midspan. The result is shown in Table 10.2. The maximum deflection recorded during the test is 14.7 mm for girder No. 3 for two side-by-side trucks.

Table 10.2. Maximum deflections measured at the center of Girder No.3, Bridge (S13-59012)

Run #	Vertical Deflection (mm)
1	6.9
2	7.3
3	6.5
4	6.7
5	4.8
6	4.9
7	4.8
8	4.8
13	14.5
14	14.7

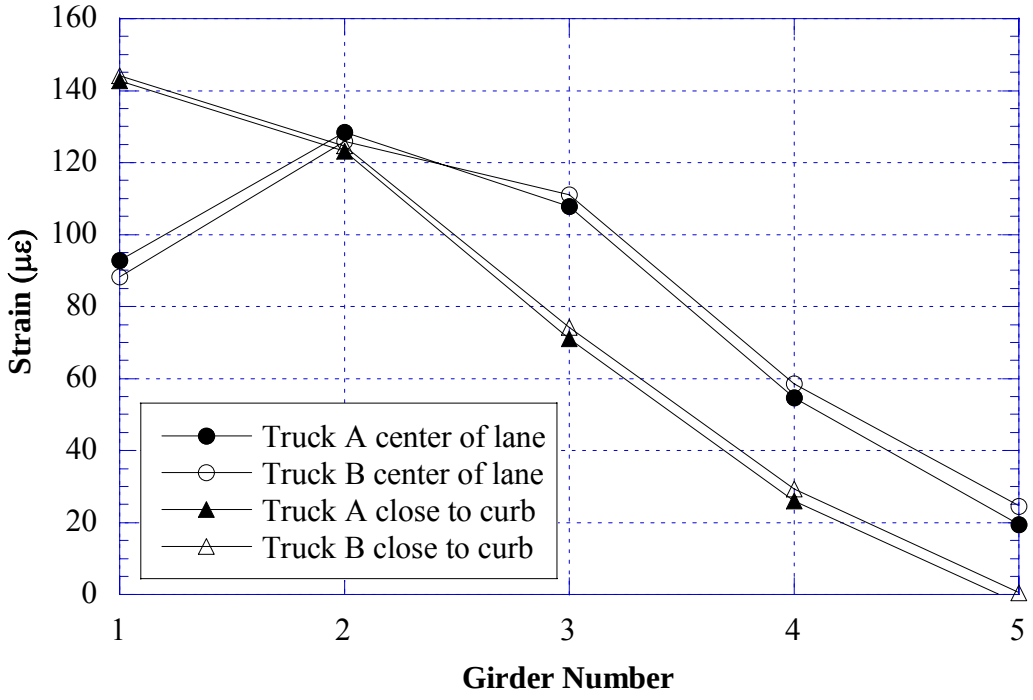

Figure 10.6 Positive Strain at Midspan of Span No.3, North Lane Loading (S13-59012)

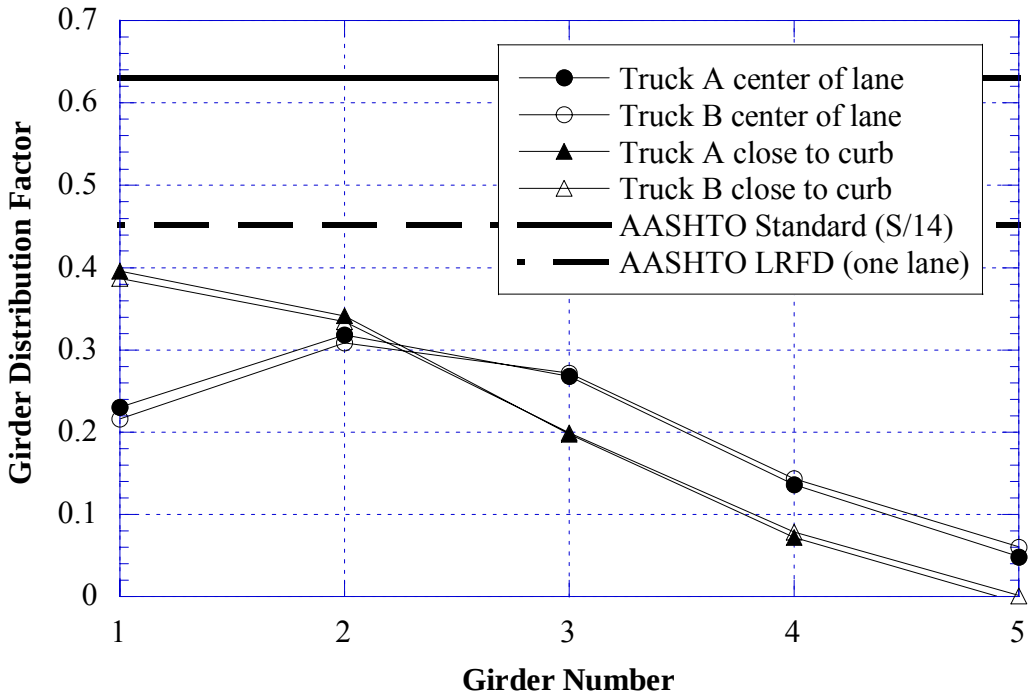

Figure 10.7 GDF from Positive Strain at Midspan of Span No.3, North Lane Loading (S13-59012)

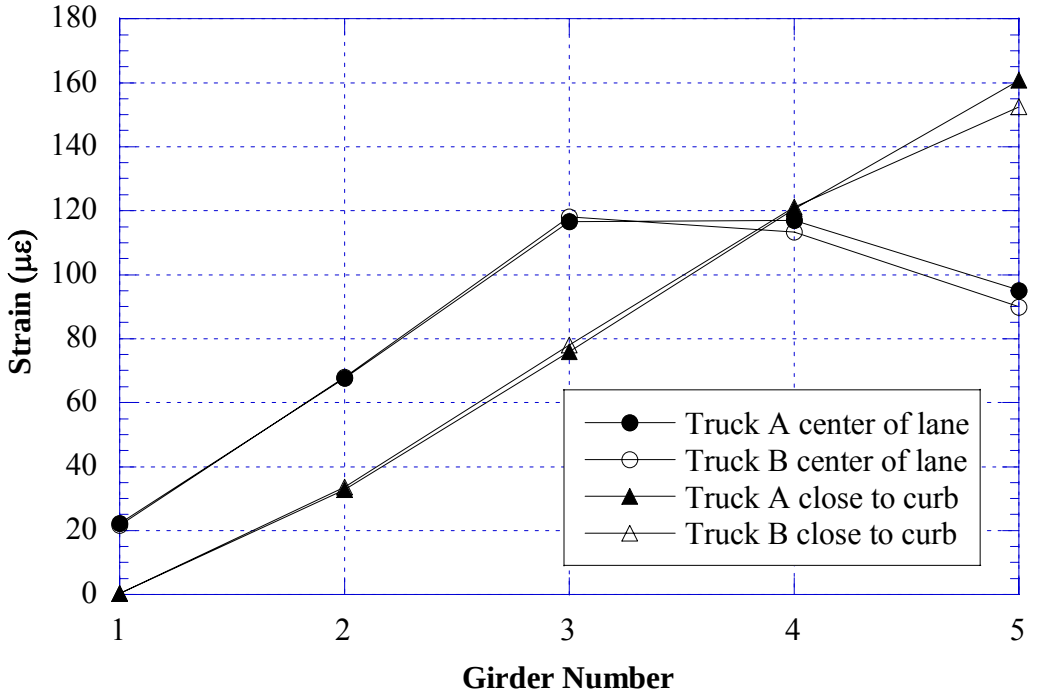

Figure 10.8 Positive Strain at Midspan of Span No.3, South Lane Loading (S13-59012)

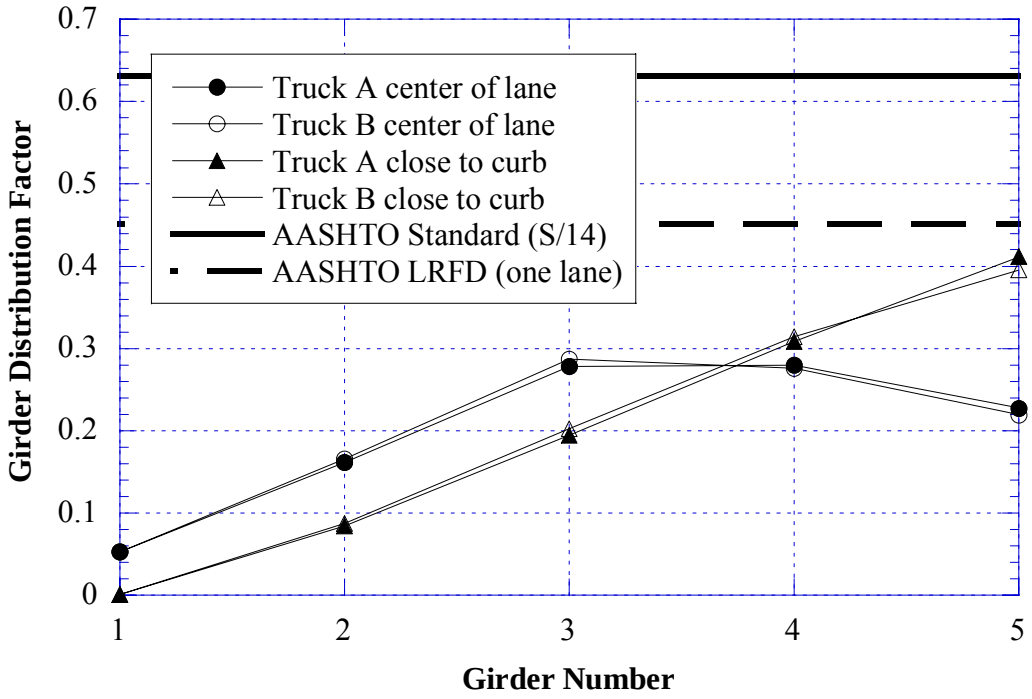

Figure 10.9 GDF from Positive Strain at Midspan of Span No.3, South Lane Loading (S13-59012)

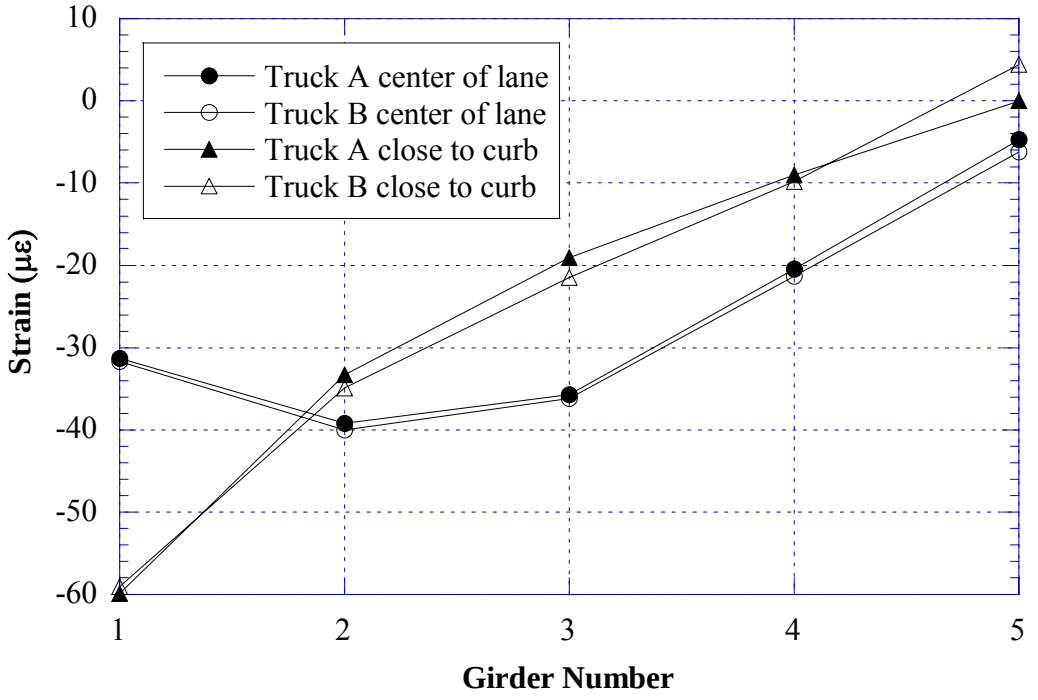

Figure 10.10 Negative Strain Near Support over East Pier, North Lane Loading, (S13-59012)

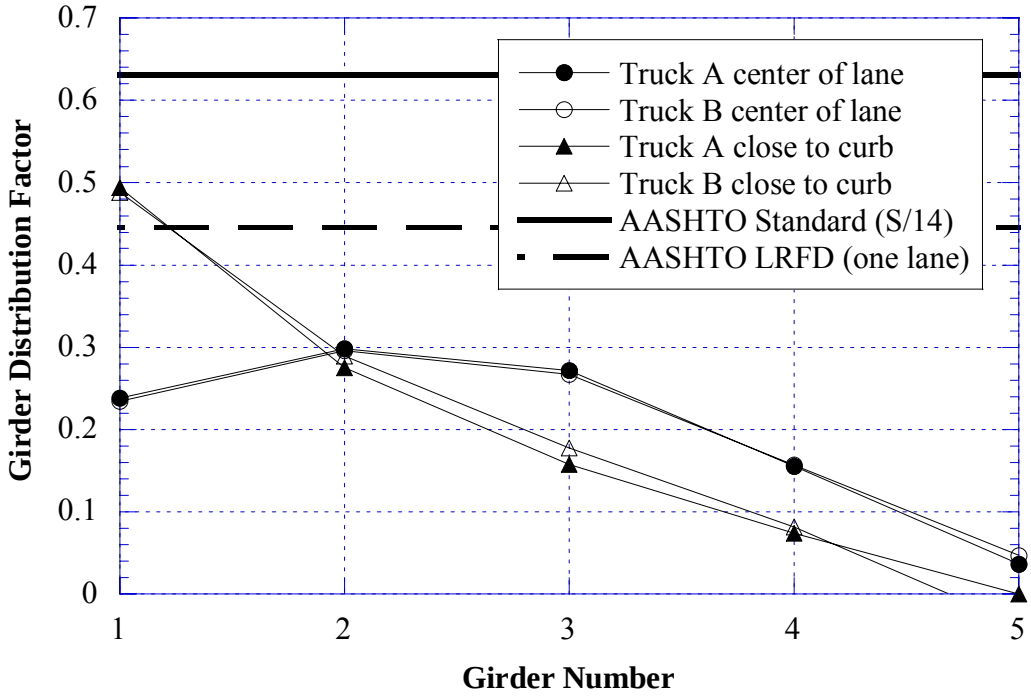

Figure 10.11 GDF from Negative Strain near Support over East Pier, North Lane Loading, (S13-59012)

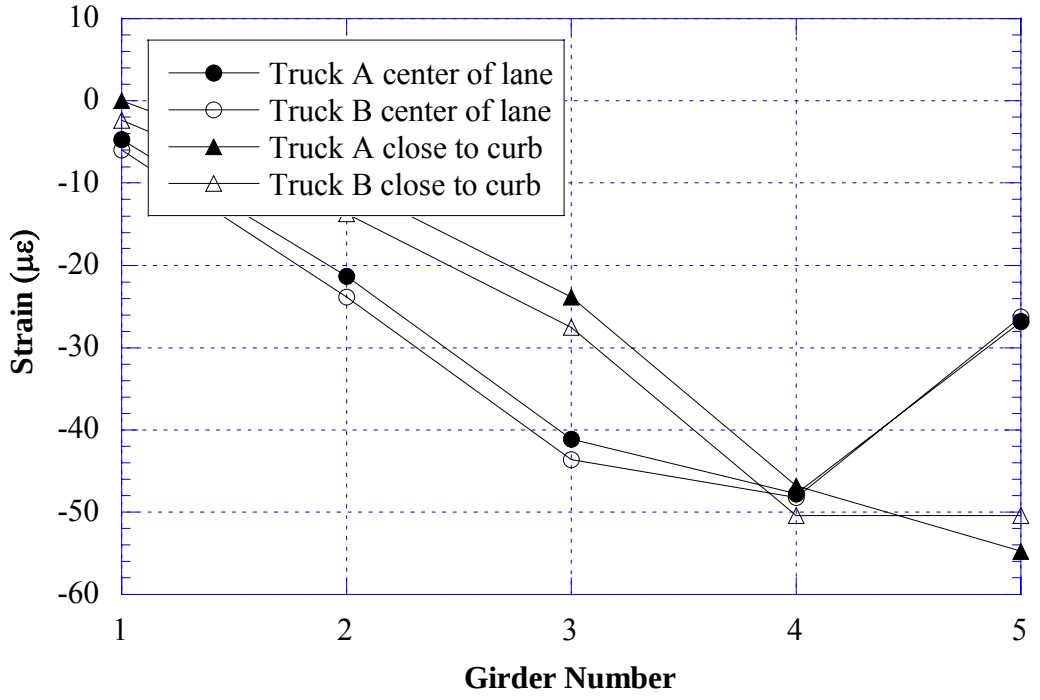

Figure 10.12 Negative Strain near Support over East Pier, South Lane Loading, (S13-59012)

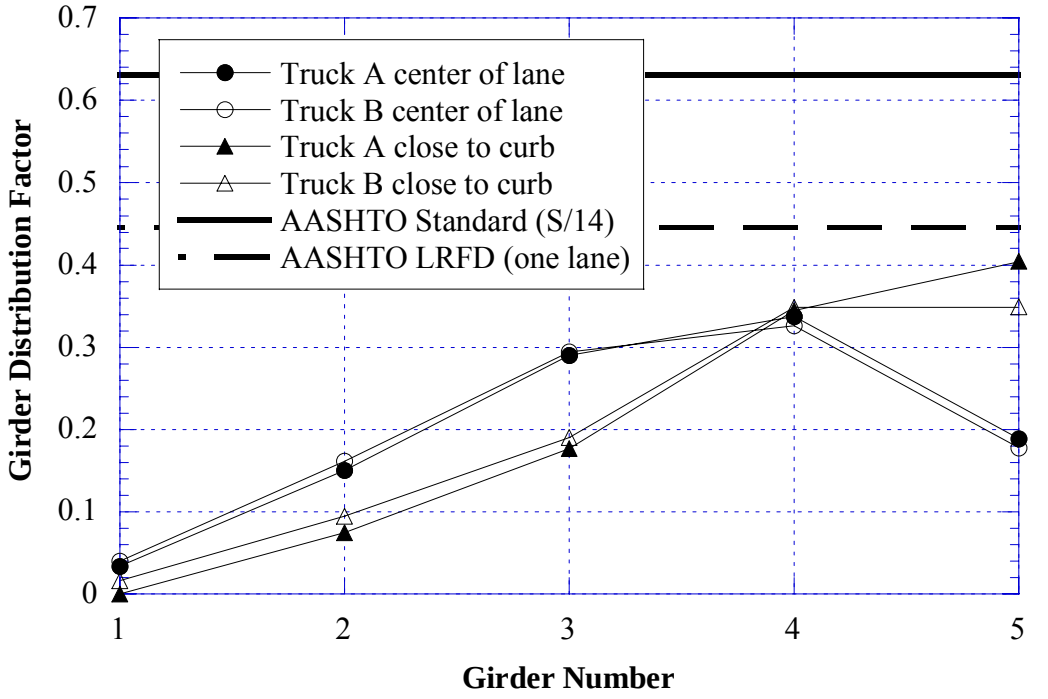

Figure 10.13 GDF from Negative Strain near Support over East Pier, South Lane Loading, (S13-59012)

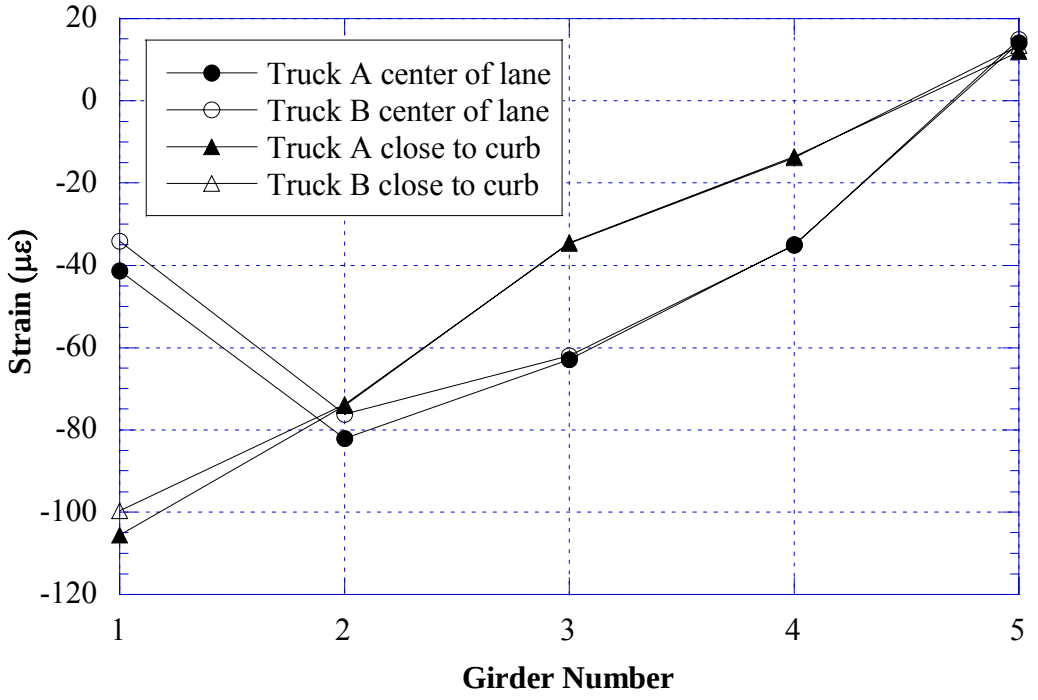

Figure 10.14 Negative Strain near Support over Center Pier, North Lane Loading, (S13-59012)

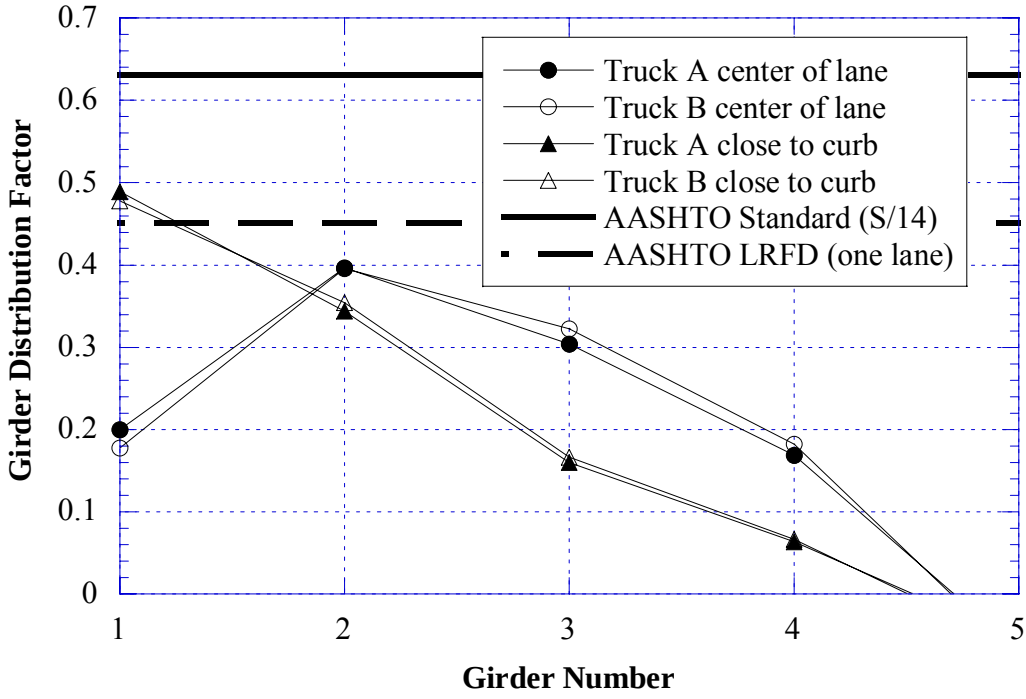

Figure 10.15 GDF from Negative Strain near Support over Center Pier, North Lane Loading, (S13-59012)

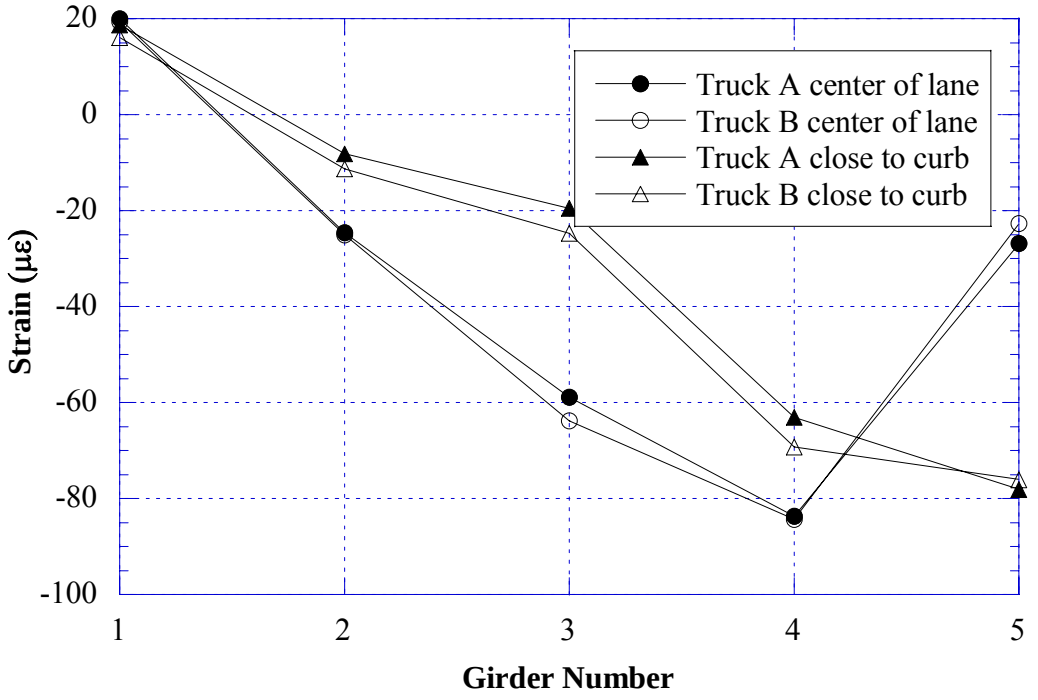

Figure 10.16 Negative Strain near Support over Center Pier, South Lane Loading, (S13-59012)

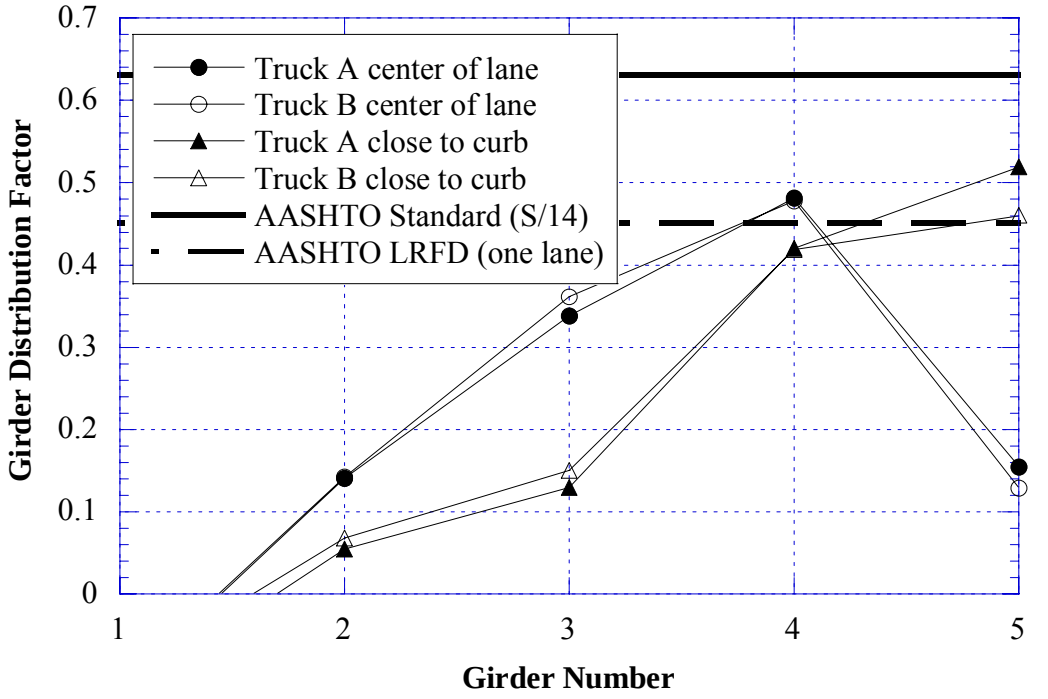

Figure 10.17 GDF from Negative Strain near Support over Center Pier, South Lane Loading, (S13-59012)

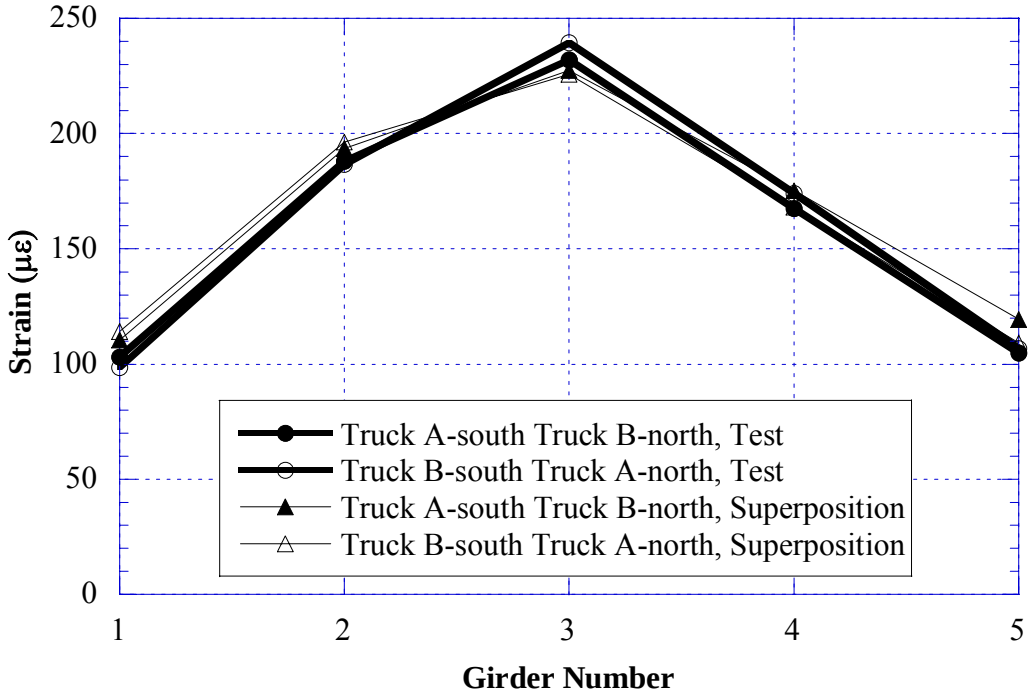

Figure 10.18 Positive Strain at Midspan of Span No.3, Side-by-Side Loading (S13-59012)

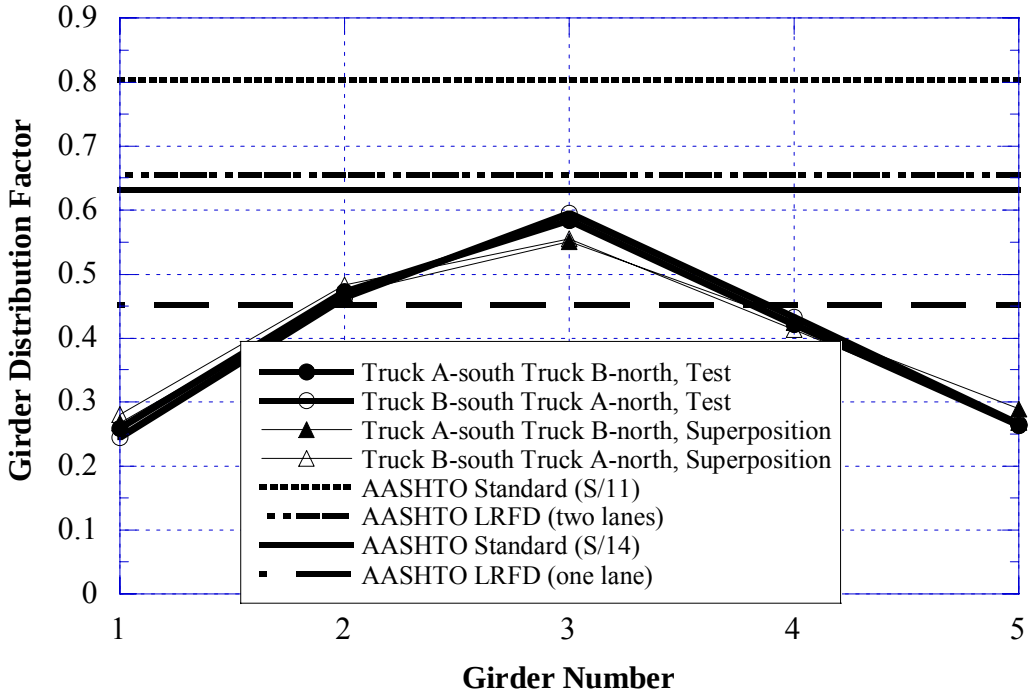

Figure 10.19 GDF from Positive Strain at Midspan of Span No.3, Side-by-Side Loading (S13-59012)

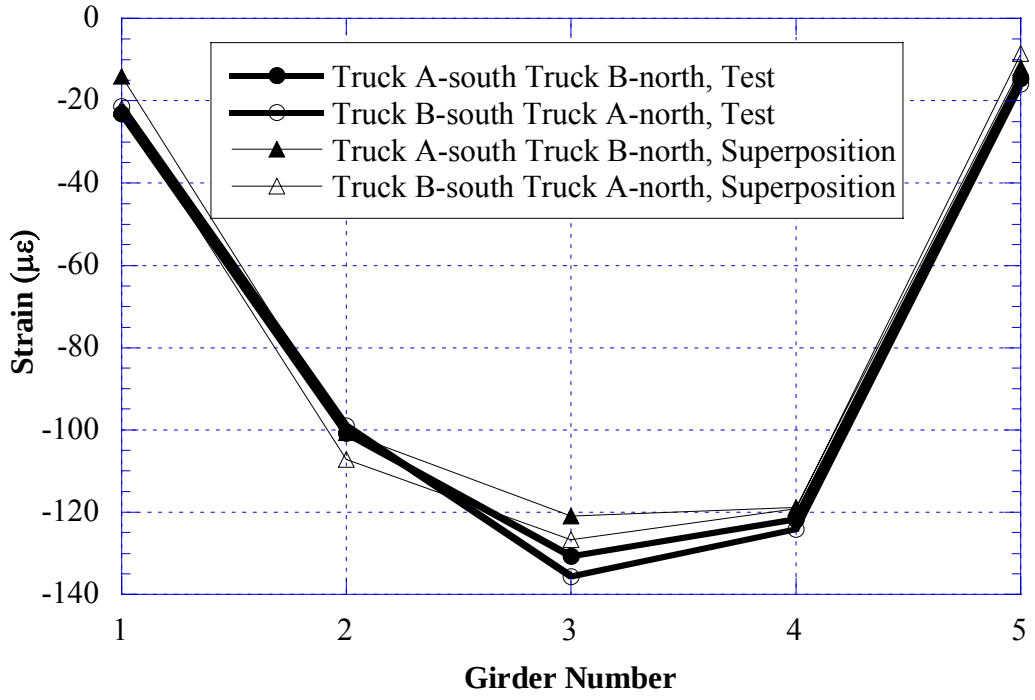

Figure 10.20 Negative Strain near Support over Center Pier, Side-by-Side Loading (S13-59012)

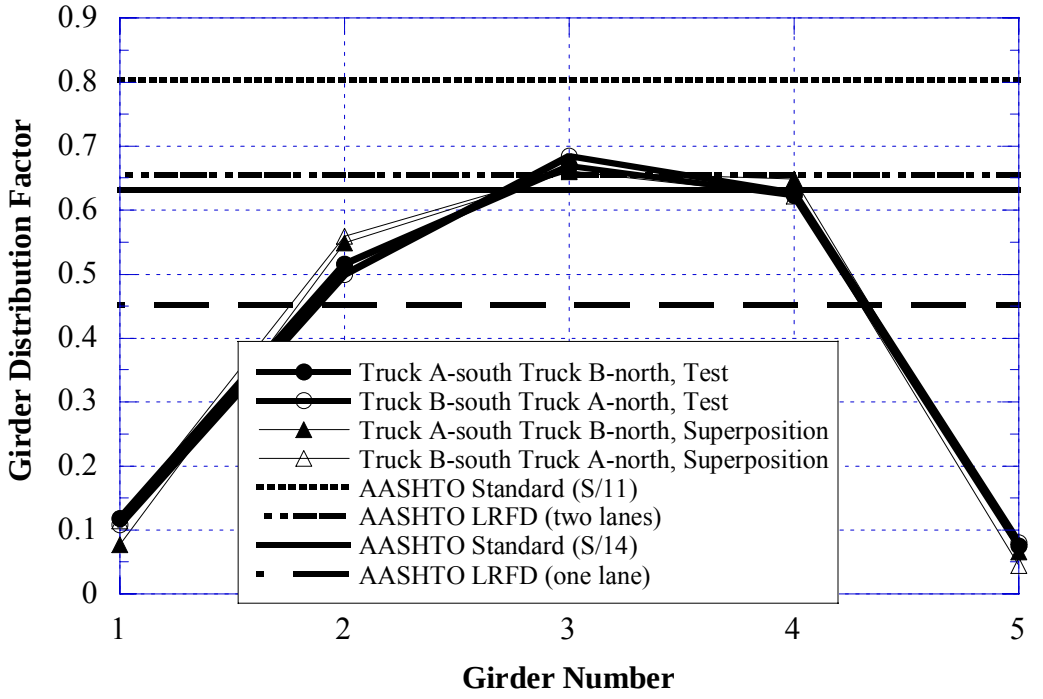

Figure 10.21 GDF from Negative Strain near Support over Center Pier, Side-by-Side Loading (S13-59012)

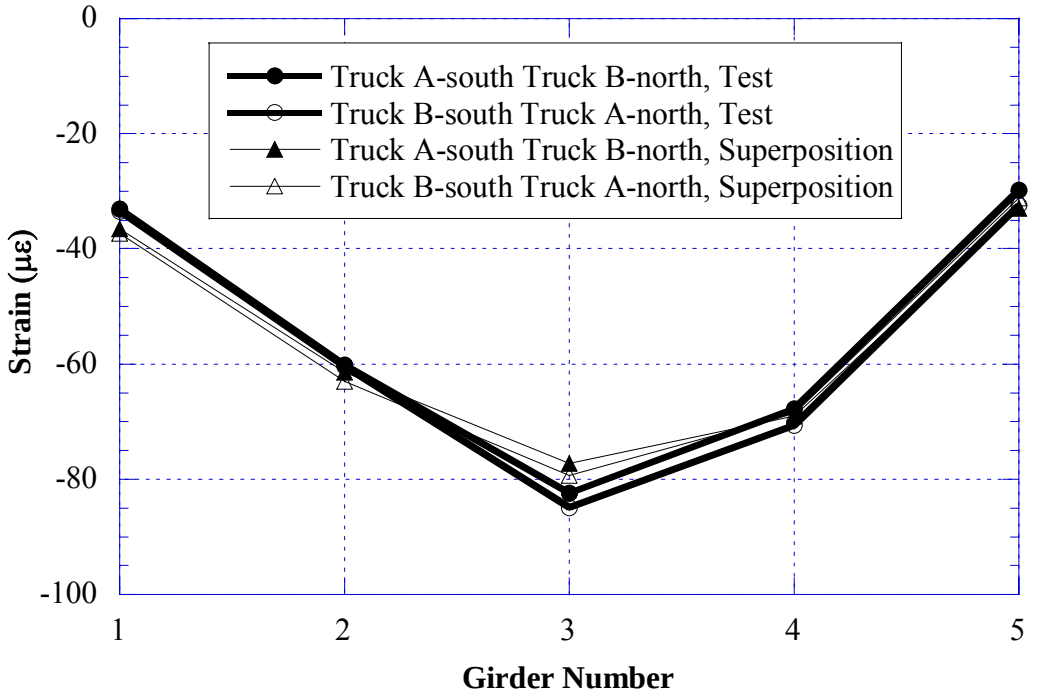

Figure 10.22 Negative Strain near Support over East Pier, Side-by-Side Loading (S13-59012)

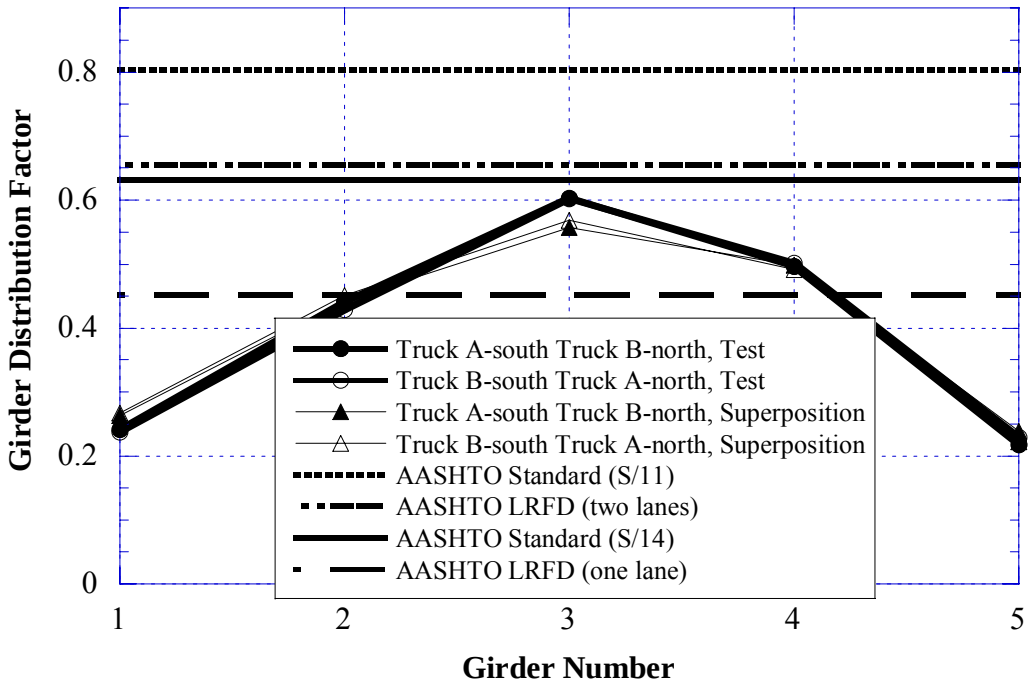

Figure 10.23 GDF from Negative Strain near Support over East Pier, Side-by-Side Loading (S13-59012)

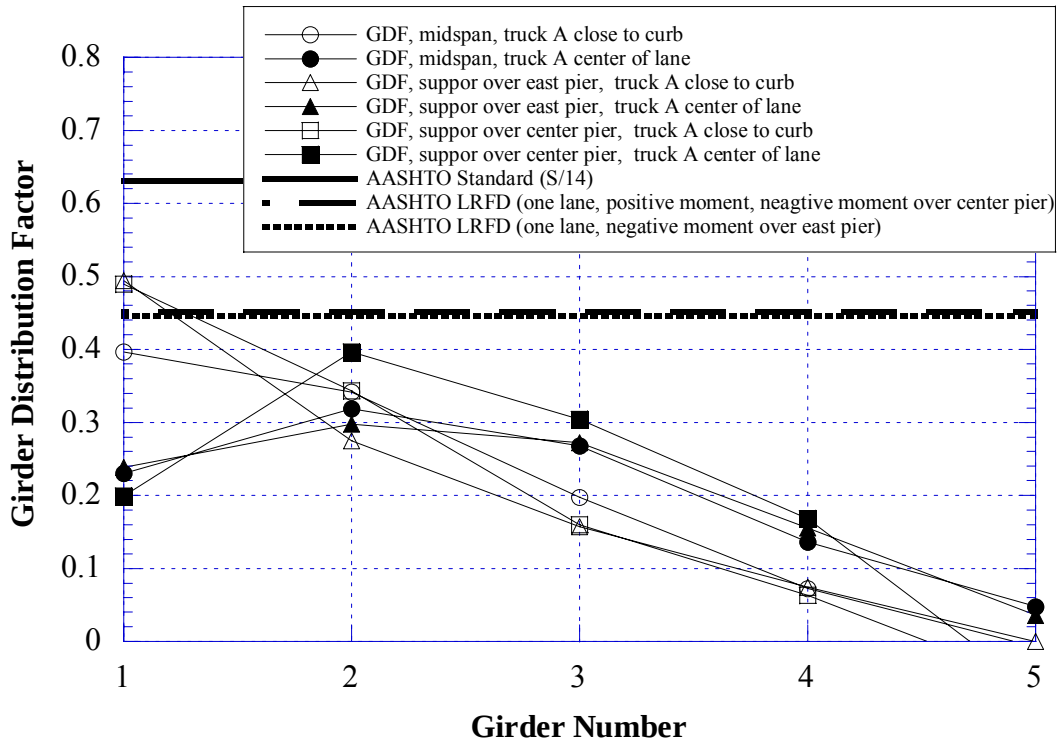

Figure 10.24 Comparison, GDF obtained from Positive Strain vs. GDF from Negative Strain, North Lane Loading (S13-59012)

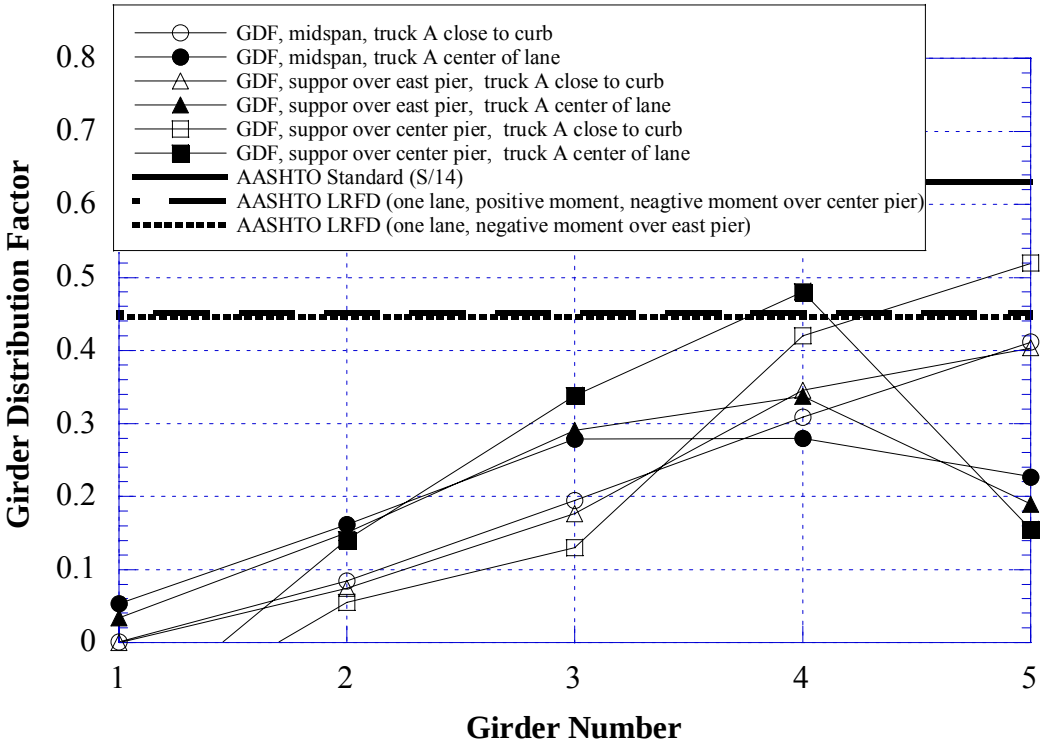

Figure 10.25 Comparison, GDF obtained from Positive Strain vs. GDF from Negative Strain, South Lane Loading (S13-59012)

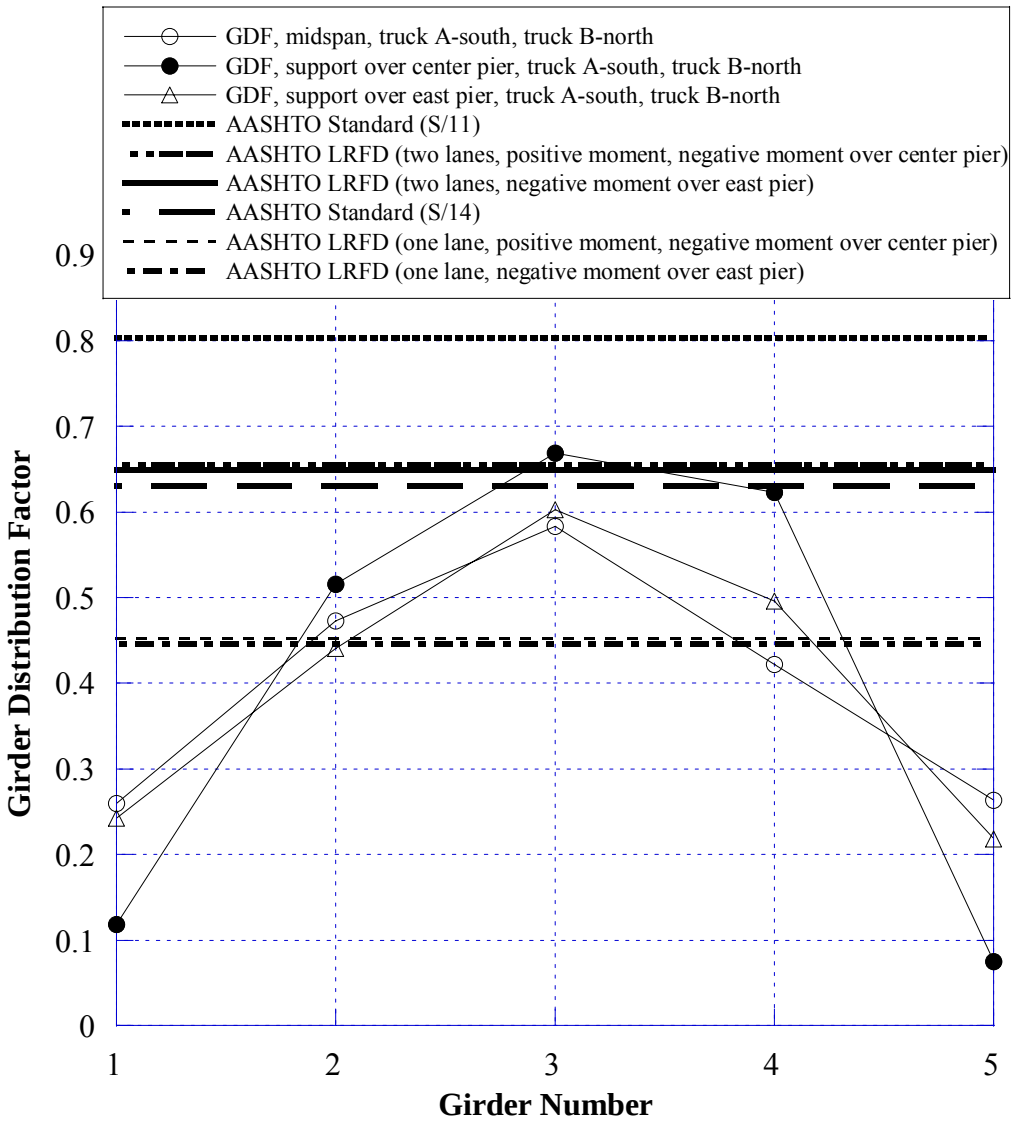

Figure 10.26 Comparison, GDF obtained from Midspan vs. GDF from Support, Side-by-Side Loading (S13-59012)

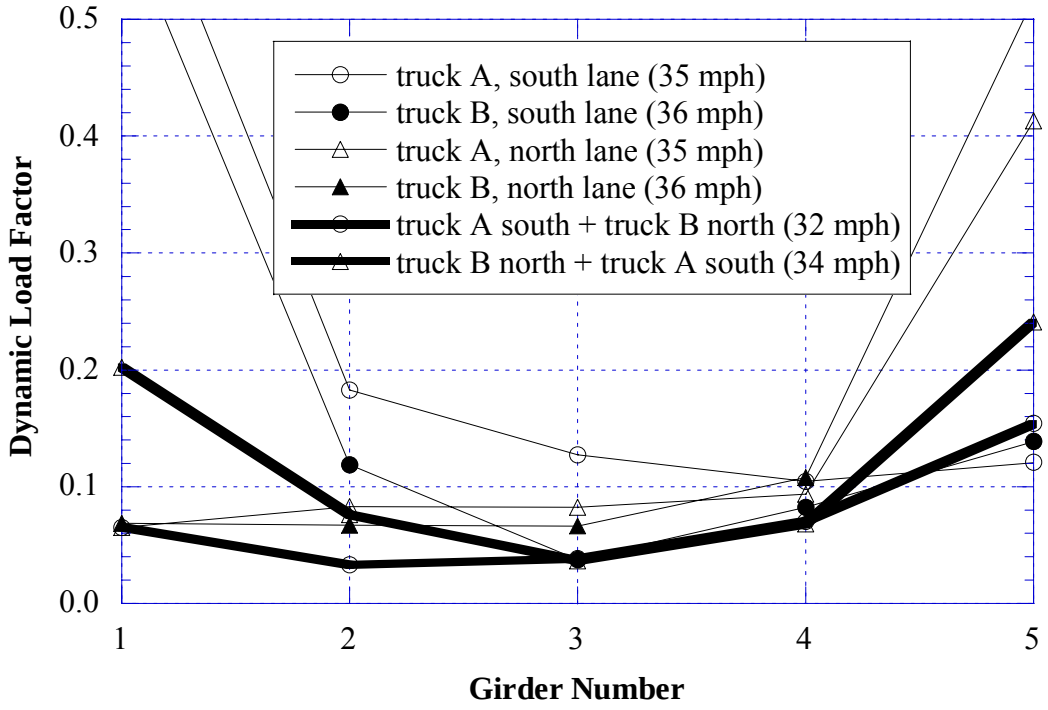

Figure 10.27 Dynamic Load Factors obtained from Positive Strain at Midspan of Span No.3 (S13-59012)

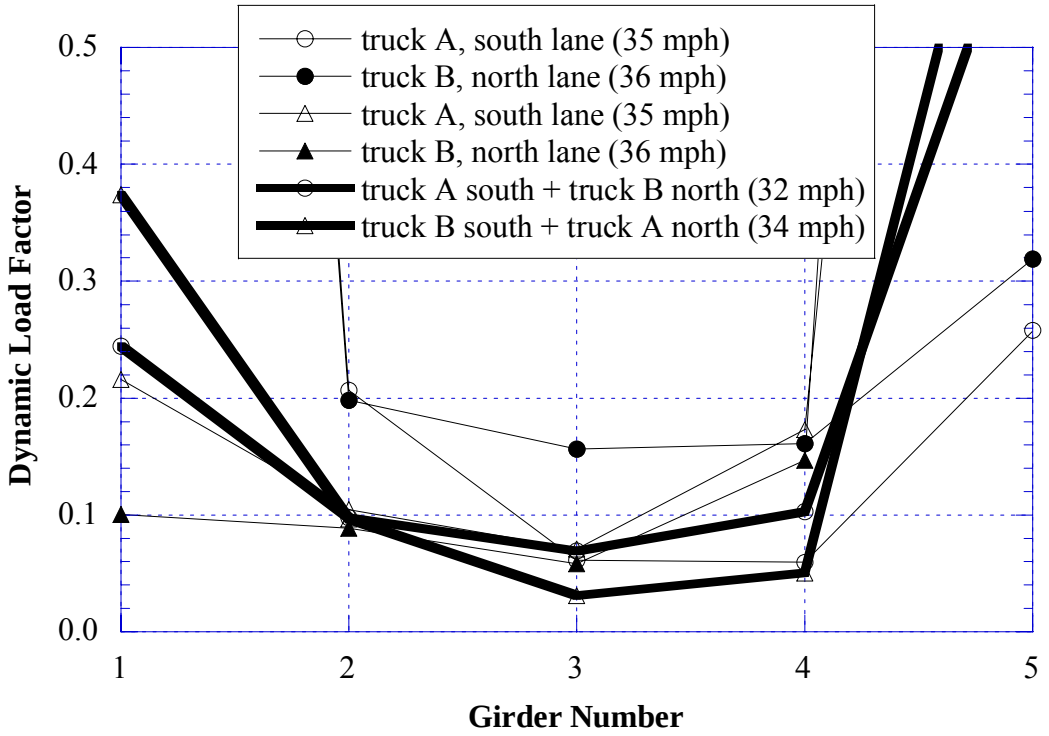

Figure 10.28 Dynamic Load Factors obtained from Negative Strain near Support over Center Pier (S13-59012)

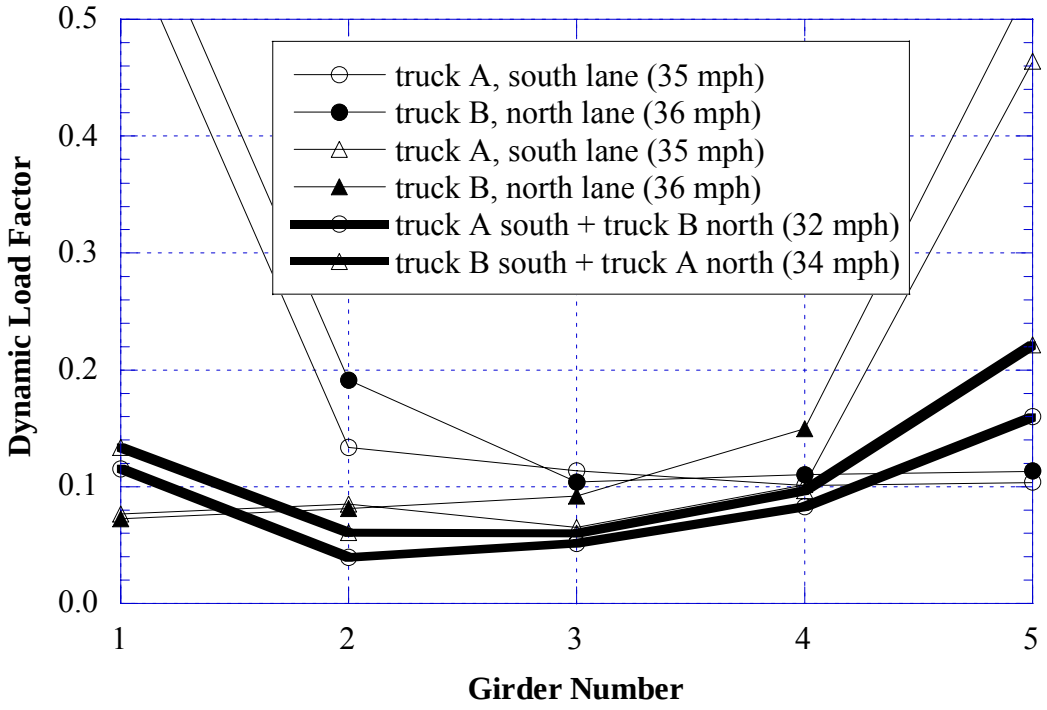

Figure 10.29 Dynamic Load Factors obtained from Negative Strain near Support over East Pier (S13-59012)

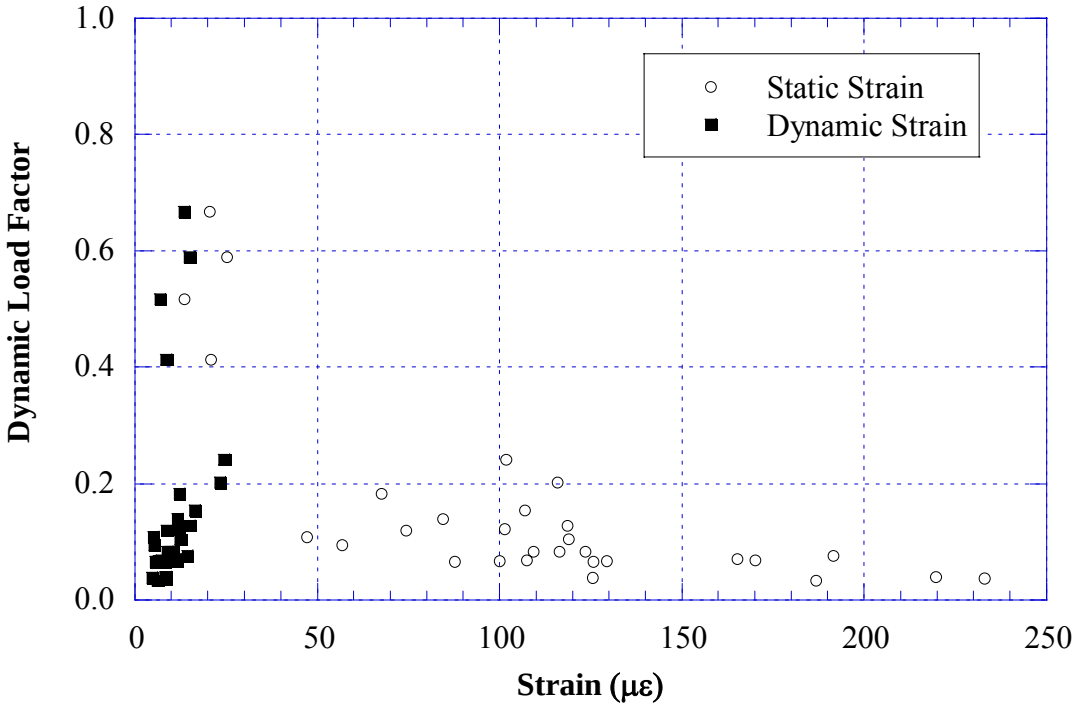

Figure 10.30 Strain vs. Dynamic Load Factors, Based on Positive Strain at Midspan of Span No.3 (S13-59012)

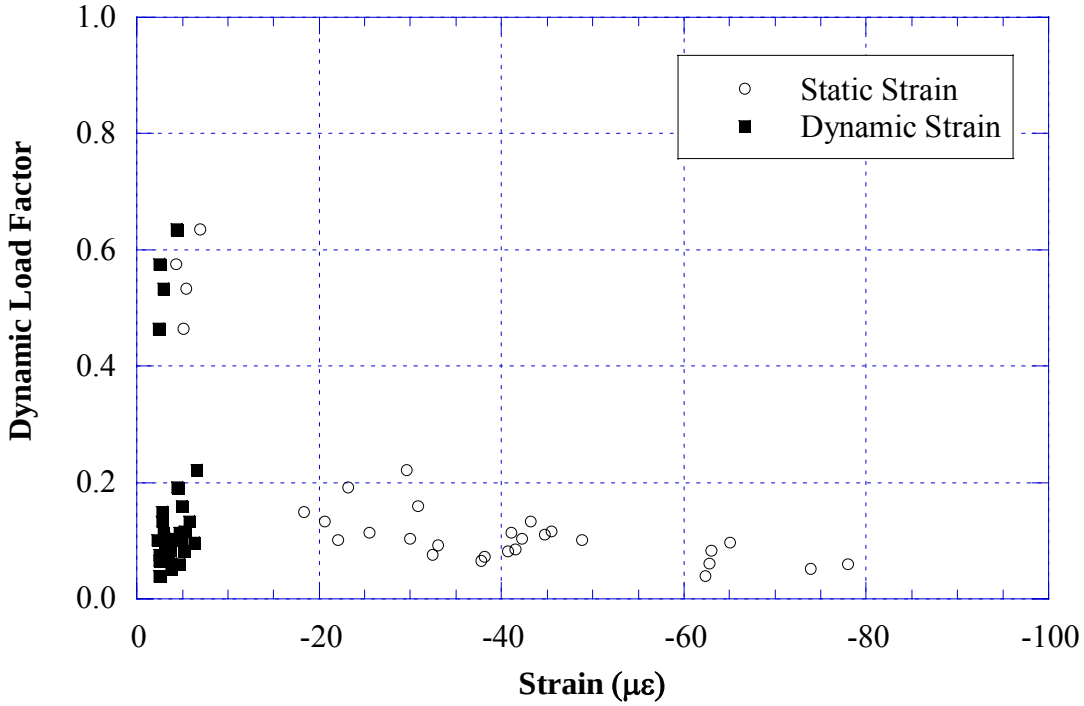

Figure 10.31 Strain vs. Dynamic Load Factors,
Based on Negative Strain near Support over East Pier (S13-59012)

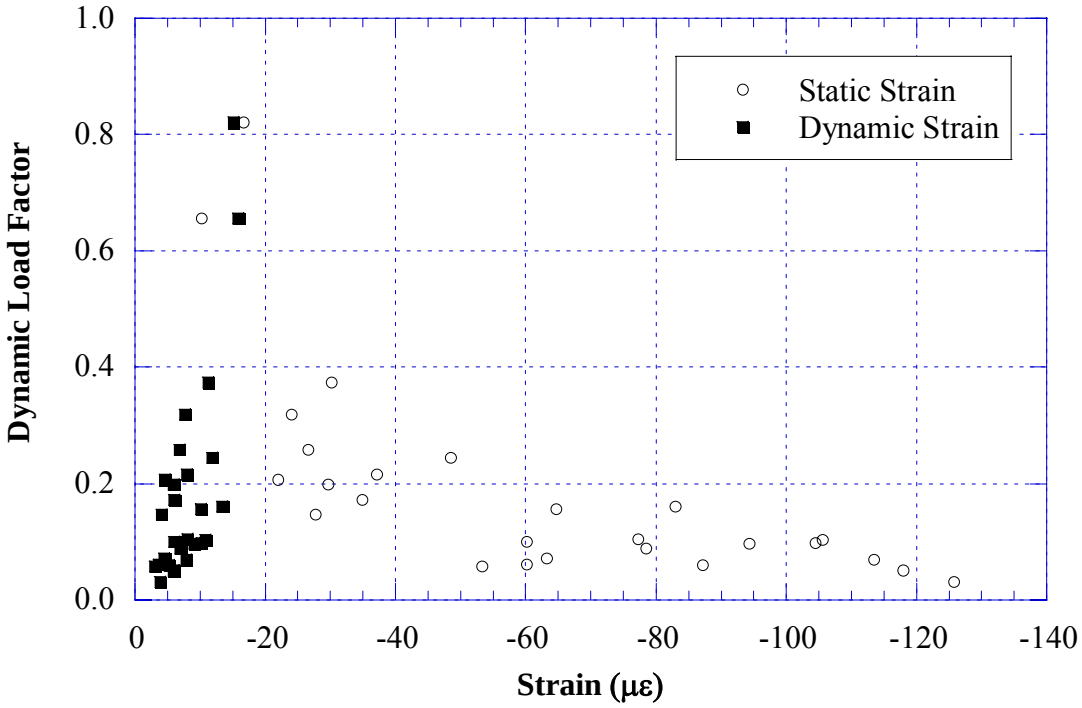

Figure 10.32 Strain vs. Dynamic Load Factors,
Based on Negative Strain near Support over Center Pier (S13-59012)

10.5 Results of Finite Element Analysis

A three-dimensional finite element method (FEM) was applied to investigate the structural behavior of the bridge S13-59012. The concrete slab was modeled with isotropic, eight node solid elements, with three degrees of freedoms at each node. The girder flanges and web were modeled using three-dimensional, quadrilateral, four node shell elements with six degrees of freedom at each node. The structural effects of the secondary members, such as the sidewalk and parapet, were also taken into account in the finite element analysis models.

The mesh of the FEM model is shown in Figure 10.33. Total number of elements is 23,072, and total number of nodes is 30,969 for this model.

Strains and GDF's calculated for the considered model is shown in Figures 10.34 to 10.43. Figures 10.34 and 10.35 present strains and GDF's from FEM model for positive moment at the midspan of span 3 under two trucks side-by-side loading. Figure 10.36 and 10.37 show the strains and GDF's from FEM model for negative moment near support over center pier under two trucks side-by-side loading. Figure 10.38 and 10.39 show the strains and GDF's from FEM model for negative moment near support over east pier under two trucks side-by-side loading. In the figures, the values obtained from FEM analysis are compared with the corresponding measured values.

The resulting strain values obtained from field tests are close to or lower than those from the finite element analysis for considered bridges. The main reason for this difference is due to the partial fixity of supports. In the previous study for simply supported bridges by University of Michigan (Nowak 2001 and 2002), the boundary conditions are simulated using the elastic spring elements in FEM models. However, for continuous bridges, it is almost impossible to obtain accurate spring coefficients satisfying multiple locations of supports with varied partial fixity condition. Therefore, in the study, the supports are assumed to behave as designed in the FEM models.

The FEM values are compared with the superposition of corresponding measured values. Figure 10.40 compares the GDF values for both positive moment and negative moment obtained from FEM analysis.

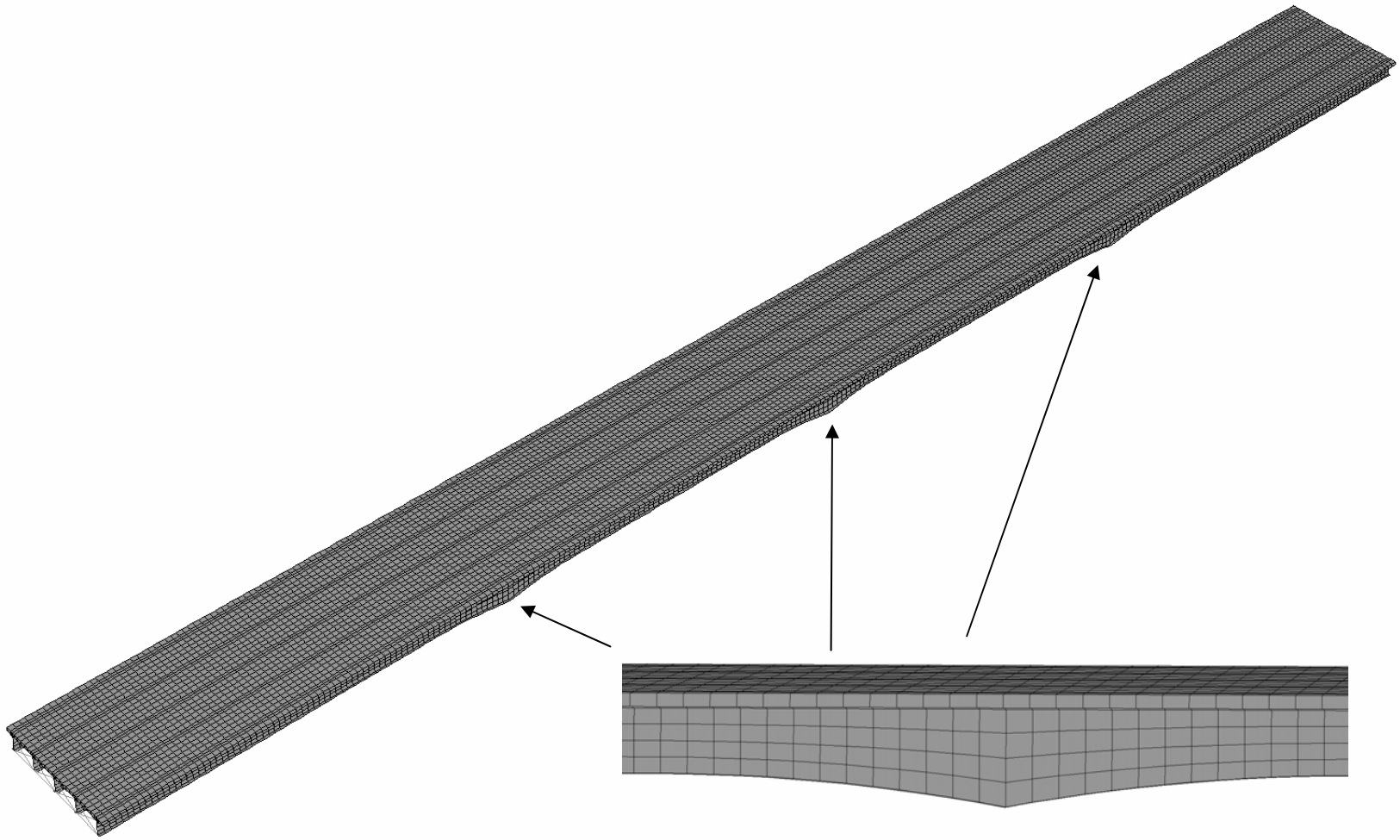

Figure 10.33 The Mesh of Finite Element Model (S13-59012)

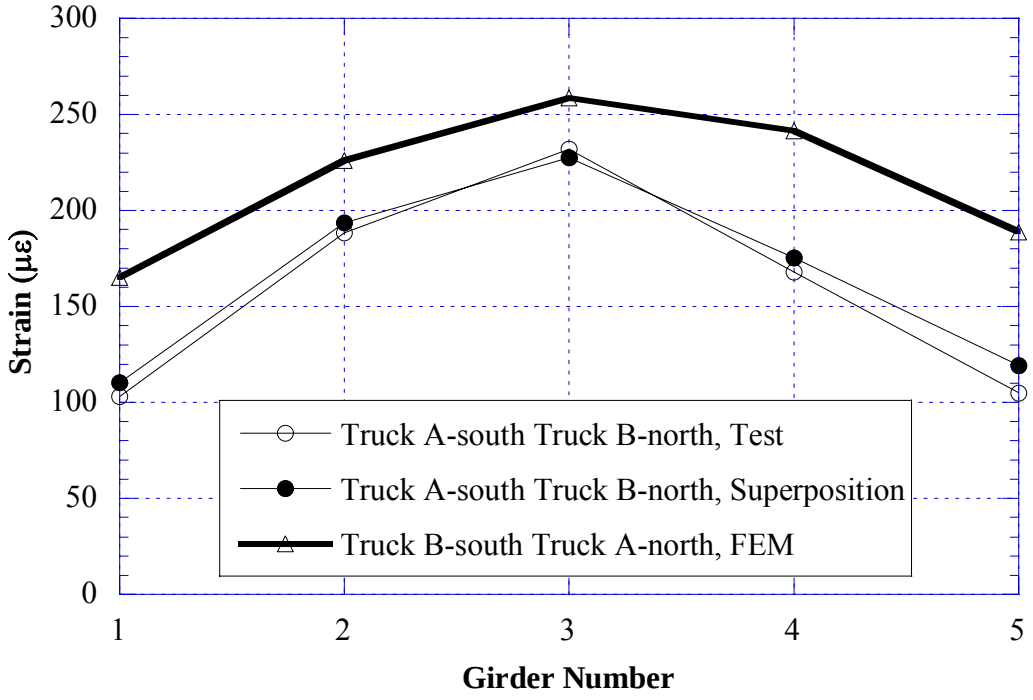

Figure 10.34 Comparison of FEM vs. Test, Positive Strain at Midspan of Span No.3, Side-by-Side Loading (S13-59012)

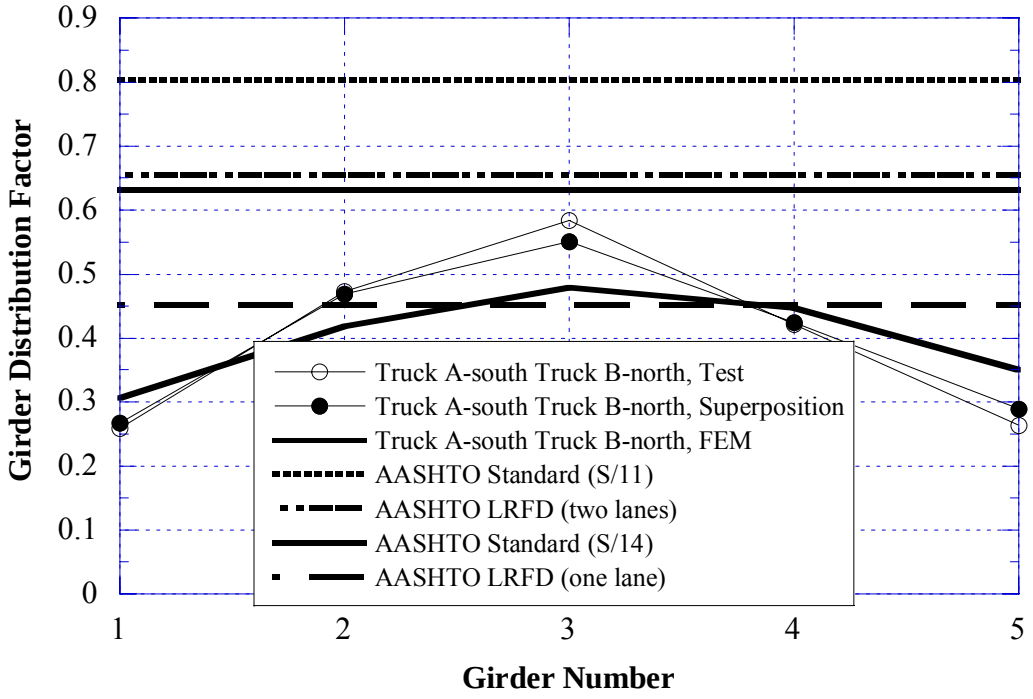

Figure 10.35 Comparison of FEM vs. Test, GDF from Positive Strain at Midspan of Span No.3, Side-by-Side Loading (S13-59012)

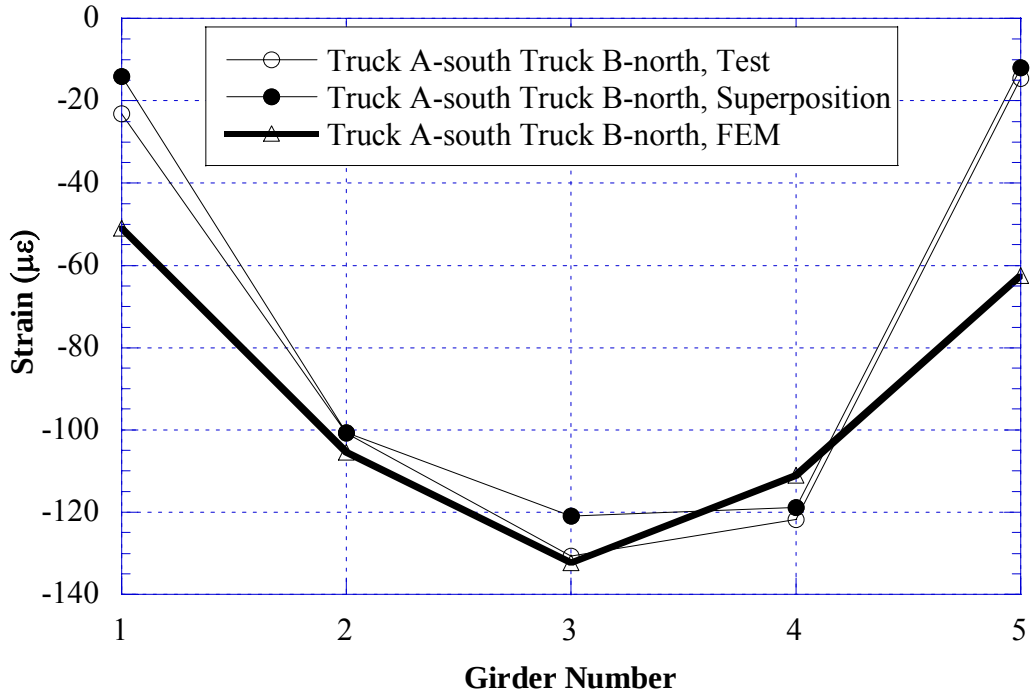

Figure 10.36 Comparison of FEM vs. Test, Negative Strain near Support over Center Pier, Side-by-Side Loading (S13-59012)

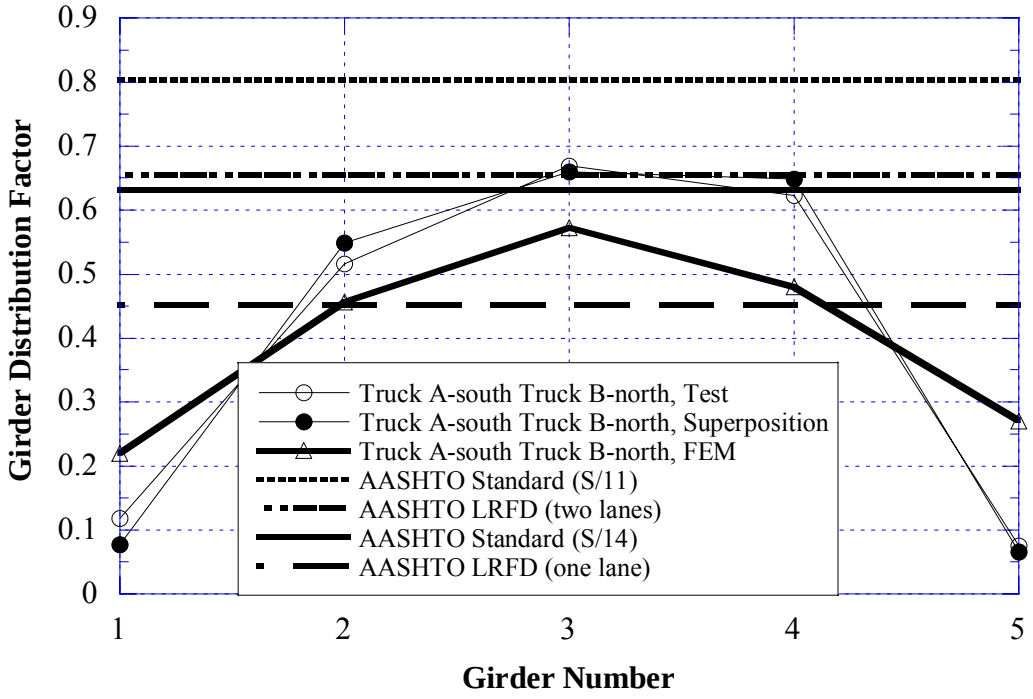

Figure 10.37 Comparison of FEM vs. Test, GDF from Negative Strain near Support over Center Pier, Side-by-Side Loading (S13-59012)

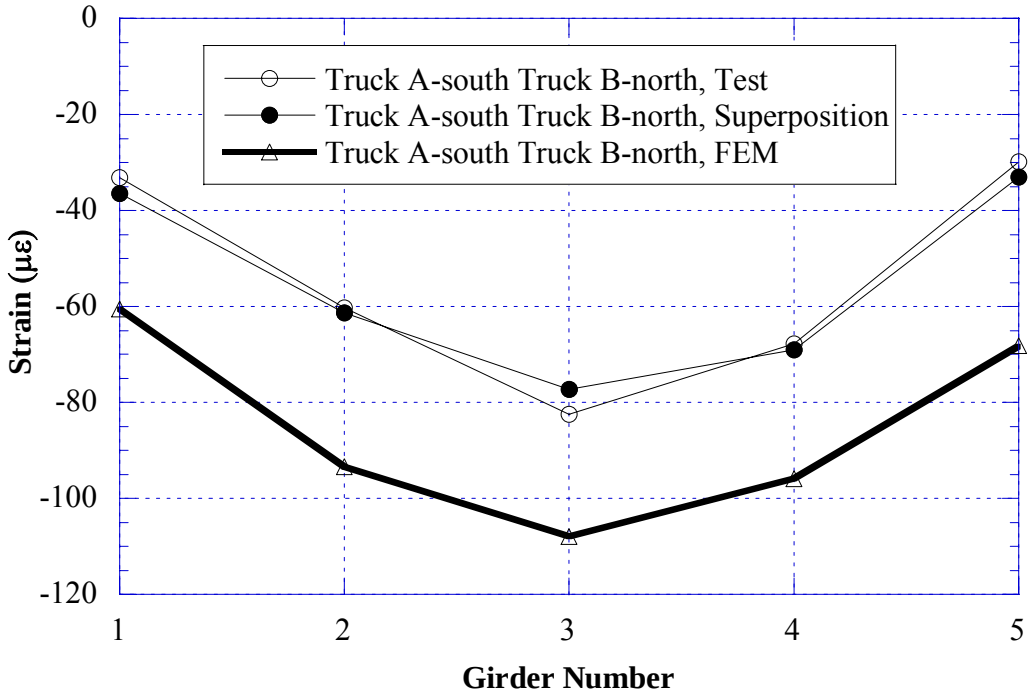

Figure 10.38 Comparison of FEM vs. Test, Negative Strain near Support over East Pier, Side-by-Side Loading (S13-59012)

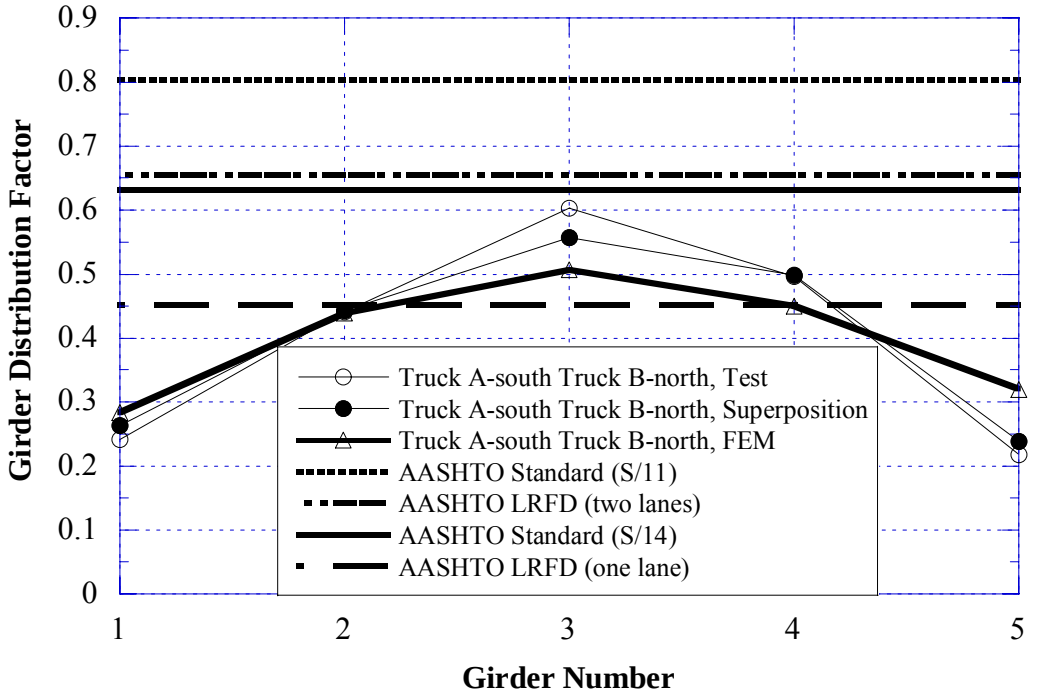

Figure 10.39 Comparison of FEM vs. Test, GDF from Negative Strain near Support over East Pier, Side-by-Side Loading (S13-59012)

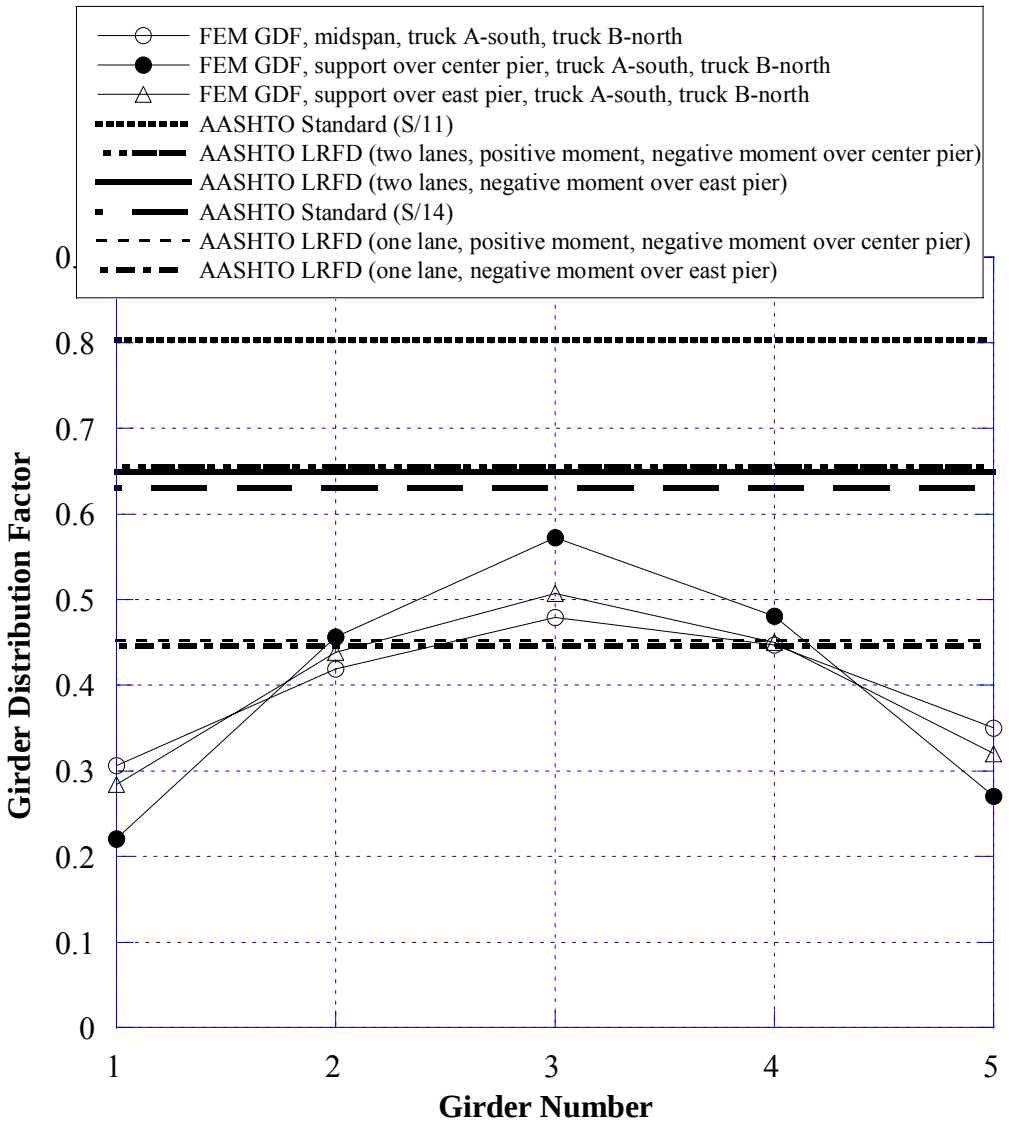

Figure 10.40 Comparison, GDF obtained from Positive Strain vs. GDF from Negative Strain, Based on Finite Element Analysis, Side-by-Side Loading (S13-59012)

11. BRIDGE ON 5 MILE ROAD OVER I-275, WAYNE COUNTY (S12-82293)

11.1 Bridge Description

This bridge was built in 1971 and it is located on 5 Mile Road over I-275 in Wayne County, Michigan. It is a six span steel structure with two continuous spans in the center of bridge, designed as a composite section. It has nine steel girders spaced at 8 ft 8 in, as shown in Figure 11.1, with 25 degree skew. The total bridge length is 594 ft. The span length of the two continuous spans is 113 ft each. The side elevation is shown in Figure 11.2. The bridge has two traffic lanes in each direction, plus one center lane used for left turn. It carries an average daily traffic (ADT) of 6,840. The operating load rating is 280 kips, according to the Michigan Structure Inventory.

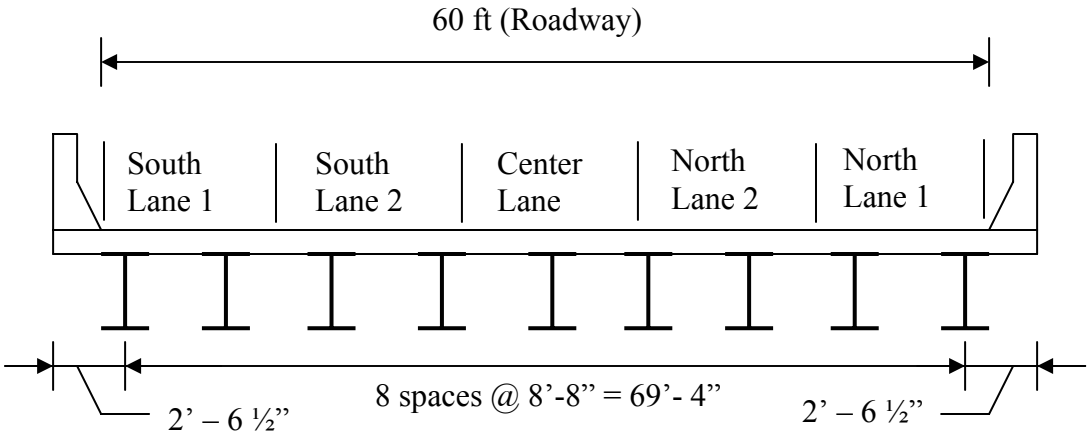

Figure 11.1 Cross Section of the bridge (S12-82293)

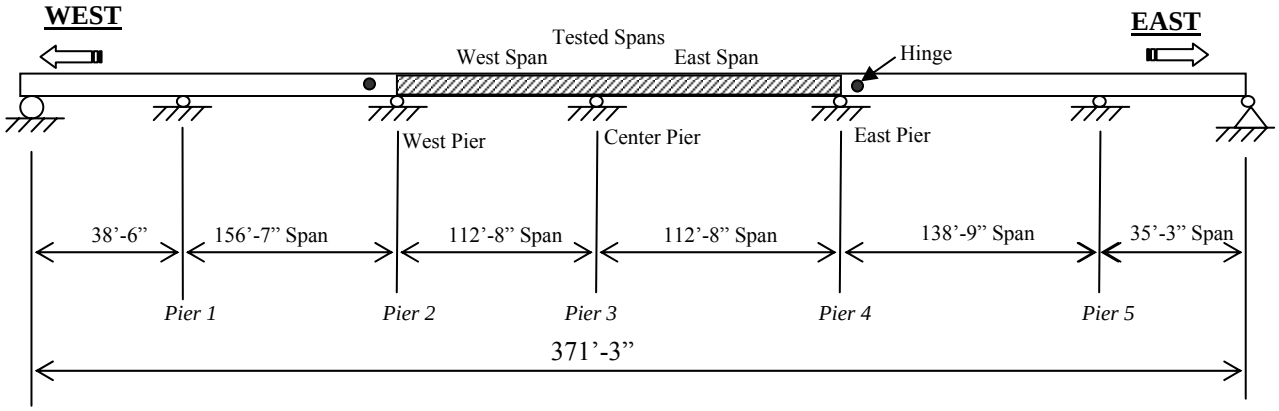

Figure 11.2 Side Elevation of Bridge (S12-82293)

11.2 Instrumentation

Strain transducers were installed on the bottom flanges of girders at midspan and at support locations, as shown in Figure 11.3. The reflector for the PSM-R device from Noptel was installed at the girder No. 5 to measure deflection. The bridge was instrumented on August 6, 2002, and bridge test were performed on August 7, 2002.

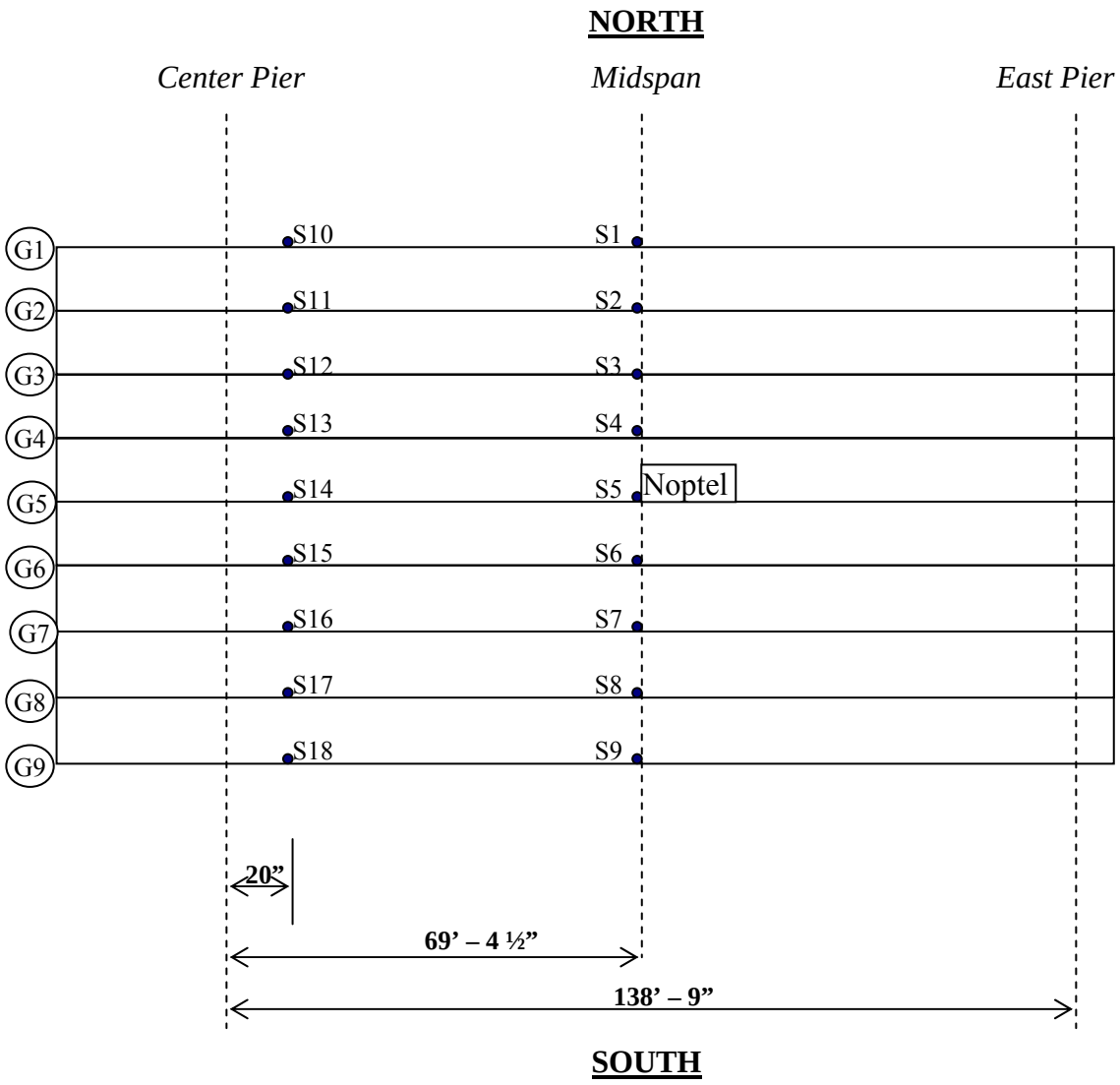

Figure 11.3 Strain Gage Location in Bridge (S12-82293)

11.3 Load cases

The girder distribution factors (GDF) and dynamic load factors (DLF) were calculated using the strains measured at midspan and near support. The bridge was loaded with two 11-axle trucks (three-unit vehicles).

The truck A and truck B have gross weights of 134 kips and 145 kips, with wheelbases of 59 ft and 57 ft, respectively. Truck configurations are shown in Figures 11.4 and 11.5.

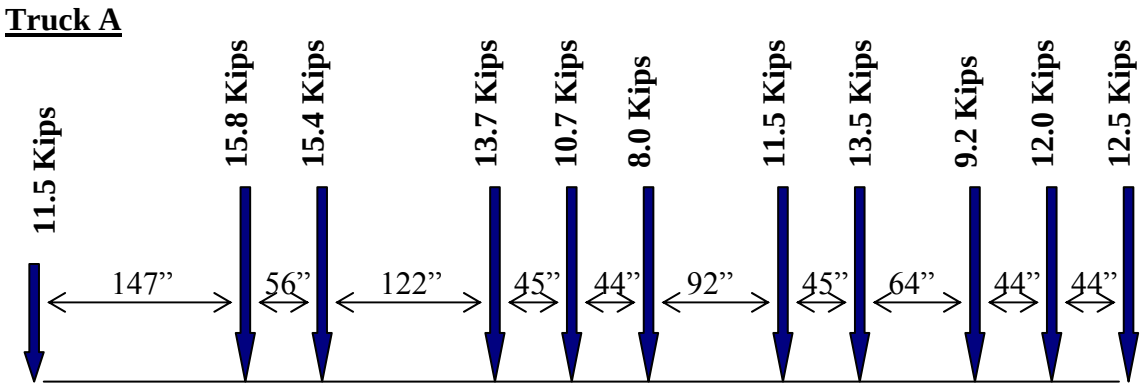

Figure 11.4 Truck A configuration, Bridge (S12-82293)

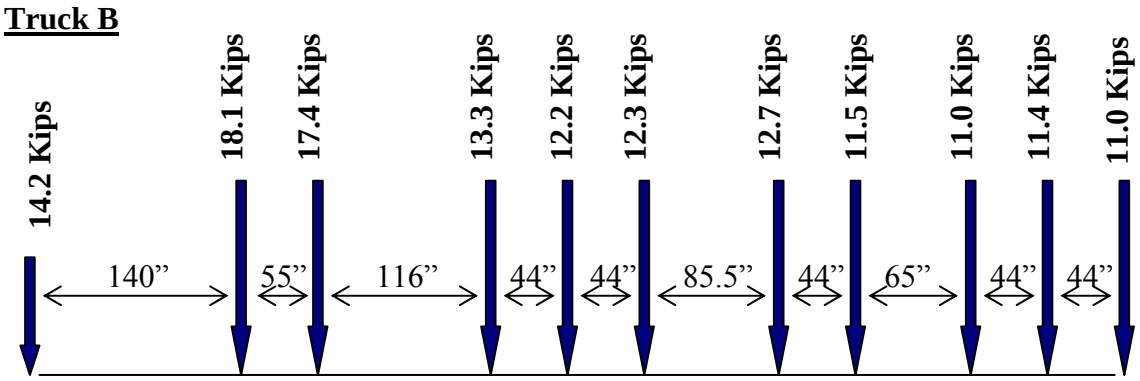

Figure 11.5 Truck B configuration, Bridge (S12-82293)

A total of 19 load cases were considered, as shown in Table 11.1. First each truck was driven by itself at the center of each lane, at crawling speed. In addition, two trucks were driven simultaneously, side-by-side, at crawling speed. In addition, trucks were stopped at predetermined position to verify pre-test calculation. For this bridge, normal speed runs were not performed due to high traffic.

Table 11.1. Sequence of Test Runs, Bridge (S12-82293)

Run#	Truck	Lane	Truck Speed
1	Truck A	South 1	Crawling
2	Truck B	South 1	Crawling
3	Truck A	South 2	Crawling
4	Truck B	South 2	Crawling
5	Truck A	Center	Crawling
6	Truck B	Center	Crawling
7	Truck A	North 2	Crawling
8	Truck B	North 2	Crawling
9	Truck A	North 1	Crawling
10	Truck B	North 1	Crawling
11	Truck A (South 1) Truck B (South 2)		Crawling
12	Truck A (South 2) Truck B (Center)		Crawling
13	Truck A (Center) Truck B (North 2)		Crawling
14	Truck A (North 2) Truck B (North 1)		Crawling
15	Truck A followed by B	South 1	Stop at fixed position
16	Truck A followed by B	South 2	Stop at fixed position
17	Truck A followed by B	Center	Stop at fixed position
18	Truck A followed by B	North 2	Stop at fixed position
19	Truck A followed by B	North 1	Stop at fixed position

11.4 Test results

The resulting strains and GDF's are shown in Figures 11.6 through 11.43. Figures 11.6 to 11.17 present the results for one truck on the bridge under crawling-speed (static) tests. For each loading condition, strains are measured and the corresponding GDF's are calculated from the strain measurement. For comparison, GDF are also calculated according to AASHTO Standard (1996) and AASHTO LRFD Code (1998). The resulting GDF's are also shown in Figures 11.6 through 11.7. Figures 11.6 to 11.11 show positive strain values recorded at the midspan of eastspan, and also resulting GDF's. Figures 11.12 to 11.17 present the negative strain values and corresponding GDF's near supports over center pier. For single lane loading, the maximum positive strain is about 100 με. This strain value corresponds about 2.9 ksi. The maximum negative strain near support is less than 85 με. This corresponds about 2.5 ksi. In all considered single lane loadings, the measured GDF's do not exceed code specified values.

Figures 11.18 to 11.33 present the results for side-by-side static loading on the bridge under crawling-speed (static) tests. For two trucks side-by-side, strains are measured and the corresponding GDF's are calculated from the strain measurement. For comparison, GDF are also calculated according to code specified values. Figures 11.18 to 11.25 present the measured positive strains under two trucks side by side, with corresponding GDF's compared with code specified values. For two trucks side by side, the maximum recorded positive strain at the midspan is about 160 με, which corresponds about 4.6 ksi. Figures 11.18 to 11.25 show that code specified GDF's are conservative. Even the single lane GDF's specifed in AASHTO Standard (1996) is sufficient for two trucks side by side. However, single lane GDF's specified in AASHTO LRFD (1998) is not sufficient for two lane load case in this bridge.

Figures 11.26 to 11.33 present the negative strains and corresponding GDF's under two truck side by side loading measured near support over center pier. The maximum recorded negative strain near support at the midspan is about 120 με, which corresponds about 3.5 ksi. The figures show that the specified GDF in AASHTO Standard (1996) for

multilane loading is conservative. In some cases (Figures 11.27 and 11.31), AASHTO LRFD (1998) for multilane loading is not conservative. However, they are not from the most critical loading case for this bridge, since this bridge has five lanes. Therefore, the corresponding strains are very low, even though the GDF's exceed specified values in AASHTO LRFD (1998).

In all cases, the superposition of strains due to a single truck produces almost the same results as strain due to two trucks side-by-side.

Figure 11.34 shows the strain superposition of two separate two trucks side-by-side loading (4 trucks) for positive strain. This simulates two trucks side-by-side loading on south lanes 1 and 2, and north lanes 1 and 2. The resulting maximum negative strain is about 160 με. The corresponding GDF's are shown in Figure 11.35. In this case, code specified values are conservative, and even the single lane GDF specifed in AASHTO Standard (1996) is sufficient.

Figures 11.36 and 11.37 show the strain superposition of two separate two trucks side-by-side loading (4 trucks). This simulates two trucks side-by-side loading on south lanes 1 and 2, and north lanes 1 and 2. The resulting maximum negative strain is about 100 με. The corresponding GDF's are shown in Figure 11.37. Again, code specified values are conservative. However, single lane GDF's specifed in the codes are not conservative in this case.

Girder No. 5 was instrumented with a remote deflection measurement device manufactured by Noptel. The reflector was installed at midspan. Due to high electric noise, not all data for deflection measurement could be processed. The available results are shown in Table 11.2. The maximum deflection recorded during the test is 10.9 mm for girder No. 5 .

Table 11.2. Maximum deflections measured at the center of Girder No.5, Bridge (S12-82293)

Run #	Vertical Deflection (mm)
1	1.5
2	1.7
3	4.5
4	4.7
5	6.8
6	7.6
7	4.4
8	N/A
9	1.6
10	1.4
11	N/A
12	10.9
13	N/A
14	N/A

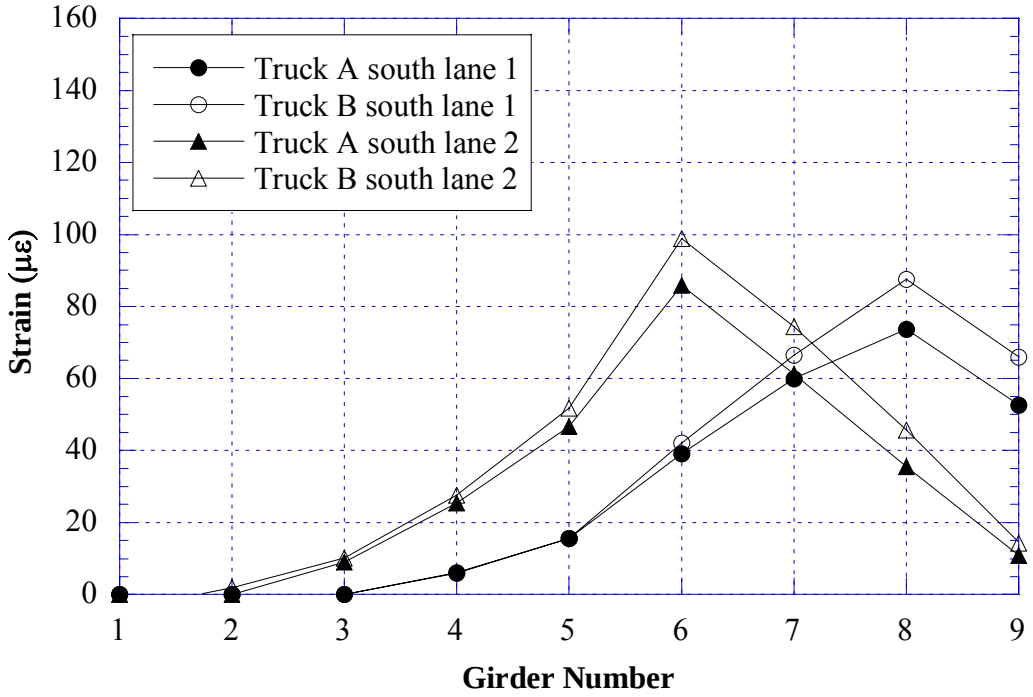

Figure 11.6 Positive Strain at Midspan of Eastspan, South Lane Loading (S12-82293)

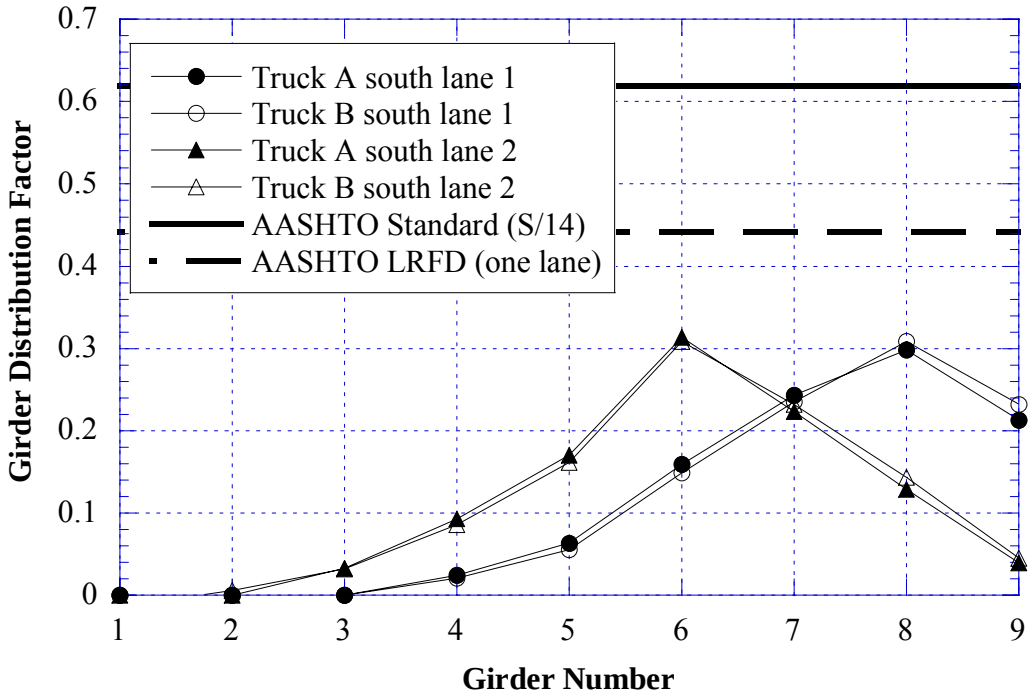

Figure 11.7 GDF from Positive Strain at Midspan of Eastspan, South Lane Loading (S12-82293)

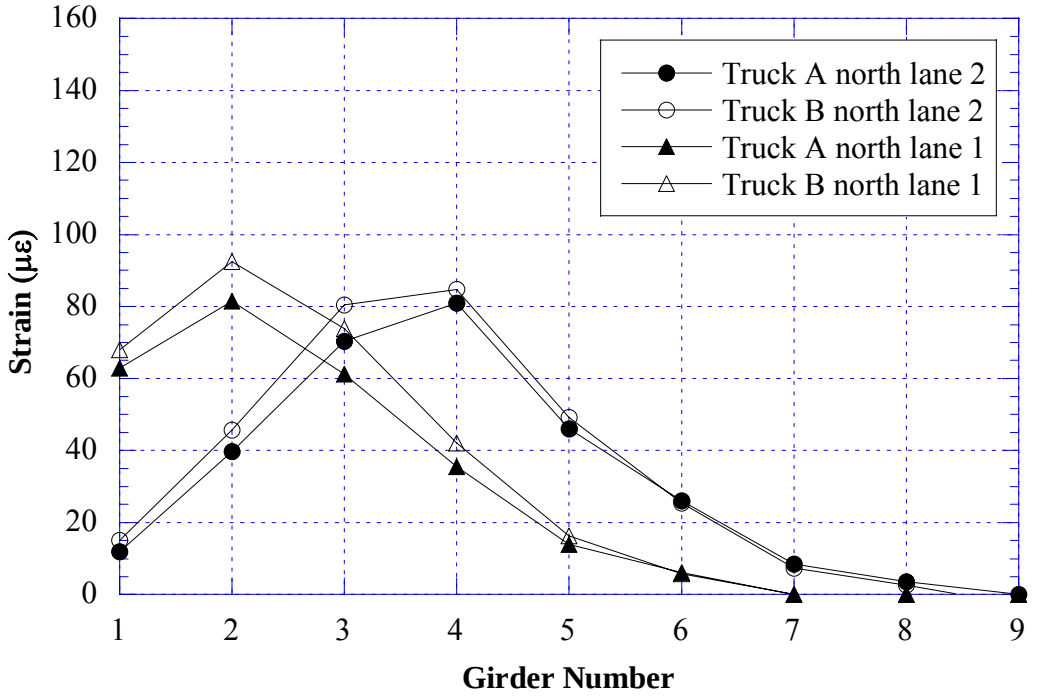

Figure 11.8 Positive Strain at Midspan of Eastspan, North Lane Loading (S12-82293)

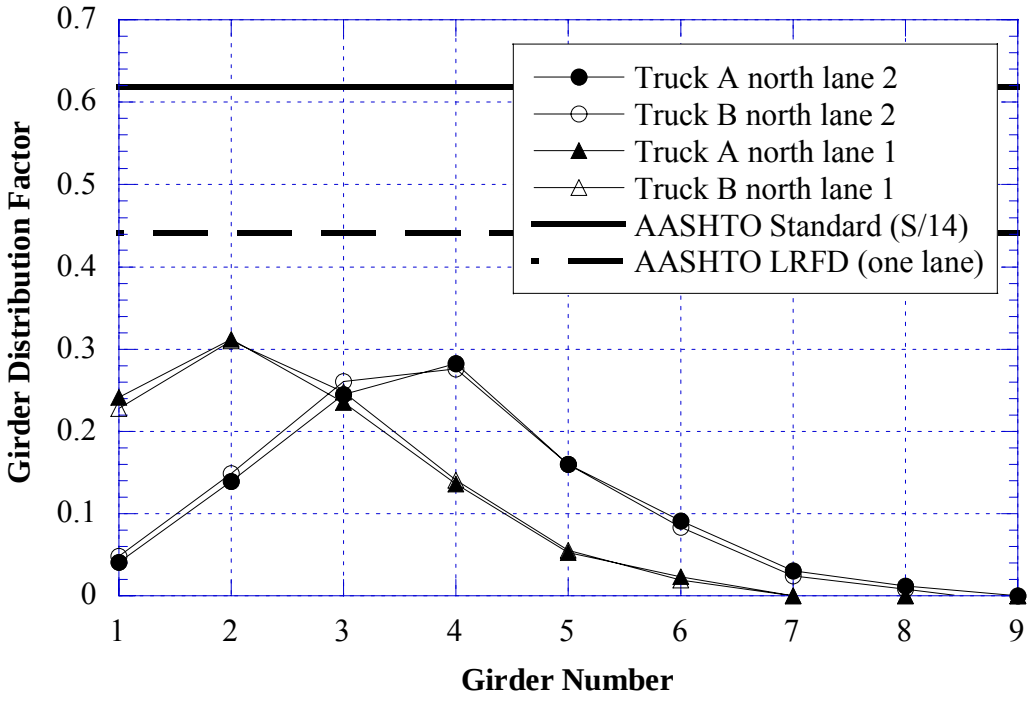

Figure 11.9 GDF from Positive Strain at Midspan of Eastspan, North Lane Loading (S12-82293)

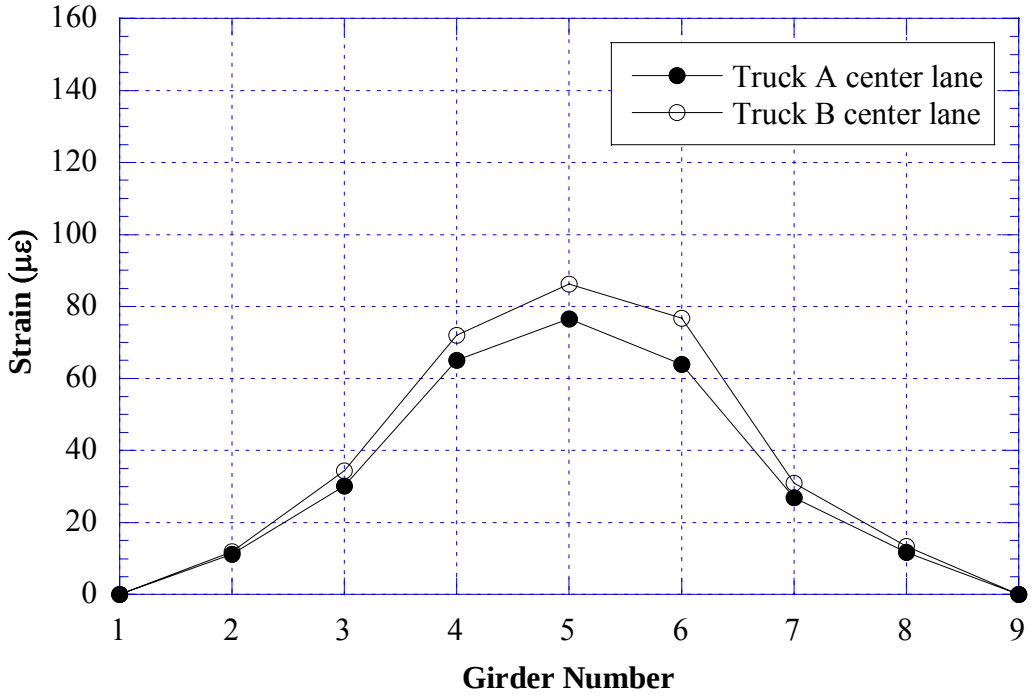

Figure 11.10 Positive Strain at Midspan of Eastspan, Center Lane Loading (S12-82293)

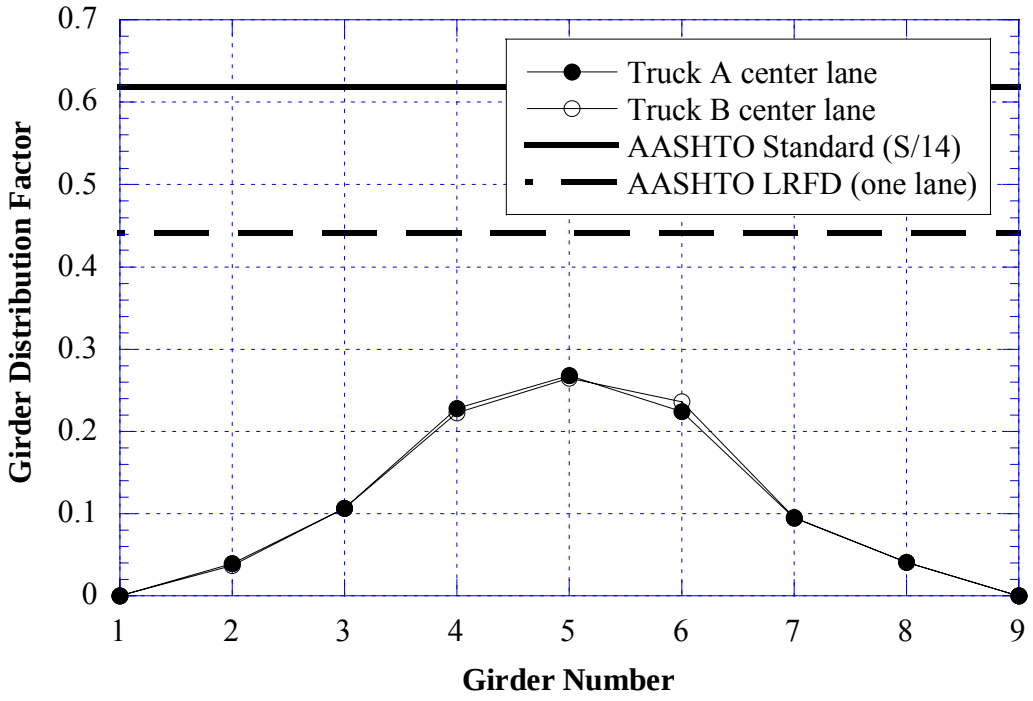

Figure 11.11 GDF from Positive Strain at Midspan of Eastspan, Center Lane Loading (S12-82293)

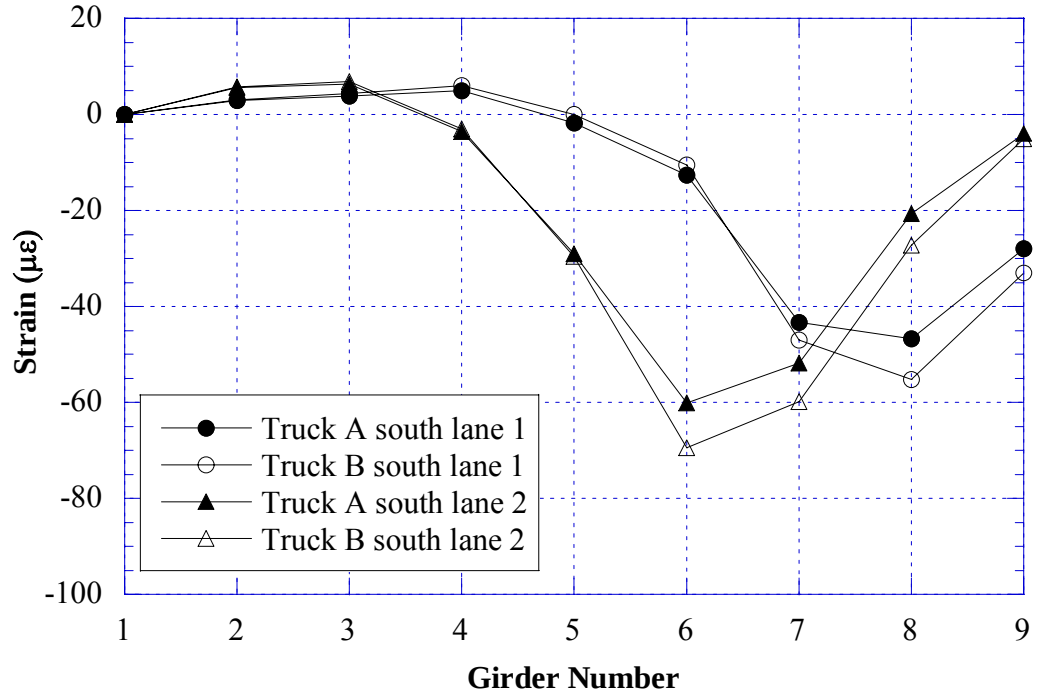

Figure 11.12 Negative Strain near Support over Center Pier, South Lane Loading (S12-82293)

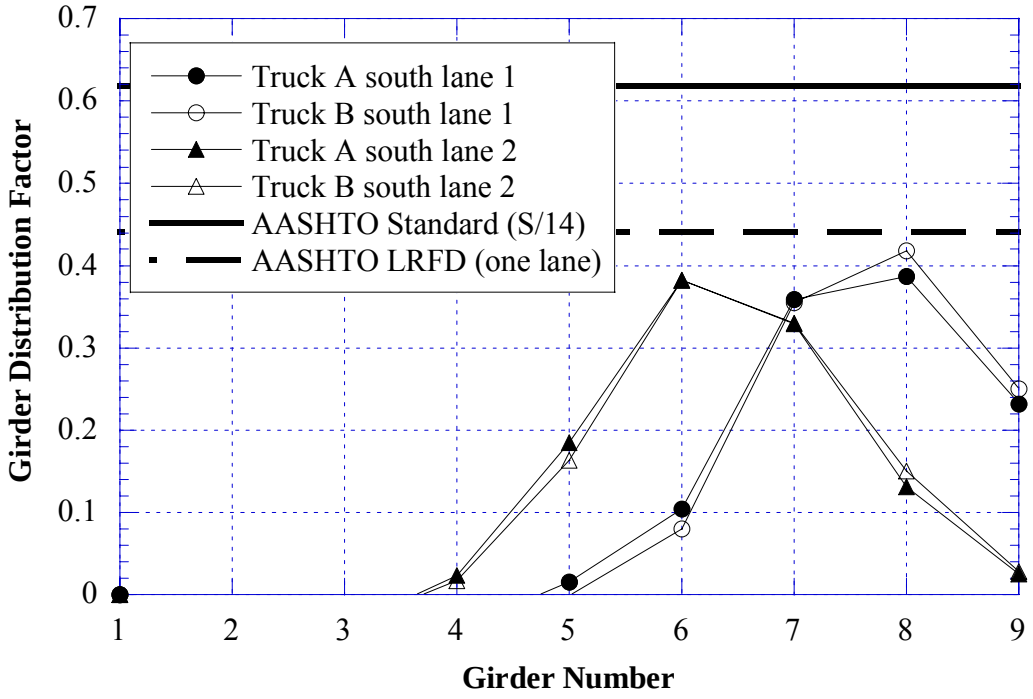

Figure 11.13 GDF from Negative Strain near Support over Center Pier, South Lane Loading (S12-82293)

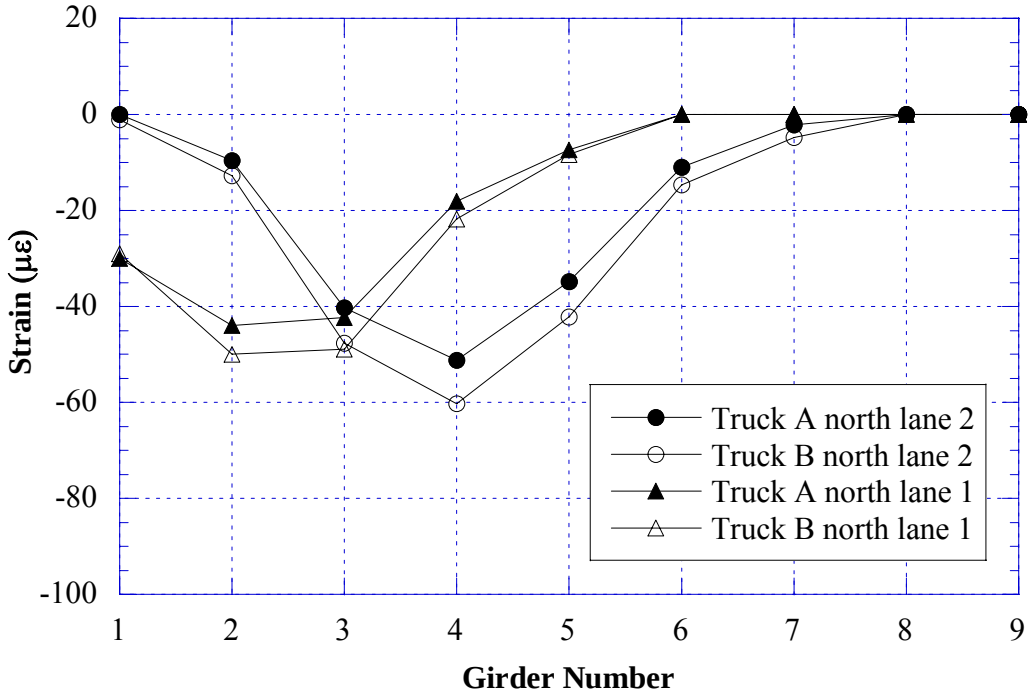

Figure 11.14 Negative Strain near Support over Center Pier, North Lane Loading (S12-82293)

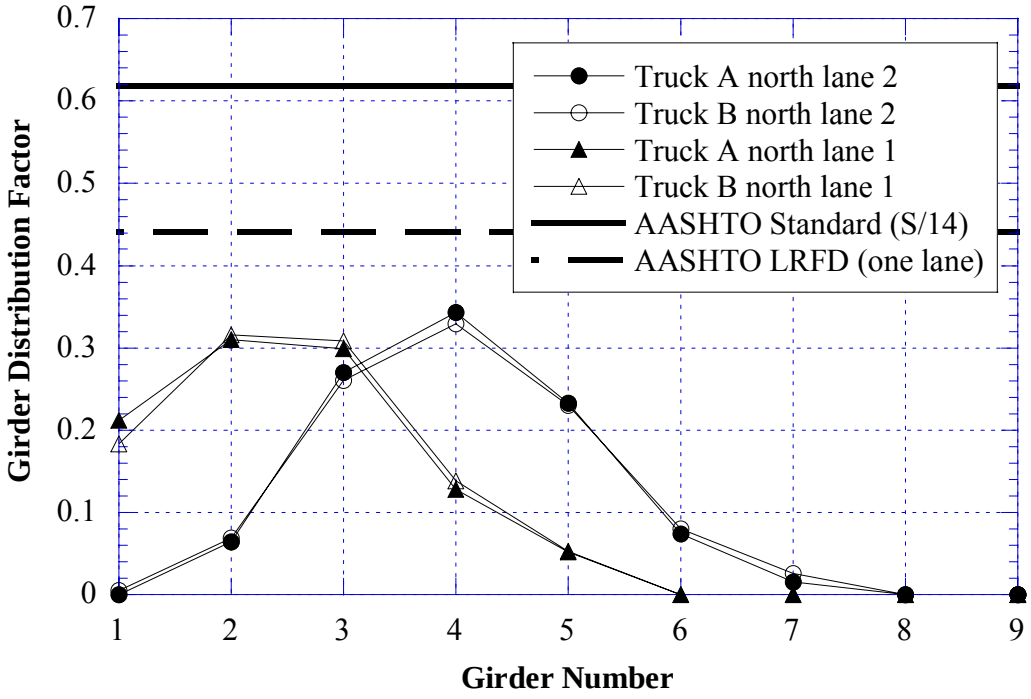

Figure 11.15 GDF from Negative Strain near Support over Center Pier, North Lane Loading (S12-82293)

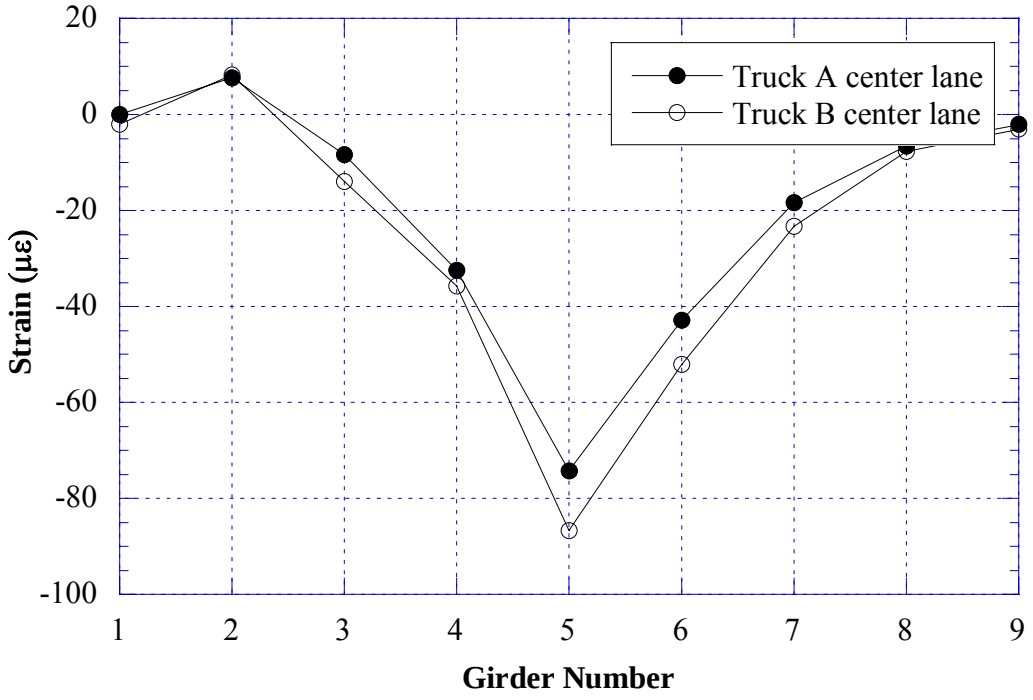

Figure 11.16 Negative Strain near Support over Center Pier, Center Lane Loading

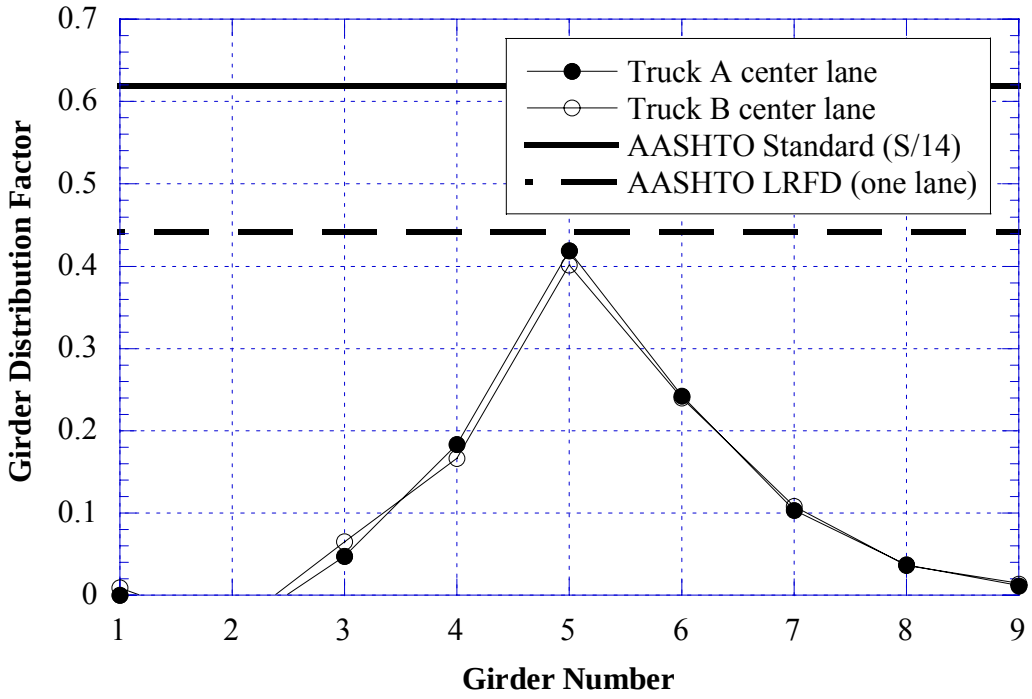

Figure 11.17 GDF from Negative Strain near Support over Center Pier, Center Lane Loading (S12-82293)

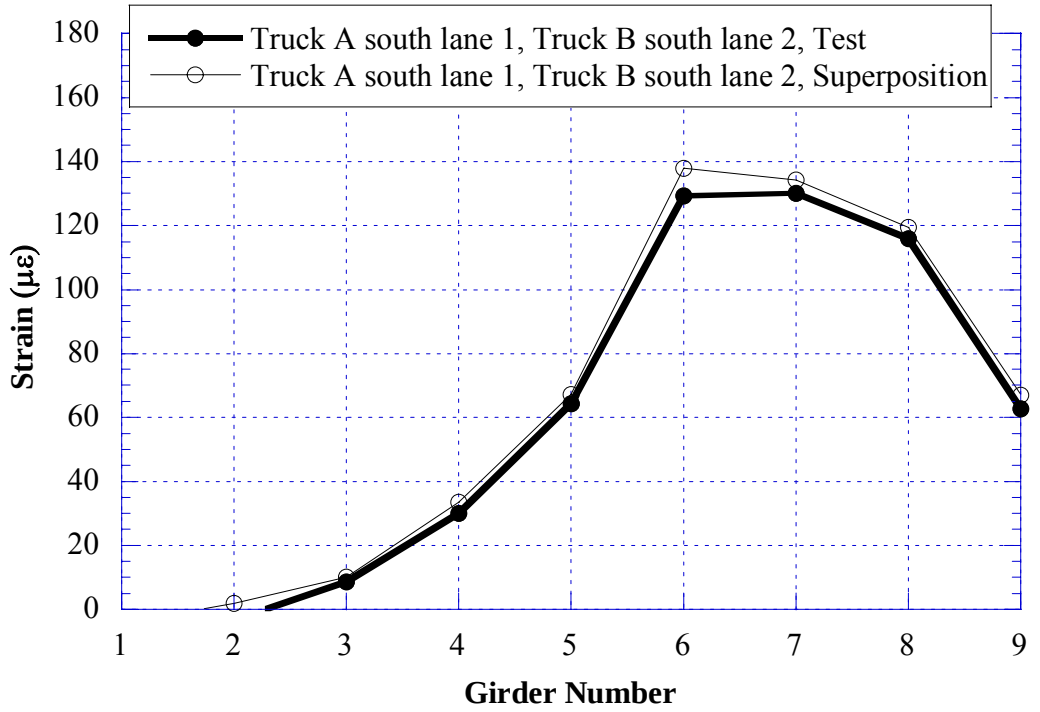

Figure 11.18 Positive Strain at Midspan of Eastspan, Two Truck Side-by-Side Loading, South Lane 1 and South Lane2 (S12-82293)

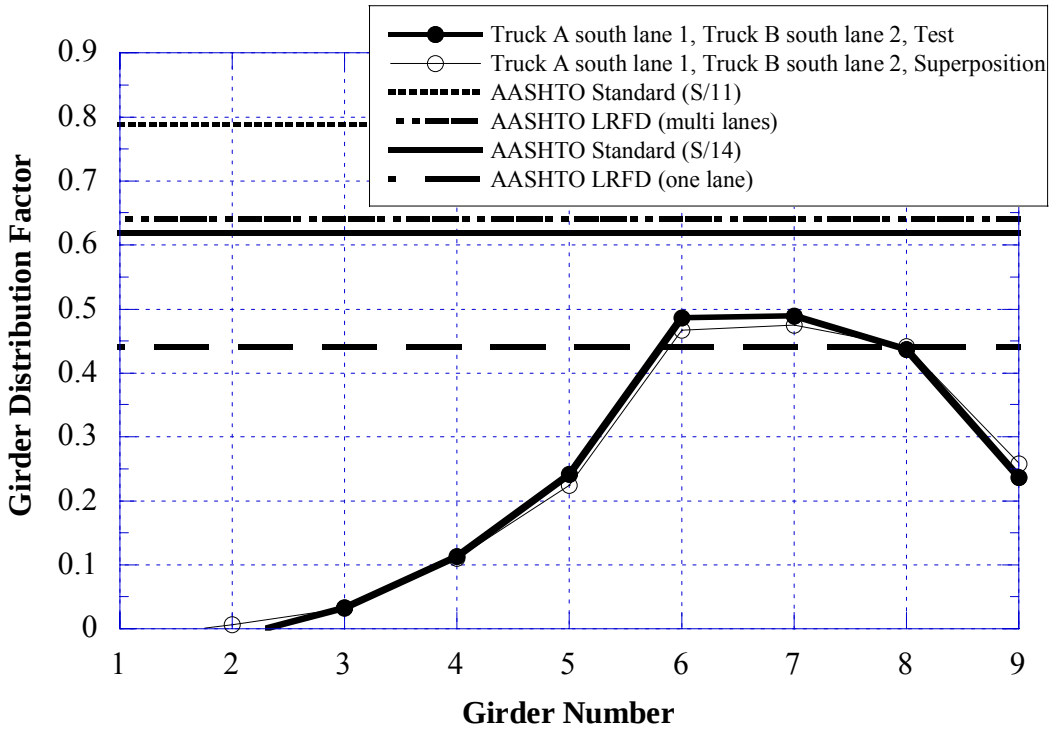

Figure 11.19 GDF from Positive Strain at Midspan of Eastspan, Two Truck Side-by-Side Loading, South Lane 1 and South Lane 2 (S12-82293)

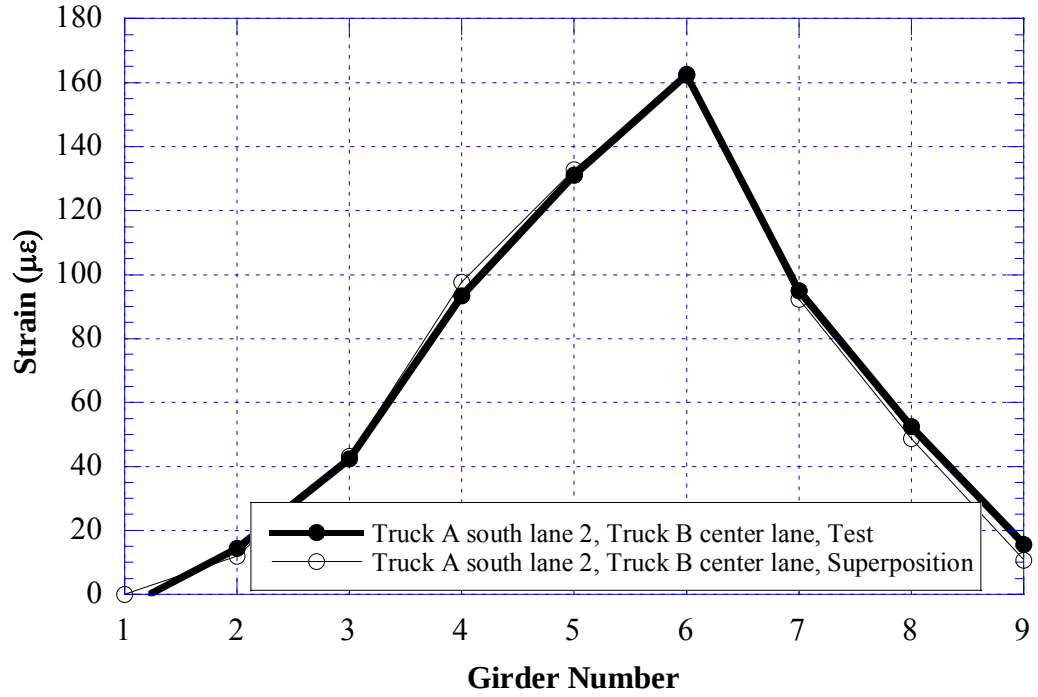

Figure 11.20 Positive Strain at Midspan of Eastspan, Two Truck Side-by-Side Loading, South Lane 2 and Center Lane (S12-82293)

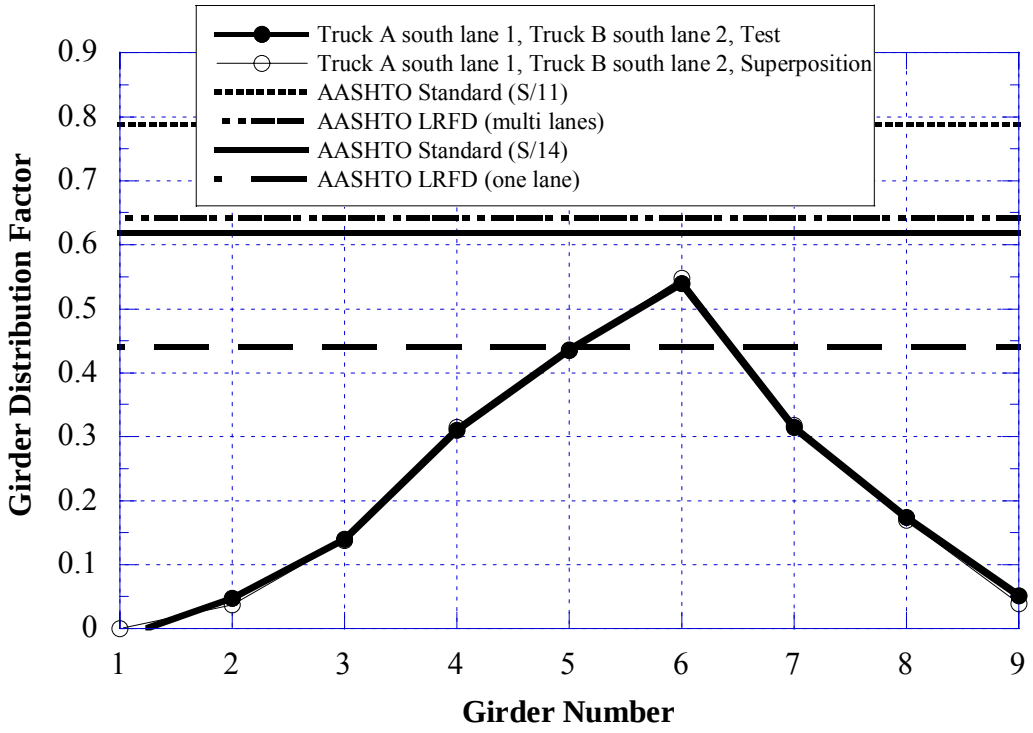

Figure 11.21 GDF from Positive Strain at Midspan of Eastspan, Two Truck Side-by-Side Loading, South Lane 2 and Center Lane (S12-82293)

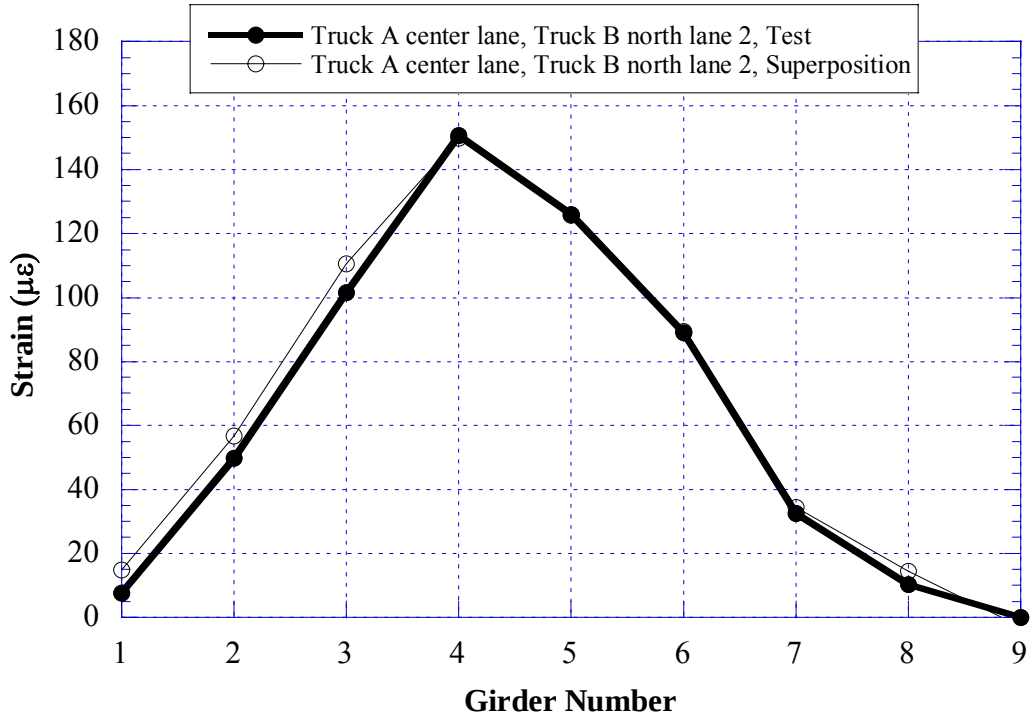

Figure 11.22 Positive Strain at Midspan of Eastspan, Two Truck Side-by-Side Loading, Center Lane and North Lane (S12-82293)

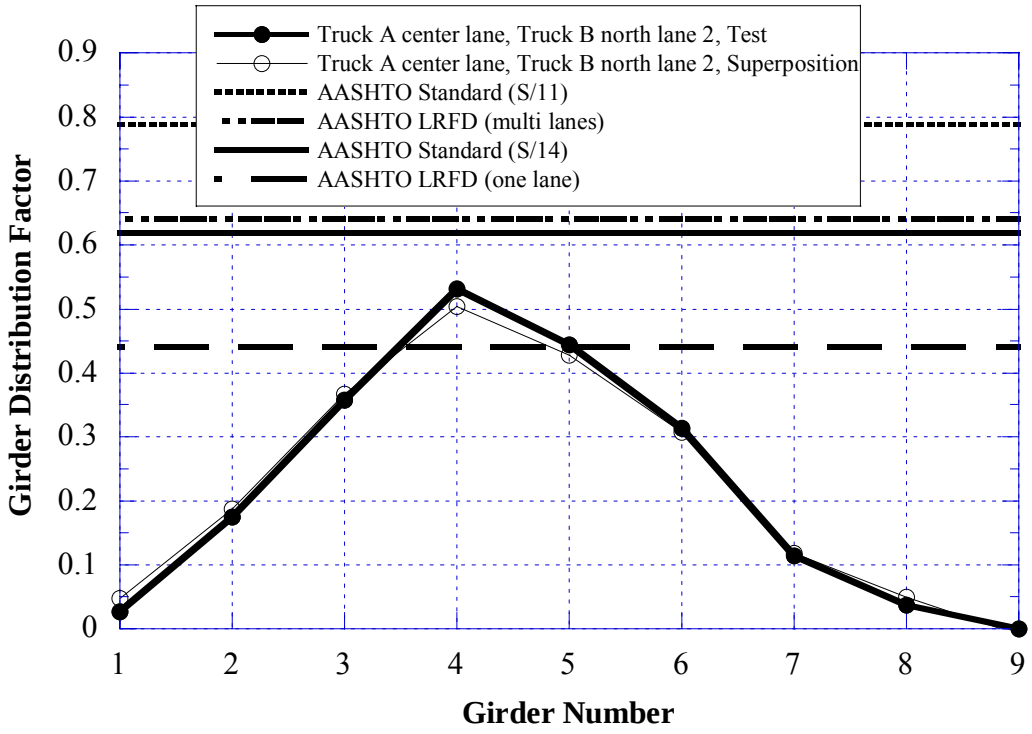

Figure 11.23 GDF from Positive Strain at Midspan of Eastspan, Two Truck Side-by-Side Loading, Center Lane and North Lane (S12-82293)

Figure 11.24 Positive Strain at Midspan of Eastspan, Two Truck Side-by-Side Loading, North Lane 2 and North Lane 1 (S12-82293)

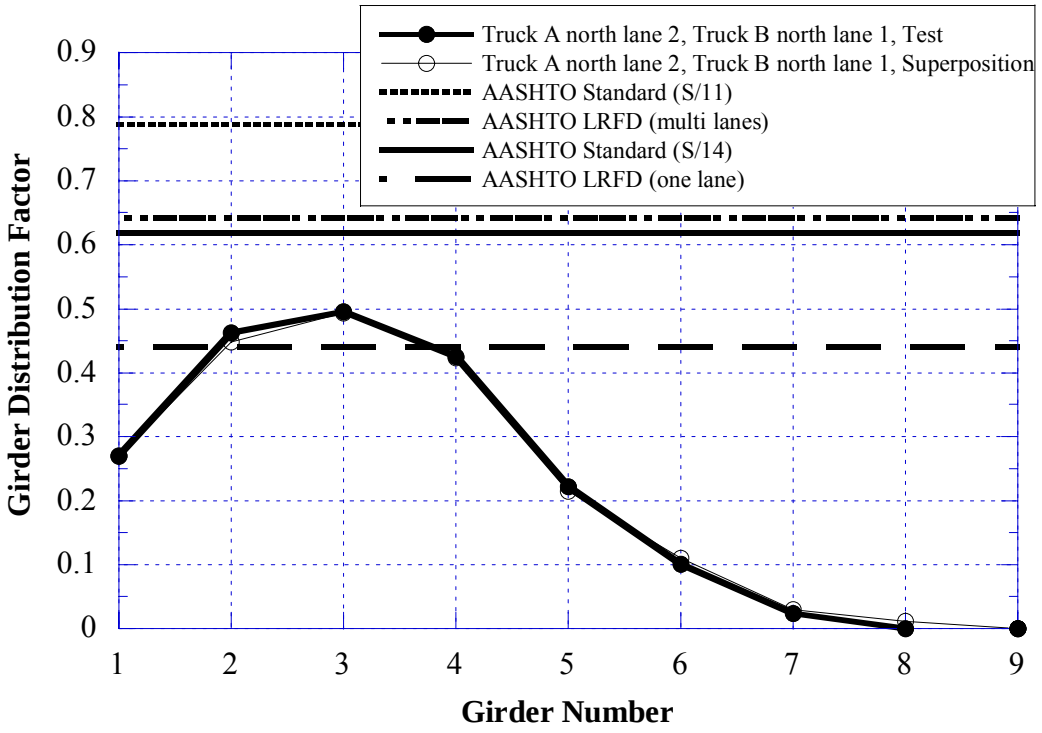

Figure 11.25 GDF from Positive Strain at Midspan of Eastspan, Two Truck Side-by-Side Loading, North Lane 2 and North Lane 1 (S12-82293)

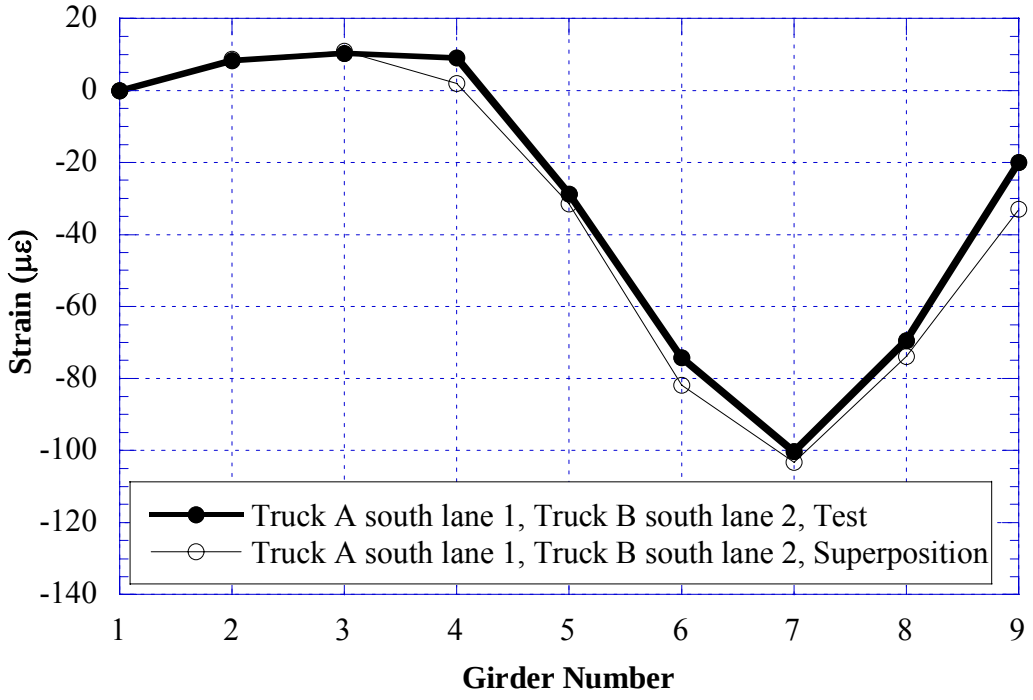

Figure 11.26 Negative Strain near Support over Center Pier, Two Truck Side-by-Side Loading,
South Lane 1 and South Lane2 (S12-82293)

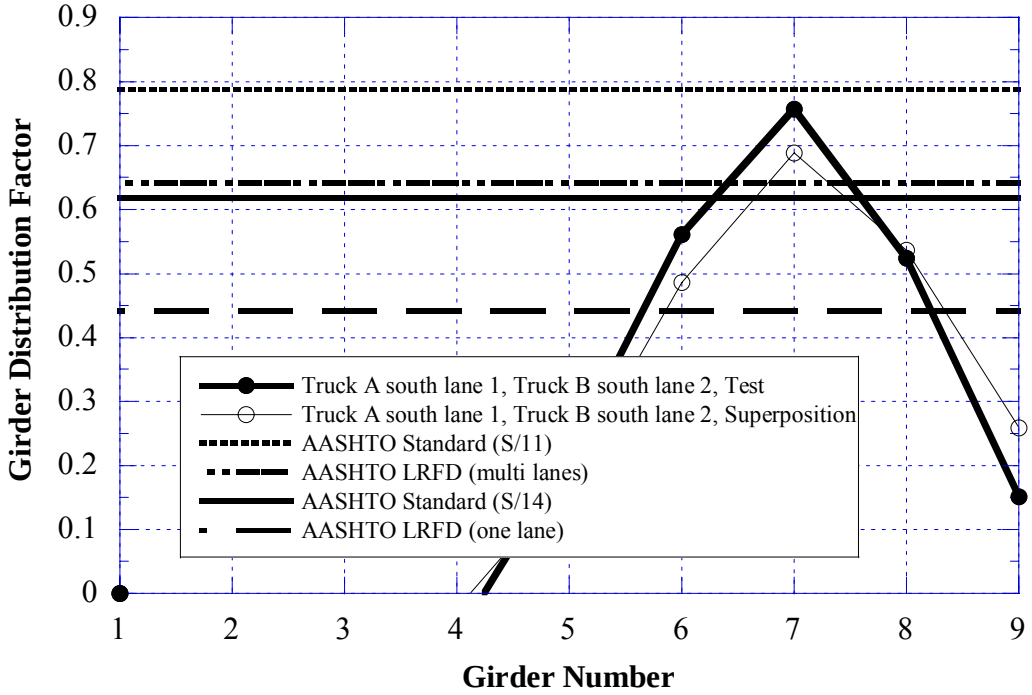

Figure 11.27 Negative Strain near Support over Center Pier,
Two Truck Side-by-Side Loading, South Lane 1 and South Lane2 (S12-82293)

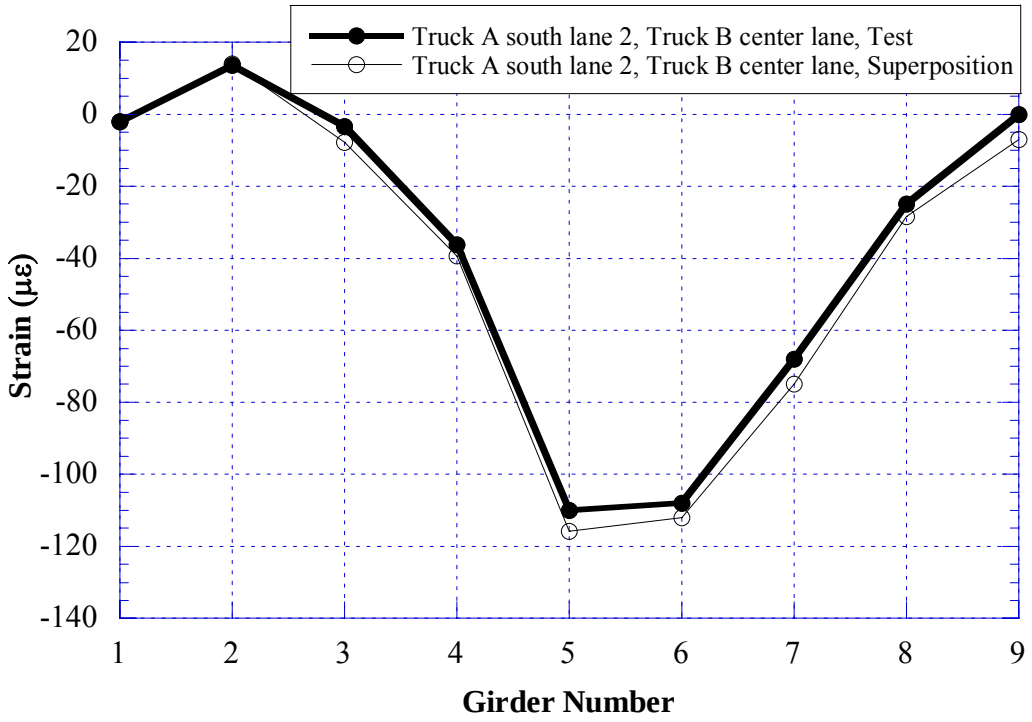

Figure 11.28 Negative Strain near Support over Center Pier, Two Truck Side-by-Side Loading, South Lane 2 and Center Lane (S12-82293)

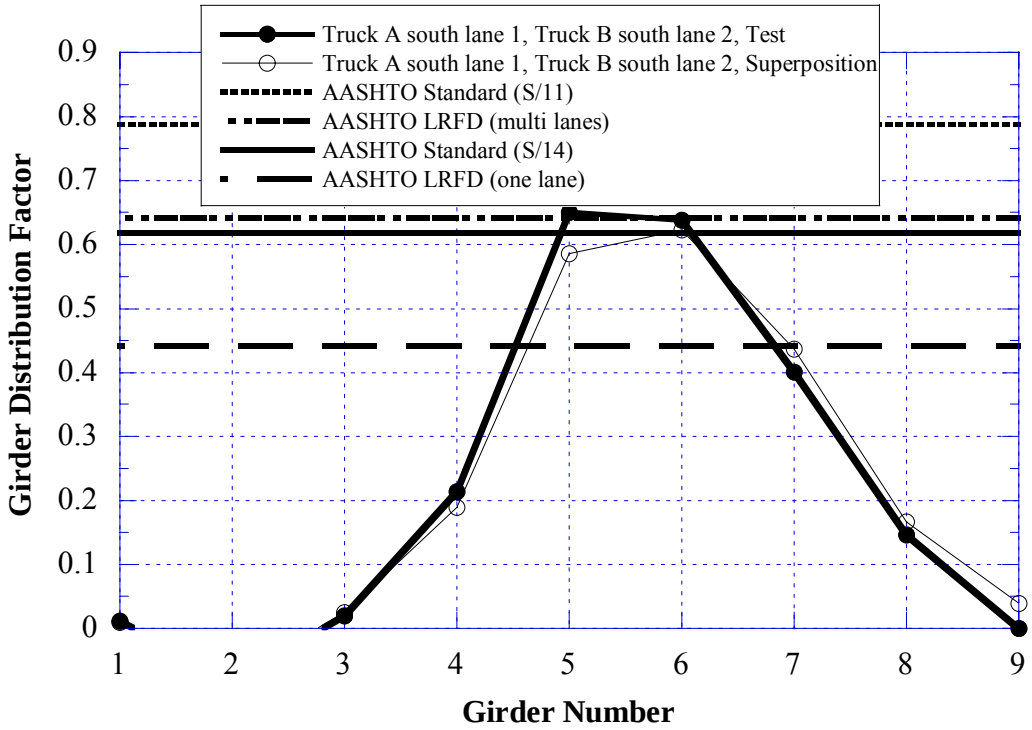

Figure 11.29 GDF from Negative Strain near Support over Center Pier, Two Truck Side-by-Side Loading, South Lane 2 and Center Lane (S12-82293)

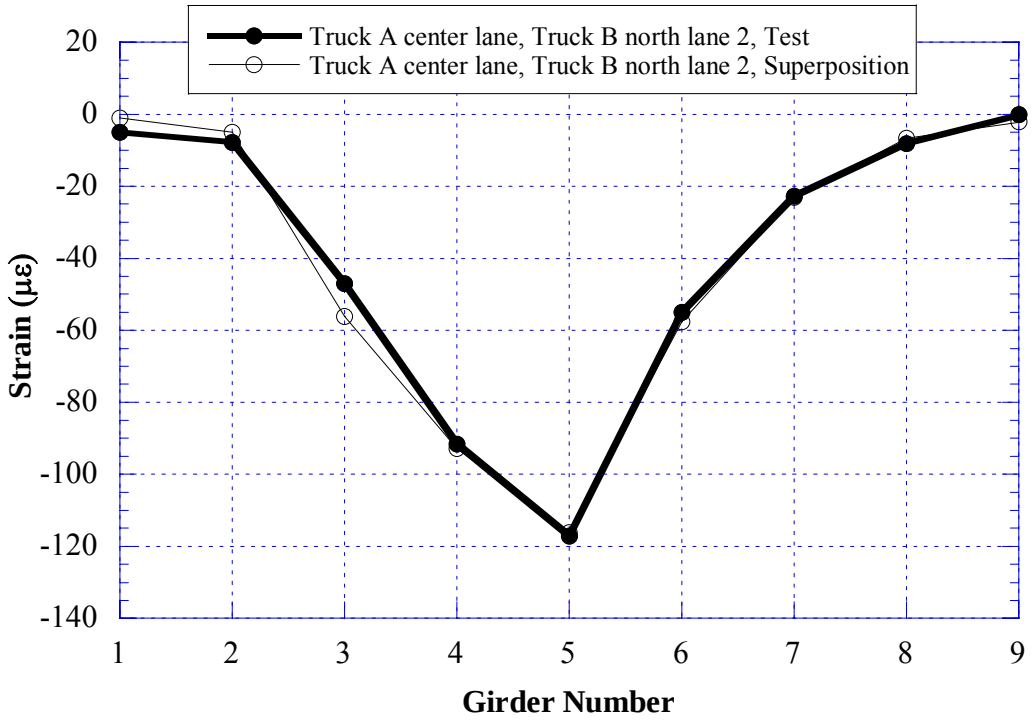

Figure 11.30 Negative Strain near Support over Center Pier, Two Truck Side-by-Side Loading, Center Lane and North Lane 1 (S12-82293)

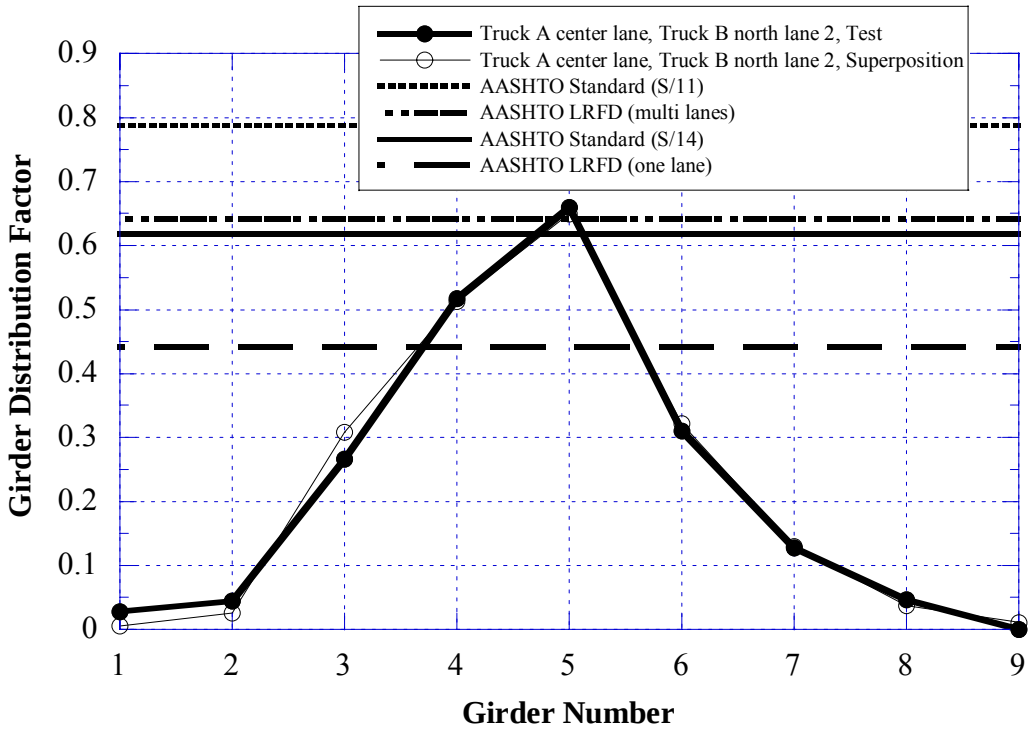

Figure 11.31 GDF from Negative Strain near Support over Center Pier, Two Truck Side-by-Side Loading, Center Lane and North Lane 1 (S12-82293)

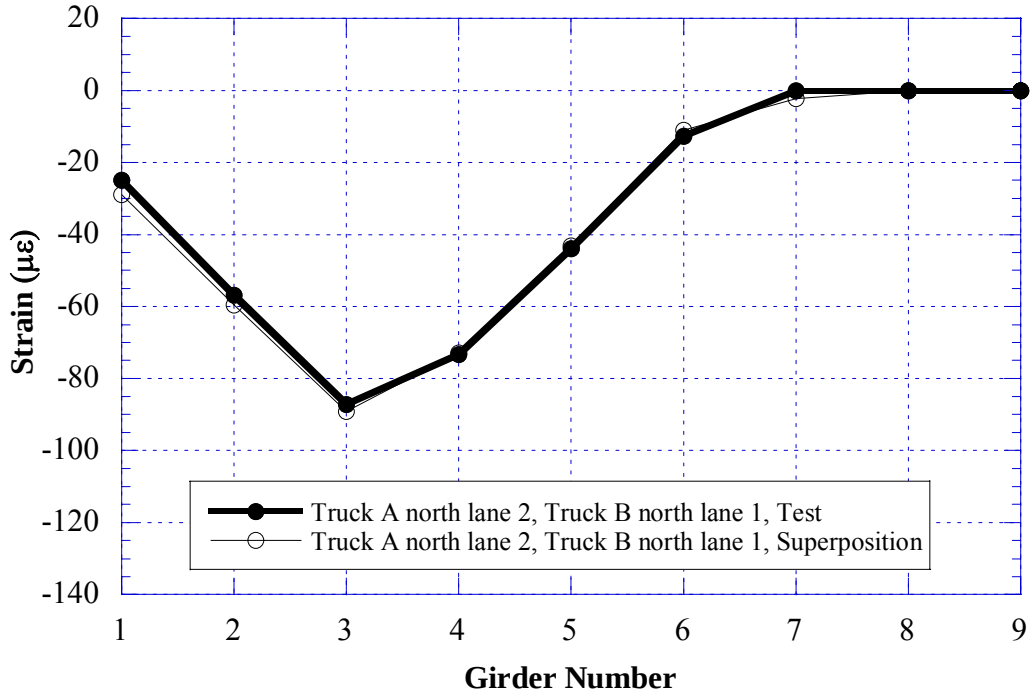

Figure 11.32 Negative Strain near Support over Center Pier, Two Truck Side-by-Side Loading, North Lane 2 and North Lane 1 (S12-82293)

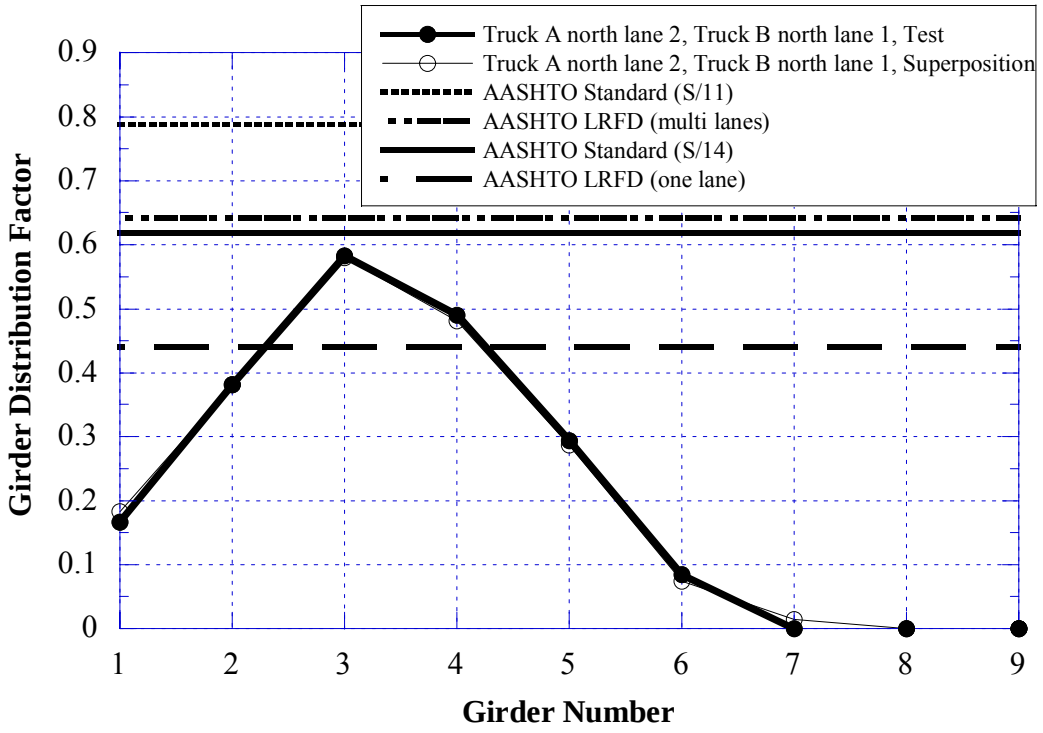

Figure 11.33 GDF from Negative Strain near Support over Center Pier, Two Truck Side-by-Side Loading, North Lane 2 and North Lane 1 (S12-82293)

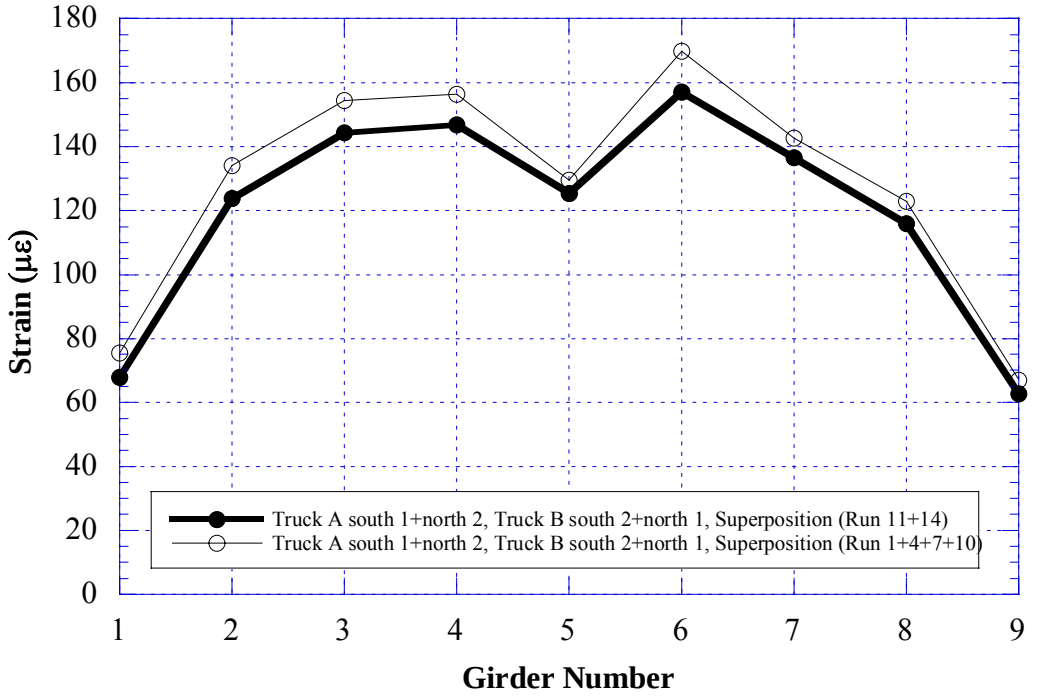

Figure 11.34 Positive Strain at Midspan of East Span due to Superposition of Side-by-Side Loading at South Lanes 1 and 2, and North Lanes 1 and 2 (4 Trucks) (S12-82293)

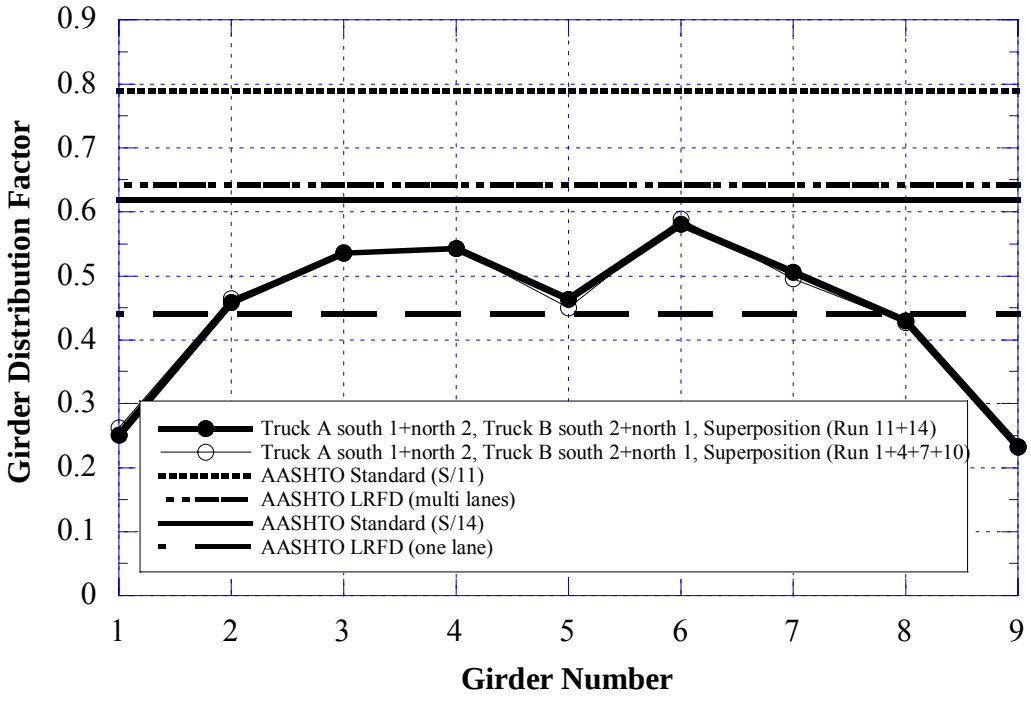

Figure 11.35 GDF from Positive Strain at Midspan of East Span due to Superposition of Side-by-Side Loading at South Lanes 1 and 2, and North Lanes 1 and 2 (4 Trucks) (S12-82293)

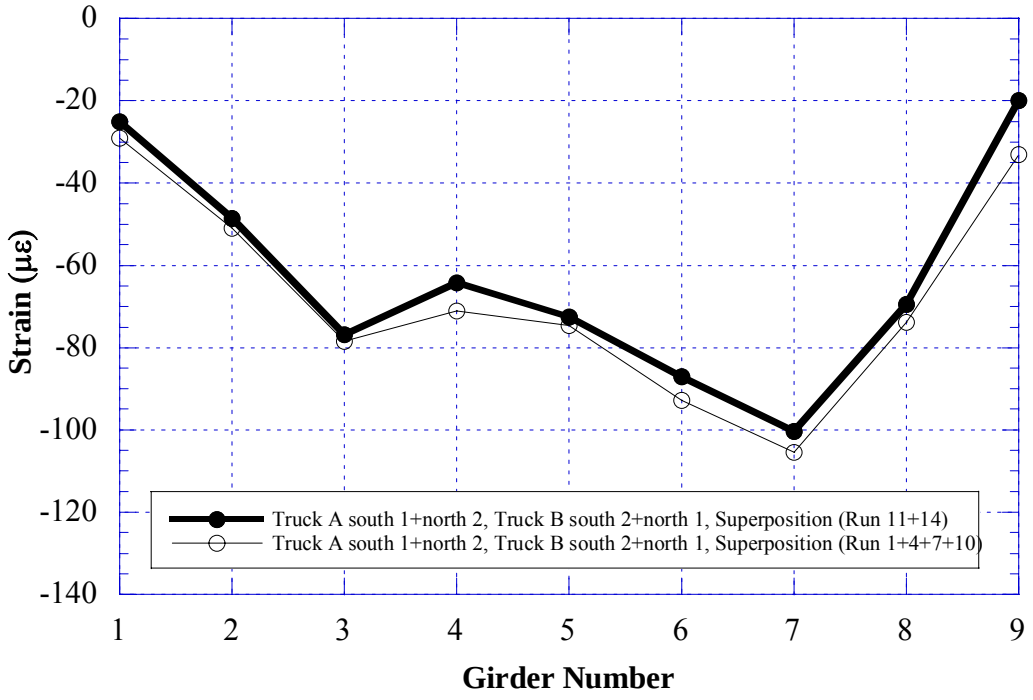

Figure 11.36 Negative Strain near Support over Center Pier due to due to Superposition of Side-by-Side Loading at South Lanes 1 and 2, and North Lanes 1 and 2 (4 Trucks) (S12-82293)

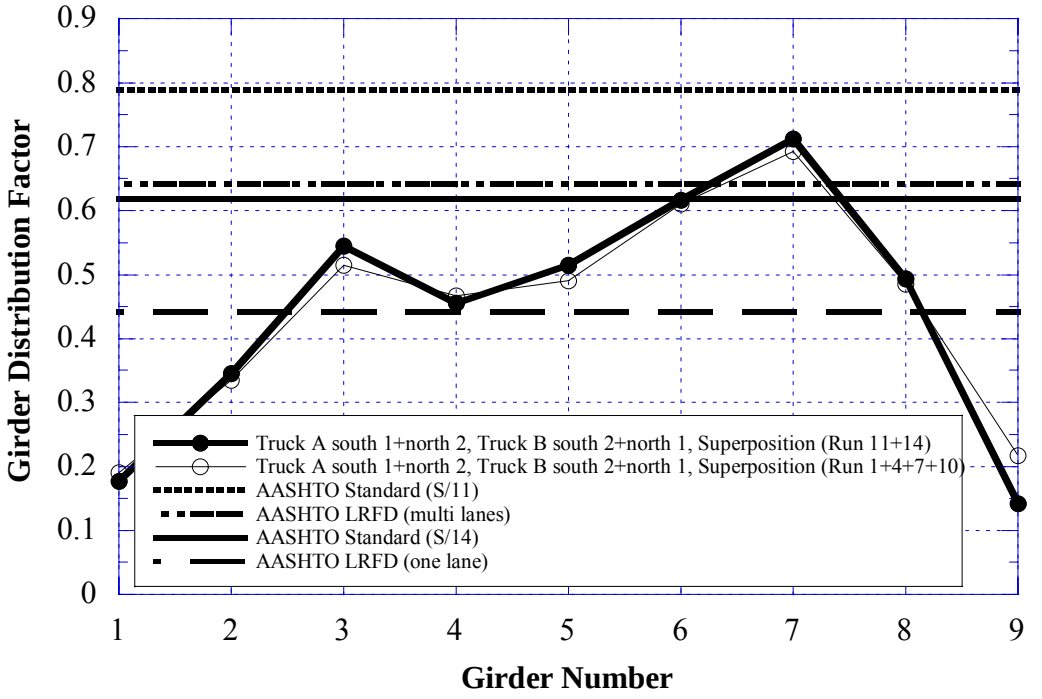

Figure 11.37 GDF from Negative Strain near Support over Center Pier due to due to Superposition of Side-by-Side Loading at South Lanes 1 and 2, and North Lanes 1 and 2 (4 Trucks) (S12-82293)

11.5 Results of Finite Element Analysis

A three-dimensional finite element method (FEM) was applied to investigate the structural behavior of the bridge S12-82293. The concrete slab was modeled with isotropic, eight node solid elements, with three degrees of freedoms at each node. The girder flanges and web were modeled using three-dimensional, quadrilateral, four node shell elements with six degrees of freedom at each node. The structural effects of the secondary members, such as the sidewalk and parapet, were also taken into account in the finite element analysis models.

The mesh of the FEM model is shown in Figure 11.38. Total number of elements is 22,896, and total number of nodes is 30,719 for this model.

Strains and GDF's calculated for the considered model is shown in Figures 11.39 to 11.50. Figures 11.39 to 11.42 present strains and GDF's from FEM model for positive moment at the midspan under two trucks side-by-side loading. Figures 11.43 to 11.46 present strains and GDF's from FEM model for negative moment near support over center pier under two trucks side-by-side loading.

Figures 11.47 to 11.48 show the positive strains at midspan and resulting GDF's from FEM model for two simultaneous loadings of two trucks side-by-side on the south lanes 1 and 2, and north lanes 1 and 2.

Figures 11.49 and 11.50 show the strains and GDF's from FEM model for negative moment near support over center pier under two simultaneous loadings of two trucks side-by-side on the south lanes 1 and 2, and north lanes 1 and 2. In the figures, the values obtained from FEM analysis are compared with the corresponding measured values.

The resulting strain values obtained from field tests are lower than those from the finite element analysis for considered bridges. The main reason for low strains is due to the partial fixity of supports. In the previous study for simply supported bridges by

University of Michigan (Nowak 2001 and 2002), the boundary conditions are simulated using the elastic spring elements in FEM models. However, for continuous bridges, it is almost impossible to obtain accurate spring coefficients satisfying multiple locations of supports with varied partial fixity condition. Therefore, in the study, the supports are assumed to behave as designed in the FEM models.

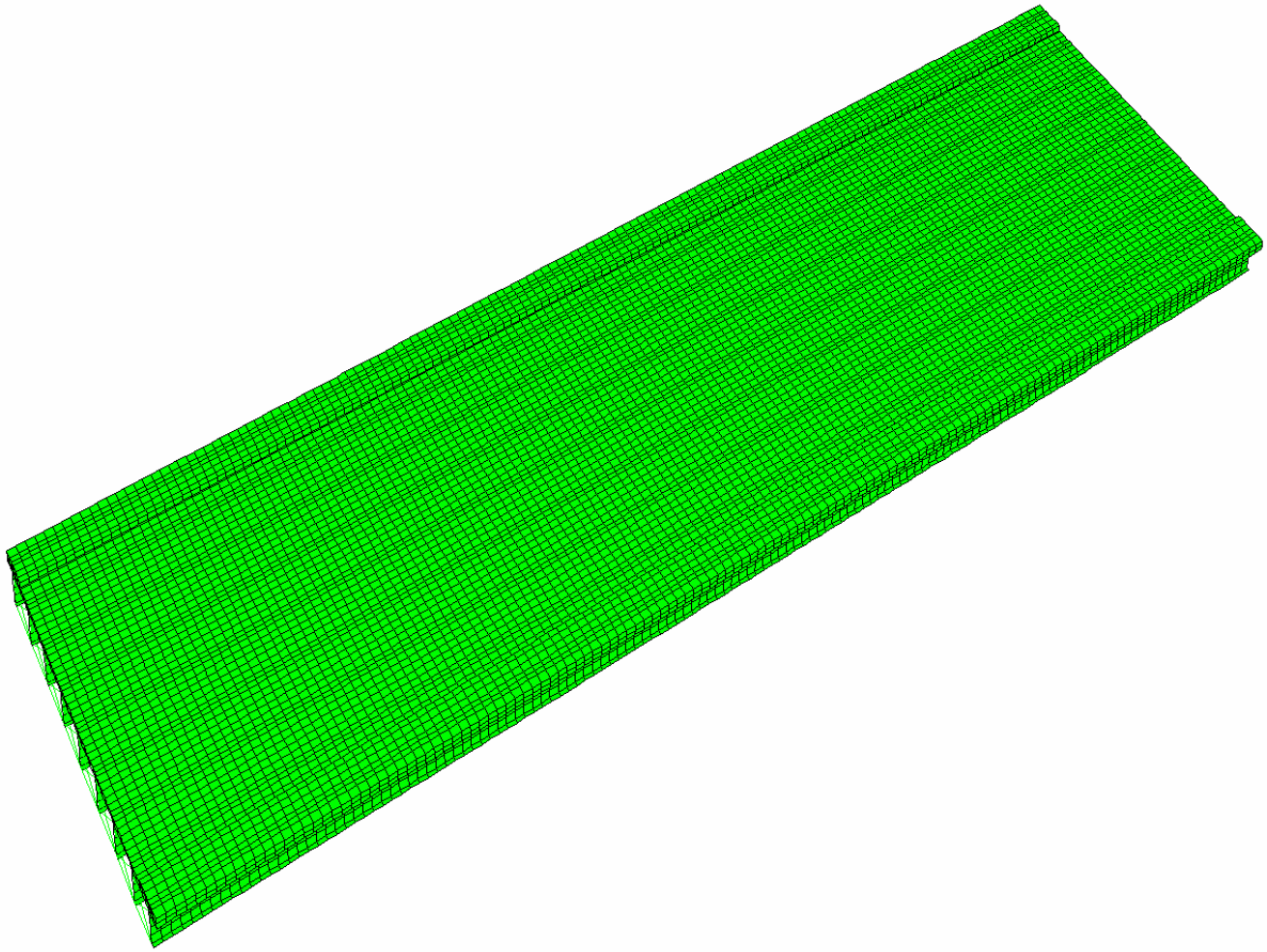

Figure 11.38 The Mesh of Finite Element Model, Bridge (S12-82293)

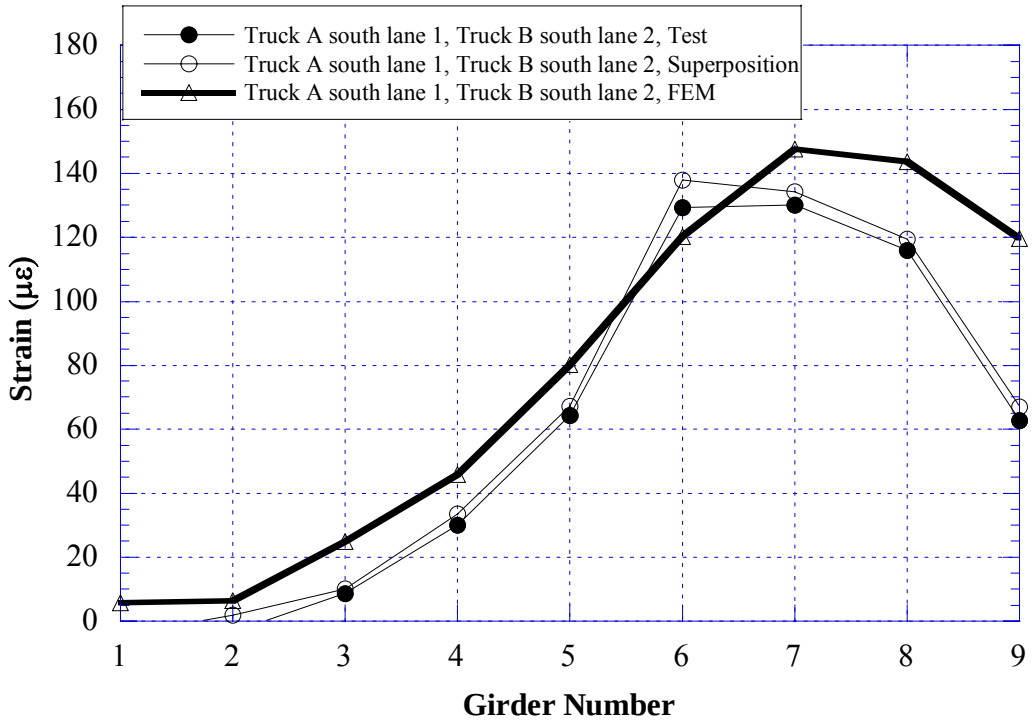

11.39 Comparison of FEM vs. Test, Positive Strain at Midspan of Eastspan, Two Truck Side-by-Side Loading, South Lane 1 and South Lane2 (S12-82293)

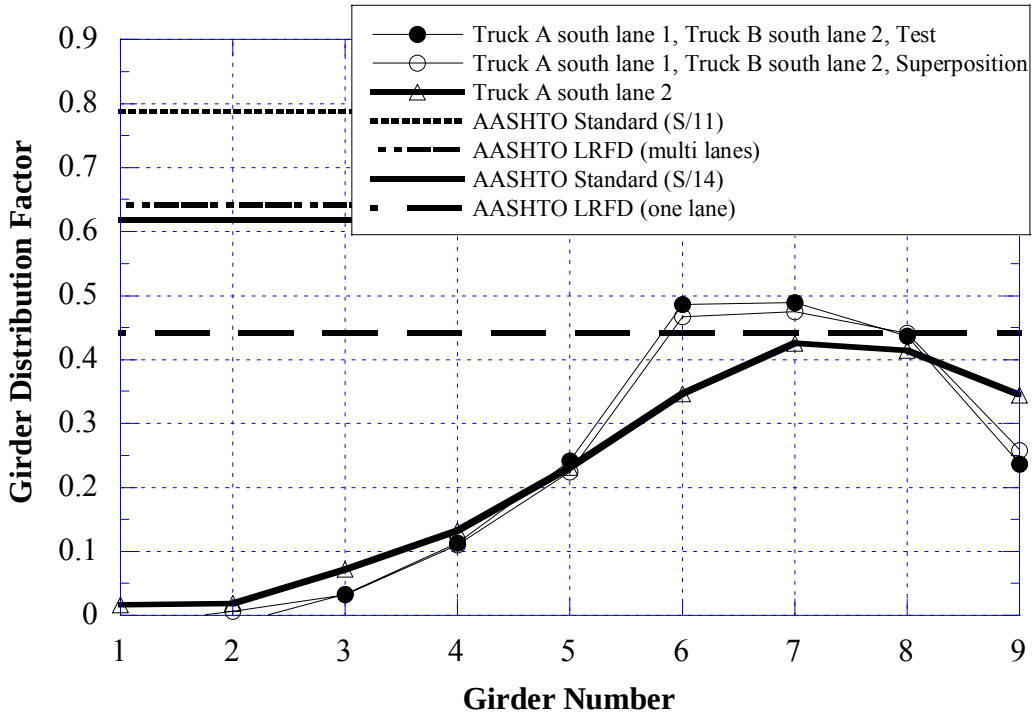

11.40 Comparison of FEM vs. Test, GDF from Positive Strain at Midspan of Eastspan, Two Truck Side-by-Side Loading, South Lane 1 and South Lane2 (S12-82293)

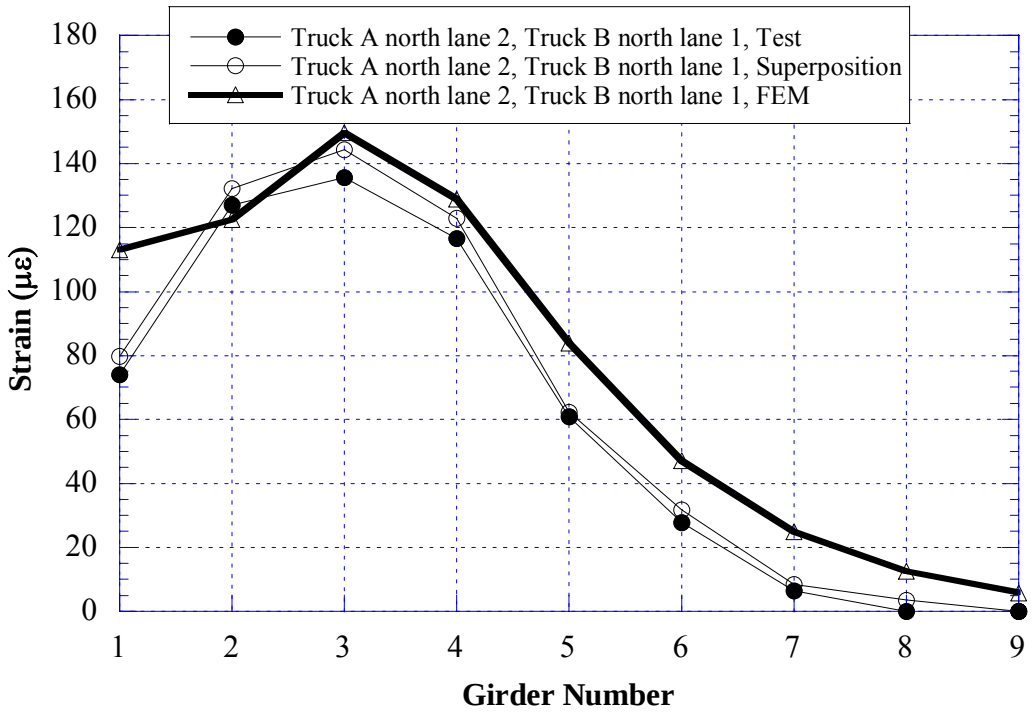

11.41 Comparison of FEM vs. Test, Positive Strain at Midspan of Eastspan, Two Truck Side-by-Side Loading, North Lane 2 and North Lane 1 (S12-82293)

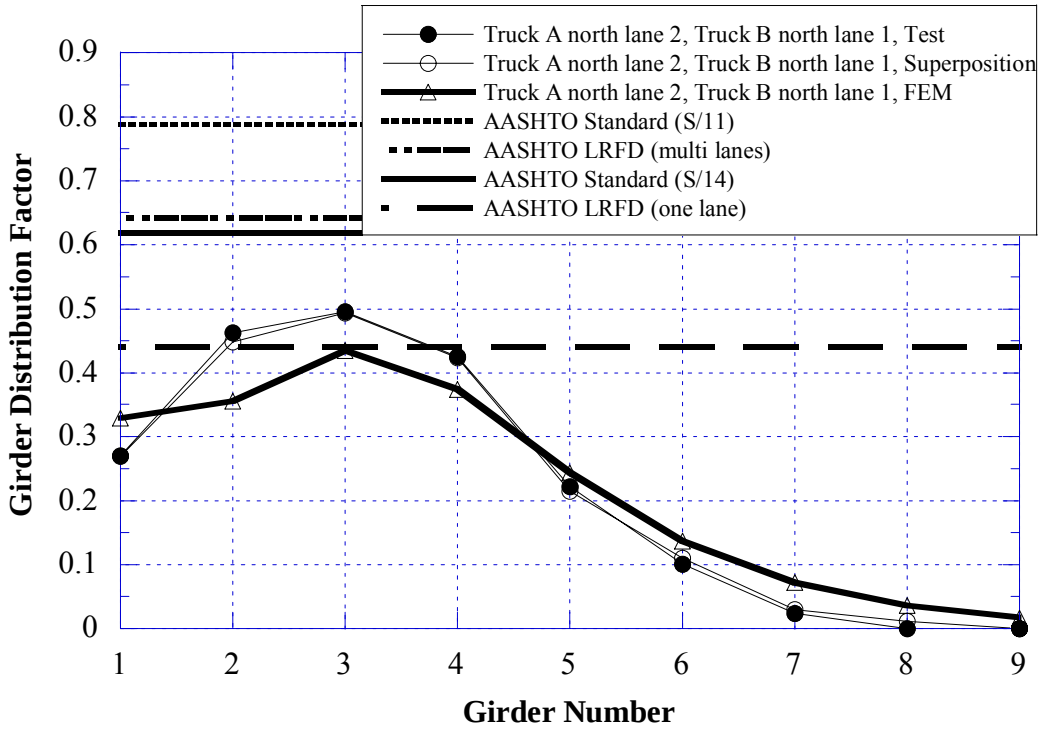

11.42 Comparison of FEM vs. Test, GDF from Positive Strain at Midspan of Eastspan, Two Truck Side-by-Side Loading, North Lane 2 and North Lane 1 (S12-82293)

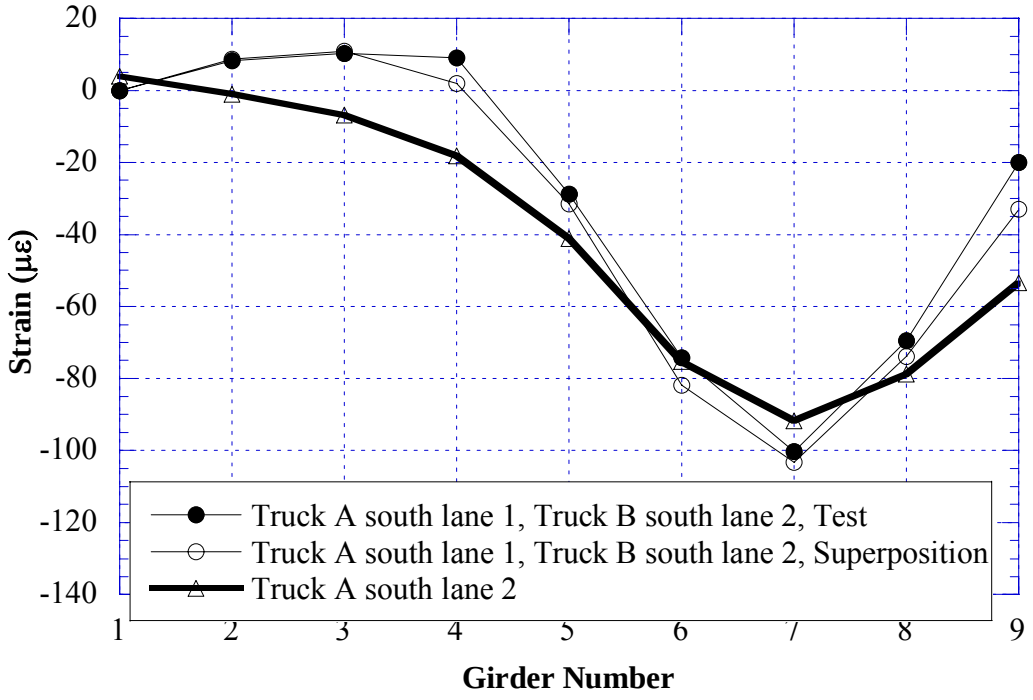

11.43 Comparison of FEM vs. Test, Negative Strain near Support over Center Pier, Two Truck Side-by-Side Loading, South Lane 1 and South Lane2 (S12-82293)

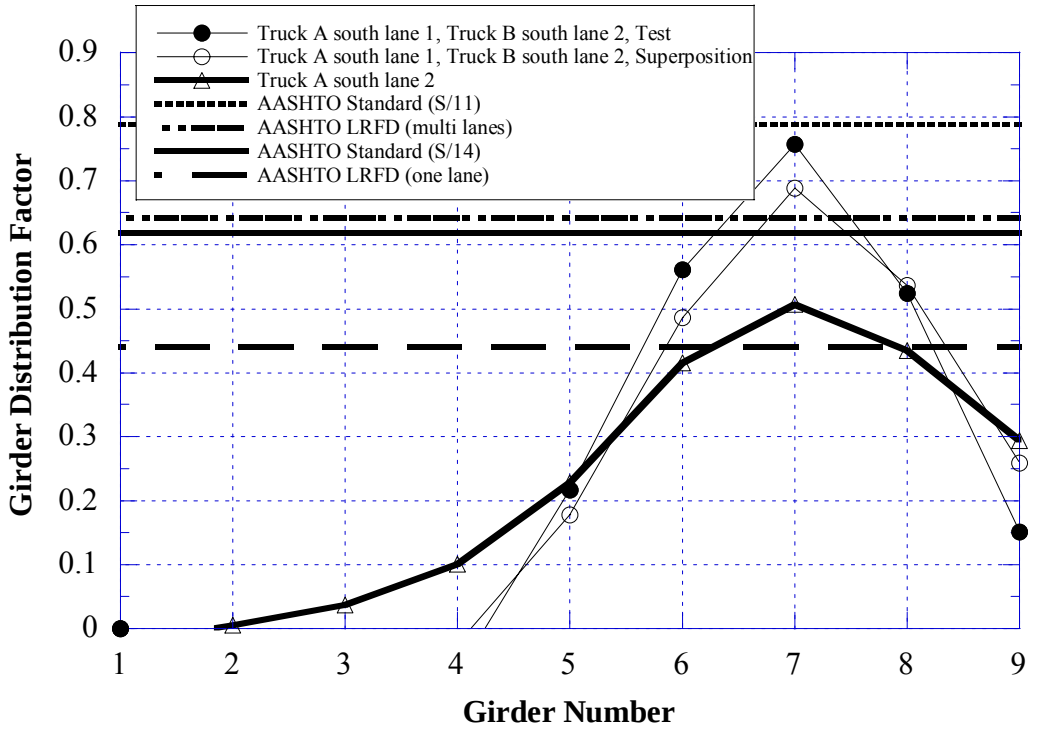

11.44 Comparison of FEM vs. Test, GDF from Negative Strain near Support over Center Pier, Two Truck Side-by-Side Loading, South Lane 1 and South Lane2 (S12-82293)

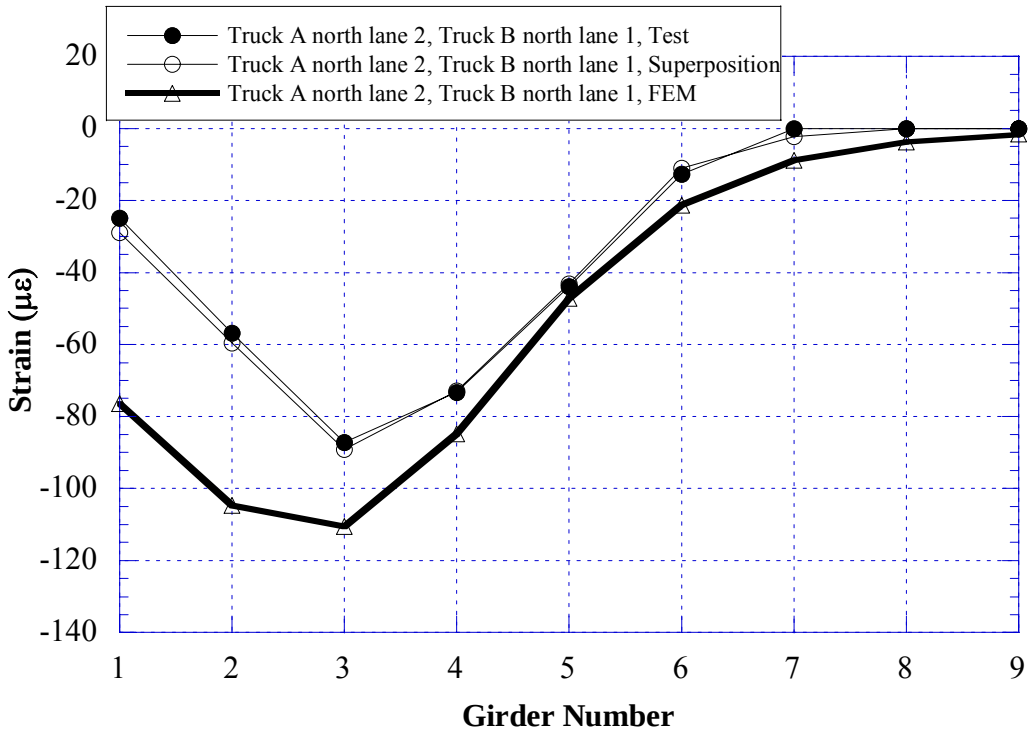

11.45 Comparison of FEM vs. Test, Negative Strain near Support over Center Pier, Two Truck Side-by-Side Loading, North Lane 2 and North Lane 1 (S12-82293)

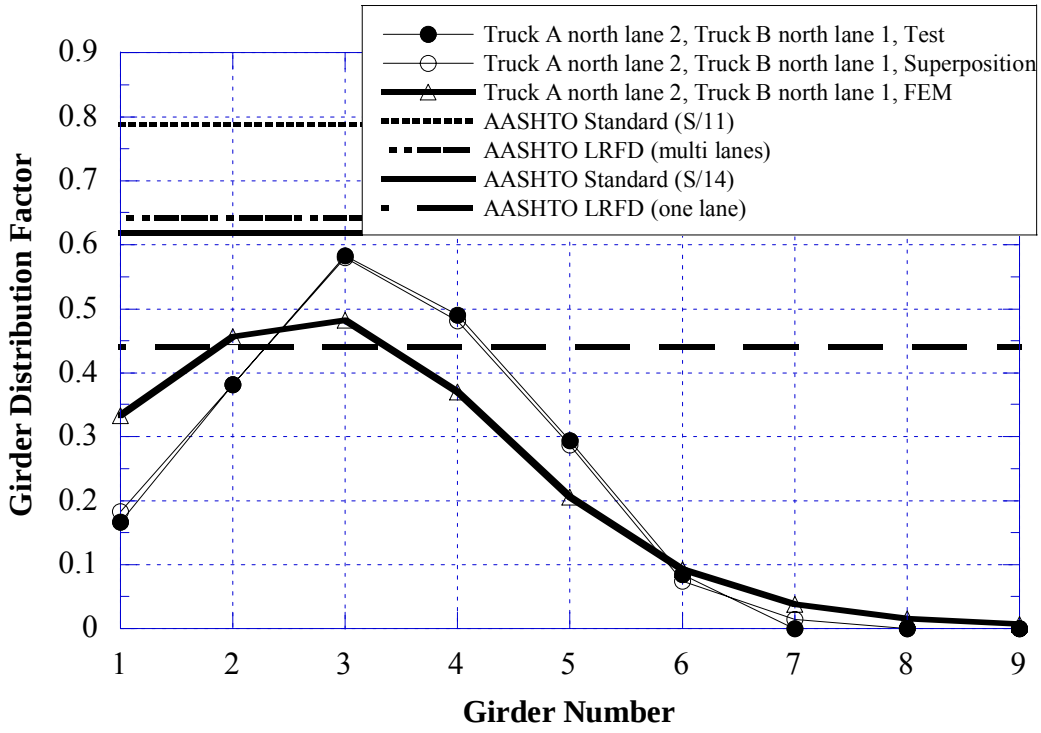

11.46 Comparison of FEM vs. Test, GDF from Negative Strain near Support over Center Pier, Two Truck Side-by-Side Loading, North Lane 2 and North Lane 1 (S12-82293)

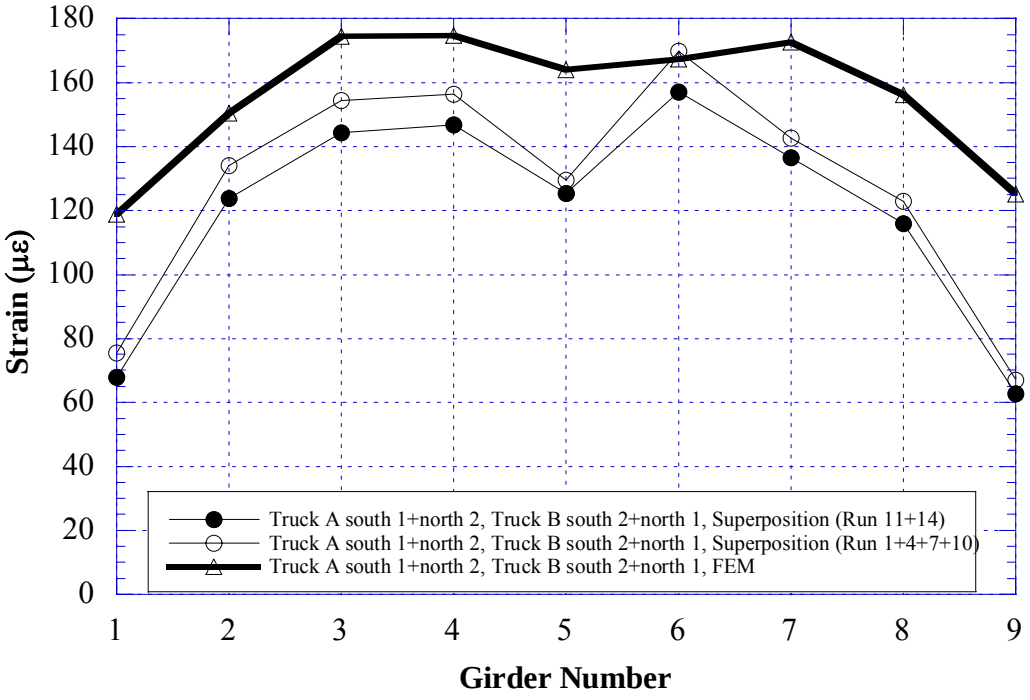

Figure 11.47 Comparison of FEM vs. Test, Positive Strain at Midspan of East Span due to Superposition of Side-by-Side Loading at South Lanes 1 and 2, and North Lanes 1 and 2 (4 Trucks) (S12-82293)

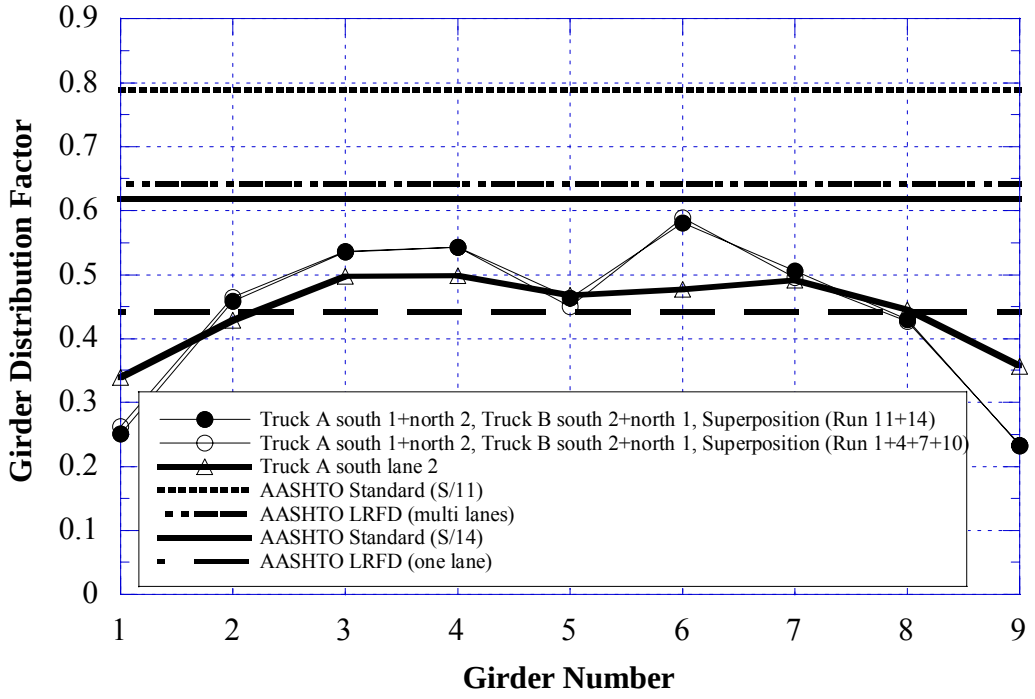

Figure 11.48 Comparison of FEM vs. Test, GDF from Positive Strain at Midspan of East Span due to Superposition of Side-by-Side Loading at South Lanes 1 and 2, and North Lanes 1 and 2 (4 Trucks) (S12-82293)

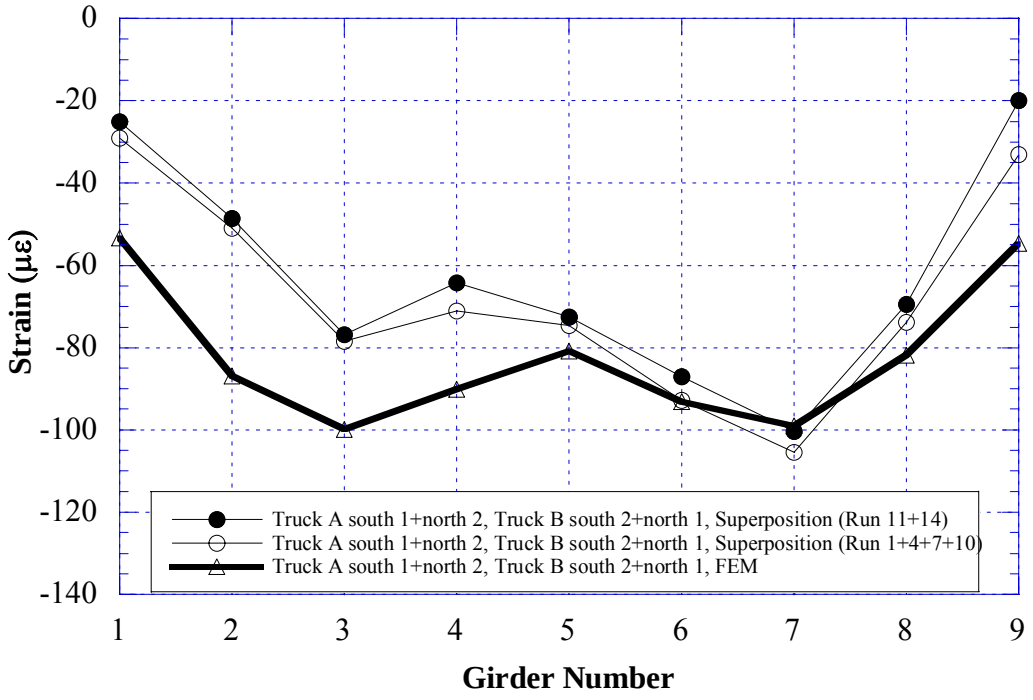

Figure 11.49 Comparison of FEM vs. Test, Negative Strain near Support over Center Pier due to due to Superposition of Side-by-Side Loading at South Lanes 1 and 2, and North Lanes 1 and 2 (4 Trucks) (S12-82293)

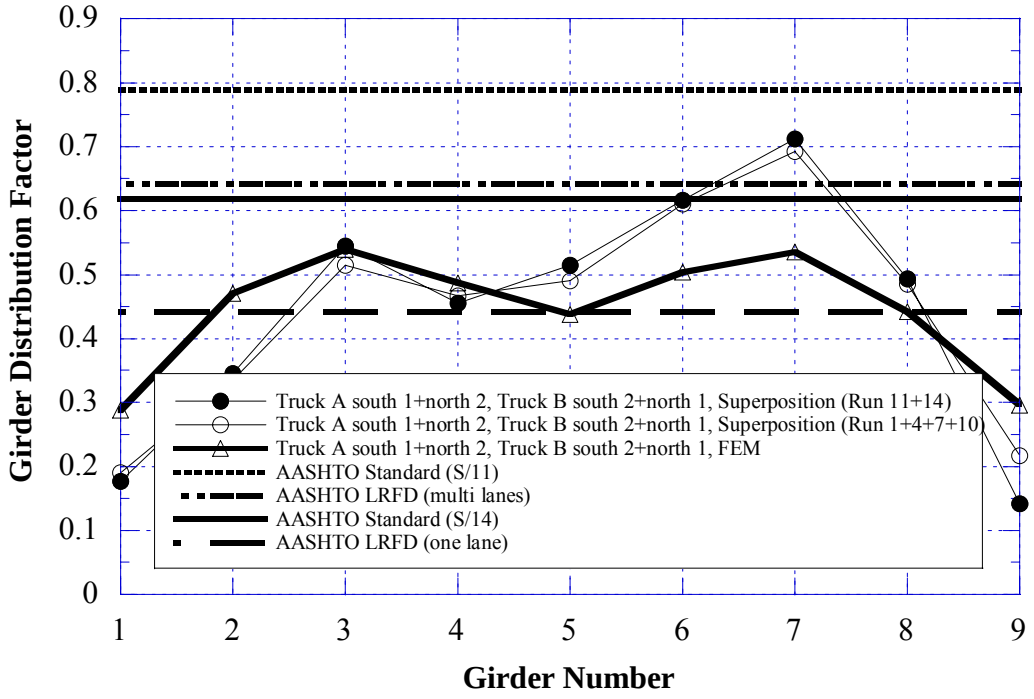

Figure 11.50 Comparison of FEM vs. Test, GDF from Negative Strain near Support over Center Pier due to due to Superposition of Side-by-Side Loading at South Lanes 1 and 2, and North Lanes 1 and 2 (4 Trucks) (S12-82293)

12. SUMMARY AND CONCLUSIONS

The field test program documented in this report covered continuous steel girder bridges. The objective of the tests was to verify girder distribution factors (GDF), and dynamic load factors (DLF).

12.1 Girder Distribution Factors

Six bridges were instrumented and loaded with fully loaded 11-axle trucks. The resulting strains are shown in Figures 12.1 to 12.5, for one truck and two trucks side-by-side. In Figure 12.1, the positive strains measured at midspan are plotted for one lane loading at crawling speed. Strains for truck A and B are practically the same, which confirms the repeatability of the results.

Figure 12.2 shows the positive strain values obtained at the midspan due to full lane loading, except bridges S01-12034 and S12-82293. For bridge S01-12034, only one truck was available for the test. For S12-82293, the bridge has five lanes. Therefore, for these two bridges, the superposition of trucks is shown in Figure 12.2 to simulate the full lane loading condition. For full lane loading (test trucks on all traffic lanes on the bridges) under crawling speed, the maximum positive strain recorded at midspan is about 240 με for bridge S13-59012.

Figures 12.3 to 12.5 present the negative strain values obatined near supports over pier. For single lane loading, the maximum negative strain is about 120 με, as shown in Figure 12.3. Figures 12.4 and 12.5 present the negative strains under full lane loading on the bridge under crawling-speed (static) tests. Figure 12.4 presents the negative strains under full lane loading measured near support over pier. The maximum recorded negative strain near supportat the midspan is less than 150 με for all tested bridges.

For all tested bridges, the superposition of strains due to a single truck produces almost the same results as strain due to full lane loading, as shown in Figures 12.2 and 12.4.

Figures 12.5 shows the strain superposition of two separate full lane loading in adjacent spans to maximize the negative moment near support over pier. The resulting maximum negative strain is about 240 με for bridge S08-77024.

The girder distribution factors are obtained from the measured strain values, and they are summarized in Figures 12.6 to 12.10. Also, measured GDF's are compared the code specified GDF's in AASHTO Standard (2002), and AASHTO LRFD (1998) for interior girders. For exterior girders, the code specified GDF's are different than for GDF's for interior girders and the test results are not compared to code specified values in this study. The Kg term was ignored in calculation of AASHTO LRFD (1998) specified GDF's.

Figure 12.6 shows the resulting GDF from positive strain due to single lane loading. For single lane loading, GDF's observed for interior girders are lower than GDF's specified in the codes. When the truck is very close to curb for Bridge S09-77023, however, the positive GDF's can exceed the specified values in AASHTO LRFD (1998) for single lane loading.

In Figure 12.7, the GDF values obtained from the strain values at midspan under full lane loading are shown, and compared with code specified values. Figure 12.7 shows that code specified GDF's are conservative. Even the single lane GDF's specifed in AASHTO Standard (2002) is sufficient for two trucks side-by-side for all bridges.

Figures 12.8 presents the negative GDF values under single lane loading measured near support over pier, compared with code specified values. Figure 12.8 shows that code specified GDF's are conservative. However, when the truck is very close to curb, the positive GDF's can exceed the specified values in AASHTO LRFD (1998) for single lane loading. Still, the GDF's specified in AASHTO Standard (2002) are in all cases conservative.

Figure 12.9 present the GDF values obtained from negative strains under full lane loading near support over pier, compared with code specified values. The figure shows that code specified GDF's are conservative. As in GDF's for positive moments, even the single lane GDF's specified in AASHTO Standard (2002) is sufficient for two trucks side by side. However, single lane GDF's specified in AASHTO LRFD (1998) is not always sufficient for multi-lane loading.

For comparison, the maximum GDF's obtained in field tests as a part of this study are plotted versus the specified values in AASHTO Standard (2002) and AASHTO LRFD (1998), as shown in Figures 12.10 and 12.11. The results are presented for single lane loading, and for multi-lane loading. Figure 12.10 shows the comparison of GDF's for positive moment at midspan, and Figure 12.11 for negative moment near support.

12.2 Dynamic Load Factors

The dynamic load factors (DLF) obtained from the tests are summarized in Figures 12.12 to 12.15. In Figure 12.12, DLF's based on the positive strains measured at the midspan of tested bridges are shown. Figure 12.13 presents DLF's based on the negative strains measured near support over pier. As shown in the figures, dynamic load factors for exterior girders are high because the static strains in these girders are very low. In other words, large values of DLF in exterior girders correspond to load cases with a single truck in the opposite lane (resulting in very low static strain).

The relationship between DLF and static and dynamic strains is shown in Figures 12.14 and 12.15, for positive moment and negative moment, respectively. Dynamic strains remain nearly constant, while static strains increase as truck loading increases. This results in large dynamic load factors for low static strains.

For all tested bridges, the DLF corresponding to the maximum static strain, is less than 0.20 for a one lane loading. For two trucks side-by-side, DLF is less than 0.10 for all the tested bridges.

12.3. Finite Element Analysis

Figures 12.16 to 12.19 show the results of the finite element analysis. Figures 12.16 and 12.17 present the positive strain values at midspan from FEM analysis, and the negative strain near support over pier from FEM analysis, respectively. They are compared with test values.

The measured strains are generally similar to those obtained from FEM analysis. However, there are some localized exceptions. This may be due to two main reasons stated as follows;

- Partial fixity of supports. All of the considered bridges were designed with simple supports. Yet, the actual supports provide some resistance to horizontal movement and rotation. This is due to collection of debris, corrosion, and counter-balancing effect of weight of structural and non-structural components on the other end of the bearing center (cantilever portion of the girder, concrete diaphragm over the support, portion of the deck slab, portion of the pavement adjacent to the bridge).
- More uniform girder distribution factors. The truck load is distributed on the girders and other components (deck slab, sidewalks, parapet, curbs). These secondary components are not considered in the simplified design practices, and their contribution to the overall stiffness of the bridge can be about 10%.

Figures 12.18 shows the positive GDF's based on the positive strain results from FEM analysis. It corresponds the strain values shown in Figure 12.16. Figure 12.19 presents GDF's based on the negative strains near support over pier obtained from FEM analysis. Figure 12.19 is based on full lane loading on one span of bridge.

The maximum measured static strains are compared to strain from the FEM analysis in Table 12.1, for full lane loading. For bridges S01-12034 and S12-82293, the measured strains shown in the table are the superposition of measured values to simulate the simulation of full lane loading. For all bridges except S12-82293, the strains are from two

trucks side-by-side loading. For bridge S12-82293, the strains are taken when all four traffic lanes are loaded with test trucks.

Table 12.1 Comparison of Strain Values from the Tests and Analysis

MDOT ID	Positive Strain at Midspan (10^{-6})			Negative Strain near Support (10^{-6})		
	Maximum Measured Strain	Maximum Strain from FEM Analysis	Ratio, Test / FEM	Maximum Measured Strain	Maximum Strain from FEM Analysis	Ratio, Test / FEM
S08-77024	177	227	0.78	-137	-147	0.93
S05-44044	108	189	0.57	-120	-113	1.06
S01-12034	223	318	0.70	-111	-134	0.83
S09-77023	201	180	1.12	-125	-120	1.04
S13-59012	232	258	0.90	-131	-132	0.99
S12-82293	157	172	0.91	-100	-100	1.00

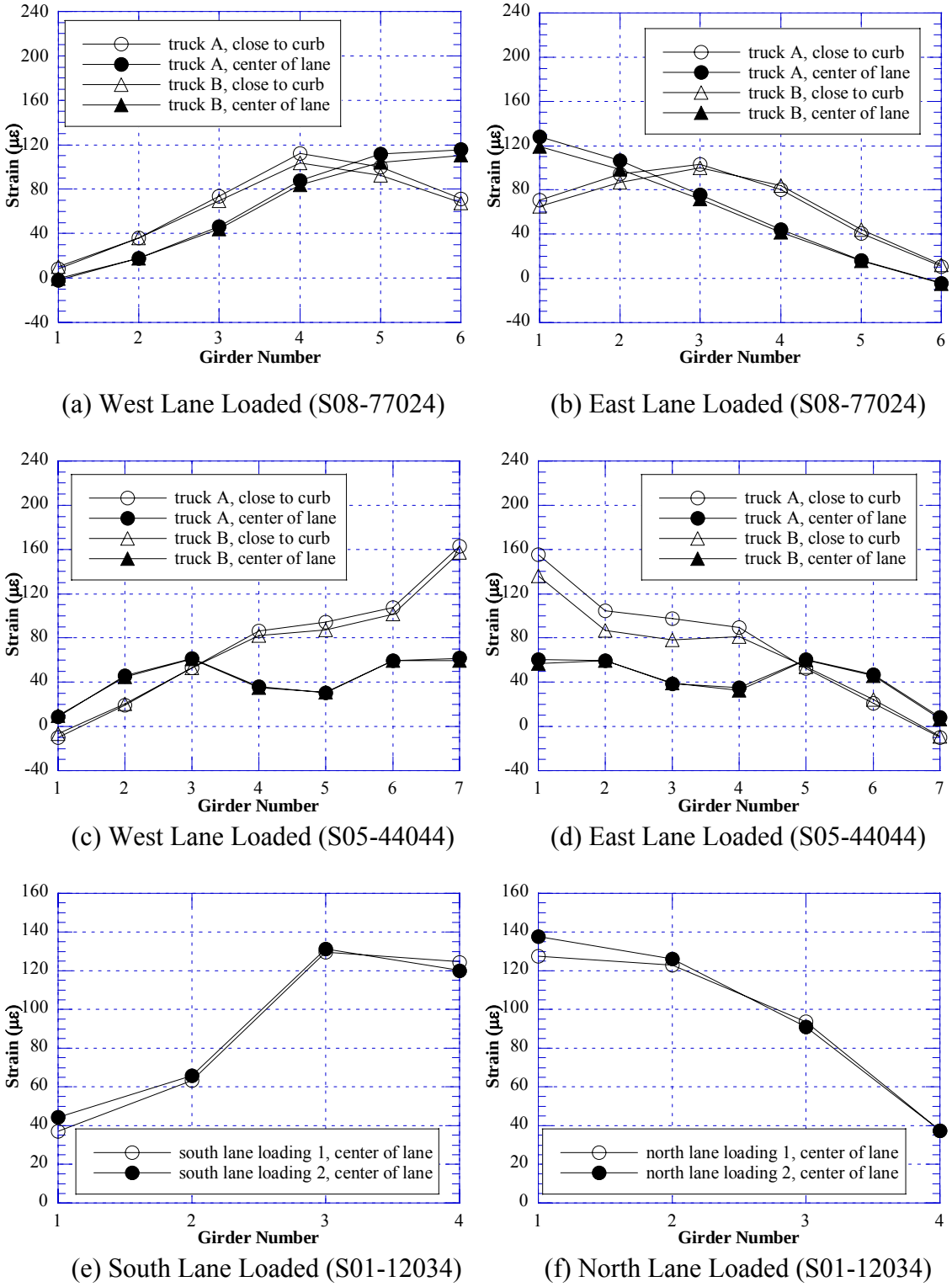

(a) West Lane Loaded (S08-77024)

(b) East Lane Loaded (S08-77024)

(c) West Lane Loaded (S05-44044)

(d) East Lane Loaded (S05-44044)

(e) South Lane Loaded (S01-12034)

(f) North Lane Loaded (S01-12034)

Figure 12.1. Positive Strains at Midspan under One Lane Loading at Crawling Speed

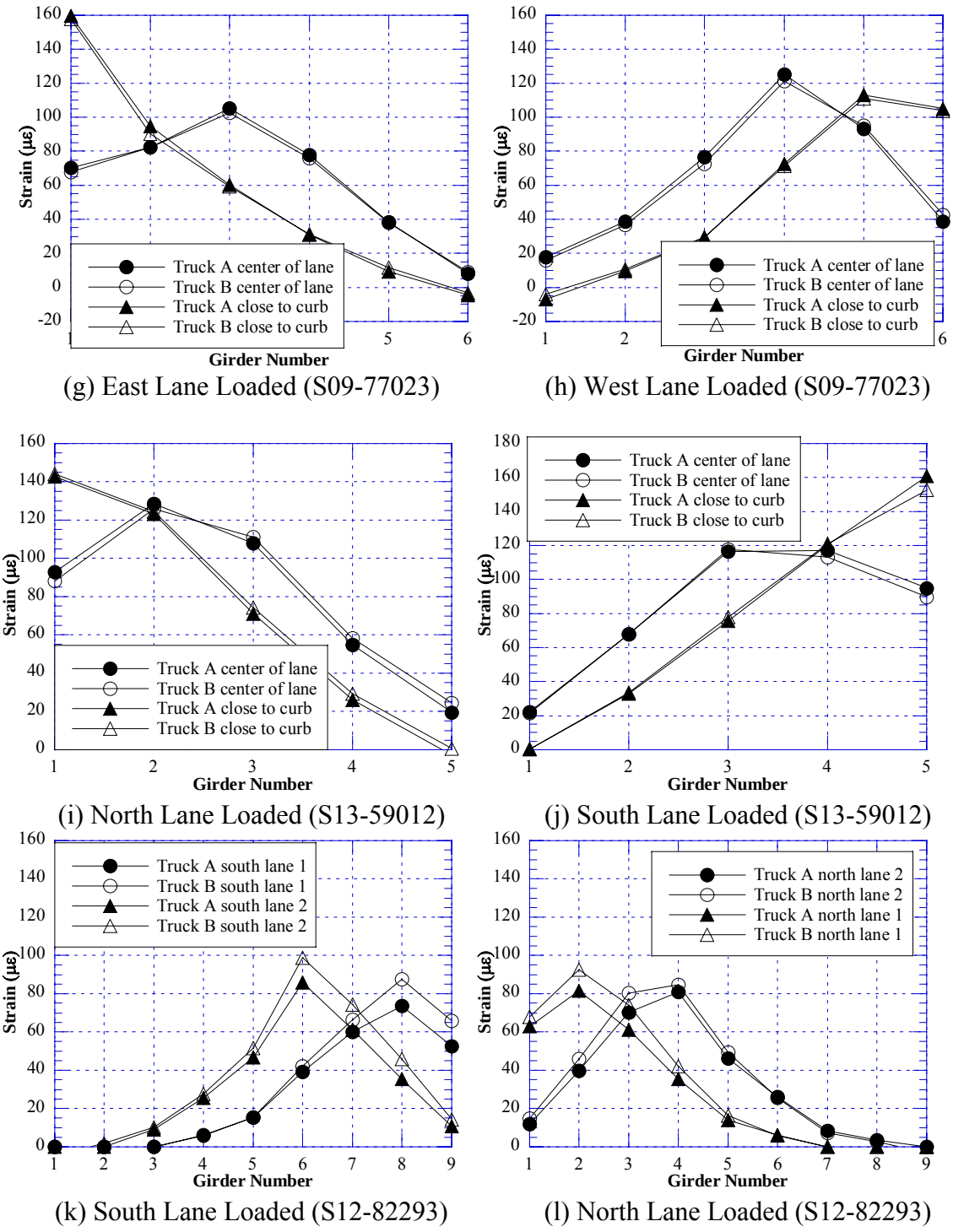

(g) East Lane Loaded (S09-77023)

(h) West Lane Loaded (S09-77023)

(i) North Lane Loaded (S13-59012)

(j) South Lane Loaded (S13-59012)

(k) South Lane Loaded (S12-82293)

(l) North Lane Loaded (S12-82293)

Figure 12.1 Positive Strains at Midspan under One Lane Loading at Crawling Speed (Continued).

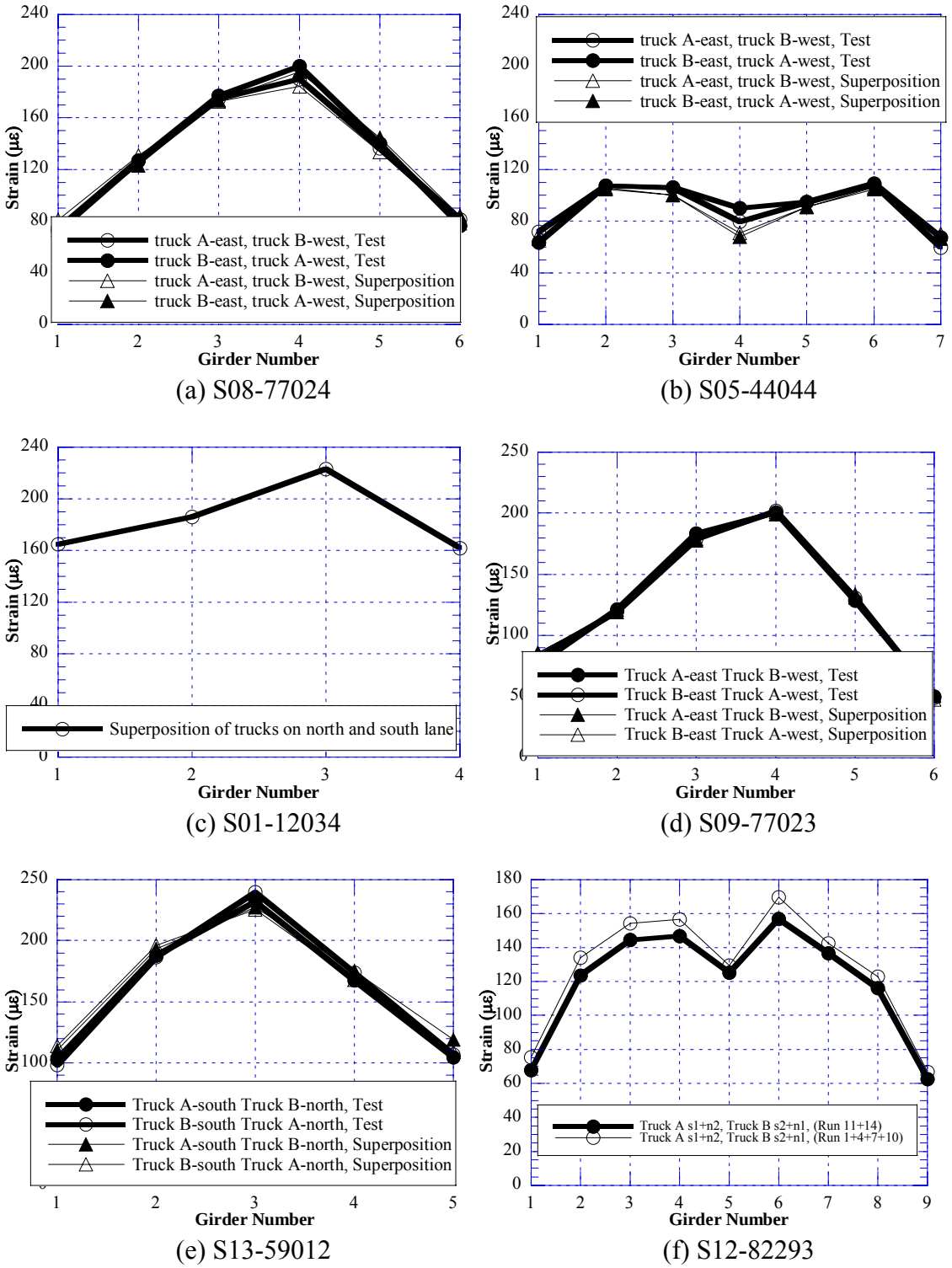

Figure 12.2 Positive Strains at Midspan under Side-by-Side Truck Loading at Crawling Speed

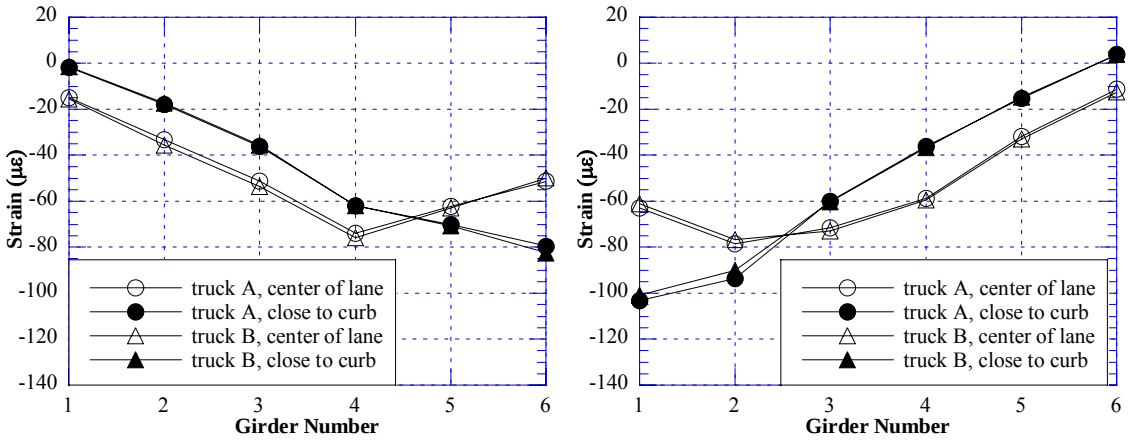

(a) West Lane Loaded (S08-77024)

(b) East Lane Loaded (S08-77024)

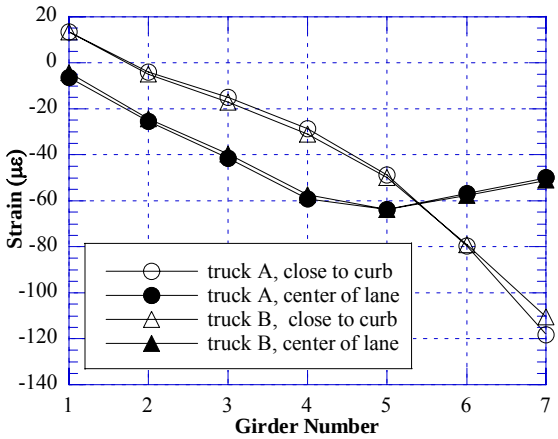

(c) West Lane Loaded (S05-44044)

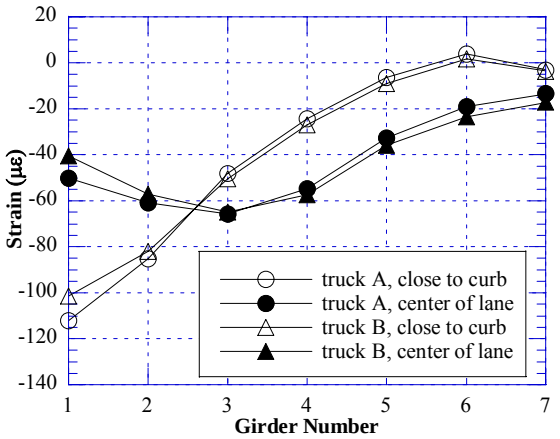

(d) East Lane Loaded (S05-44044)

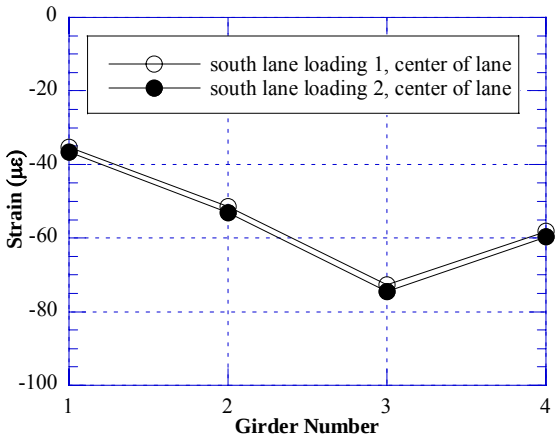

(e) South Lane Loaded (S01-12034)

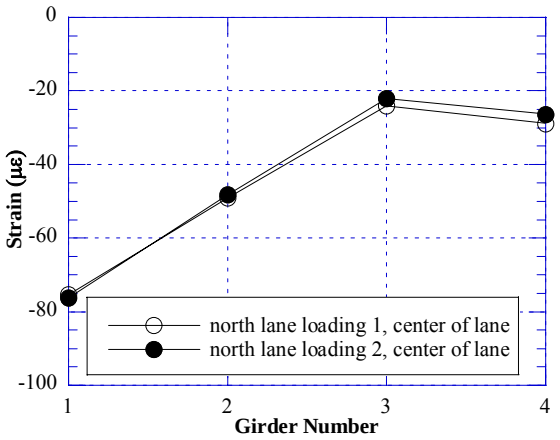

(f) North Lane Loaded (S01-12034)

Figure 12.3 Negative Strains near Support over Pier under One Lane Loading at Crawling Speed

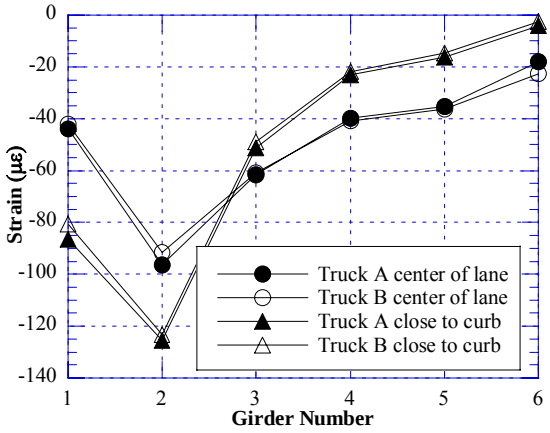

(g) East Lane Loaded (S09-77023)

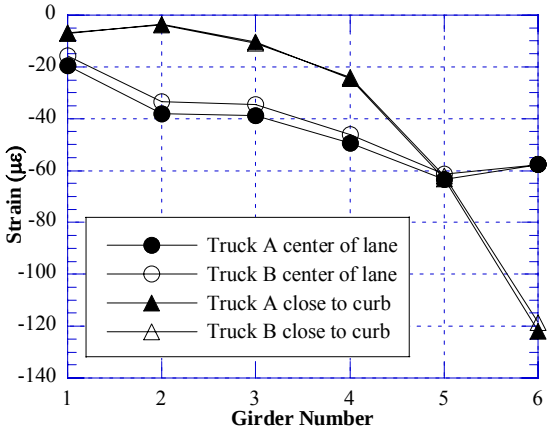

(h) West Lane Loaded (S09-77023)

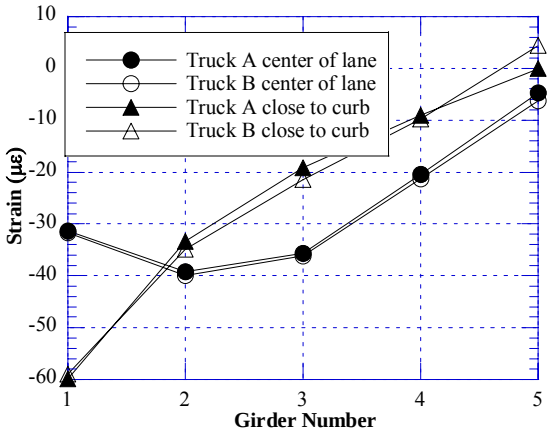

(i) North Lane Loaded (S13-59012)

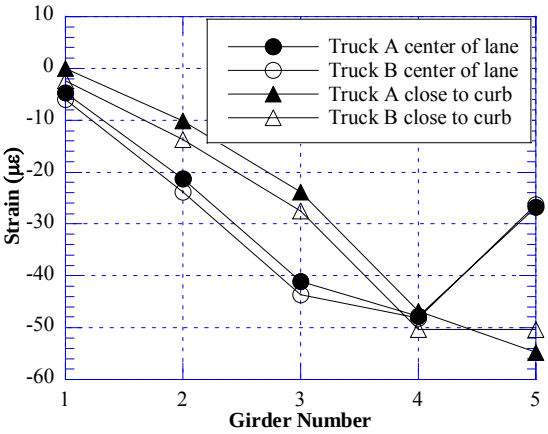

(j) South Lane Loaded (S13-59012)

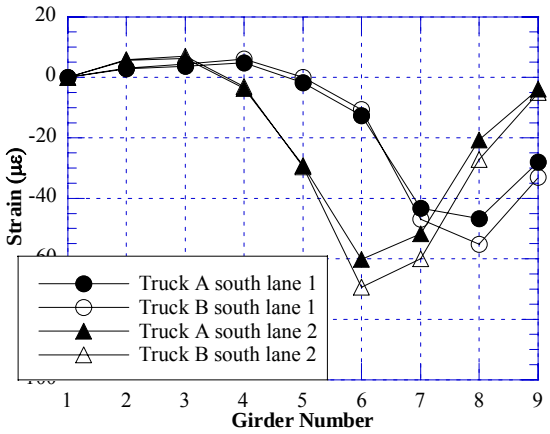

(k) South Lane Loaded (S12-82293)

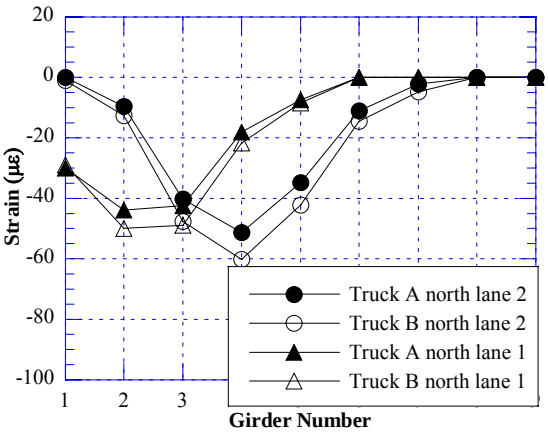

(l) North Lane Loaded (S12-82293)

Figure 12.3 Negative Strains near Support over Pier under One Lane Loading at Crawling Speed (Continued).

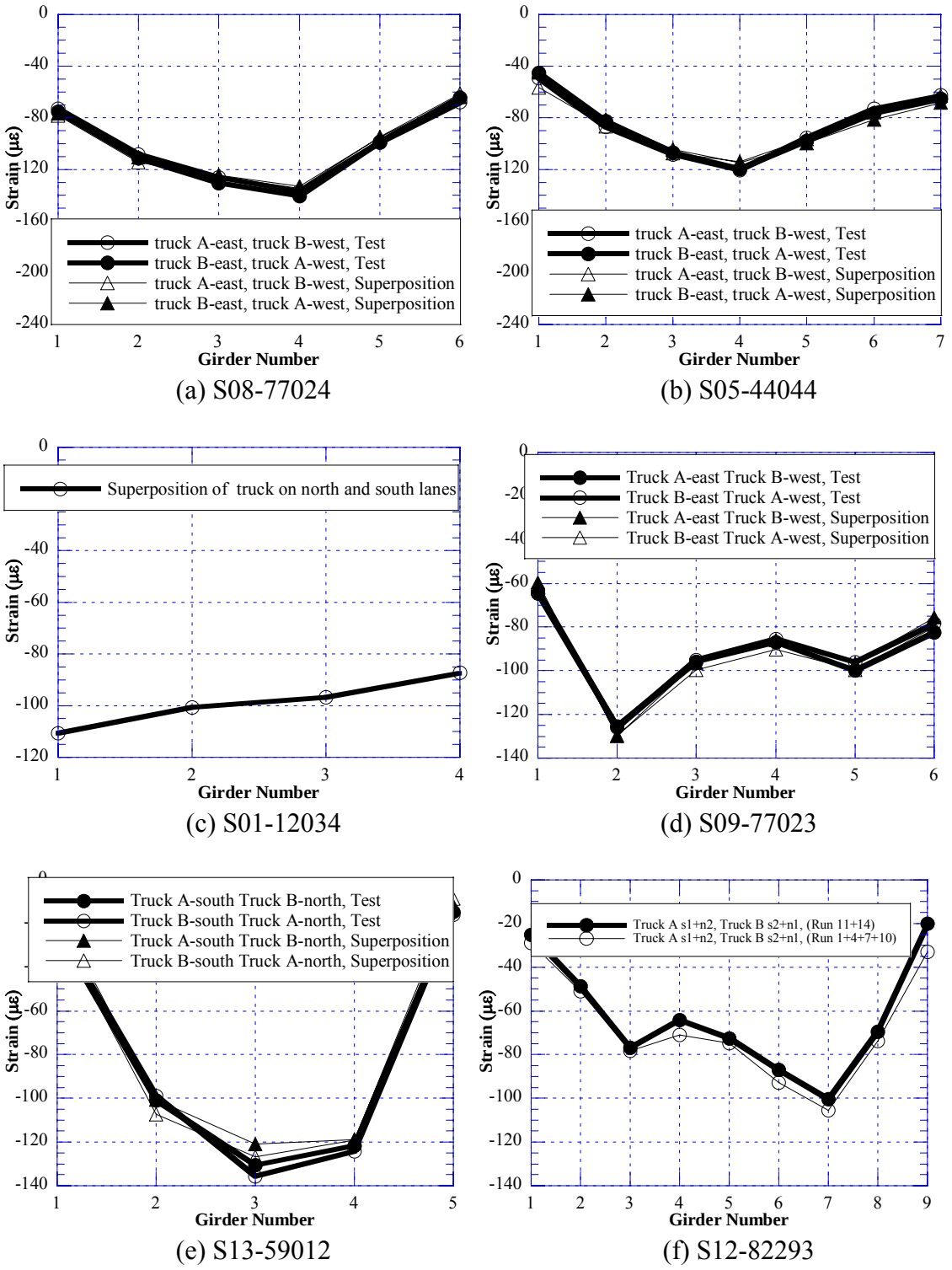

Figure 12.4 Negative Strains near Support over Pier under Side-by-Side Truck Loading at Crawling Speed

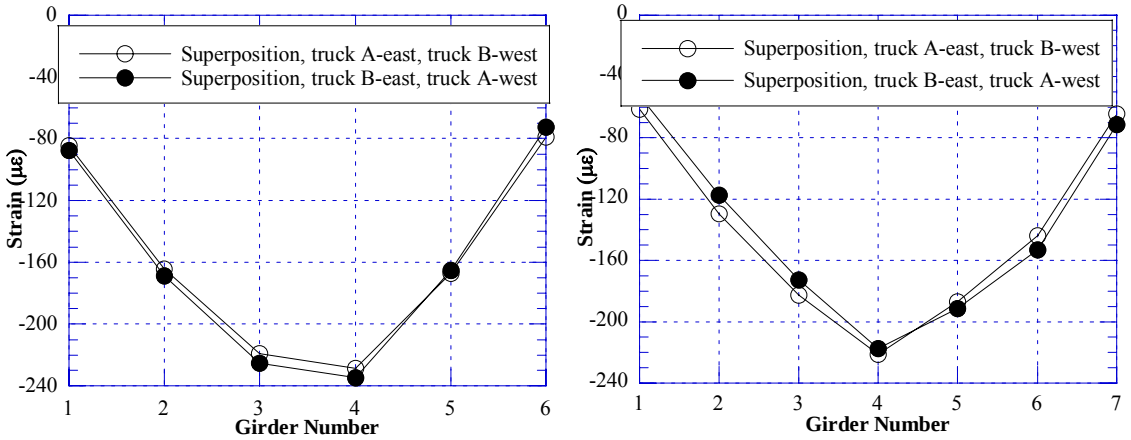

(a) S08-77024 (b) S05-44044

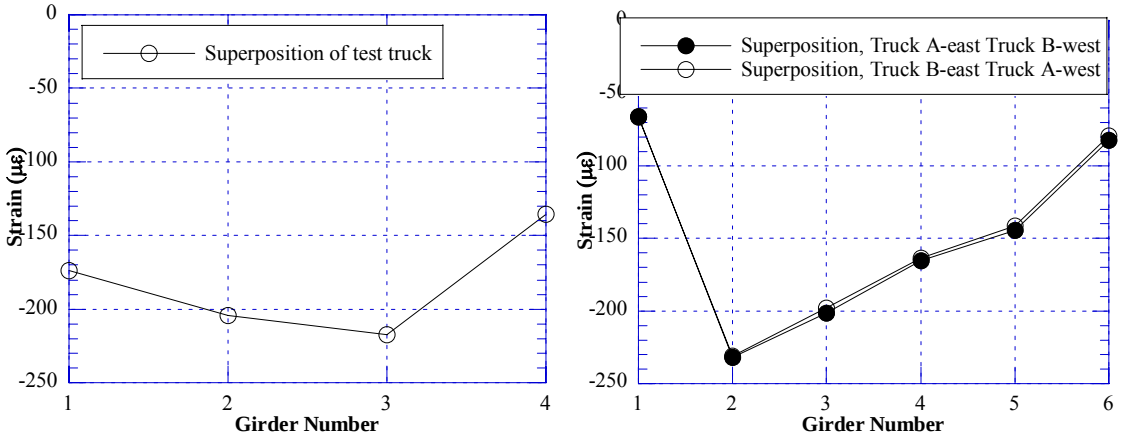

(c) S01-12034 (d) S09-77023

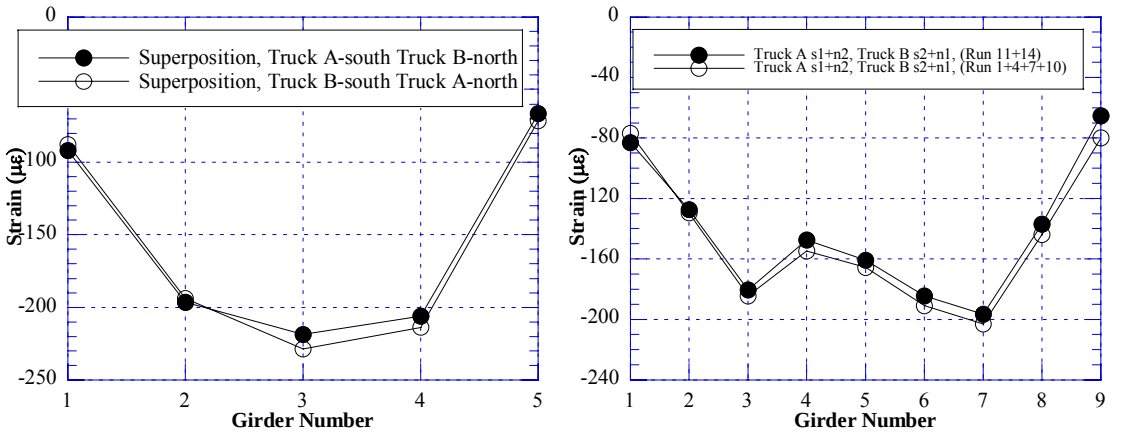

(e) S13-59012 (f) S12-82293

Figure 12.5 Negative Strain near Support over Pier due to Superposition of Side-by-Side Loading at Adjacent Spans to Maximize Negative Moment at Crawling Speed

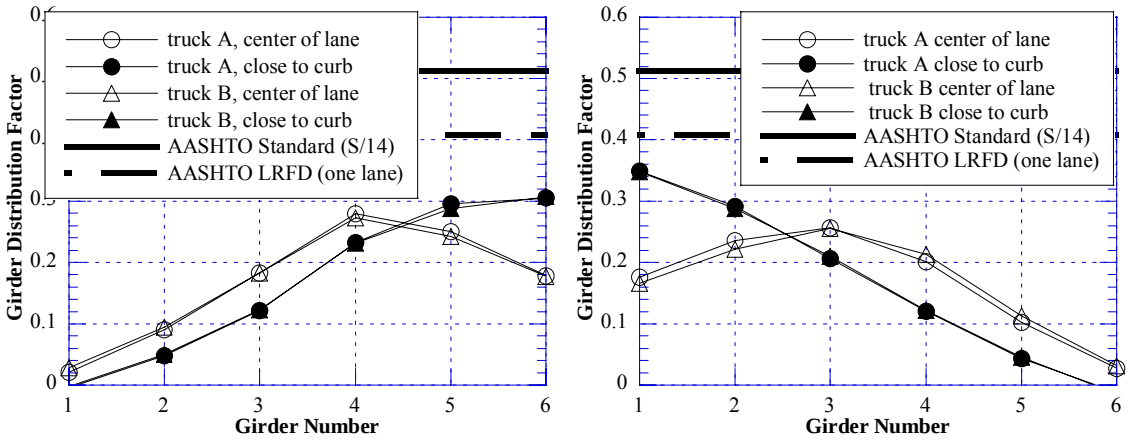

(a) West Lane Loaded (S08-77024)

(b) East Lane Loaded (S08-77024)

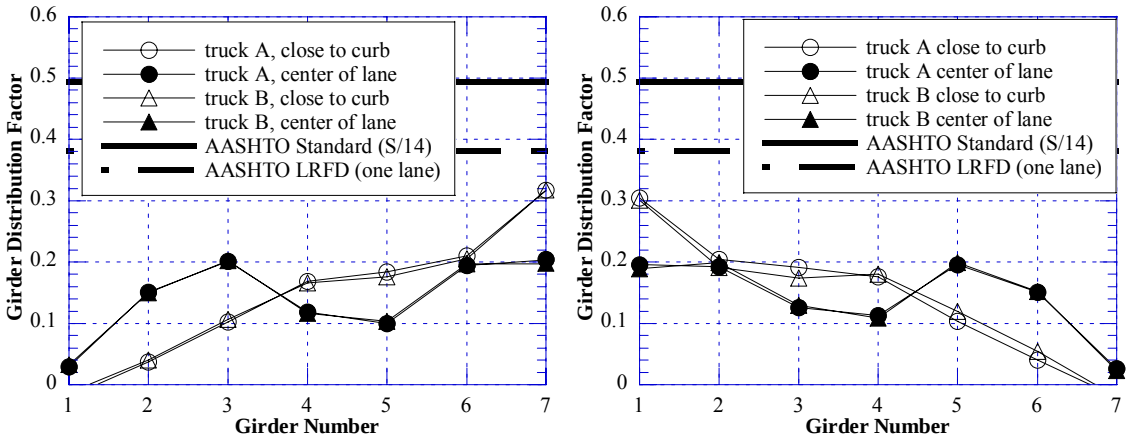

(c) West Lane Loaded (S05-44044)

(d) East Lane Loaded (S05-44044)

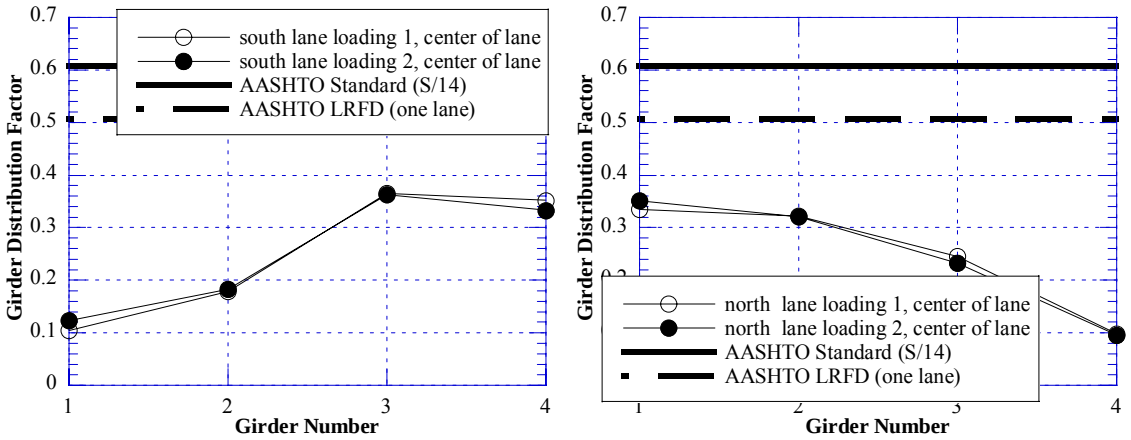

(e) South Lane Loaded (S01-12034)

(f) North Lane Loaded (S01-12034)

Figure 12.6 GDF from Positive Strain at Midspan under One Lane Loading at Crawling Speed

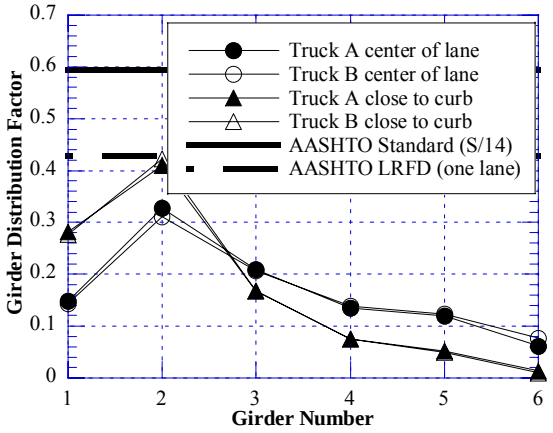

(g) East Lane Loaded (S09-77023)

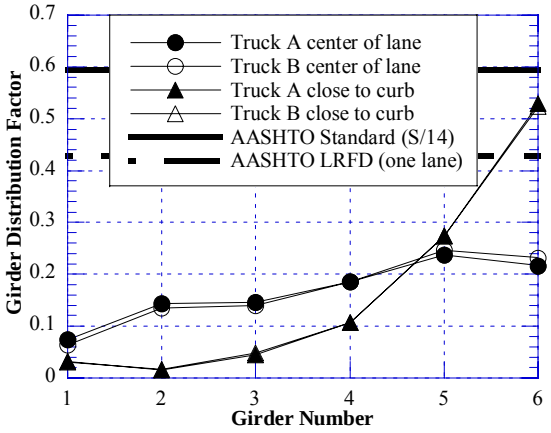

(h) West Lane Loaded (S09-77023)

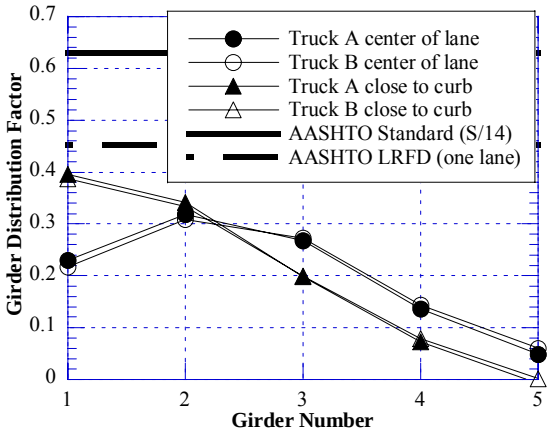

(i) North Lane Loaded (S13-59012)

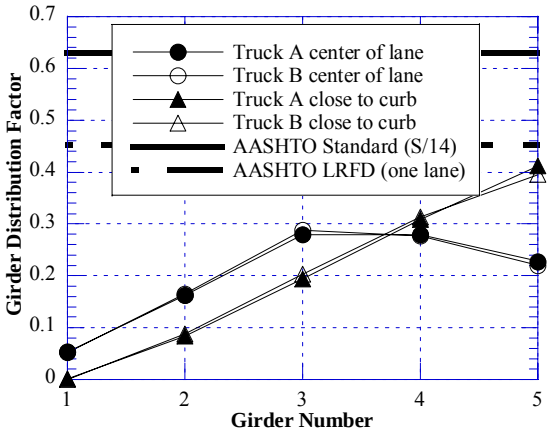

(j) South Lane Loaded (S13-59012)

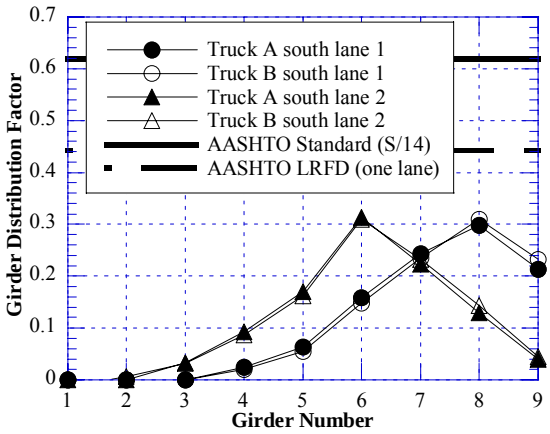

(k) South Lane Loaded (S12-82293)

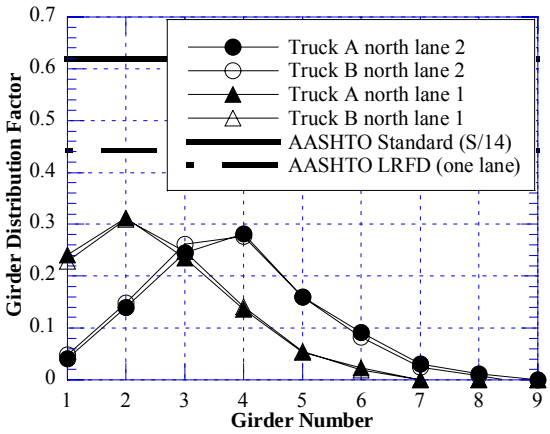

(l) North Lane Loaded (S12-82293)

Figure 12.6 GDF from Positive Strain at Midspan under One Lane Loading at Crawling Speed (Continued)

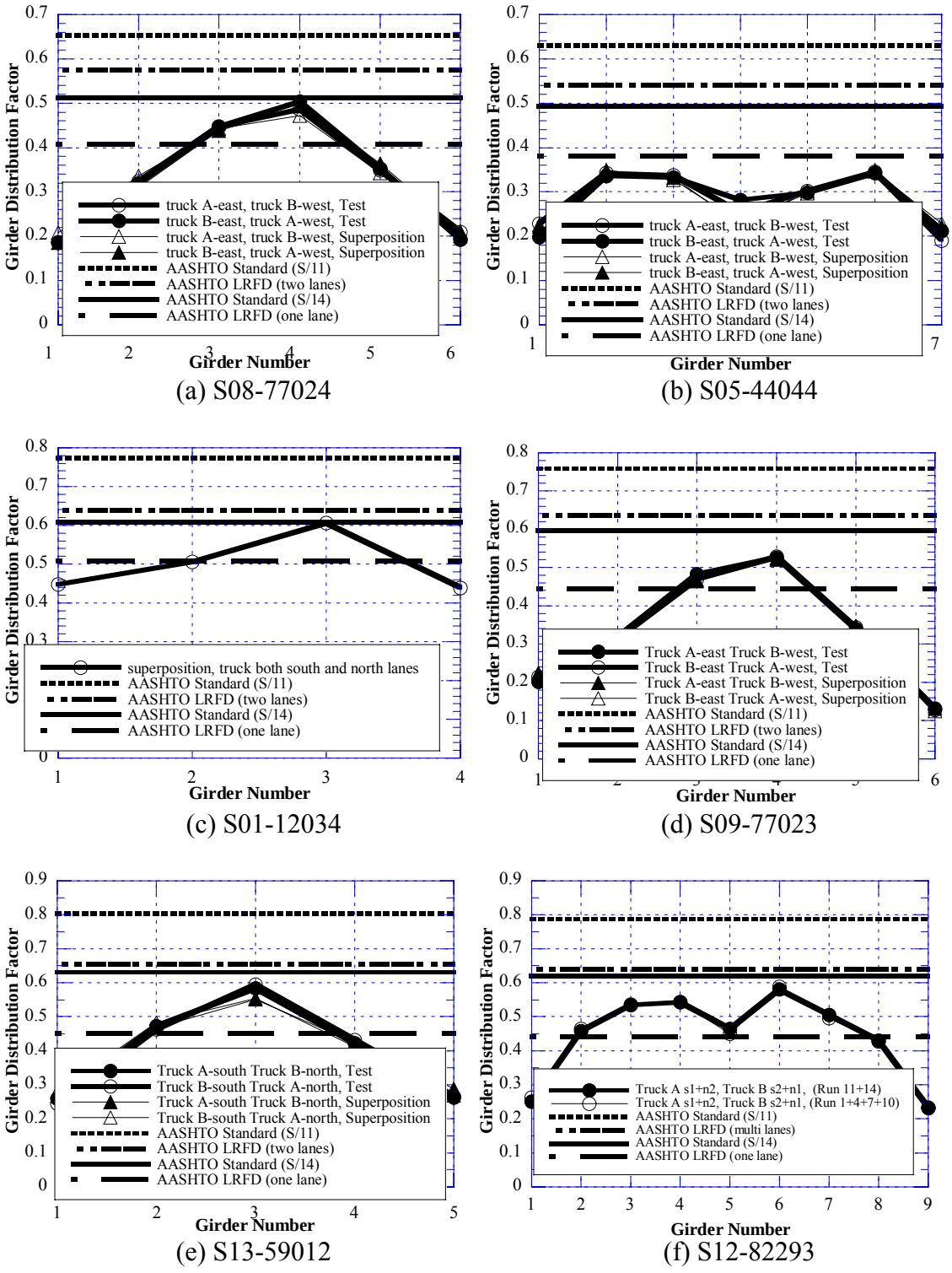

Figure 12.7 GDF from Positive Strain at Midspan under Side-by-Side Loading at Crawling Speed

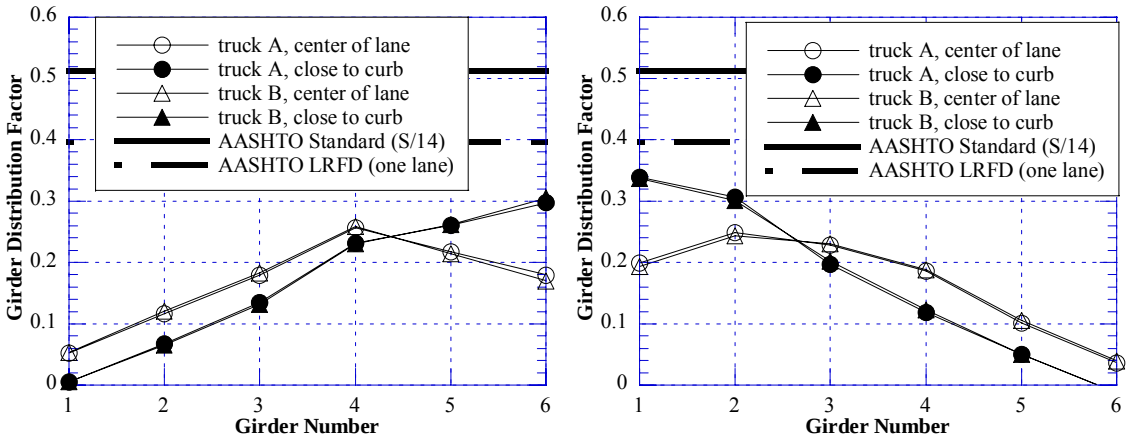

(a) West Lane Loaded (S08-77024)

(b) East Lane Loaded (S08-77024)

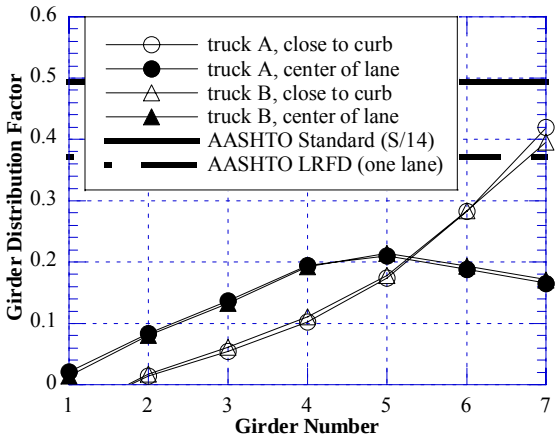

(c) West Lane Loaded (S05-44044)

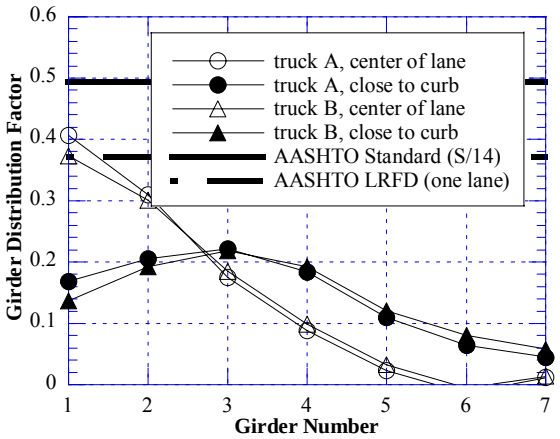

(d) East Lane Loaded (S05-44044)

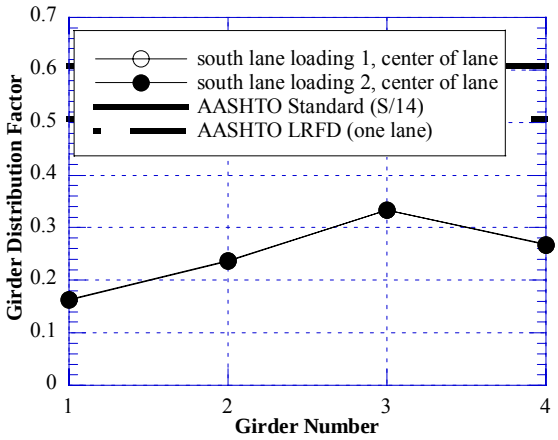

(e) South Lane Loaded (S01-12034)

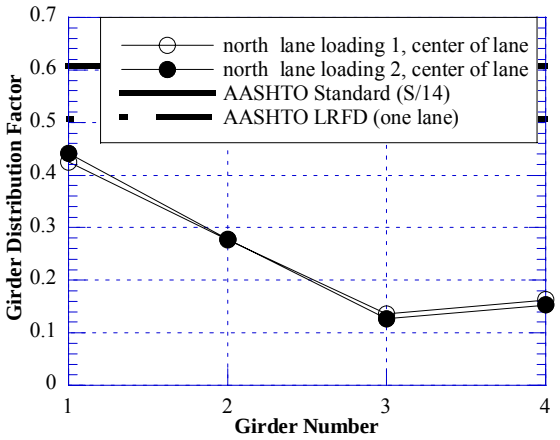

(f) North Lane Loaded (S01-12034)

Figure 12.8 GDF from Negative Strain near Support over Pier under One Lane Loading at Crawling Speed

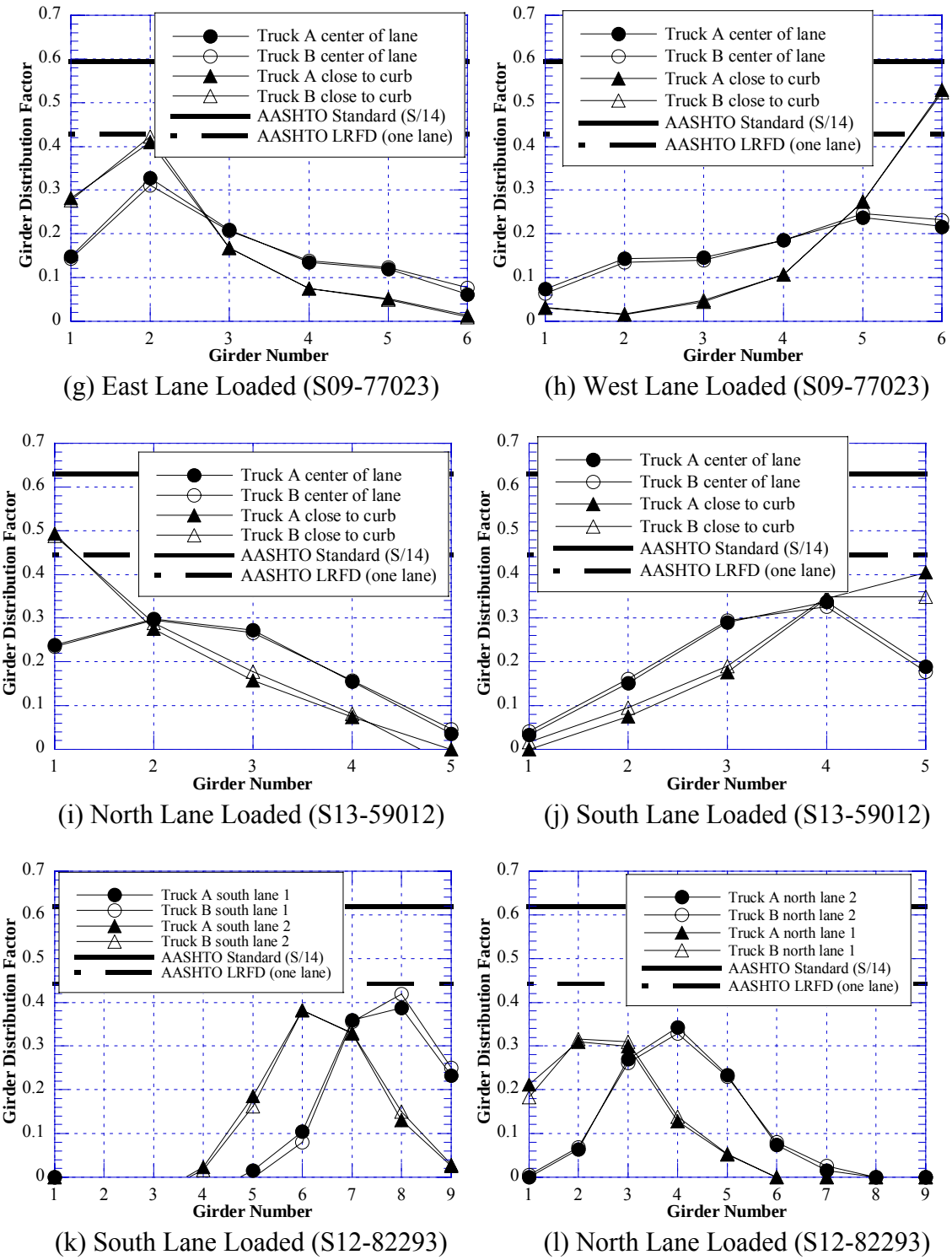

(g) East Lane Loaded (S09-77023)

(h) West Lane Loaded (S09-77023)

(i) North Lane Loaded (S13-59012)

(j) South Lane Loaded (S13-59012)

(k) South Lane Loaded (S12-82293)

(l) North Lane Loaded (S12-82293)

Figure 12.8 GDF from Negative Strain near Support over Pier under One Lane Loading at Crawling Speed (Continued)

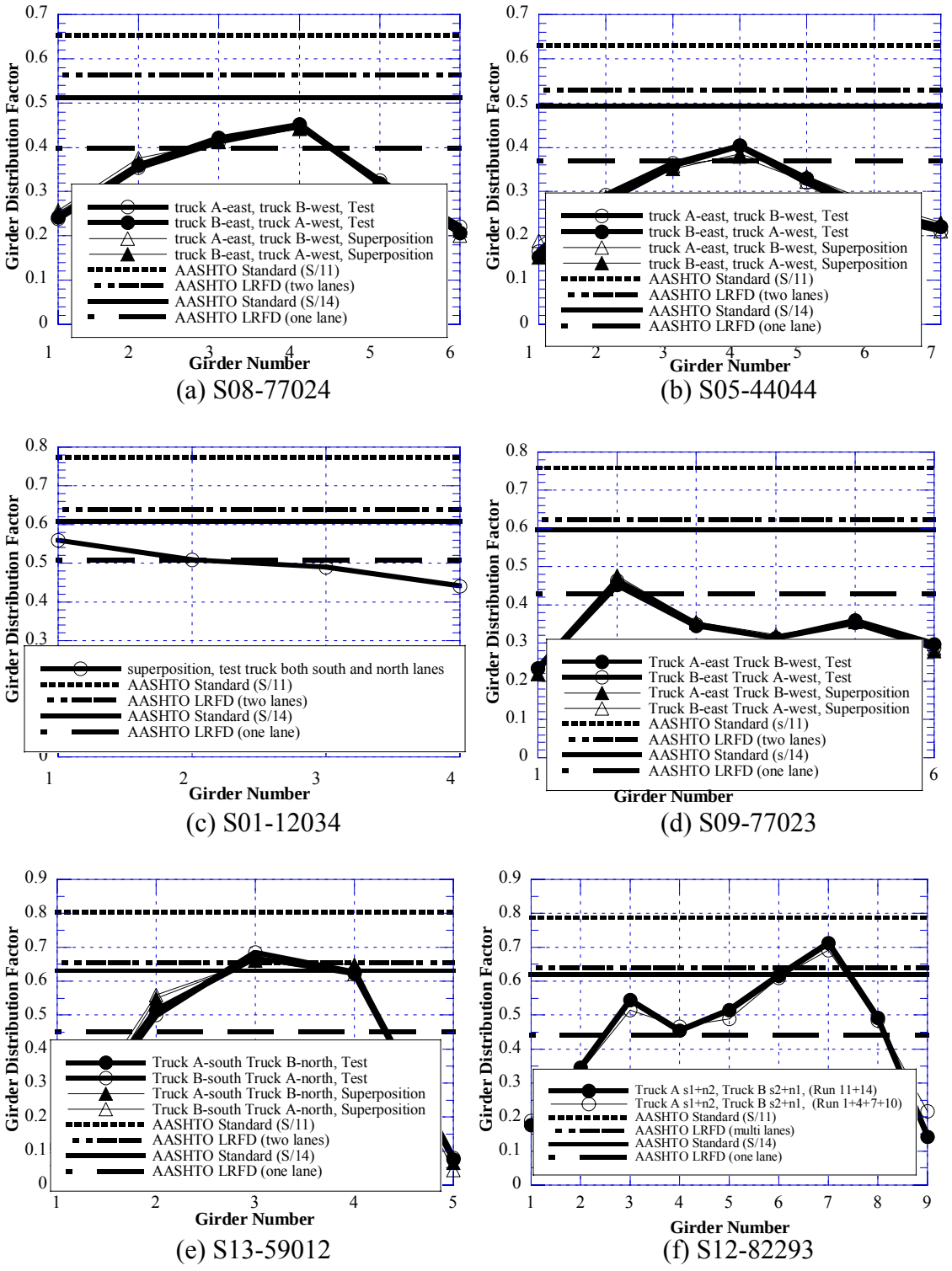

Figure 12.9 GDF from Negative Strain near Support over Pier under Side-by-Side Loading at Crawling Speed

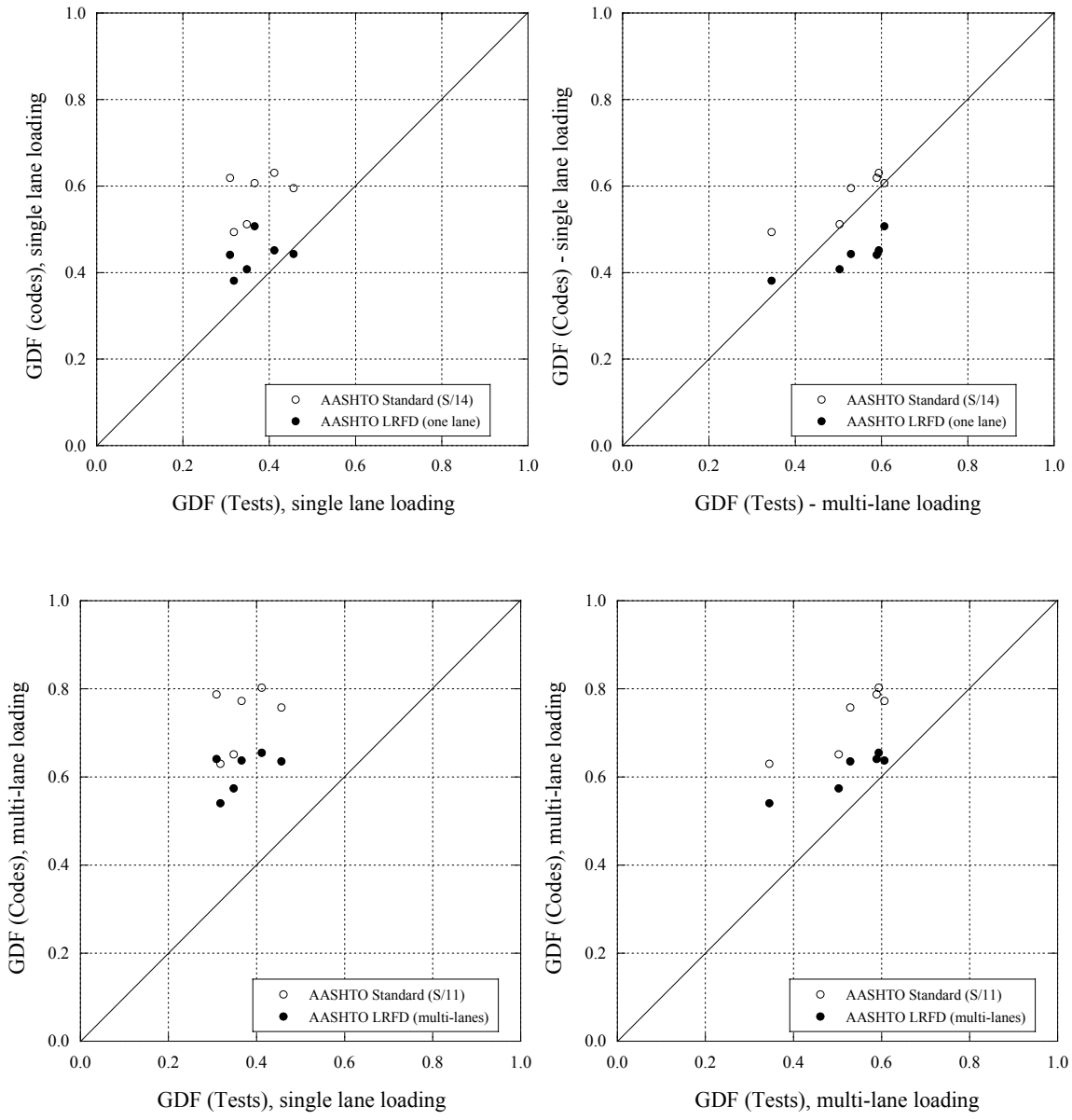

Figure 12.10 Comparison of Maximum Positive GDF's at Midspan, Tests Vs. Codes

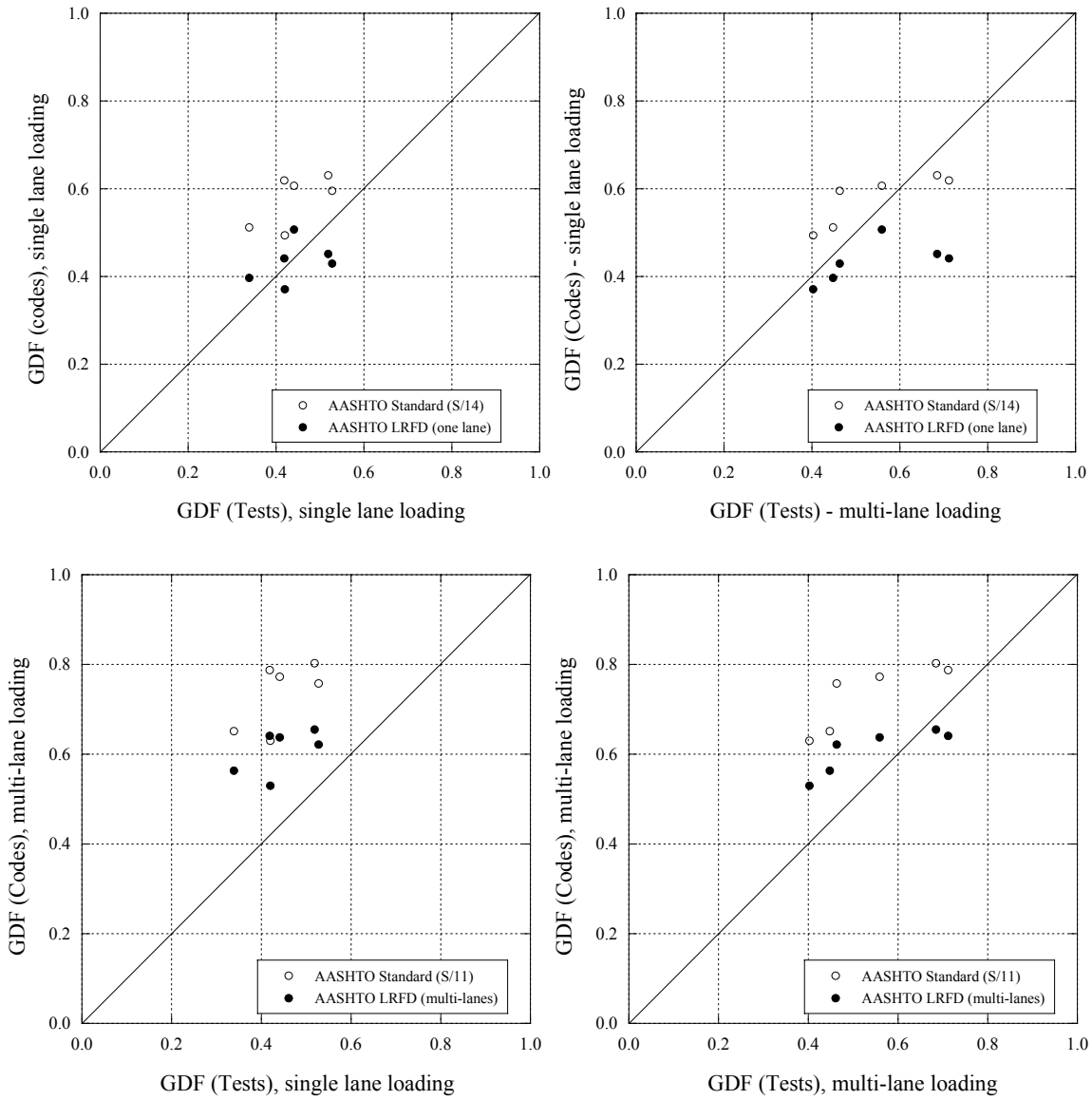

Figure 12.11 Comparison of Maximum Negative GDF's near Support, Tests Vs. Codes

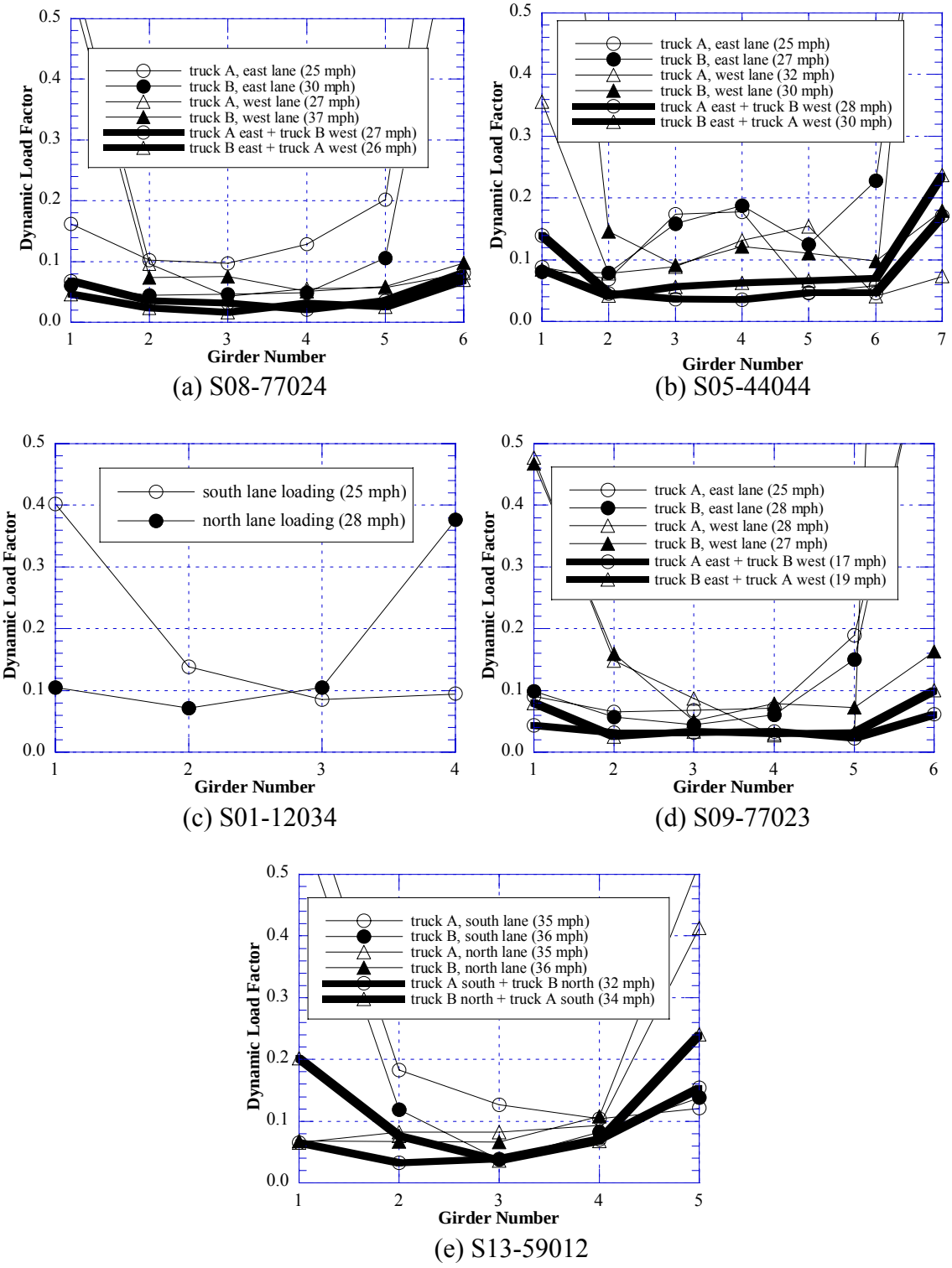

Figure 12.12 Dynamic Load Factors obtained from Positive Strain at Midspan

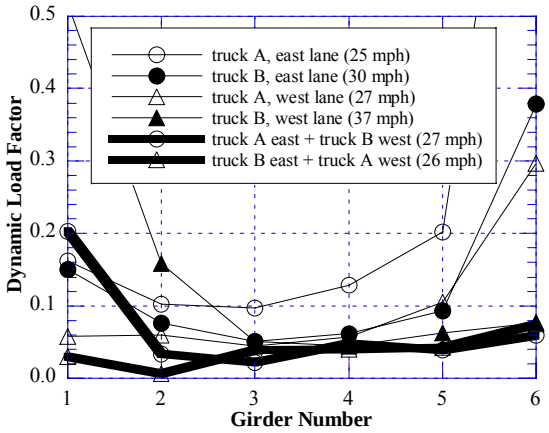

(a) S08-77024

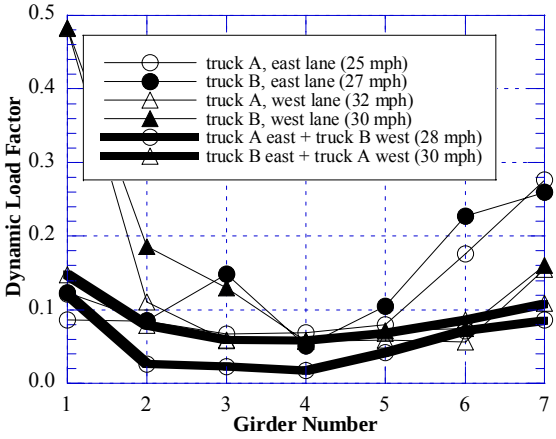

(b) S05-44044

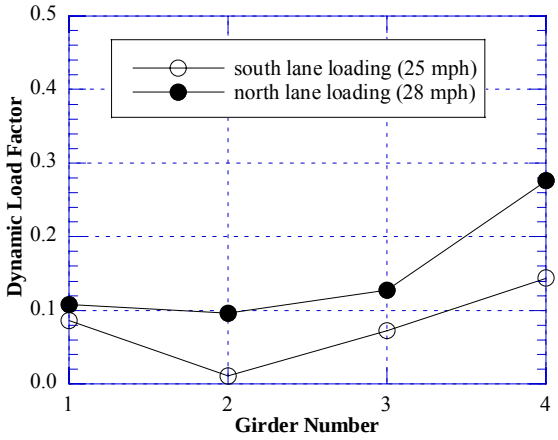

(c) S01-12034

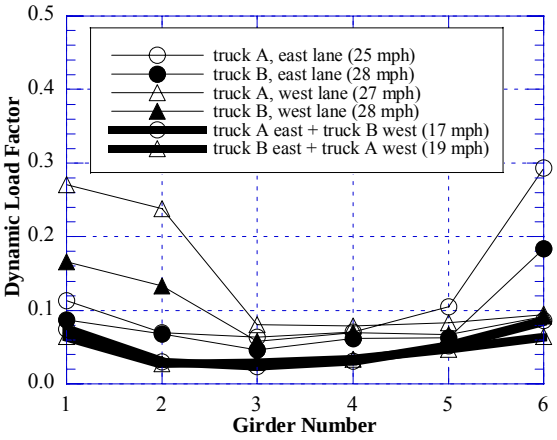

(d) S09-77023

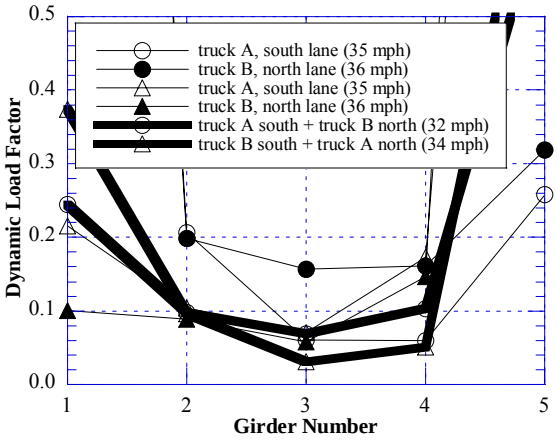

(e) S13-59012

Figure 12.13 Dynamic Load Factors obtained from Negative Strain near Support over Pier

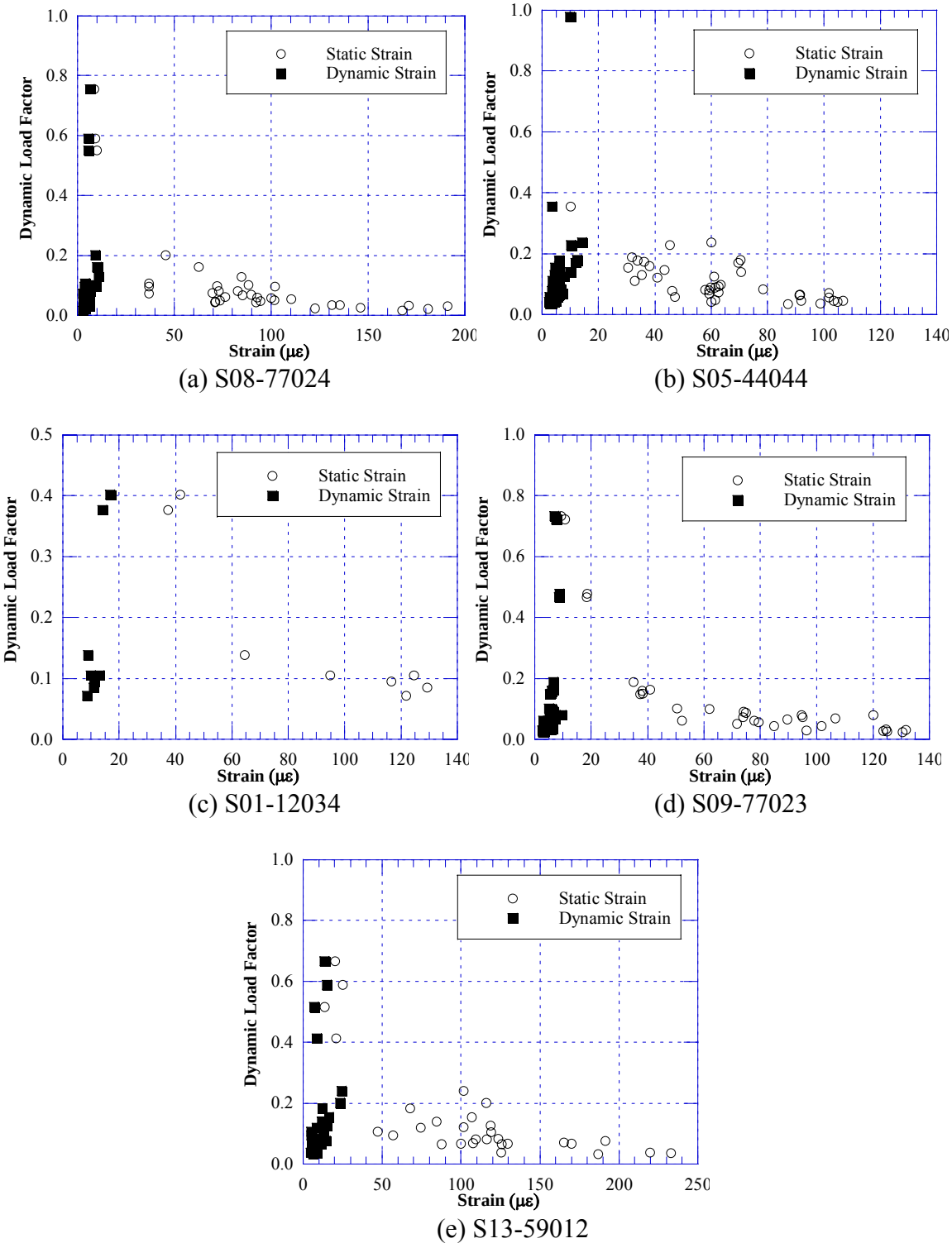

Figure 12.14 Strain vs. Dynamic Load Factors, Based on Positive Strain at Midspan

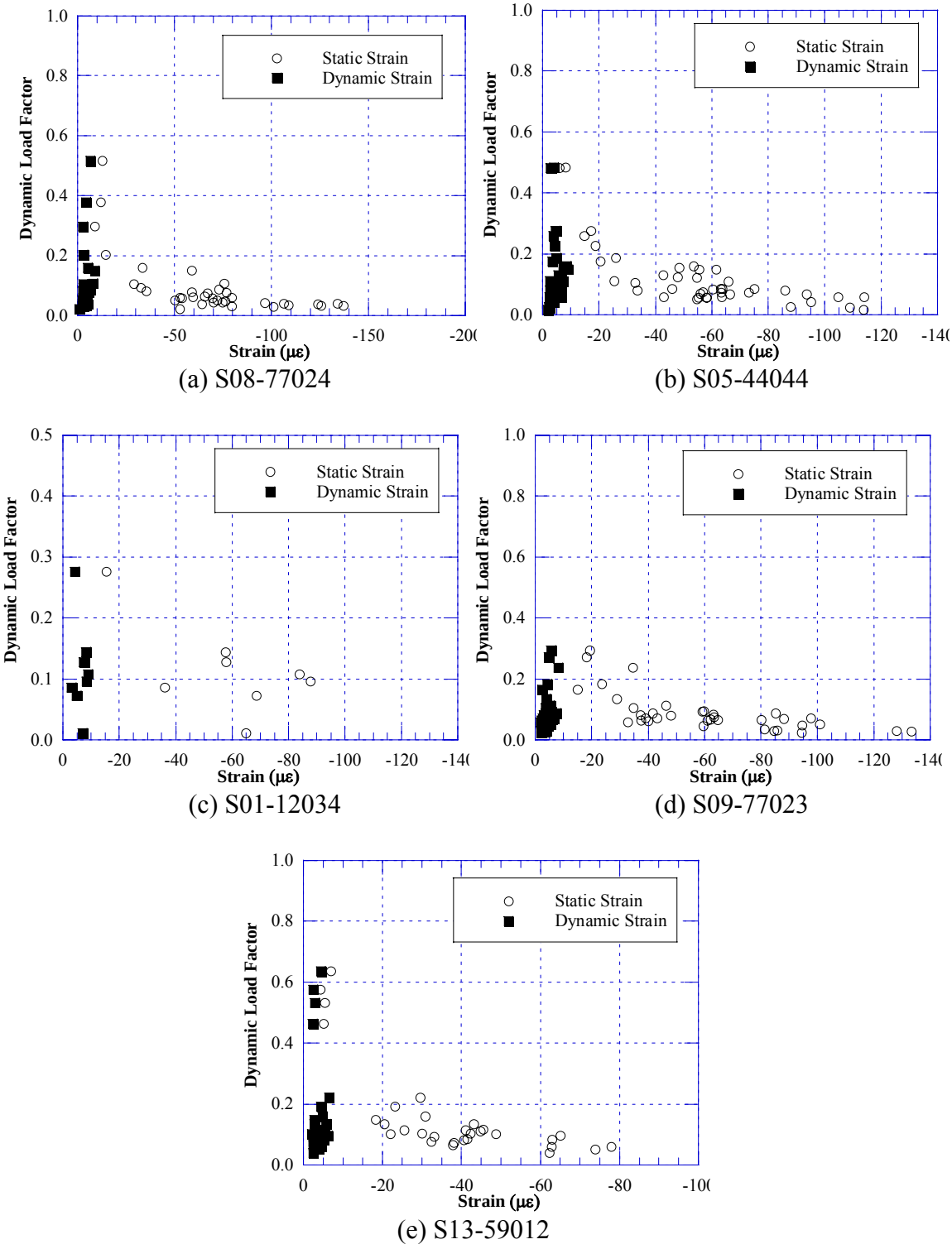

Figure 12.15 Strain vs. Dynamic Load Factors,Based on Negative Strain near Support over Pier

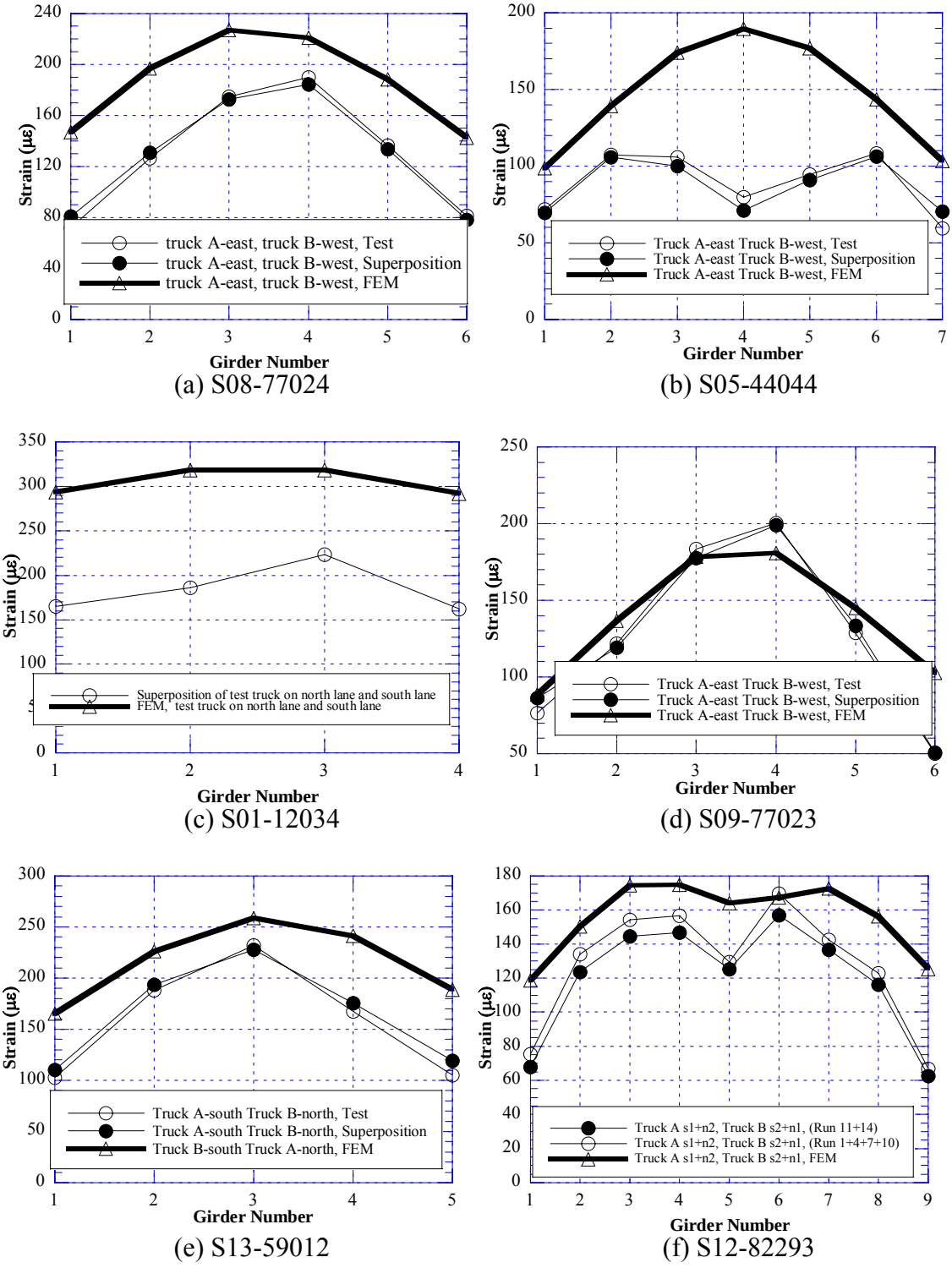

Figure 12.16 Comparison of FEM vs. Test, Positive Strain at Midspan under Side-by-Side Loading

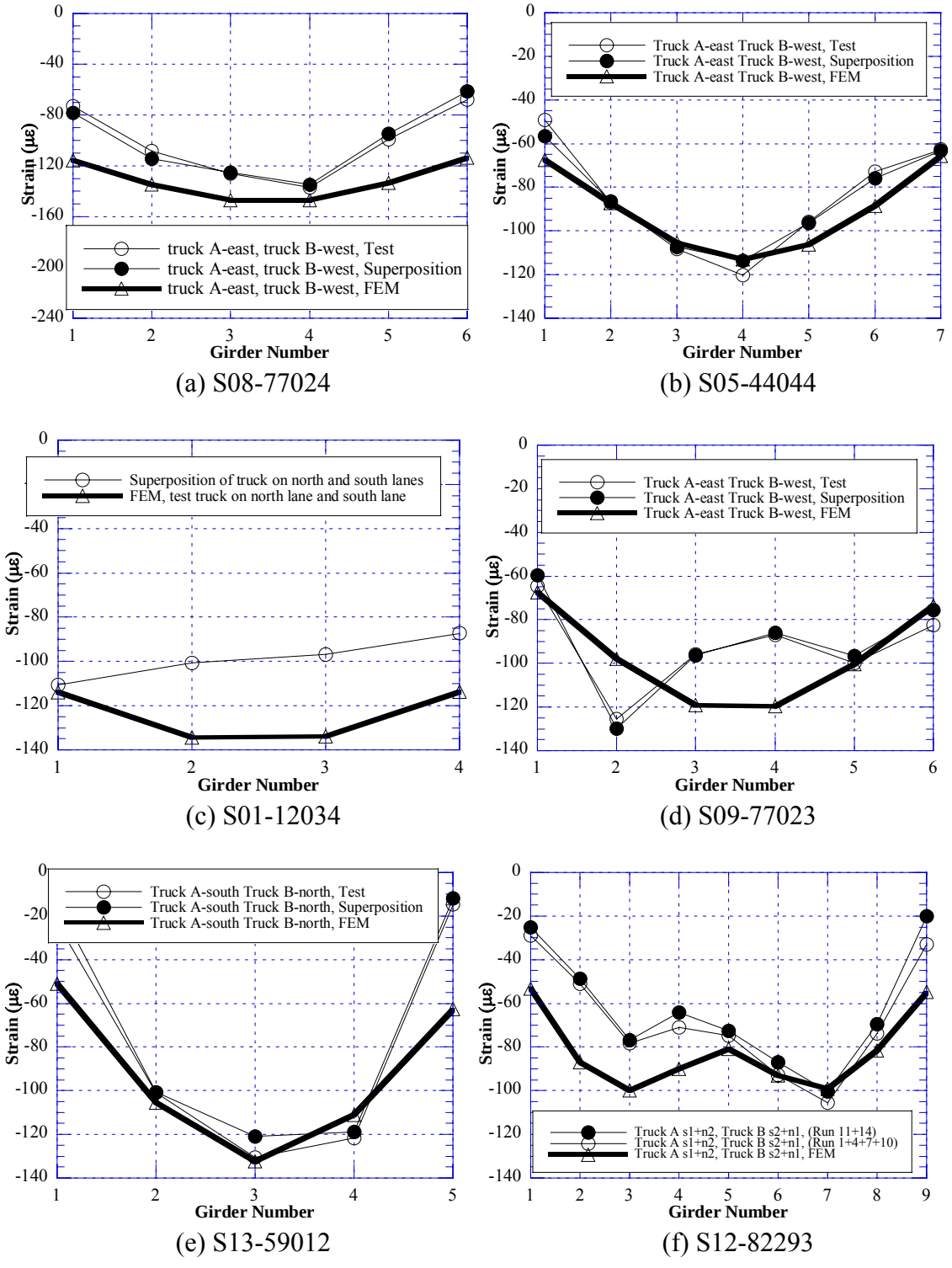

Figure 12.17 Comparison of FEM vs. Test, Negative Strain near Support over Pier, Side-by-Side Loading

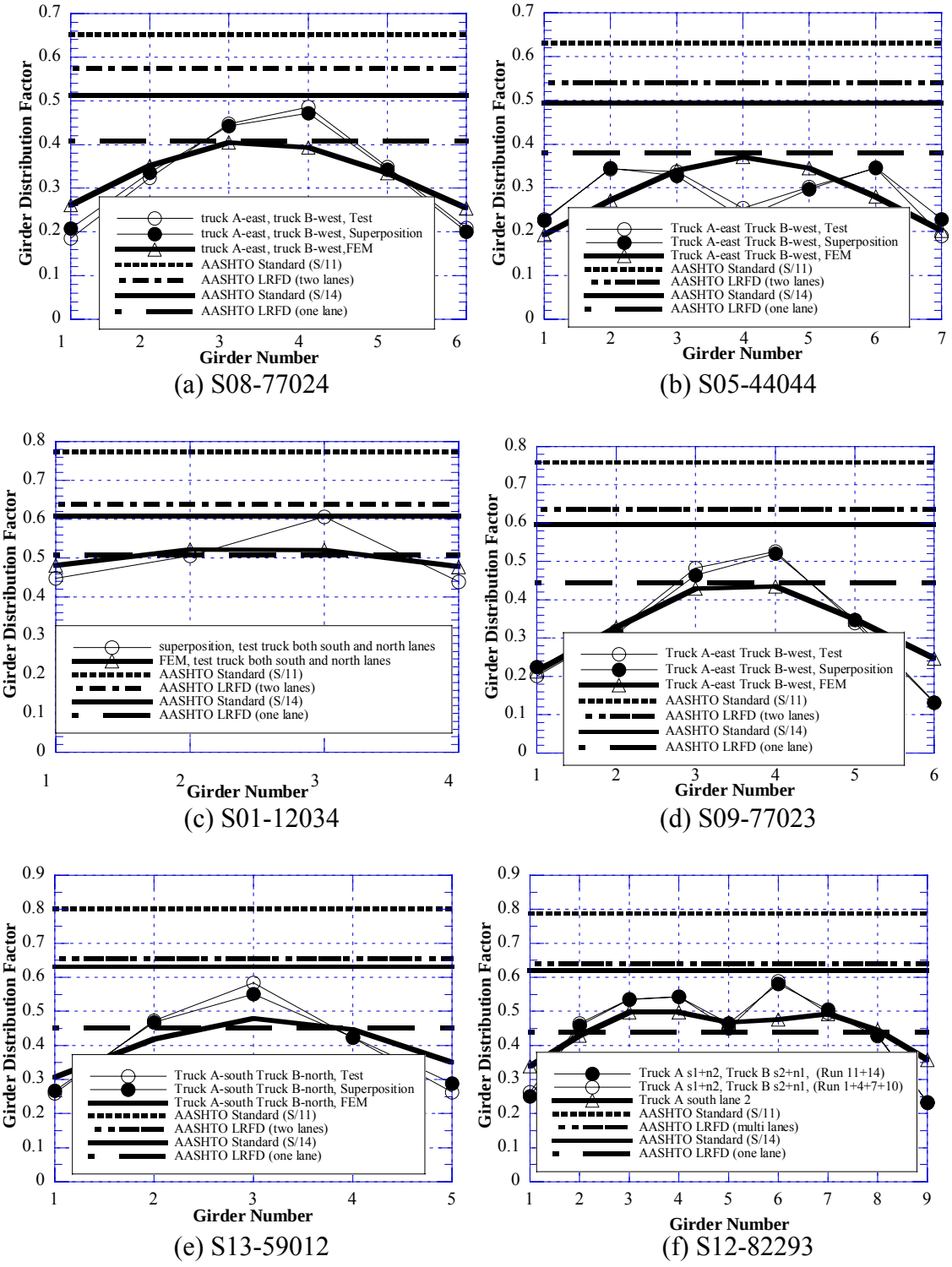

Figure 12.18Comparison of FEM vs. Test, GDF from Positive Strain at Midspan under Side-by-Side Loading

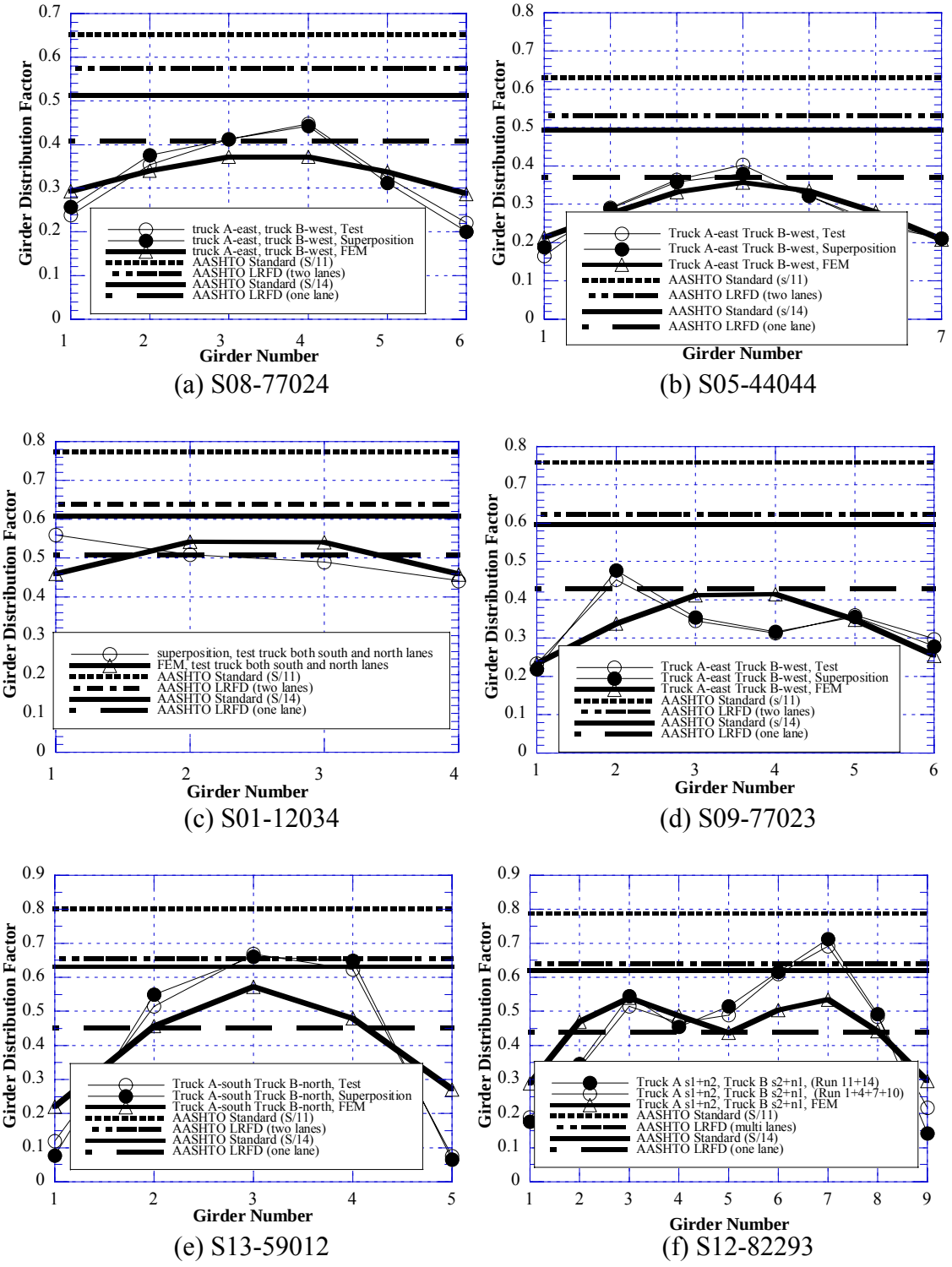

Figure 12.19 Comparison of FEM vs. Test, GDF from Negative Strain near Support over Pier under Side-by-Side Loading

12.4. Recommendations

12.4.1 Dynamic Load Factor (DLF)

In general, DLF's for continuous spans are lower than DLF's for simple spans. DLF's are lower for a negative moment (over the support) than for a positive moment (mid-span). The test results showed that DLF for a single heavy truck is less than 0.15. For two trucks side-by-side, DLF is 0.05-0.07 for the tested bridges. Therefore, for evaluation of existing steel girder bridges it is recommended, conservatively, to use DLF = 0.10 for two lane loading, and DLF = 0.20 for a single truck load case.

12.4.2 Girder Distribution Factor (GDF)

GDF's are different for continuous spans than for simple spans. In general, the distribution is more uniform for continuous spans, and this applies mostly to the negative moment. The superposition of truck loads in one lane and two adjacent spans produces a larger strain than measured during the field tests.

The code specified GDF's, for a single lane and for multi-lane traffic, are adequate or conservative, for both AASHTO LRFD (1998) and AASHTO Standard (2002). AASHTO Standard (2002) provides more conservative GDF's. Therefore, for the design of new bridges and evaluation of existing structures, it is recommended to use AASHTO LRFD (1998) GDF's. For evaluation of existing continuous steel girder bridges, it is possible to use the GDF's specified in the AASHTO Standard (2002) for a single lane even for two lane structures.

13. References

- AASHTO Standard Specifications for Highway Bridges, American Association of State and Transportation Officials, Washington, DC, 2002.
- AASHTO LRFD Bridge Design Specifications. American Association of State Highway and Transportation Officials, Washington, D.C., 1998.
- AASHTO Guide Specifications for Distribution of Loads for Highway Bridges, American Association of State Highway and Transportation Officials, Washington, D.C., 1994.
- Bakht, B., and Pinjarkar, S.G., "Dynamic Testing of Highway Bridges-A Review." Transportation Research Record 1223, Transportation Research Board, National Research Council, Washington, D.C., pp. 93-100, 1989.
- Brockenbrough, R.L., "Distribution factors for curved I-girder bridges." Journal of Structural Engineering, ASCE, Vol. 112, No. 5, 1986.
- Croce, P. and Salvatore, W., "Stochastic Model for Multilane Traffic Effects on Bridges." Journal of Bridge Engineering, ASCE, Vol. 6, No.2, pp136-143, March/April, 2001.
- Eom, J. and Nowak, A.S., "Live Load Distribution for Steel Girder Bridges", ASCE Journal of Bridge Engineering, Vol. 6, No. 6, 2001, pp. 489-497.
- Ghosn, M., Moses, F., and Gobieski, J., "Evaluation of Steel Bridges Using In-Service Testing." Transportation Research Record 1072, Transportation Research Board, National Research Council, Washington, D.C., pp. 71-78, 1986.
- Hays, C.O., Sessions, L.M., and Berry, A.J. (1986), "Further studies on lateral load distribution using FEA." Transportation Research Record 1072, Transportation Research Board, National Research Council, Washington, 1986.
- Hwang, E.S., and Nowak, A.S., "Simulation of Dynamic Load for Bridges." Journal of Structural Engineering, ASCE, Vol. 117, No.5, pp.1413-1434, July, 1991.

- Imbsen, R.A., and Nutt, R.V., "Load Distribution Study on Highway Bridge using STRUDL FEA" Proceeding, Conference on Computing in Civil Engineering, ASCE, New York, 1978.
- Lichtenstein, A. G., Manual for Bridge Rating Through Nondestructive Load Testing, NCHRP Report 12-28(13) A, 1998.
- Mabsout, M.E., Tarhini, K.M., Frederick, G.R., and Tayar, C. "Finite-Element Analysis of Steel Girder Highway Bridges." Journal of Bridge Engineering. Vol. 2, No 3, August 1997.
- Nassif, H.H. and Nowak, A.S., "Dynamic Load Spectra for Girder Bridges." Transportation Research Record 1476, Transportation Research Board, National Research Council, Washington, D.C., pp. 69-83, 1995
- Nowak, A.S. and Eom, J., "Verification of Girder Distribution Factors for Steel Girder Bridges", UMCEE 01-01, Final Report submitted to MDOT, April 2001.
- Nowak, A.S. and Kim, S. , "Development of a Guide for Evaluation of Existing Bridges, Part I", UMCEE 98-12, Final Report submitted to MDOT, June 1998.
- Nowak, A.S., Laman, J.A., and Nassif H., "Effect of Truck Loading on Bridges." Report UMCE 94-22. Department of Civil and Environmental Engineering, University of Michigan, Ann Arbor, 1994
- Nowak, A.S., Sanli, A., and Eom, J., "Development of a Guide for Evaluation of Existing Bridges, Phase II", UMCEE 99-13, Final Report submitted to MDOT, December 1999.
- O'Connor, C. and Shaw, P.A., "Bridge Loads", Spon Press, New York, 2000.
- Paultre, P., Chaallal, O., and Proulx, J., "Bridge Dynamics and Dynamic Amplification Factors-A Review of Analytical and Experimental Findings." Canadian Journal of Civil Engineering, Vol. 19, pp. 260-278, 1992.
- Schultz J.L., Commander B., Goble G.G., Frangpol D.M., Efficient field Testing and load Rating of Short – And Medium – Span Bridges, Structural Engineering review, Vol. 7, No 3 pp181-194, 1995.

- Stallings, J.M., and Yoo, C.H., “Tests and Ratings of Short-Span Steel Bridges.” Journal of Structural Engineering, ASCE, Vol. 119, No. 7, pp. 2150-2168, July, 1993.
- Tarhini K.M and Frederick, G. R. 1992. "Wheel load distribution in I-girder highway bridges" Journal of Structural Engineering Vol 118, No 5, pp1285-1294.
- Zokaie, T., Osterkamp, T.A., and Imbsen, R.A., Distribution of Wheel Loads on Highway Bridges, National Cooperative Highway Research Program Report 12-26, Transportation Research Board, Washington, D.C., 1991.